

The Role of Glycogen and Lactate in
Supporting Action Potential
Conduction in Mouse Central White
Matter and Peripheral Nerve

RICHARD DEBNEY EVANS MSci. (Hons)

Thesis submitted to the University of
Nottingham
for the degree of Doctor of Philosophy

June 2012

The Role of Glycogen and Lactate in Supporting Action Potential Conduction in Mouse Central White Matter and Peripheral Nerve

Abstract

Central white matter and peripheral nerves function by conducting action potentials, which rely on the presence of transmembrane potentials generated by ion gradients. The maintenance of these transmembrane potentials is the main energy-dependent process in the nervous system. In this thesis I investigated the ability of endogenous glycogen to support the energy requirements of nervous tissue and the role of lactate in this process. Glycogen in the CNS is located in astrocytes but is capable of supporting axonal conduction, implying axon-glia metabolic interactions. These interactions were investigated in both the mouse optic nerve (MON), a central white matter tract, and the mouse sciatic nerve (MSN), a mixed peripheral nerve. Electrophysiological techniques were used to record action potential conduction in the nerves as an index of nerve function. Parallel experiments to quantify glycogen content using biochemical assay, or simultaneous real-time measurement of lactate release from the nerves using enzyme-based lactate biosensors, correlated action potential conduction with glycogen content, or lactate release, respectively. Depletion of glycogen leaves the MON vulnerable to irreversible injury to a greater extent than exposure to moderate hyperthermia during aglycemia. Glycogen also greatly enhanced the neuroprotective effects of mild hypothermia during aglycemia. Under resting conditions lactate in the immediate vicinity of the MON was stable at ~0.5 mM, a concentration that increased with axonal activity, dependent upon stimulus intensity. Raising extracellular K^+ evoked lactate release, suggesting that increased neuronal activity promotes lactate release. Inhibition of glycogen metabolism, partly reduced lactate release from the MON, implying that glycogen metabolism is important under normal physiological conditions. The relative contribution of glycogen to lactate release increased with axonal activity, consistent with activity-induced glycogenolysis. These studies were then extended to the peripheral nervous system as the role of glycogen in this tissue has not previously been considered. Glycogen, which was present in Schwann cells, supported myelinated, but not unmyelinated axons during aglycemia, suggesting a more complex and selective neuroprotective role than that in central white matter.

These results advance our understanding of white matter energy metabolism in relation to both the contributions of glycogen and lactate. The novel functional role of glycogen in supporting peripheral nerve function has also been described.

Contents

Acknowledgements.....xiii

Declarationxv

Abbreviationsxvi

Chapter One

Introduction

1.1 Energy Metabolism in the Nervous System.....	2
1.1.1 <i>Glucose Metabolism.....</i>	<i>3</i>
1.2 Energy Metabolism in the Healthy Brain.....	14
1.2.1 <i>Energy Demands of the Brain</i>	<i>14</i>
1.2.2 <i>The Blood-Brain Barrier (BBB)</i>	<i>16</i>
1.2.3 <i>Glial Support of Neurons</i>	<i>17</i>
1.2.4 <i>Lactate in the Brain</i>	<i>19</i>
1.2.5 <i>Brain Glycogen.....</i>	<i>23</i>
1.2.6 <i>Functional Neuroimaging</i>	<i>24</i>
1.3 Energy Metabolism and Pathology.....	25
1.3.1 <i>Hypo/aglycemia</i>	<i>26</i>
1.4 Considerations in White Matter.....	27
1.5 Energy Metabolism in Peripheral Nerves	28
1.6 Aims and Hypotheses.....	29

Chapter Two

Methods

2.1 Animals.....	32
2.1.1 <i>Optic Nerve</i>	<i>32</i>
2.1.2 <i>Sciatic Nerve.....</i>	<i>32</i>
2.2 Electrophysiology.....	33
2.2.1 <i>Stimulus-Evoked Compound Action Potential</i>	<i>33</i>
2.2.2.2 <i>Analysis of Compound Action Potentials</i>	<i>36</i>
2.3 Lactate Biosensor Measurements	40
2.3.1 <i>Principles of Biosensor Measurement of Lactate.....</i>	<i>40</i>
2.3.2 <i>Biosensor protocol in the MON.....</i>	<i>40</i>
2.4 Glycogen assay.....	43
2.5 Microscopy.....	45
2.5.1 <i>Transmission Electron Microscopy</i>	<i>45</i>
2.6 Statistical Analysis.....	45

Chapter Three

Neuroprotective effect of hypothermia and glycogen in the mouse optic nerve

3.1 Introduction.....	47
3.1.1 <i>Aglycemic Injury in White Matter</i>	<i>47</i>
3.1.2 <i>The Effect of Temperature on Nerve Conduction and Injury</i>	<i>48</i>
3.1.3 <i>The Importance of Brain Glycogen.....</i>	<i>49</i>
3.1.4 <i>Aims.....</i>	<i>51</i>
3.2 Methods and Protocol	52
3.2.1 <i>Electrophysiology.....</i>	<i>52</i>
3.2.2 <i>Control of Temperature.....</i>	<i>52</i>
3.2.3 <i>Oxygen Electrode</i>	<i>53</i>
3.2.4 <i>Morphological Studies.....</i>	<i>54</i>
3.3 Results.....	56
3.3.1 <i>Extent of aglycemic injury is dependent on duration of aglycemia</i>	<i>56</i>
3.3.2 <i>Effect of temperature on the CAP profile.....</i>	<i>58</i>
3.3.3 <i>Temperature-dependence of aglycemic injury.....</i>	<i>59</i>
3.3.4 <i>Temperature-dependence of MON metabolism</i>	<i>62</i>
3.3.5 <i>Temperature-dependence of aglycemic injury in glycogen-depleted nerves.....</i>	<i>65</i>
3.3.6 <i>Comparison between control and glycogen-depleted MONs</i>	<i>66</i>

3.3.7 Morphology of aglycemic injury at 37°C	68
3.3.8 Morphology of temperature-dependence of aglycemic injury	70
3.4 Discussion.....	73
3.4.1 Prevention of Injury During Aglycemia.....	73
3.4.2 The Protective Role of Hypothermia.....	74
3.4.3 Morphometric Analysis of Nerve Injury.....	75
3.4.4 The Role of Brain Glycogen.....	77
3.4.5 Summary	79

Chapter Four

Real-time measurement of lactate using biosensors reveals that glycogenolysis contributes to extracellular lactate in the mouse optic nerve.

4.1 Introduction.....	81
4.1.1 <i>Lactate in the CNS</i>	81
4.1.2 <i>Lactate in White Matter</i>	83
4.1.3 <i>Glycogen is a Source of Lactate</i>	83
4.1.4 <i>Biosensors</i>	84
4.1.5 <i>Aims</i>	85
4.2 Methods.....	86
4.3 Results.....	87
4.3.1 <i>Biosensor Calibration and Specificity</i>	87
4.3.2 <i>Lactate is Produced by the Mouse Optic Nerve</i>	89
4.3.3 <i>The Relationship Between Glucose Supply and Extracellular Lactate</i>	91
4.3.4 <i>Extracellular Lactate with Fructose as the Sole Energy Substrate</i>	94
4.3.5 <i>Lactate Production Requires Glycolytic Metabolism of Glucose</i>	95
4.3.6 <i>Inhibition of Oxidative Metabolism in the MON</i>	97
4.3.7 <i>Glycogen Metabolism Contributes to Extracellular Lactate</i>	98

4.4 Discussion.....	105
4.4.1 <i>Biosensors for Real-Time Measurement of Lactate.....</i>	<i>105</i>
4.4.2 <i>Extracellular Lactate in White Matter</i>	<i>108</i>
4.4.3 <i>Glucose Availability and Extracellular Lactate.....</i>	<i>109</i>
4.4.4 <i>Fructose Metabolism in the Optic Nerve</i>	<i>110</i>
4.4.5 <i>Metabolic Inhibition</i>	<i>111</i>
4.4.6 <i>Glycogen as a Source of Lactate.....</i>	<i>113</i>
4.4.7 <i>Evidence for a Glycogen Shunt</i>	<i>114</i>

Chapter Five

Activity-dependent increases in white matter lactate production are mediated by extracellular potassium

5.1 Introduction.....	117
5.1.1 <i>Lactate and Increased Neural Activity.....</i>	<i>117</i>
5.1.2 <i>Lactate and Pathological Conditions.....</i>	<i>118</i>
5.1.3 <i>Aims.....</i>	<i>118</i>
5.2 Methods.....	120
5.3 Results.....	121
5.3.1 <i>Extracellular Lactate Increases During Axonal Activity ...</i>	<i>121</i>
5.3.2 <i>Extracellular Potassium Stimulates Lactate Production</i>	<i>127</i>
5.3.3 <i>Post-aglycemia Recovery.....</i>	<i>130</i>
5.4 Discussion.....	133
5.4.1 <i>The Effect of Axonal Activity on Extracellular Lactate</i>	<i>133</i>
5.4.2 <i>Time Course of Lactate Production</i>	<i>134</i>
5.4.3 <i>Potassium Homeostasis and Lactate Production</i>	<i>136</i>
5.4.4 <i>Ion Pumps and Aerobic Glycolysis.....</i>	<i>137</i>
5.4.5 <i>Lactate and Aglycemia.....</i>	<i>138</i>
5.5 An Integrated Overview of Lactate in White Matter.....	140
5.5.1 <i>Are astrocytes the Source of White Matter Lactate?</i>	<i>140</i>

5.5.2 *The Fate of Extracellular Lactate*.....142

Chapter Six

A Functional Role for Peripheral Nerve Glycogen

6.1 Introduction.....	146
6.1.1 <i>Peripheral Nerve Morphology</i>	<i>146</i>
6.1.2 <i>Glial Cells in Peripheral Nerves.....</i>	<i>147</i>
6.1.3 <i>Energy Metabolism in Peripheral Nerves</i>	<i>148</i>
6.1.4 <i>Glycogen in Peripheral Nerves.....</i>	<i>148</i>
6.1.5 <i>The Sciatic Nerve as a Model.....</i>	<i>149</i>
6.1.6 <i>Aims.....</i>	<i>150</i>
6.2 Methods.....	151
6.2.1 <i>Electrophysiology.....</i>	<i>151</i>
6.2.2 <i>Identification of Glycogen Granules.....</i>	<i>151</i>
6.2.3 <i>Immunohistochemistry.....</i>	<i>151</i>
6.3 Results.....	153
6.3.1 <i>Morphology of the Sciatic Nerve</i>	<i>153</i>
6.3.2 <i>The stimulus- evoked compound action potential (CAP) in sciatic nerve</i>	<i>154</i>
6.3.3 <i>Glycogen content of the sciatic nerve</i>	<i>155</i>
6.3.4 <i>Effects of glycogen content on the CAP during aglycemia .</i>	<i>157</i>
6.3.5 <i>Effects of aglycemia on glycogen content and relationship to CAP failure.....</i>	<i>161</i>
6.3.6 <i>Effect of inhibiting glycogen phosphorylase on the CAP</i>	<i>163</i>

6.3.7 Ultrastructural identification of glycogen in sciatic nerve	167
6.3.8 Expression of glycogen phosphorylase	171
6.3.9 Role of lactate	173
6.4 Discussion	176
6.4.1 Sciatic Nerve Morphology	176
6.4.2 The Sciatic Nerve Compound Action Potential	177
6.4.3 The Presence and Location of Glycogen in the Sciatic Nerve	178
6.4.4 Nerve Conduction During Aglycemia	180
6.4.5 A Functional Role for Peripheral Nerve Glycogen	180
6.4.6 Glycogen Metabolism Supports only Myelinated Fibres during Aglycemia	181
6.4.7 Glycogen in the PNS vs CNS	183
6.4.8 A Model of Peripheral Nerve Glycogen Metabolism	183
6.4.9 Summary	185

Chapter Seven

Summary

7.1 *Central white matter*187

7.2 *Peripheral Nerves*188

References190

Publications215

Acknowledgements

I wish to acknowledge the following contributions to this work:

Dr. Susan Anderson, Denise Christie and Marie Smith (University of Nottingham) for their work producing electron microscope images in Chapter 3.

Dr. Joel Black (Yale University) for the electron micrographs and immunohistochemistry images in Chapter 6

Garry Clarke (University of Nottingham) for the H&E staining images in Chapter 6.

Dr. Bruce Ransom (University of Washington, Seattle) for the purchase of the potentiostat used for biosensor experiments.

Dr. Paul Smith (University of Nottingham) for guidance and use of his apparatus for oxygen electrode experiments.

Dr. Ian Mellor and Mark Burton (University of Nottingham) for supplying TTX.

I would like to thank my supervisors Dr Angus Brown and Dr Rob Mason for their input and supervision during the past three years.

I wish to further extend my thanks to everyone who has helped in providing me with the education that has brought me to this point.



Finally, I would like to thank my parents for their unwavering support.

Oh, and julia too.

Declaration

I declare that the work contained in this thesis is original research which I have carried out during the registration for this degree under the supervision of Dr. Angus Brown and Dr. Rob Mason at the University of Nottingham with the following exceptions:

- Processing of tissue and acquisition of electron microscope images in Chapter 3 was performed by the AMU at Nottingham University (Dr. Susan Anderson, Denise Christie and Marie Smith).
- Electron microscope and immunohistochemistry images in Chapter 6 were supplied by Dr. Joel Black (Yale University).
- H&E staining of mouse sciatic nerve in Chapter 6 was performed by Garry Clarke.

Richard Debney Evans, November 2011.

Abbreviations

4-CIN	alpha-cyano-4-hydroxycinnamate
aCSF	Artificial cerebrospinal fluid
ANLSH	Astrocyte-neuron lactate shuttle hypothesis
ATP	Adenosine triphosphate
CAP	Compound action potential
CNS	Central nervous system
DAB	1,4-dideoxy-1,4-imino-D-arabinitol
FA	Fluoroacetate
GP	Glycogen phosphorylase
IA	Iodoacetate
LDH	Lactate dehydrogenase
MCT	Monocarboxylate transporter
MON	Mouse optic nerve
MSN	Mouse sciatic nerve
NADH/ NAD ⁺	Nicotinamide adenine dinucleotide
PNS	Peripheral nervous system
ROI	Region of interest
S.D.	Standard deviation
TEA	Tetraethylammonium
TEM	Transmission electron microscope
TTX	Tetrodotoxin

Chapter One

Introduction

I.1 Energy Metabolism in the Nervous System

The mammalian nervous system is responsible for performing a vast number of tasks critical for survival. Performing these functions requires energy which is obtained from food. The focus of this thesis is the energy requirements of the parts of the nervous system that conduct action potentials between cells, namely central white matter and peripheral nerves. This introductory chapter provides a general overview of energy metabolism and the idiosyncrasies of the nervous system.

The energy used to drive biochemical process in cells and keep them alive is obtained from energy stored in the chemical bonds of food molecules. Food molecules that are potential sources of energy come from three main categories: polysaccharides, fats and proteins (See Fig. 1.1). The reactions of energy metabolism ultimately generate ATP (adenosine 5'-triphosphate) which is used to store energy, and as a cellular energy currency to power the myriad reactions that occur inside every cell.

The brain is particularly reliant on the metabolism of glucose to generate the vast majority of its ATP. The traditional view maintains that the brain requires a constant supply of glucose from the blood (Greutter et al., 1992; Chih and Roberts, 2003). This is based on the following evidence: (1) hormonal mechanisms which maintain a stable blood glucose concentration; (2) gluconeogenesis converts non-glucose substrates into glucose; (3) the brain contains glucose sensing neurons; (4) the arterial-venous difference of blood glucose is positive; (5) labelled glucose metabolites are detected by magnetic resonance studies in the brain; (6) during insulin overdose there is no alternative blood-borne energy substrate that supports brain function;..

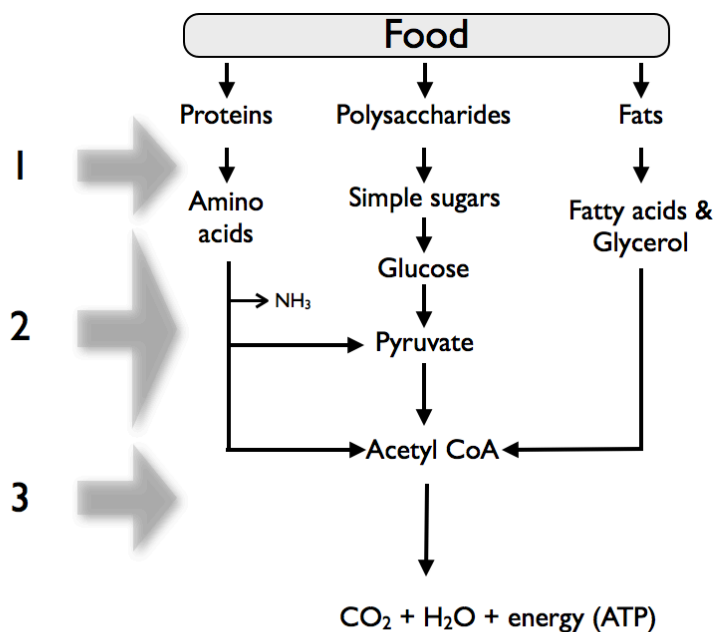


Figure 1.1 Simplified diagram of the routes of energy production from food showing conservation of metabolic pathways. 1. The first stage is the breakdown of macromolecules into their constituent sub-units. 2. Stage 2 occurs mainly in the cytosol and is the breakdown of the simple sub-units to acetyl CoA. This stage yields limited amounts of ATP and NADH. 3. The final stage is the complete oxidation of acetyl CoA to CO_2 and H_2O , which yields large amounts of ATP and NADH in the mitochondrion.

1.1.1 Glucose Metabolism

Glucose is the most biologically important carbohydrate molecule. The glucose molecule is the starting point of cellular energy metabolism and it is the only fuel that can be used by all cells in the body.

1.1.1.1 Glycolysis

The metabolism of glucose begins with the glycolytic pathway. Glycolysis (the Embden-Meyerhof pathway) is the term given to the set of reactions that split

glucose and form two molecules of pyruvate and a small amount of energy. The reactions of glycolysis are shown in Fig. 1.2 below. The first reaction is the phosphorylation of glucose to form glucose-6-phosphate by the enzyme hexokinase. This reaction, which occurs intracellularly, is the rate-limiting step for glucose metabolism in the brain (Whitesell et al., 1995). Phosphorylation traps glucose inside the cell, but consumes one molecule of ATP per glucose molecule. A further molecule of ATP is used in the reaction catalysed by phosphofructokinase. Following this step the 6 carbon molecule is cleaved to produce two 3 carbon molecules which means that for each glucose molecule the steps after this reaction occur two times. From glyceraldehyde-3-phosphate a series of enzymes produce pyruvate, yielding 1 molecule of NADH and 2 of ATP. Pyruvate can then enter the TCA cycle where it is oxidatively metabolised to yield ATP. Alternatively pyruvate can be converted to lactate (see below). Glycolysis produces relatively little ATP in comparison to oxidative metabolism, but does not require molecular oxygen and is therefore how cells that lack mitochondria generate their ATP (e.g. red blood cells).

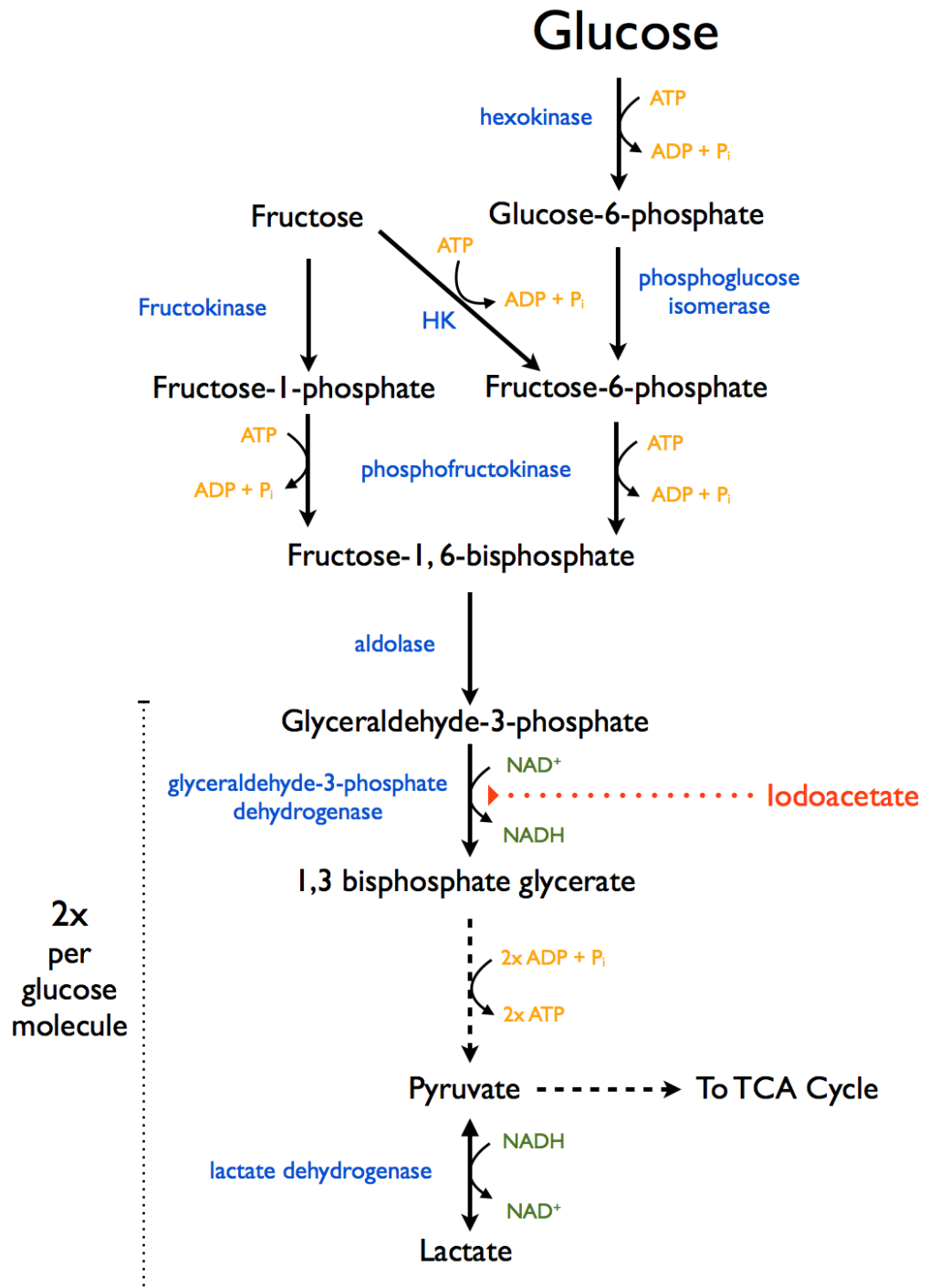


Figure 1.2 An outline of glycolysis. Key enzymes are shown in blue (HK = hexokinase). Iodoacetate, a known glycolytic inhibitor was used in Chapter 4, its site of action is shown. Glycolysis can either proceed to pyruvate, which then enters the TCA cycle, or to produce lactate.

1.1.1.2 Oxidative Metabolism

As the reactions of glycolysis only yield a small amount of ATP, the vast majority of ATP is generated by reactions which occur in the mitochondria and require oxygen (Fernie et al., 2004). Pyruvate generated from the breakdown of glucose in the reactions of glycolysis forms the starting point for oxidative metabolism. Pyruvate is converted into acetyl CoA which is then fed into the series of reactions collectively known as the tricarboxylic acid (TCA) cycle (Fig. 1.3.A). The reactions of the TCA cycle catalyse the reduction of NAD^+ to NADH and FAD to FADH_2 , which then act as electron donors for the electron transport chain. Electrons are donated to a series of enzyme complexes located in the mitochondrial inner membrane (Fig. 1.3.B). Electrons that pass through this system are left in an increasingly lower energy state, and the free energy derived from this process is used to pump hydrogen ions into the space between the mitochondrial membranes. The proton gradient is then used by ATP synthase to produce ATP.

The reactions of the TCA cycle and electron transport chain require molecular oxygen in order to proceed. No oxygen is directly consumed in the TCA cycle but it is required for the recycling of electron accepting molecules e.g. NAD^+ . When oxygen is not available the supply of NAD^+ is exhausted and the reactions of the TCA cycle cannot proceed.

The purpose of the TCA cycle is not restricted to the production of energy, it also plays a crucial role in the biosynthesis of many important molecules in the cell. Non-essential amino acids are among the products which can be made from TCA cycle intermediaries and the synthesis of molecules such as these will depend upon the energy state of the cell as well as demand.

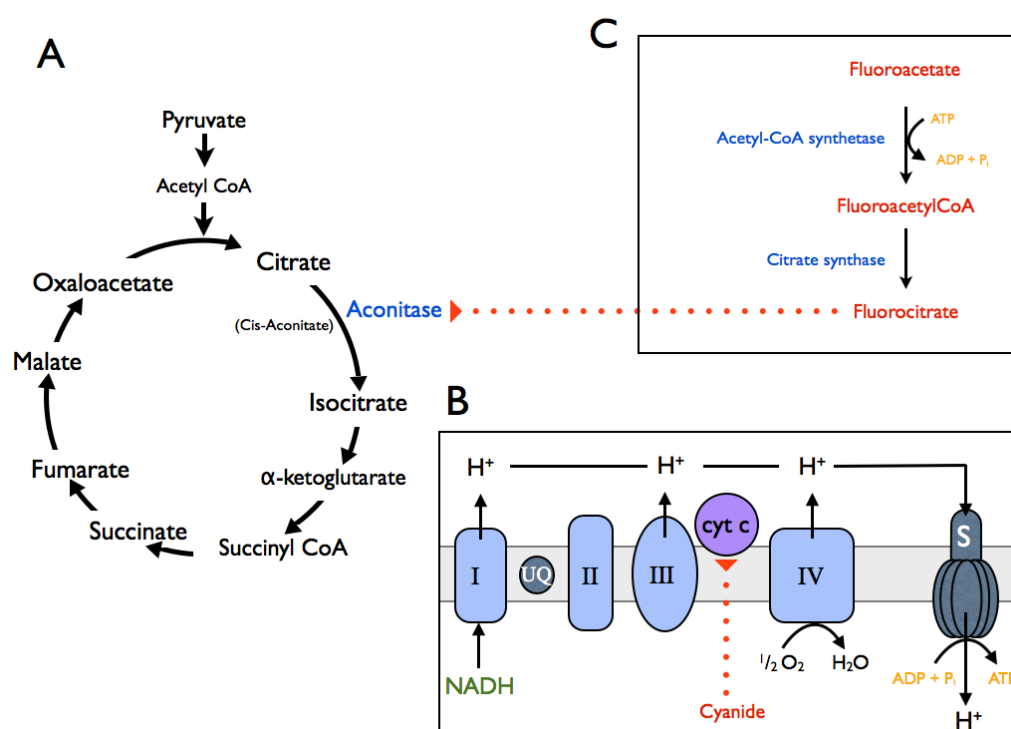


Figure 1.3 An overview of oxidative phosphorylation. **A.** TCA cycle **B.** The electron transport chain. The inner mitochondrial membrane is shown with the chain of electron donors / acceptors (Complex I - IV, ubiquinone (UQ), and cytochrome c (cyt c)). The H⁺ ion gradient created by the passage of electrons along the chain is used to drive ATP Synthase (S) which forms ATP. **C.** Fluoroacetate (FA) is an inhibitor of the TCA cycle. FA is converted to fluorocitrate which inhibits the enzyme aconitase. Key enzymes are shown in blue.

In the brain, as with almost all tissues, oxidative metabolism is the largest contributor to ATP synthesis. Not all glucose consumed by the brain is fully oxidised. The brain uses 31 mmol of glucose per 100g of tissue per minute, a value greater than the 26.6 mmol/100g.min that can be accounted for by the brain's oxygen consumption, which leaves 4.4 mmol/100g.min for other pathways (Magistretti et al., 2000).

1.1.1.3 Lactate

Lactate is an alternate end product of glycolysis which is typically described as only being produced under anaerobic conditions. Lactate is formed from pyruvate by the enzyme lactate dehydrogenase (LDH), a reaction that also results in the production of NAD^+ from NADH. LDH is also capable of catalysing the reverse reaction, i.e. the formation of pyruvate from lactate. The direction with which the reaction proceeds depends upon the relative concentrations of lactate and pyruvate and also the LDH isoenzyme in question. LDH is a tetramer composed of a combination of two subunits: the heart (H) and muscle (M) subunits. A homo-tetramer of the H subunit forms the LDH-1 isoenzyme and LDH composed of four M subunits forms the LDH-5 isoenzyme. For this reason the H subunit has been referred to as the LDH-1 subunit and the M subunit as the LDH-5 subunit (Bittar et al 1996). The LDH-1 isoform is more suited to the oxidation of lactate to form pyruvate. LDH-5 favours the conversion of pyruvate to lactate and is found in tissues that produce lactate (Cahn et al., 1962). The cellular expression pattern of these subunits in the brain is of importance when determining the role in this organ (see below).

Under anaerobic conditions and in red blood cells, which do not possess mitochondria, the formation of lactate is a method of regenerating the NAD^+ , which is required for the continuation of glycolysis. Lactate is then released from the cell as a waste product. This view has led to the presence of lactate in tissue being viewed as potentially harmful and an indication of disrupted energy metabolism. On the contrary, healthy tissue does produce lactate. In muscle and the brain, lactate is produced under aerobic conditions. The term aerobic glycolysis is given to this formation of lactate as the end product of glycolysis in fully oxygenated tissue. Lactate is also no longer viewed as a metabolic dead-end: rather than being a waste product lactate can enter the pathway of oxidative metabolism and yield more ATP. A single lactate molecule, after conversion to pyruvate by lactate dehydrogenase, can enter the

pathway of oxidative phosphorylation to produce 18 molecules of ATP (Magistretti and Pellerin, 1999). Further references to the oxidation of lactate refer to this process. Despite changing attitudes towards the possible metabolic fate of lactate, there still is no exact consensus as to the importance of lactate oxidation. This is particularly relevant to brain energy metabolism and is discussed later in this thesis.

Lactate transport into and out of cells is performed by members of a family of membrane proteins called monocarboxylate transporters (MCTs). The most important members of this family with regards to lactate transport are MCT1-MCT4 as these have been shown to transport lactate and other monocarboxylates such as pyruvate and ketone bodies (Halestrap and Meredith, 2004). Generally, MCT1 and 2 are associated with lactate uptake in the liver, heart, kidney and red skeletal muscle. MCT4 is expressed by cells that exhibit a high rate of glycolysis and is associated with lactate efflux (Juel and Halestrap, 1999). MCT1, 2 and 4 are widely expressed in the brain, with MCT3 restricted to the choroid plexus and pigment cells in the retina (Simpson et al, 2007). Because of the limited expression of MCT3 in the brain a focus will be placed on MCT1, 2 and 4. The association of MCT subtypes with lactate uptake or release is central to the role of lactate in the brain which will be discussed below (1.2.4). Each of the MCTs has a different affinity for lactate and inhibitors (Halestrap and Price, 1999). Table 1.1 summarises some of the characteristics of the three MCTs expressed in the brain.

	Expression	Lactate Km (mM)	Suggested Function	Inhibitors*
MCT1	Blood vessels, astrocytes, neurons	3.5	Ketone body transport (1)	
MCT2	Neurons	0.7	Lactate uptake	4-CIN (2 & 3) pCMBS (3)
MCT4	Astrocytes	35	Lactate release	Quercetin (4)

Table 1.1 A summary of the three main MCTs of importance in the brain. The predominant cell type expressing the transporter is listed along with the Km for lactate transport, the simplified suggested function and some inhibitors of note. * Specific MCT inhibitors are not currently in widespread use. Most inhibitors will affect all three MCTs but those listed are examples which have been used a concentration designed to target the specific subtype. This table summarises the text of Pellerin et al. (2005). Other sources used are: (1) Simpson et al., 2007; (2) Erlichman et al. (2008); (3) Wender et al (2000); (4) McKenna et al. (1998).

The data in Table 1.1 shows that MCT2 has the highest affinity for lactate, MCT1 is intermediate and MCT4 the lowest affinity. The significance of the brain expression is discussed later (1.2.4.1) but it is worth noting that the location of expression listed is the predominant one. Some studies have shown that MCT expression can vary depending upon the conditions, particularly in cell culture (Pellerin et al., 2005). It is thought that MCT1 is particularly important in the transport of ketone bodies during suckling as its expression declines during development (Simpson et al., 2007). The inhibitors listed are those which have been used in attempts to selectively block specific MCTs. Most MCT inhibitors will affect all MCTs but differences in affinity enable a careful choice of concentration to achieve a selective block. For example, 4-CIN at a concentration of 100 μ M has been used to block the neuronal uptake of lactate via MCT2 (Wender et al., 2000; Erlichman et al., 2008).

1.1.1.4 Carbohydrate Storage

Carbohydrates can be stored as polymers of glucose, and glycogen is the primary storage carbohydrate in the mammalian body. Glycogen is a branched polymer of glucose that can readily be stored or broken down depending upon the availability of glucose. Storing glucose in the form of glycogen provides an energy reserve that does not affect the osmotic balance of cells due to the insolubility of glycogen. The main locations of glycogen storage are the liver and skeletal muscles where it accounts for 6-8% and 1-2% of the masses of these tissues, respectively. The function of glycogen in the liver is to act as a buffer for plasma glucose ensuring that the concentration of glucose in the blood remains steady (between 4 and 7.2 mM is considered normal in humans). When blood glucose drops glycogen in the liver is mobilised to buffer the glucose concentration. Glycogen stored in the liver can be replenished when blood glucose is raised due to intake of nutrients after feeding.

The function of glycogen in other tissues is different to that in the liver, glycogen acts as a local energy reserve. The best known and characterised example of glycogen acting as a local energy reserve is skeletal muscle. This is perhaps not surprising due to this tissue having the next highest concentration of glycogen after liver (Hargreaves, 2004).

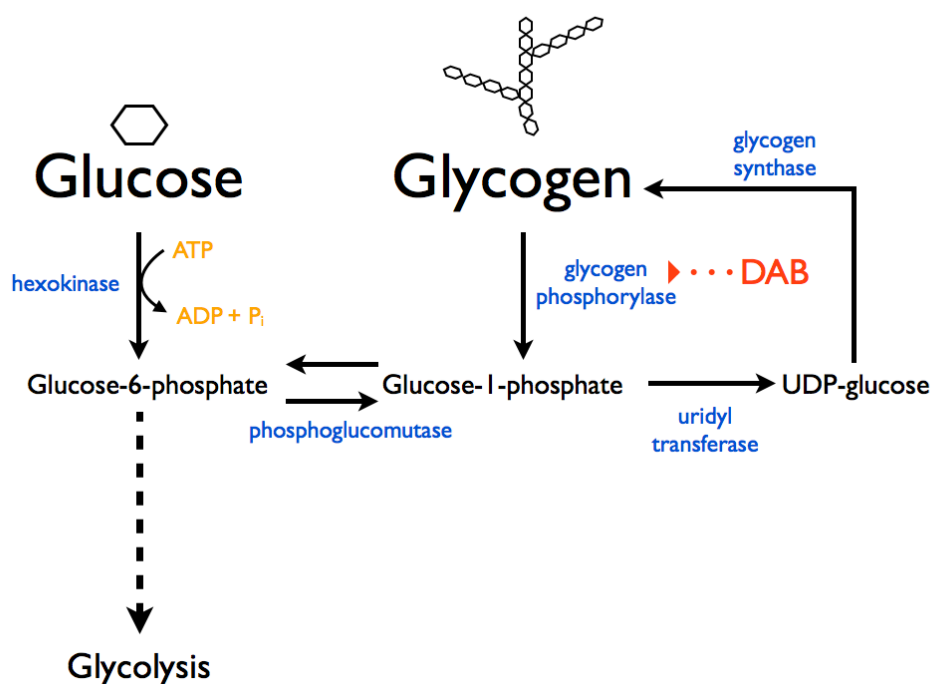


Figure 1.4 An outline of glycogen synthesis and breakdown. Key enzymes are shown in blue. DAB is an inhibitor of glycogen phosphorylase.

The reactions involved in glycogen metabolism are summarised in Fig. 1.4, where glycogen acts as a storage depot for phosphorylated glucose molecules. Glycogen phosphorylase (GP) is the key enzyme involved in glycogenolysis which liberates the glucose stored in the glycogen molecule. GP acts on the linear chains of glucose residues contained within the glycogen molecule, a de-branching enzyme is required to completely digest glycogen. GP is in its active state when it is phosphorylated and this is governed by phosphorylase kinase (Brown, 2004). The transition of GP from its inactive to active form is very rapid which allows glycogen to be quickly mobilised when needed (Schulman and Rothman, 2001). Allosteric interactions with molecules such as glucose and AMP allow the activity of GP to be responsive to the energy state of the cell (Johnson, 1992). It exists in tissue-specific isoenzymes: muscle

(GPMM), liver (GPLL) and brain (GPBB), although expression is not restricted to these specific tissues (Newgard et al., 1989). Glycogen breakdown and therefore access to the stored glucose can be inhibited by compounds that bind to GP, an example of an inhibitor of GP is the compound DAB (Walls et al., 2008).

1.2 Energy Metabolism in the Healthy Brain

1.2.1 Energy Demands of the Brain

The Central Nervous System (CNS) is a very demanding tissue in terms of its requirements of both glucose and oxygen supply. Despite only accounting for 2 % of body mass, the brain consumes 20 % of the oxygen and 25 % of plasma glucose (Raichle and Gusnard, 2002). The first measurements of whole brain blood flow were determined by measuring the cerebral arterial and venous concentrations of nitrous oxide after inhaling a small amount of the gas (Kety and Schmidt, 1948). This technique was used to show that total cerebral blood flow and oxygen consumption remains relatively constant irrespective of the degree of brain activity. Both variables were found to be unaltered by mental exertion in the form of mental arithmetic (Sokoloff et al., 1955). Cerebral oxygen consumption is also unchanged during natural sleep (Mangold et al., 1955). The dependence of the brain on a steady supply of glucose and oxygen from the blood was vividly demonstrated by a study carried out during World War II. Blood supply to the brain was temporarily interrupted in healthy volunteers by applying pressure to the neck with an inflatable device; consciousness in all 141 subjects was lost in 4 to 10 seconds (Rossen et al., 1943).

The energy-dependence of the brain largely arises from the amount of energy required to maintain the ion distribution that is responsible for generating resting membrane potential. The electrochemical ion gradient across the cell membrane underlies many cellular functions such as action potential conduction, neurotransmitter signalling and nutrient transport. These processes cause Na^+ to enter the cell, and for function to continue as normal the Na^+ must be actively pumped back into the extracellular space (i.e. homeostasis must be maintained). The extrusion of Na^+ is performed by the Na^+/K^+ ATPase which has been estimated to consume around 40 - 50 % of the

energy required by the brain (Whittam, 1962; Astrup et al., 1981; Attwell and Laughlin, 2001). The other major functions of the brain which consume the majority of energy are estimated as follows: vegetative metabolism (5 -15 %), Ca^{2+} flux (3 - 7 %), processing of neurotransmitters (10 - 20 %), intracellular signalling (20 - 30 %) and axonal transport (20 - 30%) (Ames, 2000).

The observed lack of a response in total cerebral blood flow during mental activity led early researchers to speculate that neural activity was not accompanied by an increase in energy demand (Sokoloff et al., 1955). However, neural activity involves an increase in the energy-consuming processes described above and does require more energy to support it. It was only when regional blood flow and oxygen consumption were measured that activity-dependent changes were observed. Interestingly, this phenomenon was demonstrated by an unusual clinical case of a patient who had unsuccessful surgery to remove a malformed blood vessel in his visual cortex (Fulton, 1928). The surgery left the patient with an auscultatory bruit that became more prominent after exposure to visual stimuli. The increased prominence of the bruit was due to enhanced regional blood flow to the visual cortex in the occipital lobe. This was long before the same response was demonstrated with the modern neuroimaging techniques of positron emission tomography (PET) (Shulman et al., 1997) and magnetic resonance imaging (MRI) (Kruger et al., 1996).

As well as increases in blood flow and oxygen consumption, regional activity increases glucose utilisation which can be measured by PET (Wienhard et al., 1985). Surprisingly, the increases in glycolysis and oxidative phosphorylation are not of the same magnitude (Fox et al., 1988; Frahm et al., 1996). The increase in oxygen consumption is not as great as that for glucose. The mismatch between increases in glycolysis versus oxidative metabolism are thought to be responsible for the increase in lactate observed during and after neural activation and will be further discussed in Chapters 4 and 5.

1.2.2 The Blood-Brain Barrier (BBB)

The blood-brain barrier is an anatomical and physiological barrier that separates the brain from circulating blood. The BBB is formed by capillary endothelial cells which are in close contact with astrocytes (Hawkins and Davis, 2005). Molecules in the blood that have free access to other tissues are often not able to cross into the brain. Substances that can cross into the brain from the blood are limited to those that can diffuse across the BBB or those that are substrates for transporters expressed in the BBB. Energy metabolism in the brain is dependent upon the BBB due to this selective permeability. Sugars are transported across the BBB to enter the brain, although this process is not usually rate-limiting for cerebral energy metabolism (Buschiazzo et al., 1970). Glucose is transported by a family of membrane-bound transporters known as GLUTs which exist in a number of isoforms (Barros et al., 2007). The importance of glucose transport into the brain is demonstrated by a clinical condition in which a deficit in the GLUT1 transporter in the BBB of infants leads to low glucose concentrations in CSF, seizures and impaired development (De Vivo et al., 1991). The deficiency in glucose transport results in the brain being more dependent on ketone bodies as a fuel.

The structure of the BBB has been found to be disrupted in a variety of neurological disorders (Hawkins et al., 2005). Post-concussion syndrome (Korn et al., 2005), epilepsy (van Vliet et al., 2007), depression (Niklasson and Agren, 1984) and stroke (Sandoval and Witt, 2008) are all conditions where an increase in the permeability of the BBB has been observed. Disruption of the BBB has also been suggested as the cause of seizures in some patients that receive Interferon-alpha therapy (Pavlovsky et al., 2005). Increased permeability of the BBB alters the composition of the extracellular fluid within in the brain, affecting the osmolarity, resulting in increased excitability and seizures (van Vliet et al., 2007). The opening of the blood brain barrier also affects energy metabolism by removing fine control of the substrate

availability in the brain and allowing in toxins such as bilirubin that impair mitochondrial function (Wennberg et al., 1991; Hansen, 2001).

1.2.3 Glial Support of Neurons

Glia is the collective name given to non-neuronal cell types within the nervous system (Hartline, 2011). For many years after glia had been identified they were somewhat neglected despite there being an equal number of glia and neurons in the human brain (Azevedo et al., 2009). The term glia arose because these cells were regarded as simply the “glue” of the nervous system. Although, not all early research dismissed functional roles for glia. Ramon y Cajal postulated that they may have a role in executive brain function (Garcia-Martin et al., 2007). However, it was as techniques improved and more research was conducted into glial cells that their importance truly emerged. When the modern understanding of glial biology was in its infancy it was recognised that these cells play vital roles in brain function (Ransom and Sontheimer, 1992). The way glial cells are now viewed ascribes them prominent and active roles in the brain and the way it works. The functional abilities of the human brain are now, to an extent, thought to depend upon the functional and anatomical complexity of astrocytes in comparison to the equivalent cells in rodents (Oberheim et al., 2009).

There are two main categories of glia: microglia and macroglia. Microglia are frequently referred to as the immune system cells of the CNS, but this view may be too simplistic (Graeber and Streit, 2010). Types of macroglia include: the aforementioned astrocytes as well as oligodendrocytes, radial glia and ependymal cells. These are all found in the CNS. The PNS macroglia population consists of: Schwann cells, satellite cells and enteric glial cells. The roles of glial cells are diverse but a brief overview of some examples is provided below.

The idea that glia were passive constituents of the nervous system could be not be maintained after the discovery of gliotransmission. Glial cells are capable of releasing chemicals such as glutamate, ATP and D-serine which are able to modulate neurons and other glial cells (Angulo et al., 2004; Newman, 2003; Mustafa et al., 2004). Astrocytes are the cell type most associated with gliotransmission. They can be considered as a component of the “tripartite synapse”, along with the neuronal pre- and post-synaptic terminals (Araque et al., 1999). In this model the astrocyte can provide signals to the neurons and receive them too, allowing fine control of excitability. This type of communication between neurons and glia is important in a diverse array of physiological processes including nociception (Foley et al., 2011), regulation of breathing (Housley, 2011) and memory (Henneberger et al., 2010).

Important functions performed by glia are not restricted to the astrocytes. Glial cells produce myelin which wraps around axons and acts as an electrical insulator speeding up action potential velocity. In the CNS oligodendrocytes are responsible for myelinating axons and a similar role is performed by Schwann cells in peripheral nerves. The presence of myelin is critical for normal nervous system function. When myelin is disrupted or defective, such as is seen in multiple sclerosis, neurological function is impaired due to disrupted axonal signalling (Steinman, 1996). While myelin is important to the axons it ensheaths not all axons are myelinated. Peripheral nerves and CNS white matter contain un-myelinated axons (Murrinson and Griffin, 2004; Ziskin et al., 2007). When space is at a premium, small un-myelinated axons offer an advantage with their compact size (Wyatt et al., 2005). Large myelinated axons appear to be necessary for neurons that form vast numbers of synaptic connections (Harris and Atwell, 2012).

Further to providing insulation for axons in the form of myelin it has been suggested that oligodendrocytes may provide trophic support to the axons that they ensheath (Nave, 2010). This intercellular support is a two-way relationship. For example, neurons release growth factors that promote

oligodendrocyte survival (Fernandez et al., 2000). The provision of energy substrate from glia to neurons has been explored in great detail with regards to astrocytes. Astrocytic glycogen and lactate are thought to be important substrates for neurons, although, the extent of this is hotly debated (see below, 1.2.4-5). The role of glial cells in nervous system energy metabolism is discussed throughout this thesis. Discoveries concerning glial biology have revealed a previously unknown level of complexity for cellular interactions in the brain.

1.2.4 Lactate in the Brain

The ability of the brain to use lactate as an energy substrate has been shown *in vitro* where it supports synaptic activity (Schurr et al., 1989) and axonal conduction (Brown et al., 2001). There is also evidence of lactate utilisation *in vivo*, Plasma lactate may be a major fuel for the brain of newborn mammals (Hellmann et al., 1982). Transport of lactate into the brain declines during development into adulthood (Cremer et al., 1976), but the adult human brain still retains some capacity for lactate uptake from blood (Rivers et al., 1991). At rest there is a net lactate release from the brain, but during exercise when blood lactate rises the brain takes up blood-borne lactate and uses it as a fuel (Quistorff et al., 2008; van Hall et al., 2009). Lactate is capable of supplementing glucose as a fuel during hypoglycemia, lowering the glucose concentration at which deterioration in brain function is seen (Maran et al., 1994). Despite some lactate uptake and metabolism, the limited permeability of the BBB for lactate is the main reason why lactate is not capable of fully substituting for plasma glucose (Lubow et al., 2006).

Lactate is also produced locally within the brain (Hu and Wilson, 1997; Leegsma-Vogt et al., 2003) and is present in the brain, typically at a concentration of around 1.5 mM (Medina et al., 1975). Lactate production increases with neural activity (During et al., 1994). The fate of lactate produced

within the brain has been at the centre of an intense debate. There is evidence that lactate is oxidised away from its site of production to yield more ATP (Wyss et al., 2011).

The most contentious of the hypotheses which this field has generated is the astrocyte-neuron lactate shuttle hypothesis (Pellerin and Magistretti, 1994).

1.2.4.1 Astrocyte-Neuron Lactate Shuttle Hypothesis (ANLSH)

The astrocyte-neuron lactate shuttle hypothesis (ANLSH) has been responsible for igniting one of the most ferocious debates in neuroscience of recent years. In 1994 Pellerin and Magistretti proposed that astrocytes were responsible for glucose uptake from the blood and that this glucose underwent glycolysis in the astrocytes resulting in the formation of lactate (Pellerin and Magistretti, 1994). They went on to propose that this lactate was then released into the extracellular space where it was then transported into neurons and used as a fuel for oxidative metabolism. The theory has undergone several modifications since its inception (Magistretti et al., 1999; Pellerin and Magistretti, 2003) but still persists, neither having been fully discredited or fully accepted.

In its current form the model states that glutamate released during synaptic activity triggers astrocytes to release lactate to support the energy requirements of neurons (Bouzier-Sore et al., 2002). Lactate produced by glycolysis in the astrocytes is released into the extracellular space before being taken up, converted into pyruvate and oxidised by neurons. The pathway is shown in Fig. 1.5. It is now well established that lactate can support neuronal activity (e.g. Brown et al., 2001). Henry McIlwain observed this in brain slices in the 1950s (McIlwain, 1953). However, the relative contribution that this pathway provides to normal neuronal energy metabolism is central to the ANLSH debate.

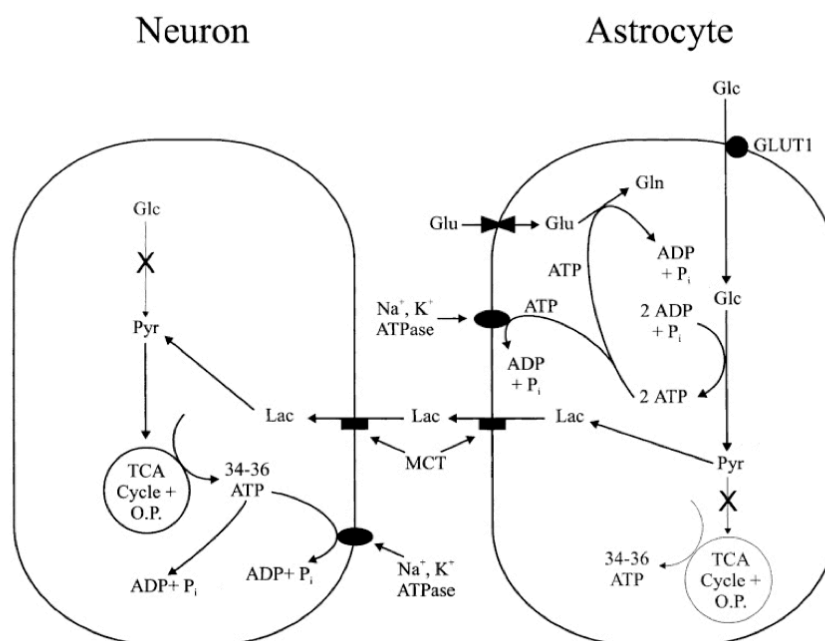


Figure 1.3 Diagram of the astrocyte-neuron lactate shuttle hypothesis. Astrocytes take up glucose (Glc) which then passes through the glycolytic pathway via pyruvate (Pyr) to produce lactate (Lac). The ATP produced is used to fuel the uptake of glutamate (Glu) and its conversion to glutamine (Gln). Lactate is released from the astrocyte into the extracellular space where it is taken up by the neuron by monocarboxylate transporters (MCT). Lactate in the neuron is converted to pyruvate which yields energy via oxidative phosphorylation. This pathway can co-exist with neuronal glucose uptake and metabolism. Figure adapted from Chih and Roberts (2003).

The ANLSH is supported by evidence drawn from a number of experiments and observations which complement the initial discovery of astrocytic lactate release. Neurons express the LDH-1 subunit which favours the conversion of lactate to pyruvate. This suggests neurons are primed for the oxidation of lactate. Astrocytes also contain the LDH-1 subunit but express the LDH-5 subunit which favours the formation of lactate from pyruvate (Bittar et al, 1996). The LDH-5 subunit is associated with glycolytic, lactate-producing cells which is the role given to astrocytes in the ANLSH model.

The distribution of MCTs also has been used to support the theory that astrocytes predominantly release lactate into the extracellular space and neurons are responsible for its uptake (Pellerin and Magistretti, 2003). Neurons express high levels of MCT2 (Debernardi et al., 2003), whereas, astrocytes express MCT 1 and MCT4 (Rafiki et al., 2003). As neurons express the MCT (MCT2) with the greatest affinity for lactate it has been suggested neurons are less suited to lactate release and will retain and oxidise lactate. Meanwhile, MCT4 expressed by astrocytes is able to rapidly release lactate when the intracellular concentration rises (Broer et al., 1997). However, whether this supports the model of lactate flow from astrocytes to neurons is not universally accepted (Hertz and Dienel, 2005). Evidence that does appear to support the idea of a lactate shuttle comes from the results of experiments which have used MCT inhibitors to block lactate transport. This approach has revealed that, in both rodent optic nerve and hippocampal slices, lactate trafficking is important for neuronal survival when the supply of energy substrate is restricted (Tekkok et al., 2005; Cater et al., 2001). Knockdown of MCTs by antisense nucleotides disrupts long-term memory formation, indicating that lactate transport has a role in this physiological function (Suzuki et al., 2011).

A further criticism of evidence used to support the ANLSH is that the majority of it comes from *in vitro* experiments such as cell culture systems that are far departed from the situation *in vivo* (Chih and Roberts, 2003). However, the use of labelled lactate and glucose has shown that even *in vivo* lactate is oxidised in an activity-dependent manner (Wyss et al., 2011). Wyss et al. concluded that the brain preferentially utilises lactate over glucose as an energy substrate when they are both available. Measurement of brain glucose and lactate uptake and release during exercise in human subjects has also revealed an activity-dependent increase in lactate consumption by the brain (Rasmussen et al., 2011).

The role of lactate in the brain is not fully established and forms the focus of Chapters 4 and 5 where it is discussed in further detail.

1.2.5 Brain Glycogen

As discussed above (1.1.1.3) glycogen is a storage carbohydrate that can be used as an alternative supply of glucose molecules. The brain contains glycogen at a concentration that is relatively low in comparison to that seen in liver and skeletal muscle. Glycogen contributes about 0.1 % of total brain weight, whereas, in muscle it accounts for 1 - 2 % of tissue mass (Brown, 2004). The low concentration of glycogen in the brain led to it largely being overlooked in terms of playing an important role in energy metabolism in this organ. In recent years brain glycogen has emerged as a topic which has received substantial interest (Brown, 2004). A variety of experiments have shown that nervous tissue contains glycogen and this glycogen content can be metabolised to provide energy substrates under both pathological and physiological conditions.

Glycogen in the brain is almost exclusively located in astrocytes (Brown and Ransom, 2007). Astrocytes also express the enzyme GPBB, necessary for glycogenolysis (Pfeiffer et al., 1990). Cultured astrocytes have been extensively used as a model to investigate factors affecting brain glycogen. Astrocytes are able to take up a number of substrates and synthesise glycogen (Dringen et al., 1993) and this process is sensitive to modulation by insulin (Kum et al., 1992). Glycogenolysis is stimulated by the action of some neurotransmitters. Vasoactive intestinal peptide (VIP) and noradrenaline both act on cultured astrocytes to induce glycogenolysis (Magistretti et al., 1993; Pellerin et al., 1997). Noradrenaline-induced glycogenolysis has also been observed in isolated rat pineal glands (Eugenin et al., 1997). Furthermore, the toxic effects of ammonia in the brain may be mediated by its inhibition of glycogenolysis (Dombro et al., 1993) These experiments demonstrate that astrocytic glycogen is labile and under the dynamic control of neurotransmitters.

Glycogen has been shown to be utilised as an energy substrate in the rodent optic nerve to support high frequency firing or conduction under aglycemic conditions (Wender et al., 2000; Brown et al., 2003). Glycogen is known to play an important role in the developing brain (Rust, 1994), for example, preventing glycogen breakdown interferes with memory consolidation in young chicks (Gibbs et al., 2006; Hutchinson et al., 2008). This process is mediated by beta2-adrenoceptors (Gibbs et al., 2008), which corroborates the observations from astrocyte cultures. In the adult brain transport of glycogen-derived lactate has been shown to be necessary for the maintenance of long-term potentiation, a process suggested to be linked to memory formation (Suzuki et al., 2011). Evidence continues to emerge that adds more weight to the argument that brain glycogen plays important physiological roles.

1.2.6 Functional Neuroimaging

An understanding of energy metabolism in the brain is vital in order to fully appreciate and understand the results of functional imaging studies. Non-invasive functional imaging has become one of the most widely used techniques in neuroscience and psychology (Raichle, 2003). The widespread use of functional neuroimaging has been, in part, responsible for much of the interest in brain energy metabolism. The local changes in glucose and oxygen consumption which occur in response to brain activity form the principal behind functional neuroimaging (Magistretti and Pellerin, 1999). The debate surrounding brain lactate has been fuelled by experiments that have sought to understand the energetics behind neuroimaging signals. Although functional imaging does not form the focus of the work described in the following chapters, it is important to consider that any enhancement in our knowledge of brain energy metabolism holds the possibility of helping further understand the basis of neuroimaging.

1.3 Energy Metabolism and Pathology

Increasing knowledge of energy metabolism in the nervous system holds the possibility of better understanding and ultimately treating diseases. Alterations in nervous system energy metabolism have been associated with a vast array of pathologies (Blass et al., 1988; Sas et al., 2007). Some conditions appear to be triggered by disruptions in energy metabolism, whereas, others the changes in energy metabolism are secondary to the disease. Disruptions in energy metabolism are most obvious in cerebral hypoxia, traumatic brain injury and stroke (Zauner et al., 2002). In these conditions the supply of oxygen, in the case of hypoxia, and both oxygen and glucose for trauma and stroke, is interrupted. This leads to impaired energy metabolism and pathological damage in brain tissue. An example of a secondary disruption in brain energy metabolism is seen in diabetic patients who can be unaware of their hypoglycemia (Boyle et al., 1995). During a hypoglycemic episode brain glucose falls and this can lead to seizures and coma (Bingham et al., 2005).

Evidence is emerging that metabolic dysfunctions may form part of the aetiology and pathophysiology of psychiatric syndromes, including major depression, obsessive-compulsive disorder, bipolar disorder and schizophrenia (Saxena et al., 2001; Martins-de-Souza et al., 2011). Schizophrenia is a condition of which the precise causes still remain an enigma, but mitochondrial dysfunction is frequently observed in affected brain areas (Bubber et al., 2011; Clay et al., 2011). Glycogen metabolism in astrocytes has also been identified as potentially disrupted in schizophrenia (Lavoie et al., 2011). A direct effect on energy metabolism may underlie the therapeutic effects of anti-psychotics (Ma et al., 2009) and anti-depressants (Moretti et al., 2003), but some of the major side-effects of these drugs, such as weight gain, are also caused by their effects on metabolic pathways (Baig et al., 2010). A similar body of evidence emphasising the importance of energy metabolism in neurodegenerative diseases, such as Alzheimer's, has appeared (Allaman, 2011). As perturbations in energy metabolism may underlie

numerous disease states, clear and accurate understanding of energy metabolism in the brain is needed in order to develop future treatments.

1.3.1 Hypo/aglycemia

Blood glucose concentration is tightly regulated by hormonal homeostatic mechanisms. The normal range for humans is between 4 - 7.2 mM. The critical nature of normoglycemia (i.e. normal blood glucose) means that hypoglycemia is seldom seen outside of patients who are treated with drugs that lower plasma glucose. Hypoglycemia may be rare, but non-systemic shortages of glucose can occur under other conditions. Interruptions in the supply of blood to tissue cause ischemic injury by depriving cells of glucose and oxygen. Ischemic events are particularly notable in the CNS due to its critical dependence upon blood-borne glucose. Stroke and traumatic brain injury are two notable causes of ischemic brain injury which result in significant levels of disability and mortality for sufferers worldwide.

I.4 Considerations in White Matter

The majority of the brain is composed of either one of two types of tissue, grey or white matter. Grey matter contains neuronal cell bodies and synapses whereas, white matter is mostly made up of myelinated axons. White matter accounts for 50% of the volume of the central nervous system (CNS). The total length of myelinated fibres in a 20 year old male has been calculated as 176,000 km (Marner et al., 2003). In terms of the focus of research into both health and disease, white matter has often played second fiddle to grey matter. The bias towards grey matter is probably understandable if white matter is seen as merely tissue that connects different areas of grey matter. However, dysfunction in white matter is an important factor in a number of pathologies that affect the brain. Injury to white matter causes a large proportion of the functional deficit seen in patients who have suffered an ischemic stroke (Goldberg and Ransom, 2003). White matter anomalies have been documented in cases of chronic schizophrenia (Agartz et al., 2001) and in the brains of children diagnosed with attention deficit hyperactivity disorder (Silk et al., 2009). Changes in white matter also accompany the ageing process and the development of dementia (Malloy et al., 2007). These findings have been achieved by applying neuroimaging techniques to white matter. Therefore, as for grey matter, understanding the bioenergetic basis of imaging signals in this tissue is essential.

It cannot be assumed that white matter energy metabolism is the same as that in grey matter. The differences in structure and function of white matter mean that the tissue has different energetic demands and perhaps different ways of fuelling these. The ANLSH (1.2.2.1) is an example of this. The hypothesis ties lactate production to re-uptake of synaptic glutamate, which is a process that does not occur in white matter as it is devoid of synapses. The processing of neurotransmitters has been estimated to consume 20 - 30 % of the energy usage of the whole brain (Ames, 2000), which will not be the case for white matter. In white matter the energy required for ion fluxes and axonal transport

will be proportionally greater and ion movement is likely to be the most activity-dependent consumer of energy.

1.5 Energy Metabolism in Peripheral Nerves

The importance of energy metabolism is not restricted to the axons of the CNS. The peripheral nervous system (PNS) is affected by conditions which lead to alterations in its energy metabolism (Low et al., 1997). Due to differences in the structure and physiology of the PNS, the physiological and pathological alterations which affect energy metabolism are not the same as those in the CNS. An immediately visible difference is that the PNS is not surrounded by the blood brain barrier or any structure with a similar role. The glial cell population in the PNS is also composed of different types of cells (Barron et al., 1990). Myelination in the PNS is performed by Schwann cells rather than oligodendrocytes. Each myelinating Schwann cell is associated with one axon, whereas, CNS oligodendrocytes contribute to the myelination of many axons. There are also Schwann cells which surround un-myelinated axons in peripheral nerves, forming structures called Remak bundles (Murrinson and Griffin, 2004). Differences between these two areas of the nervous system raise questions as to whether adaptations in energy metabolism vary between the tissues. The role of glycogen in the CNS has received growing attention. However, the same is not true of peripheral nerve glycogen. The role of glycogen in CNS axons has been mostly examined in the adult rodent optic nerve which contains exclusively myelinated axons. Studying the role of glycogen in a peripheral nerve will allow a comparison to be made between myelinated and un-myelinated axons. The aim of Chapter 6 was to begin to explore whether peripheral nerves possess glycogen and if the role of glycogen is analogous to that seen in the CNS.

1.6 Aims and Hypotheses

The central aim of this thesis was to investigate the role of glycogen and lactate in supporting action potential conduction in both central white matter and peripheral nerves. Axonal activity in peripheral and central nerves will be monitored by recording CAPs using the suction electrode technique (Stys et al., 1991). A brief overview of the aims of the work carried out in this thesis is given here. Specific aims and their backgrounds are given in the introduction for each results chapter.

The first group of aims focus on the role of glycogen and lactate in central white matter. This subject has been explored previously using the MON as a model CNS white matter tract (Wender et al., 2000; Brown et al., 2003; Tekkok et al., 2005). The objectives to be set out here build on this prior knowledge by using the same model. From this previous work it is known that glycogen in the mouse optic can support axonal activity during aglycemia. My aim is to compare and contrast the neuroprotective role of glycogen against that of temperature. As moderate hypothermia ($\sim 2^{\circ}\text{C}$) is a clinically utilised neuroprotective strategy (Levi et al., 2009), it is hoped that showing similar benefits from glycogen will highlight its potential.

During aglycemia, glycogen in astrocytes is metabolised to form lactate which is then released into the extracellular space and taken up by axons to sustain their energy demands. Lactate concentration in the MON has not been directly measured. It is an aim of this thesis to measure extracellular lactate in the optic nerve using an enzyme-based biosensor. The lactate dynamics during aglycemia will be investigated together with the effect of up- and down-regulating the availability of glycogen. As neural tissue produces lactate during times of increased activity. I will use the biosensor measurement of lactate to see whether this is true in the MON and begin to explore mechanisms which underlie any changes in lactate production.

Finally, I will examine the role of glycogen in peripheral nerves by using the mouse sciatic nerve (MSN) as a model. I will replicate the original experiments that demonstrated a functional role for glycogen in CNS white matter in the peripheral nerve. It is likely that glycogen will be present in the sciatic nerve as it expresses enzymes necessary for glycogen metabolism (Pfeiffer-Guglielmi et al., 2007). A functional role for glycogen in supporting axonal conduction is also expected as the structure of peripheral nerves can leave them susceptible to metabolic isolation (Low et al., 1997; Nave, 2010). As CNS glycogen is located in astrocytes and these cells are not present in the PNS it will be necessary to determine the location of glycogen. Due to the large extracellular spaces in peripheral nerves and also the size of axons it would not be surprising if glycogen was located in the axons rather than surrounding glia.

Chapter Two

Methods

This chapter provides an overview of all methods used within this thesis. Minor points, which are specific to individual chapters, are detailed prior to the relevant results.

2.1 Animals

All procedures involving animals were carried out in accordance with the Animals (Scientific Procedures) Act 1986.

All animals used in these studies were adult male CD-1 mice (Charles Rivers, UK) weighing between 35-45 g (aged 40 days plus) and were killed by Schedule 1 dislocation of the cervical vertebrae.

2.1.1 *Optic Nerve*

Optic nerves were obtained by making an incision at the rear of the orbit and cutting each optic nerve at the eye. The skull was then opened and the brain reflected to expose the optic chiasm and the optic nerves which were cut free and gently removed. The dissection process took approximately three minutes from sacrifice till the nerves were placed in the tissue bath. Each nerve was approximately 8 mm in length.

2.1.2 *Sciatic Nerve*

After sacrifice, mice were placed prone and the limbs secured to a cork board with dissecting pins. Sciatic nerves were obtained by dissecting the overlying tissue to expose the nerve in the thigh. The nerve was cut proximally near the sciatic notch and distally near the knee, and was then gently freed from surrounding connective tissue and gently removed. This dissection took a maximum of five minutes to fully remove the nerve and place in the tissue bath. The length of sciatic nerve removed was typically between 1.5 - 2 cm.

2.2 Electrophysiology

2.2.1 *Stimulus-Evoked Compound Action Potential*

2.2.1.1 Background of the Compound Action Potential

The primary function of axons in CNS white matter and peripheral nerves is the conduction of action potentials. This process consumes most of the energy required by these tissues (Ames, 2000) and is therefore impacted by disruptions in the supply of energy substrate. Recording the electrophysiological activity of an isolated nerve provides an index of nerve function that can be used to assess the effects of different metabolic conditions on the viability of CNS white matter.

Conduction in isolated nerves can be studied by using a pair of electrodes and stimulating the nerve at one end whilst recording the evoked response distally. Such extracellular recording techniques allow monitoring of all the axons in the nerve. The evoked response is called the compound action potential (CAP). The CAP is the summation of all the individual action potentials in the axons comprising the nerve (Stys et al., 1991). The CAP encodes information about various parameters of the nerve and its individual fibres; information that relates to characteristics such as the number of axons activated by the stimulus and their conduction velocities.

The CAP recorded from peripheral nerves has a distinctive profile when recorded with extracellular electrodes. Fig. 2.1 shows the CAP recording from a rat sural nerve by Potocnik et al. (2006). It shows that the CAP from the sural nerve consists of one main peak with a small peak merging with it (Fig. 2.1.A). A much smaller peak (around a tenth of the amplitude of the first peak) can be seen when the time scale is extended (Fig. 2.1.B). A similar pattern of peaks can be seen in human nerves when CAPs are recorded by electrodes placed on the skin of healthy subjects (Van Veen et al., 1995). Axons of fast conducting,

thick, myelinated nerve fibres with a conduction velocity of greater than 40 ms^{-1} produce the high amplitude first peaks with slower, smaller, unmyelinated fibres generating the later peaks which are of much smaller amplitude (Schoonhoven and Stegeman, 1991).

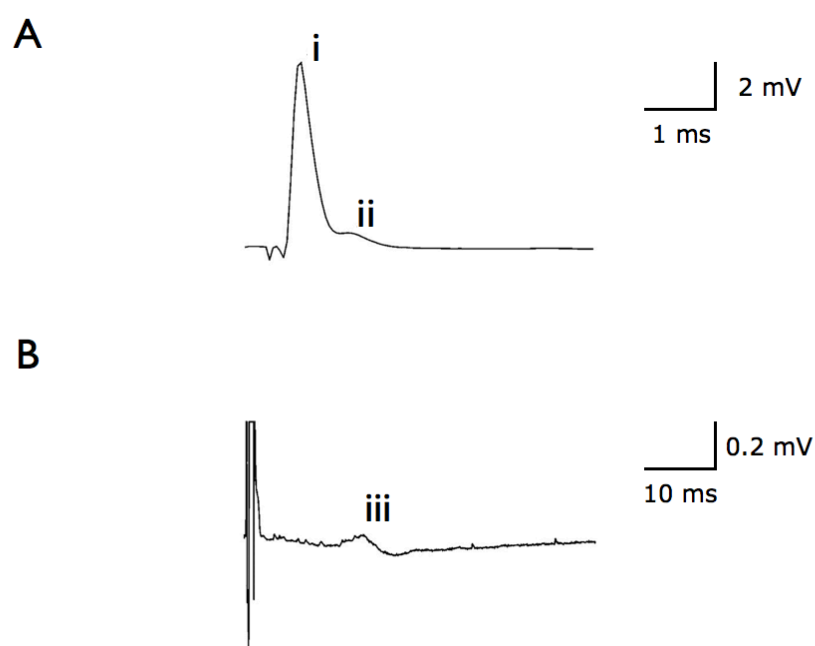


Figure 2.1 Compound action potential (CAP) recorded from the rat sural nerve by Potocnik et al. (2006). CAPs were recorded with hook electrodes applied to isolated nerves in a liquid paraffin bath. **A.** The fast component of the CAP consists of a large positive peak (i) and is generated by myelinated axons, a slight shoulder to this peak can be seen (ii) which is the response of slightly slower sub-population of myelinated axons. **B.** There is a third component (iii) which is the response of unmyelinated axons and is roughly a tenth of the amplitude of the fast response and ten times slower. Figure is adapted from Potocnik et al. (2006).

Some nerves exhibit CAPs which have considerably different profiles compared to that seen in the sural nerve. When recording from the rodent optic nerve the CAP observed is formed by three large positive peaks which overlap, in contrast to the main single peak seen in the example in Fig. 2.1. Fig. 2.2 shows the typical CAP recorded in response to a supramaximal stimulus in the mouse optic nerve. The contrast in the number of peaks seen is due to differences in the diameter and conduction velocities of axons which make up the nerve. The time at which a peak occurs after the stimulus acts as an index of sub-population conduction velocity.

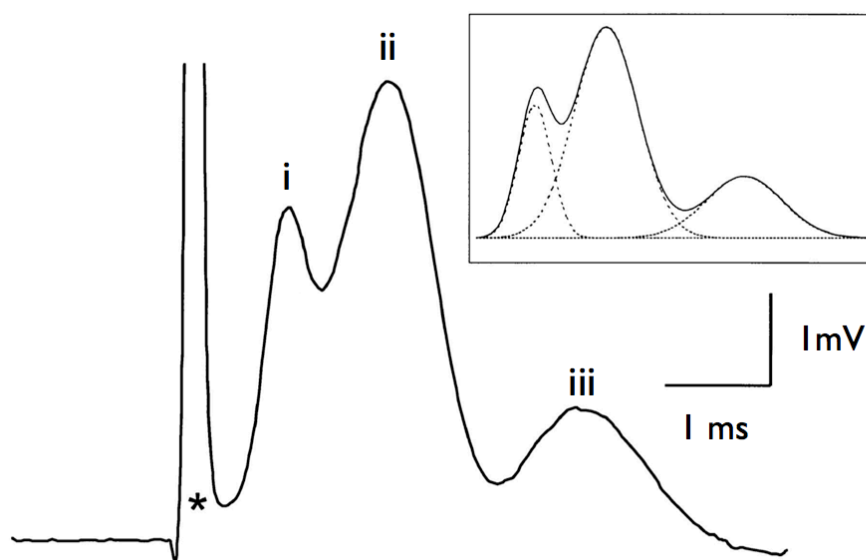


Figure 2.2 The compound action potential recorded from rodent optic nerve. The CAP consists of three positive peaks (i, ii and iii), which are thought to originate from three distinct sub-populations of axon. The peak marked * is the stimulus artefact. The inset shows how the three peaks are each described accurately by a Gaussian function, where the dotted lines are the individual Gaussian best fit functions, and the solid line is the recorded CAP. Figure adapted from Allen et al. (2006) and Brown (2006).

Nerves can vary widely in the number of axons they contain, and in the degree that specific sub-populations of axons contribute to the CAP profile. Anatomical studies have produced histograms to describe in detail the distribution patterns of these individual fibres that make up a nerve (see van Veen et al., 1995 and Allen et al., 2006). The difference in the CAP traces seen between the peripheral nerve and the optic nerve would suggest that there are indeed fundamental differences in the axon populations relating to myelination and conduction velocity. The rodent optic nerve has been studied in great anatomical detail and contains around 24,000 axons in mice (Allen et al., 2006) and around 100,000 in the rat (Lam et al., 1982). The nerve fibres in the adult rodent optic nerve are all myelinated (Foster et al., 1982), whereas, peripheral nerves such as the sural nerve contain un-myelinated fibres (van Veen et al., 1995). It is these differences that result in contrasting CAP profiles. Analysis of the CAP can then be used to make inferences about the axon composition of the nerve, and the effects of experimental paradigms on sub-populations of axons.

2.2.2.2 Analysis of Compound Action Potentials

Interpretation of CAPs requires mathematical and electrical models in order to obtain data suitable for analysis. When CAPs were first used to measure electrical activity in the rat optic nerve using suction electrodes the amplitude of the CAP seen under control conditions was highly variable over time. An electrical model was required which took into account factors such as changes in resistance and stimulus artefacts that contribute to CAP variability. Stys et al. (1991) devised a model which took into account these factors and allowed reproducible recordings to be made. The model was validated experimentally and has formed the basis for other studies using suction electrodes and isolated nerves (e.g. Stys et al., 1992; Brown et al., 2003; Meakin et al., 2007). Modelling is required for detailed CAP analysis since the summation of all the individual action potentials to form a CAP is not straightforward as axons

contribute voltage according to their size. Some of the models commonly used for this purpose are extensively reviewed by Schoonhoven and Stegeman (1991). Whilst detailed analysis of the CAP is possible, the amplitude of the range of CAP peaks, and the conduction velocity measured by the latency of these peaks, provides a simple, but effective, measure of how nerve activity is affected by physiological or pathological interventions.

As described above, several characteristics of the compound action potential can be considered for analysis. These include the stimulus-response latency, the peak amplitude of the response or an area under the curve. When the mouse or rat optic nerve is used, a response with three identifiable peaks is always seen, which raises the question of whether to interpret the response as a whole or to look at the individual peaks. Dong and Hare (2005) elected to use the area under the curve for the complete compound action potential response despite the presence of three peaks. They noted that whilst the compound action potential could change in its timing and amplitude without a change in overall area under the curve, total area under the curve still provided a useful measurement for their purpose of investigating the contribution of Na⁺ to ischemic injury. On the other hand, monitoring changes in the individual peaks has previously allowed conclusions about specific sub-populations of axons in the nerve to be made. For example, it was found that the large axons, which make up the first peak in the mouse optic nerve compound action potential, are not supported by fructose (Allen et al., 2006; Meakin et al., 2007). This information can only be gathered by considering each peak as an individual population of axons (see Fig. 2.2). A method for interpreting CAPs in this manner has been described (Brown, 2006; Evans et al., 2010).

2.2.2.3 Protocol for Recording CAPs

After removal from the animal, nerves were immediately placed in a laminar flow interface perfusion chamber (Harvard Apparatus) supplied with a constant flow (2 ml / min) of artificial cerebrospinal fluid (aCSF) maintained at 37°C and bubbled with a gas mixture of 95% O₂ / 5% CO₂. The aCSF comprised of a solution of (in mM): 126 NaCl, 3 KCl, 2CaCl₂, 2 MgCl₂, 1.2 NaH₂PO₄, 26 NaHCO₃ and 0 - 10 glucose, pH 7.4. When required for aglycemic conditions an aCSF solution omitting 10 mM glucose was used. For other experiments the glucose concentration was adjusted or further compounds added as necessary (see protocol sections in other chapters). Since the manipulation of glucose did not alter osmolarity by more than 5% no osmotic compensations were made. Historic data revealed no difference between results whether osmotic compensation was made or not (Wender et al., 2000).

Axonal conduction was monitored in both optic and sciatic nerves using suction electrodes to record the stimulus-evoked CAP in a manner similar to that described by Stys et al. (1991). A diagram of the setup is shown in Fig. 2.3.

Suction electrodes back-filled with the appropriate aCSF were used for stimulation and recording. One electrode was attached to the rostral end of the nerve for stimulation and the second suction electrode was attached to the caudal end of the nerve to record the CAP, thus all recordings were orthodromic. A WPI Isostim A320 constant current stimulator (WPI, Stevenage, UK) was used to generate a stimulus of 30 μs duration and the strength adjusted to evoke the maximum CAP possible and then increased another 25% (i.e. supramaximal stimulation, Stys et al. 1991). During an experiment, the supramaximal CAP was elicited every 30 seconds. The signal was amplified 10x by an Axoprobe 1A amplifier, then amplified a further 100x by an SRS560 Preamplifier (Stanford Research Systems, Inc., Sunnyvale, CA, USA), filtered at 10 kHz and acquired at 20 kHz (Digidata 1320A with

Clampex 9.2, Molecular Devices, Wokingham, UK). Optic nerve axon function was monitored quantitatively as the area under the supramaximal CAP. The area under the CAP represents the best measure of the number of active axons because currents generated by individual axons within a fibre tract are considered to sum linearly (Cummins et al. 1979; Stys et al. 1991). The curve fitting routine for detecting the latency to CAP failure has previously been described (Wender et al. 2000) and involves measuring where the CAP falls to 95 % of its baseline area. For the sciatic nerve CAP area was not used, but rather CAP amplitude, see Chapter 6 for details. All CAP areas or amplitudes were normalised to control conditions unless indicated.

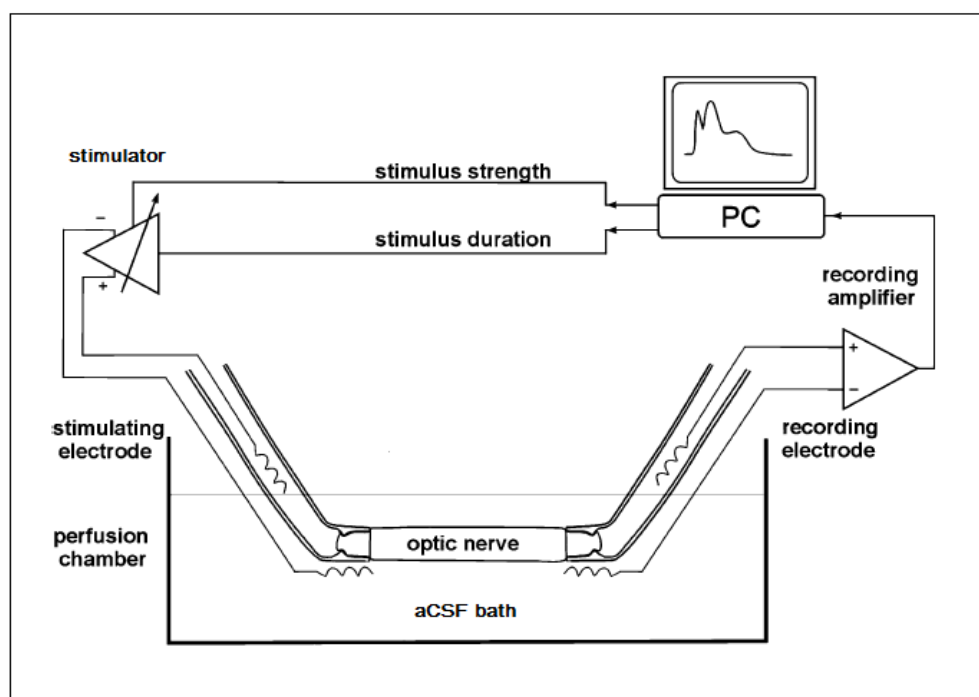


Figure 2.3 Illustration of the experimental setup used to record compound action potentials from rodent optic nerves. Figure adapted from Dong and Hare (2005) and represents an updated diagram of the setup used by Stys et al. (1991).

2.3 Lactate Biosensor Measurements

2.3.1 Principles of Biosensor Measurement of Lactate

The measurement of specific compounds within the brain and how their concentrations are affected by physiological variables is an important tool in neuroscience. In the field of nervous system energy metabolism, measurement of brain lactate concentration can provide evidence as to the role of lactate in brain physiology. Monitoring of lactate has often been performed by using microdialysis, but this technique has its limitations (See Chapter 4 for discussion). In the experiments described here an enzyme-based biosensor was used to measure lactate in nervous tissue. The principles that underlie biosensor measurement of chemicals combine a biological component and a physical component. In the case of the lactate biosensor utilised here, the biological component is the interaction of lactate with the enzyme lactate oxidase which is immobilised in the tip of the sensor. Lactate oxidase catalyses the formation of pyruvate from lactate and oxygen, forming hydrogen peroxide (H_2O_2) in the process. The physical component of the sensor is the amperometric detection of hydrogen peroxide by a polarised platinum electrode. The current produced, by the oxidation of H_2O_2 is proportional to the concentration of lactate present at the sensor tip. Biosensors are designed such that a selectively permeable layer surrounds the enzyme layer and electrode, which allows for recording specific signals from the analyte of choice.

2.3.2 Biosensor protocol in the MON

Lactate in the vicinity of the MON was quantified amperometrically by using an enzyme-based lactate biosensor. Biosensor experiments were performed simultaneously alongside CAP recordings in the perfusion chamber set up described above. Commercially available lactate biosensors (2 mm length, 50

μm diameter) were purchased from Sarissa Biomedical (Coventry, UK). Prior to experimental use a sensor was rehydrated in a buffer composed of: 10 mM NaPi, 100 mM NaCl, 1 mM MgCl_2 and 2 mM glycerol, the pH was adjusted to 7.4. After rehydration experiments were carried out in aCSF (see above) with the addition of 2 mM glycerol.

At the start of an experiment a rehydrated sensor was mounted on a micro-manipulator and gently lowered into the perfusion chamber so that the sensing tip was fully submerged in aCSF. The sensor was connected to a potentiostat (Micro C, WPI, Sarasota, FA, USA) and polarised to + 500 mV relative to the Ag/AgCl reference electrode located in the bath. The potentiostat output was digitised and acquired at 1 Hz (Digidata 1320A with Clampex 9.2, Molecular Devices, Wokingham, UK)

Before commencing measurements from tissue the sensor was cycled and calibrated. Cycling was achieved by using an external signal generator to apply a current to the sensor. This process helps to sustain the useful life of the sensor. When the current from the sensor was stable calibration was performed by pipetting a 1 mM solution of lactate onto the sensor *in situ*, this process was repeated at the end of the experiment to determine if sensitivity was lost during the experiment. Following calibration, the sensor was slowly positioned against the nerve and the output was again allowed to stabilise for 30 minutes. The sensor was positioned relative to the nerve so that the maximum area of the sensing tip came into contact with the outside of the nerve (Fig. 2.4). Time for further equilibration was needed because after initial positioning of the sensor in contact with the nerve the lactate signal increased before returning to a stable value. The cause of this raised signal is most likely due to mechanical disruption of the tissue causing lactate release.

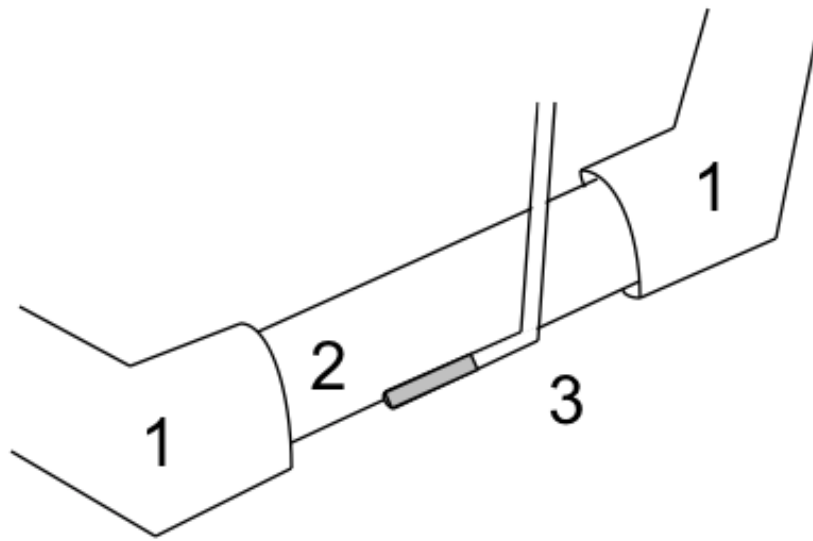


Figure 2.4 Schematic of the arrangement of nerve, biosensor and suction electrodes within the tissue bath. **1.** Suction electrodes. **2.** Optic or sciatic nerve. **3.** Lactate biosensor; the biosensor tip was flexed to fit alongside the nerve, the shaded area represents the sensing tip.

2.4 Glycogen assay

A biochemical assay was used to quantify nerve glycogen content. The assay was based on that described by Brown et al. (2003) with nerve glycogen content being expressed as pmol glycogen ($\mu\text{g protein}$)⁻¹.

Nerves were obtained as described above (2.1) and at completion of the relevant experimental paradigm the nerves were placed in a ice-cold solution of 85% ethanol / 15% 30 mM HCl – this solution prevents glycogen metabolism occurring. Nerves were stored in solution at -30°C until required for assay. A total of 5 pairs of optic nerves or 2 pairs of sciatic nerves, a total net weight of 10 mg, were pooled for each data point.

On the day of the assay tissue was washed in 30 mM HCl and then transferred to ice-cold 0.1 M NaOH/0.01% SDS. The tissue was sonicated and re-acidified with 1M HCl. At this point the homogenate was divided into two equal volumes, one used to determine glycogen content the other for protein quantification. The protein assay was performed following the instructions supplied with the BCA protein assay (BioRad), in which a BSA standard was used and the samples read at a wavelength of 740 nm on a spectrophotometer.

Glycogen content was determined by first further dividing the homogenate and treating one sample with amylo- α -1,4- α -1,6-glucosidase (0.08 units per sample) (AG: EC 3.2.1.3) to digest glycogen to glucose. This step was performed at 37°C with gentle agitation. Leaving one sample untreated with AG allowed determination of any background glucose in the tissue, which was subtracted from the value obtained in the AG-treated samples. Samples were then added to a reaction mixture containing 260 μM ATP, 50 μM NADP and 2.27 and 6.25 units of the enzymes glucose-6-phosphate dehydrogenase (EC 1.1.1.49) and hexokinase (EC 2.7.1.1), respectively. Addition of glucose to the reaction mixture results in the formation of NADPH from NADP. NADPH can be detected by monitoring absorbance on a spectrophotometer at 340 nm.

The concentration of glucose was estimated by comparison with a standard curve of increasing glucose concentrations (0 - 200 μM). The glucose concentration was then factored for the dilutions which occurred during the assay and divided by the homogenate protein concentration to establish the final glycogen concentration.

2.5 Microscopy

2.5.1 Transmission Electron Microscopy

Following electrophysiological recordings, optic or sciatic nerves were removed from chambers and fixed with 4% glutaraldehyde in 140 mM Sorensen's phosphate buffer, post-fixed with OsO₄, and embedded in plastic resin according to standard procedures. Semi-thin (0.5 μm) and ultra-thin (70 - 90 nm) cross-sections of sciatic nerves were cut. Ultra-thin sections were stained with uranyl acetate and lead citrate and examined with a JEM-1011 electron microscope (JEOL USA, Peabody, MA) operating at 80 kV. Images were acquired at 10,000x magnification with an AMT-TR-111 digital camera (Advanced Microscopy Techniques, Danvers, MA).

2.6 Statistical Analysis

Data presented as the mean ± the standard deviation. Paired Student *t*-tests were used to determine significance between control and treated CAPs (Microsoft Excel for Mac). Differences between control and multiple conditions were calculated using one way ANOVA with the appropriate *post-hoc* test (Graphpad Prism for Mac).

Chapter Three

Neuroprotective effect of hypothermia and glycogen in the mouse optic nerve

3.1 Introduction

The human brain is reliant on the blood-borne delivery of glucose and oxygen at levels in excess of demand in order to function normally. Blood-glucose concentration can fall and be incapable of meeting the energy requirements of the brain in patients receiving intensive insulin treatment for Type-1 diabetes. This is due to management of blood-glucose concentration; patients inject insulin to prevent hyperglycaemia which carries the risk of accidental hypoglycemia (Frier and Fisher, 2007). Insulin-induced hypoglycemia leads to a rapid deterioration of brain function, evidenced by the appearance of symptoms such as confusion, anxiety and lethargy (Hepburn et al, 1991). Historically research has focused on the effects of hypoglycaemia in CNS grey matter due to its close association with the cognitive processes that appear to be first affected by the drop in glucose availability. However, evidence has emerged to suggest that white matter is also vulnerable to hypoglycaemic injury and should not be over-looked (Mori et al, 2006).

3.1.1 Aglycemic Injury in White Matter

Studying white matter in isolation is possible with the acutely isolated rodent optic nerve preparation. The optic nerve is ideal as a white matter model as it lacks the constituents of grey matter: neuronal cell bodies and glutamatergic synapses. The rodent optic nerve can be maintained *in vitro* for many hours with physiological variables controlled as determined by the experiment. Nerve conduction during this time can be monitored by recording stimulus-evoked compound action potentials (CAPs). Using these methods the mechanisms behind aglycemic injury in rodent optic nerve have been identified as (1) toxic Ca^{2+} influx via L-type Ca^{2+} channels, and (2) reverse operation of the Na^{+} - Ca^{2+} exchanger (Brown et al, 2001). The mechanisms of aglycemic injury can be delayed; temperature can influence the injury process as can endogenous stores of energy in the form of glycogen.

3.1.2 The Effect of Temperature on Nerve Conduction and Injury

Temperature is one of the most important physiological variables, as it influences all cellular processes, and exposure to a temperature outside optimal range can result in cell or organism death. The effect of temperature on individual action potentials was investigated as part of the pioneering work on conduction in the squid giant axon (Hodgkin and Katz, 1949). Variations in temperature altered the profile of action potentials, with the falling phase most sensitive. The effect of temperature on mammalian nervous tissue has also been examined: peripheral nerves (Kiernan et al., 2001) and brain EEG activity (Kochs, 1995) are both temperature sensitive.

Changes in temperature slow down or speed up the ionic mechanisms that underlie aglycemic injury. The effect of temperature on injury in the CNS has been used as a therapeutic strategy, as controlled cooling of the body can help protect against cell death (Levi et al., 2009). Preventing increases in temperature is another rationale behind cooling as transient hyperthermia 24 hours after ischemia greatly increases the neuronal injury that occurs (Baena et al., 1997). Additionally, moderate hypothermia post-ischemia can reduce the extent of brain injury and cell death (Edwards et al., 1998). A key factor behind the beneficial effects of hypothermia during ischemia is likely to be the slowing down of metabolism and reductions in the energy demand and oxygen consumption that have been demonstrated to occur during hypothermia (Michenfelder and Milde, 1991). The rate of ion transport by the Na^+ - Ca^{2+} exchanger and the slowing down of enzyme reactions may also provide an important role in producing the neuroprotective effects of hypothermia (Stys et al., 1992). There is also evidence that Zn^{2+} ion movement which, plays a role in brain injuries, is inhibited by hypothermia and enhanced by hyperthermia (Suh et al., 2006). The relative importance of the effect of temperature on these processes and their relevance to therapeutic hypothermia is likely to be a balance between the contribution they make to

cell death and their temperature sensitivity. It is possible that understanding the contribution of each of these injury processes could allow selective targeting of interventions which will be most effective in ameliorating aglycemic injury.

3.1.3 The Importance of Brain Glycogen

Recent studies in both human and rodent models have highlighted the potential clinical use of brain glycogen as an endogenous therapeutic target (Gruetter, 2003; Seaquist and Gruetter, 2002). The influence of temperature on metabolic rate means that an effect on the utilisation of glycogen stores in white matter is likely. Glycogen is used as an energy reserve when glucose is withdrawn and can delay conduction failure for up to 30 minutes in the rodent optic nerve (Wender et al., 2000; Brown et al, 2003). Glycogen is therefore considered an endogenous neuroprotective agent of clinical relevance. Up-regulation of endogenous glycogen content has been proposed as a potential therapy to stave off hypoglycemic brain injury (Swanson and Choi, 1993; Suh et al., 2005; Suh et al., 2007). However, performing such therapeutic interventions depends upon the successful development of clinical methods of regulating brain glycogen. The track record for many neuroprotective therapies transitioning from the lab to the clinic has frequently been poor, notably in the treatment of stroke (Green and Shuaib, 2006). For this reason caution should be adopted when assessing the clinical possibilities of glycogen regulation.

While interventions targeting glycogen are not yet clinically available to prevent neuronal damage, hypothermia is, and has been shown to reduce neuronal damage during aglycemia in *in vitro* models (Shin et al, 2010). Comparing the neuroprotective ability of glycogen to that afforded by hypothermia may help highlight the potential clinical importance of glycogen. Further to this, the effects of hypothermia combined with the neuroprotective

effect of glycogen on white matter injury during aglycemia have not been previously tested.

3.1.4 Aims

The aim of this study was to evaluate the neuroprotective effects of hypothermia and glycogen in the optic nerve. Whilst the benefit of hypothermia and the dangers of hyperthermia occurring during brain injury are widely accepted, the role of brain glycogen is overlooked. Demonstrating the beneficial effect of metabolically available glycogen in astrocytes upon prevention of aglycemic injury, and comparing this to the effect of temperature will highlight the potential importance of glycogen.

3.2 Methods and Protocol

3.2.1 *Electrophysiology*

Compound action potentials (CAPs) were recorded using suction electrodes from isolated mouse optic nerves, which were obtained as described in Chapter 2.

Parameters of CAP failure during aglycemia expressed in Fig. 3.6 and 3.10 were calculated as described by Wender et al. (2000). A template which used the Solver function in Microsoft Excel (Brown, 2001) was used to fit a Boltzman equation to the CAP area during aglycemia which then determined the time at which CAP area reached 95 % of its pre-aglycemic value. This equation also gave a value for the gradient of the slope of CAP failure which indicates the rate of CAP failure. A lower value indicates a steeper slope and therefore more rapid CAP failure. CAP recovery was measured as the CAP area at 37°C remaining post-aglycemia as a percentage of the initial CAP area at 37°C. This was the case for all temperatures as at the end of each experiment the nerve was returned to 37°C for the recovery phase.

3.2.2 *Control of Temperature*

A temperature controller (Model TC 202A, Harvard Apparatus, UK) allowed control of temperatures above room temperature of the perfusion chamber, thus we chose to carry out experiments at 27°C, 32°C, 37°C and 42°C. Temperature readings were obtained via the dedicated output (100 mV °C⁻¹). The slow time course of the temperature changes illustrated in Fig. 3.4.A highlights the delay in heating the chamber. To accelerate the transition of temperature changes, the reservoir was drained of water via a sump in the base of the unit and water at the desired temperature was injected into the

reservoir. In experiments where the temperature sensitivity of aglycemia was tested, the bath was allowed to reach the desired temperature prior to switching to glucose-free aCSF.

3.2.3 Oxygen Electrode

The O₂ consumption was measured polarographically using Clark oxygen electrodes (Rank Brothers, Bottisham, UK). The partial pressure of O₂ was measured at a polarographic voltage of -600 mV with electrodes calibrated at 100% saturation in aCSF bubbled with 95% O₂ / 5% CO₂, and at 0% with addition of Na₂S₂O₄. aCSF was bubbled with 95% O₂ / 5% CO₂ for 2 hours at the test temperature to ensure maximal solution saturation of gas. The rate of O₂ consumption was measured as the change in pO₂ over a period of time, which being linear, was the pO₂ slope. The PO₂ was converted to molarities based on assumptions of solubility of O₂ at 35°C being 19.82 μmoles / mole H₂O, and 22.90 μmoles / mole H₂O at 25°C (Lide 2006), and corrected for tissue weight.

3.2.4 Morphological Studies

As described in Chapter 2 electron microscope images of nerves were obtained by providing treated tissue to The University of Nottingham Advanced Microscopy Unit.

Axon counting was performed by undergraduate students within the laboratory and these data are included here to augment and illuminate the functional data. The protocol was carried out as described by Allen et al., (2006). Firstly, a transverse section of the MON was viewed at low magnification (300x). The hexagonal pattern on the copper grid used to support the specimen was used to randomly select areas to record at the higher magnification (10,000x). Prior to acquiring the image for analysis the samples were focussed at 20,000x then returned to 10,000x. This improves the sharpness of the image by reducing the effect of hysteresis in the lens. Two fields which measured 18.8 μm by 12.5 μm were selected from opposite corners of each hexagon. The hexagons can be seen superimposed over an image of the MON in Fig. 3.1.A. The total image shown in Fig. 3.1.B shows an example field of the measurements described above. Axon counting and measurement was then performed in a smaller region of interest (ROI) within these fields. Each ROI measured 9.0 μm by 6.33 μm (total area 56 μm^2). The ROI is shown in Fig. 3.1.B by the solid rectangle. Only axons that were judged to be more than 50 % inside the ROI were included in the analysis. For example, axon 1 (Fig. 3.1.B) would be included in the count, whereas, axon 2 in the same figure would not. The surface area of each axon judged to be inside each ROI was measured using Openlab software (Improvision).

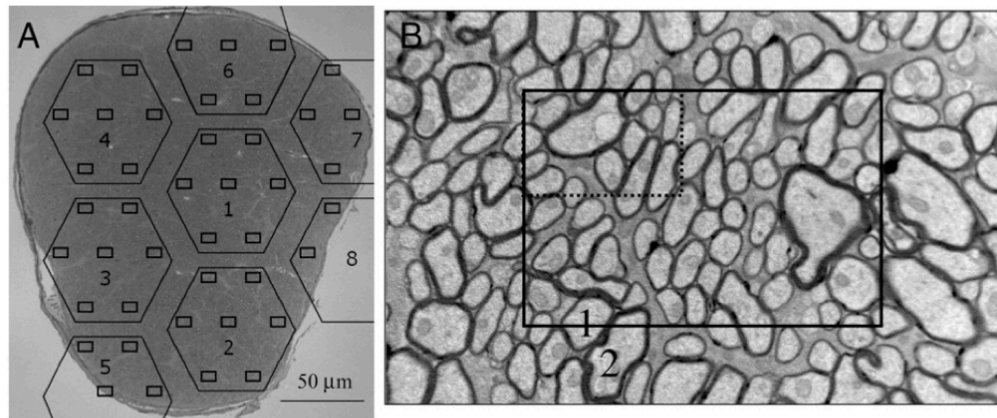


Figure 3.1 Method for axon counting. **A.** Transverse section of the MON with hexagonal grid overlaid. **B.** High power image of a single rectangular grid from A. For analysis two rectangular fields were acquired from opposite sides of each hexagon in A. Axons were then counted and measured from a smaller region of interest in each field, shown by the solid rectangle in B. Axons that were over 50% within the ROI (1) were included in the analysis and axons more than 50% outside the ROI (2) were excluded. Figure reproduced from Allen et al., 2006.

3.3 Results

3.3.1 *Extent of aglycemic injury is dependent on duration of aglycemia*

The effects of aglycemia on axon conduction were assessed by exposing MONs to either 1 or 2-hour periods of aglycemia followed by 1-hour recovery in control aCSF containing 10 mM glucose. Figure 3.2.A-B (insets) illustrates that the control CAP is composed of three peaks, an initial 1st CAP peak, a larger 2nd CAP peak, and a smaller 3rd CAP peak. Figure 3.2.A shows that in MONs exposed to aglycemia, the CAP began to fall after 21.0 ± 3.7 minutes ($n = 6$) and fell rapidly to zero, where it remained for the duration of the aglycemic insult (Fig 3.2.A-B). In MONs that were exposed to 1 hour of aglycemia followed by a 1 hour recovery period in 10 mM glucose aCSF, the CAP area slowly increased and recovered to 45.5 ± 18.8 % by the end of the 1 hour recovery period (Fig. 3.2.A, $n = 6$). In MONs exposed to 2 hours of aglycemia the CAP fell after 19.3 ± 3.4 minutes, and recovered to 16.6 ± 7.7 % of control (Figure 3.2.B, $n = 5$) Figure 3.3 shows that the difference between the CAP area prior to aglycemia and post-insult was significant for both 1 and 2 hours of aglycemia (for 1 hour $p = 0.00024$ vs. baseline and $p = 0.00005$ vs. baseline for 2 hours). The difference between CAP area recovery between a 1 hour and a 2 hour glucose withdrawal followed by a 1 hour recovery in 10 mM glucose aCSF was also significant ($p = 0.018$).

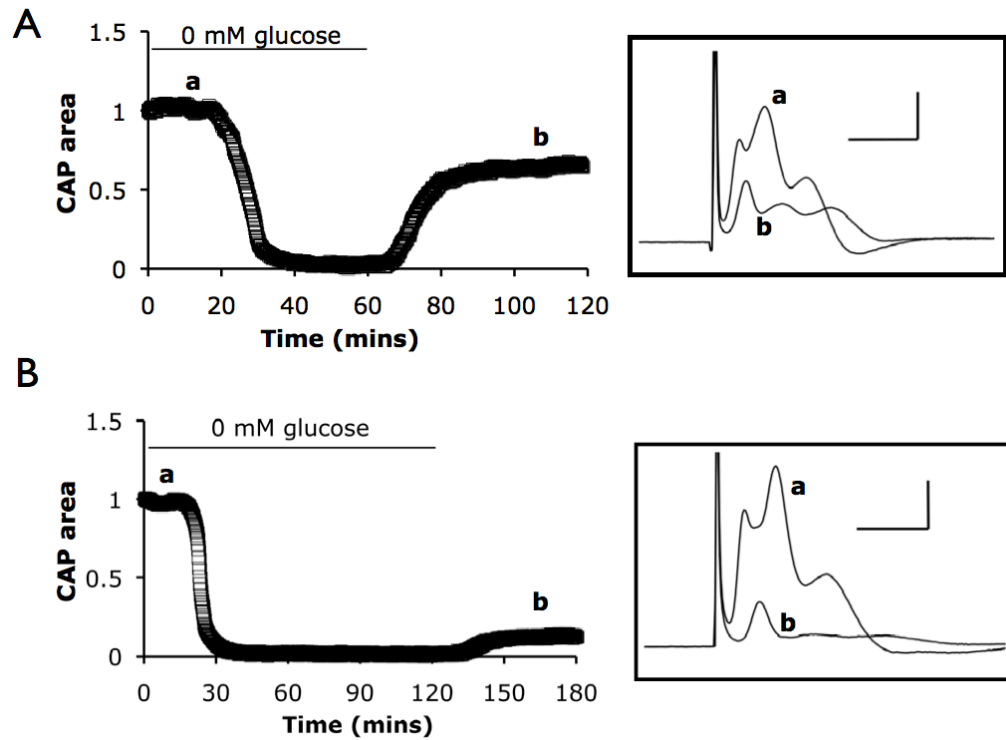


Figure 3.2 The effect of aglycemia on axonal conduction. **A.** Exposure to 1 hour of aglycemia followed by a 1 hour recovery in 10 mM glucose aCSF resulted in a delayed fall followed by incomplete recovery of the CAP ($n = 6$). Inset shows the control triple peaked CAP (a) and the attenuated CAP after the recovery phase (b). **B.** Aglycemia for 2 hours resulted in total abolition of the CAP with minimal recovery ($n = 5$). Inset shows a control CAP (a) and the post-aglycemia CAP (b). Scale bars for insets are 2 mV (y-axis) and 1 ms (x-axis).

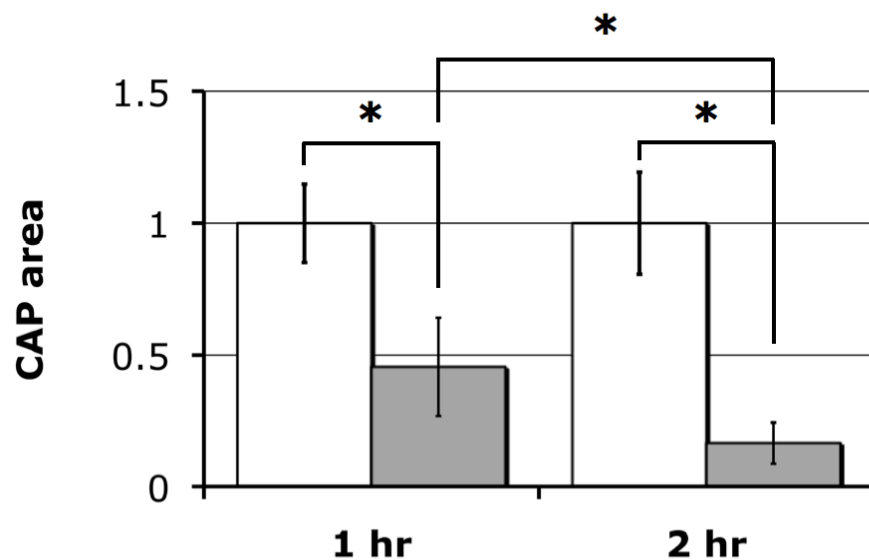


Figure 3.3 Functional recovery of the MON depends upon the duration of aglycemia. The degree of CAP recovery was dependent upon the duration of aglycemia, with 1 hour producing greater recovery than 2 hours. * denotes $p < 0.05$, see text for details. White bars show CAP area before aglycemia and shaded bars show CAP area after 1 hour of recovery in 10 mM glucose aCSF; ($n = 6$ for 1 hr and $n = 5$ for 2 hr).

3.3.2 Effect of temperature on the CAP profile.

The effect of temperature on the CAP profile was examined by recording the CAP at 27°C then increasing the temperature in 5°C steps to 42°C. Figure 3.4 clearly shows an inverse relationship between temperature and CAP area. Individual CAPs recorded at the four test temperatures are illustrated in Fig. 3.4.C, demonstrating that whereas conduction velocity decreases with hypothermia the CAP amplitude increases. The CAP area is plotted versus temperature to illustrate the non-linear relationship (Fig. 3.4.B, $n = 4$).

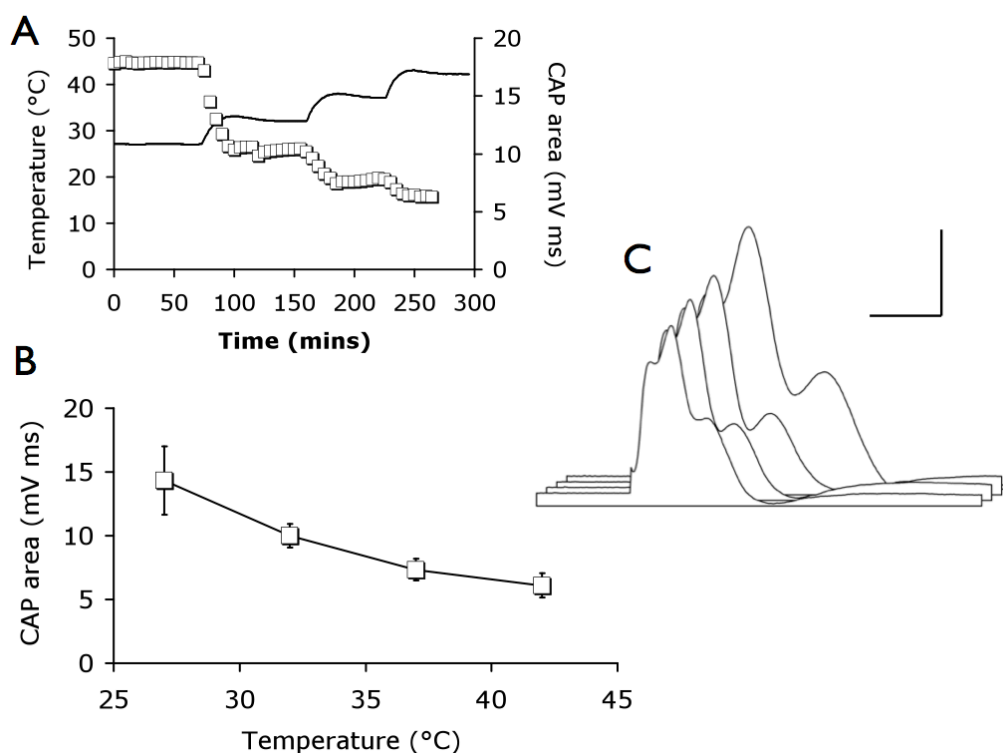


Figure 3.4 Effect of temperature on MON CAP profile. **A.** CAP area was temperature sensitive, hypothermia resulting in increased CAP area. The open squares denote individual CAP areas (right y-axis), the solid line denotes temperature (left y-axis). **B.** CAP area plotted against temperature. **C.** Example CAPs recorded at 27°C, 32°C, 37°C or 42°C, with the CAPs at the back of the stack recorded at the lower temperatures. Scale bars 2 mV (y-axis) and 1 ms (x-axis).

3.3.3 Temperature-dependence of aglycemic injury

In order to test the temperature-dependence of aglycemic injury, MONs were incubated in 10 mM glucose aCSF for 90 minutes, whereupon 0 mM glucose aCSF was introduced. At 60 minutes the temperature was altered from 37°C to the test temperature, where it remained until 150 minutes. At 150 minutes the temperature was returned to 37°C and 10 mM glucose aCSF was reintroduced, thus the temperature had stabilised to the test temperature at the onset of aglycemia and remained stable at that temperature for the duration of the aglycemic insult (see Fig. 3.5). The temperature-dependence was reflected in

both the latency to CAP failure and the degree of CAP recovery. Decreasing temperatures were associated with increased latency durations: at 27°C, 32°C, 37°C or 42°C, respectively, the latencies to failure were 19.9 ± 4.5 , 17.7 ± 3.8 , 15.7 ± 2.9 or 13.0 ± 4.3 minutes, respectively (Fig. 3.5 & 3.6.A). Similarly the slope of the CAP failure was temperature-dependent indicating that the CAP fell most rapidly at higher temperatures (Fig. 3.6.B). The degree of recovery of the CAP after the aglycemic injury was temperature dependent, not surprisingly showing that MONs incubated at lower temperatures during exposure to aglycemia displayed greater recovery: at 27°C, 32°C, 37°C or 42°C, respectively, the CAP recovery was 73.8 ± 5.9 , 50.3 ± 9.9 , 34.7 ± 3.8 or 15.6 ± 5.3 %, respectively (Fig. 3.6.C, $n = 4$ for each temperature).

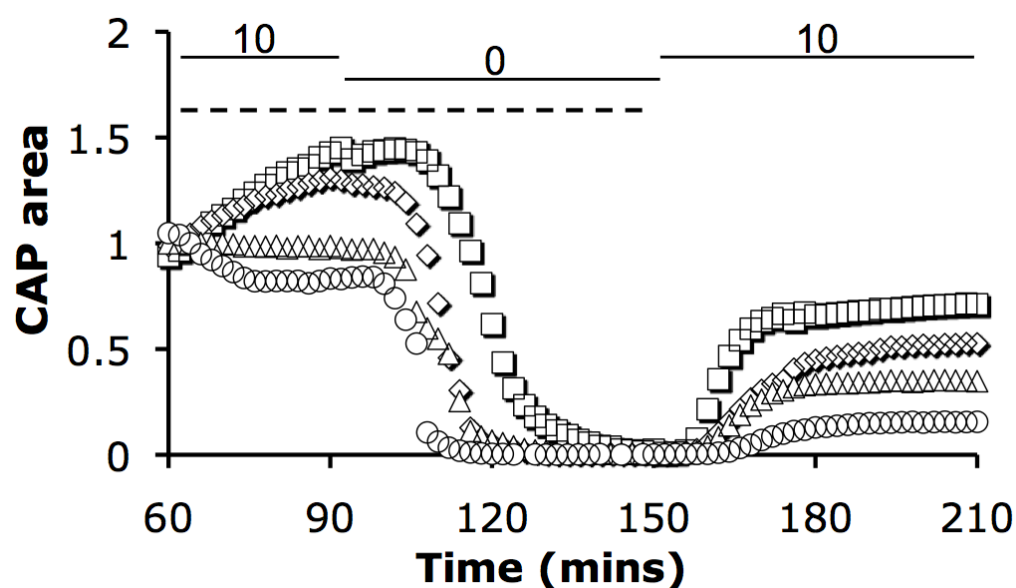


Figure 3.5 The effect of temperature on CAP area during aglycemia. Plot of average CAP area versus time during exposure to aglycemia at 27°C (\square), 32°C (\diamond), 37°C (\triangle) or 42°C (\circ). The dotted line indicates the period of test temperature, and the numerals denote the aCSF [glucose] in mM ($n = 4$ for each condition).

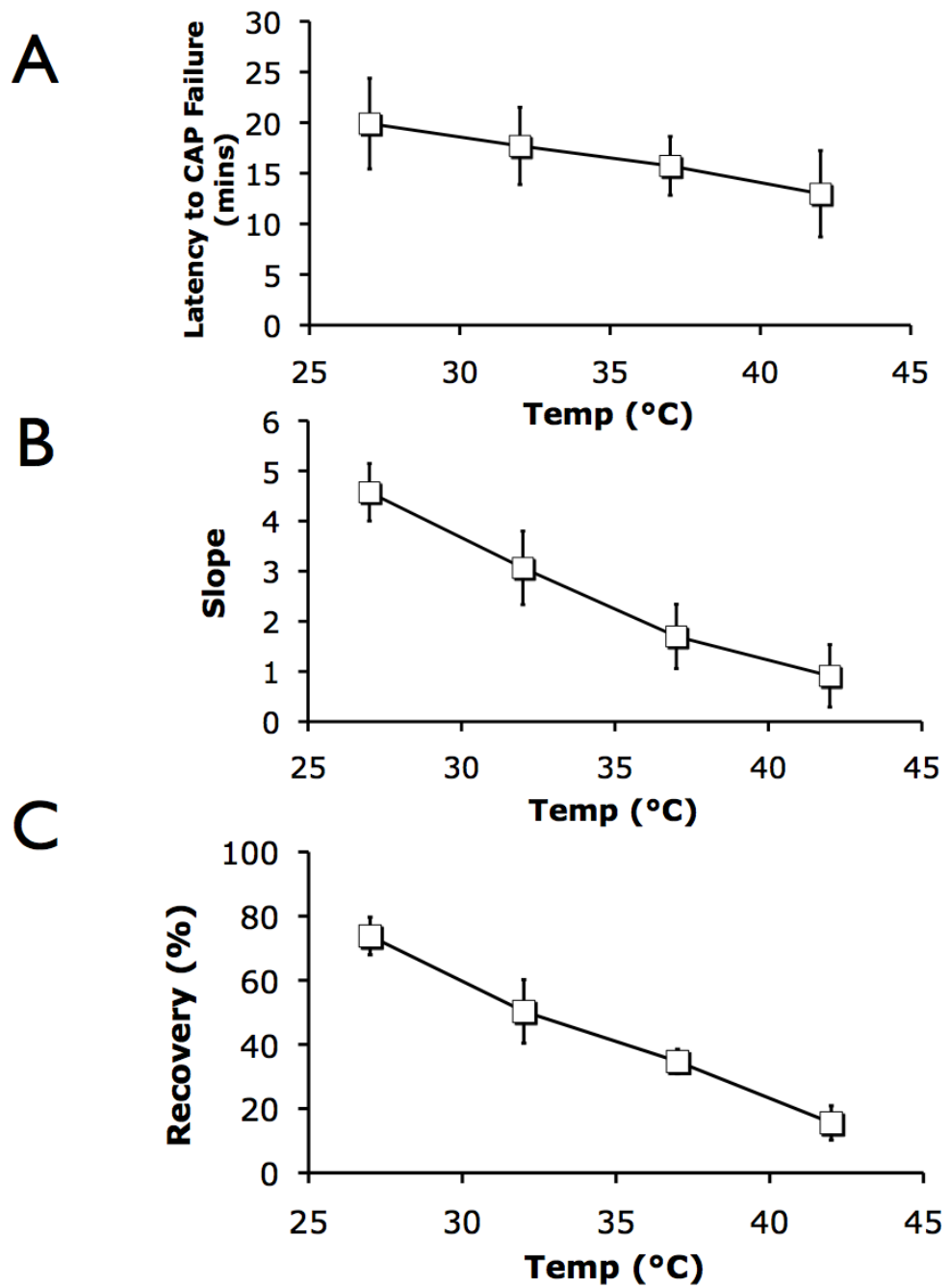


Figure 3.6 The effect of temperature on CAP area for a 1 hour period of aglycemia. **A.** Latency to CAP failure. **B.** Slope of CAP fall. **C.** Recovery of CAP after 1 hour 10 mM glucose post-aglycemia. (n = 4).

3.3.4 Temperature-dependence of MON metabolism

Glycogen is present in the MON and prolongs latency to CAP failure during periods of aglycemia (Brown et al., 2003). Thus, isolation of the neuroprotective effects of glycogen from the aglycemia-induced injury mechanism was sought. As a first step the effect of increasing temperature on glycogen breakdown during aglycemia was measured. MONs were maintained as described in Fig. 3.5 at 37°C or 27°C and harvested at 110 minutes, thus nerves were exposed to aglycemia for 20 minutes at either 27°C or 37°C. Figure 3.7.A shows that there was a significant decrease in the glycogen content of MONs incubated at 37°C (2.92 ± 0.58 pmoles $\mu\text{g protein}^{-1}$) compared to 27°C (6.18 ± 0.61 pmoles $\mu\text{g protein}^{-1}$, $p = 0.009$, $n = 3$), indicating that at lower temperatures the rate of glycogen metabolism is decreased.

As a second step in isolating the neuroprotective effects on glycogen MONs were incubated in aCSF containing either 2 mM glucose or 10 mM glucose for 2 hours at 37°C (Fig. 3.7.B). Glycogen content was 7.18 ± 0.13 pmoles $\mu\text{g protein}^{-1}$ in MONs incubated in 10 mM glucose, whereas content fell significantly to 2.61 ± 0.65 pmoles $\mu\text{g protein}^{-1}$ in MONs incubated in 2 mM glucose ($p = 0.0003$, $n = 3$). Thus incubating MONs in low glucose aCSF is an effective means of depleting glycogen content and could be performed prior to examining the effect of temperature on aglycemic injury.

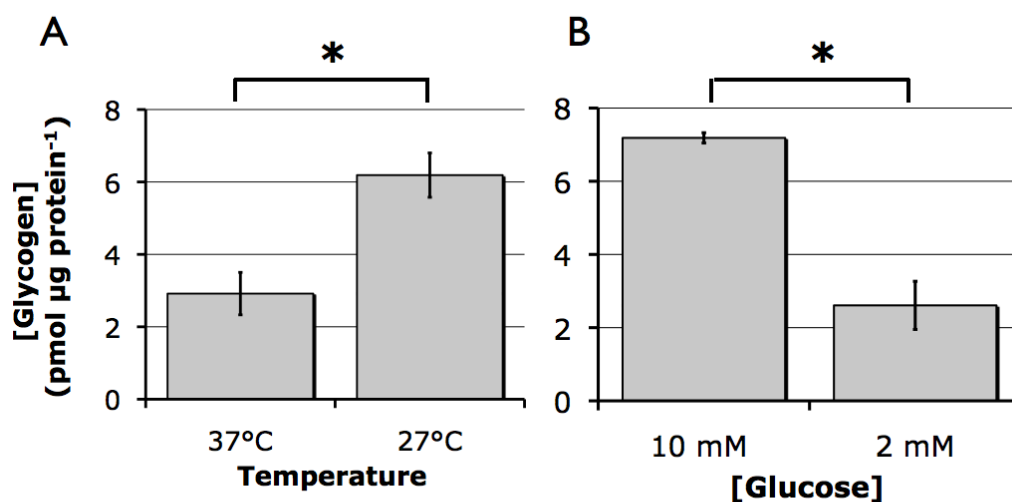


Figure 3.7 Glycogen metabolism is affected by temperature and ambient glucose concentration. **A.** Glycogen content (pmoles $\mu\text{g protein}^{-1}$ – also applies to B) of MONs incubated for 20 minutes at either 37°C or 27°C in the absence of glucose. Glycogen stores are used less rapidly during aglycemia at lower temperatures ($n = 3$). **B.** Glycogen content of MONs incubated for 2 hours in either 10 mM glucose or 2 mM glucose ($n = 3$). The glycogen content of the MON can be modulated prior to aglycemia by changing the ambient glucose concentration. * denotes $p < 0.05$.

Recording oxygen uptake can be used to monitor tissue metabolic rate. Accordingly, the oxygen consumption of MONs incubated at either 27°C or 37°C, in the presence and absence of glucose was measured. MONs incubated at 27°C in the presence of 10 mM glucose had a significantly lower rate of O_2 consumption than MONs incubated at 37°C (1.09 ± 0.28 vs. 2.09 ± 0.85 $\mu\text{moles O}_2 \text{ g}^{-1} \text{ min}^{-1}$, $p = 0.020$, $n = 5$, Fig. 3.8.A). Similarly in MONs incubated in the absence of glucose the O_2 consumption was significantly lower at 27°C than 37°C (1.13 ± 0.49 vs. 1.82 ± 0.45 $\mu\text{moles O}_2 \text{ g}^{-1} \text{ min}^{-1}$, $p = 0.040$, $n = 5$, Fig. 3.8.B). There was no significant difference in the rate of O_2 consumption at either

temperature of MONs incubated in the presence or absence of glucose (27°C - 1.13 ± 0.49 vs. 1.09 ± 0.27 $\mu\text{moles O}_2 \text{ g}^{-1} \text{ min}^{-1}$; 37°C - 1.82 ± 0.45 vs. 2.01 ± 0.85 $\mu\text{moles O}_2 \text{ g}^{-1} \text{ min}^{-1}$) (Fig 3.8.B), indicative of glycogen metabolism in the glucose-free MONs requiring equivalent oxygen as does glucose metabolism.

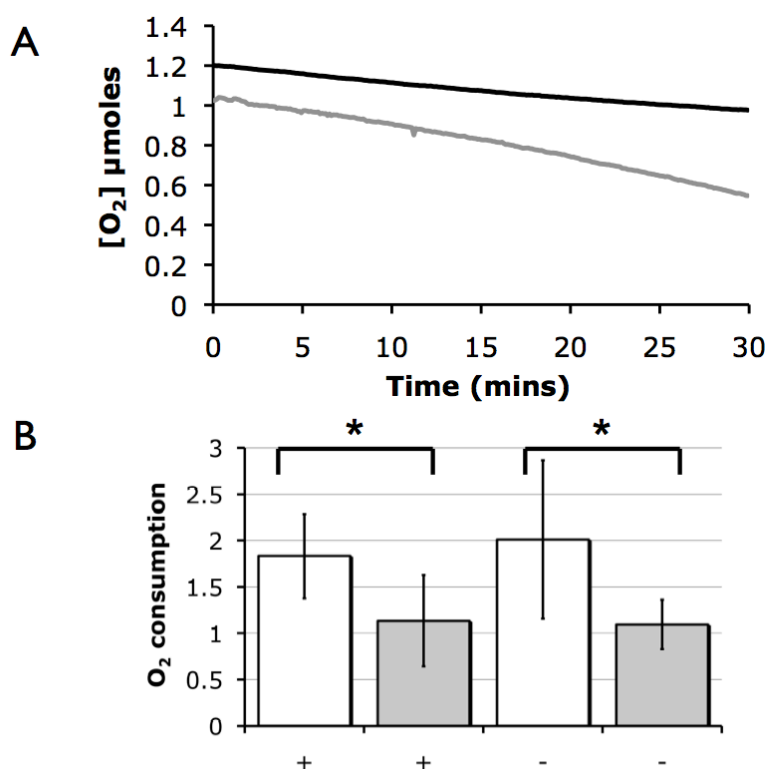


Figure 3.8 Temperature sensitivity of oxygen consumption in the MON. **A.** Oxygen consumption of MONs incubated in aCSF containing 10 mM glucose at 27°C (black line) or 37°C (grey line). **B.** Oxygen consumption ($\mu\text{moles O}_2 \text{ g}^{-1} \text{ min}^{-1}$) in MONs incubated at either 27°C (grey columns) or 37°C (open columns) in the presence (+) or absence (-) of 10 mM glucose. * denotes $p < 0.05$, $n = 5$.

3.3.5 Temperature-dependence of aglycemic injury in glycogen-depleted nerves

The presence of glycogen in the MON and the slowing down of the metabolic rate at low temperatures means that the exact relationship between temperature and injury mechanisms may be masked. Glycogen content was therefore depleted from the nerves prior to exposing them to aglycemia to reduce its influence. Depletion of glycogen was achieved by incubating nerves for 2 hours in 2 mM glucose aCSF, which has previously been shown to reduce glycogen to its nadir (Brown et al 2003). MONs were incubated in 10 mM glucose for 60 minutes then 2 mM glucose aCSF was introduced for 120 minutes (60 – 180 minutes), whereupon glucose-free aCSF was introduced (180 – 240 minutes), followed by a 60-minute recovery period in 10 mM glucose aCSF (240 – 300 minutes, see Fig. 3.9). MONs were maintained at 37°C until 165 minutes when temperatures were changed to the test temperature. At 240 minutes the temperature was restored to 37°C to coincide with the period of recovery. Qualitatively the effects of temperature were similar to those shown in Fig. 3.5 and 3.6, however, there were significant quantitative differences. The latency to CAP failure at 27°C, 32°C, 37°C or 42°C, respectively, was 11.2 ± 1.0 , 9.4 ± 1.9 , 8.0 ± 2.5 , or 5.3 ± 3.2 minutes, respectively (Fig. 3.9 & 3.10.A). The rate of CAP failure was temperature-dependent, being fastest at higher temperatures (Fig. 3.11.B), and the greatest CAP recovery occurred when exposure to aglycemia occurred at low temperatures. The CAP recovery at 27°C, 32°C, 37°C or 42°C, respectively, was 61.0 ± 8.5 , 37.7 ± 13.4 , 13.2 ± 6.0 or $0 \pm 0\%$, respectively (Fig. 3.11.C, $n = 4$ for all temperatures).

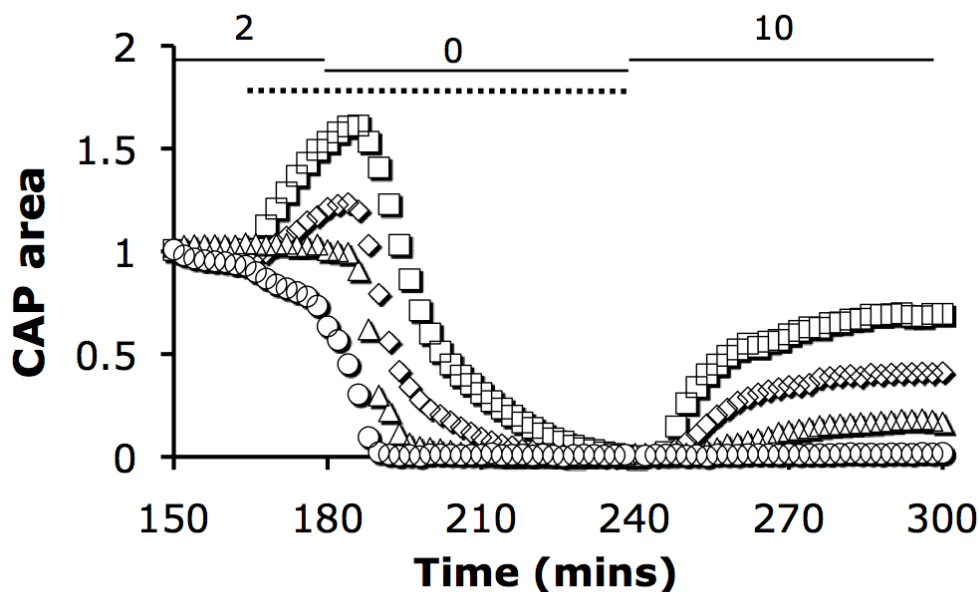


Figure 3.9 The effect of temperature on CAP area during aglycemia for glycogen-depleted nerves. Plot of average CAP area versus time during exposure to aglycemia at 27°C (\square), 32°C (\diamond), 37°C (\triangle) or 42°C (\circ). The dotted line indicates the period of test temperature, and the numerals denote the aCSF [glucose] in mM ($n = 4$ for each condition).

3.3.6 Comparison between control and glycogen-depleted MONs

Comparing the data shown in Figs 3.5 and 3.9 allows us to quantify the neuroprotective effects of glycogen at all four test temperatures using unpaired t-tests. For CAP recovery at 27°C, 32°C, 37°C or 42°C the p values were 0.287, 0.182, 0.003, 0.007, respectively: for the slope at 27°C, 32°C, 37°C or 42°C the p values were 0.048, 0.347, 0.403, 0.519, respectively, and for the latency at 27°C, 32°C, 37°C or 42°C the p values were 0.042, 0.046, 0.013, 0.048, respectively.

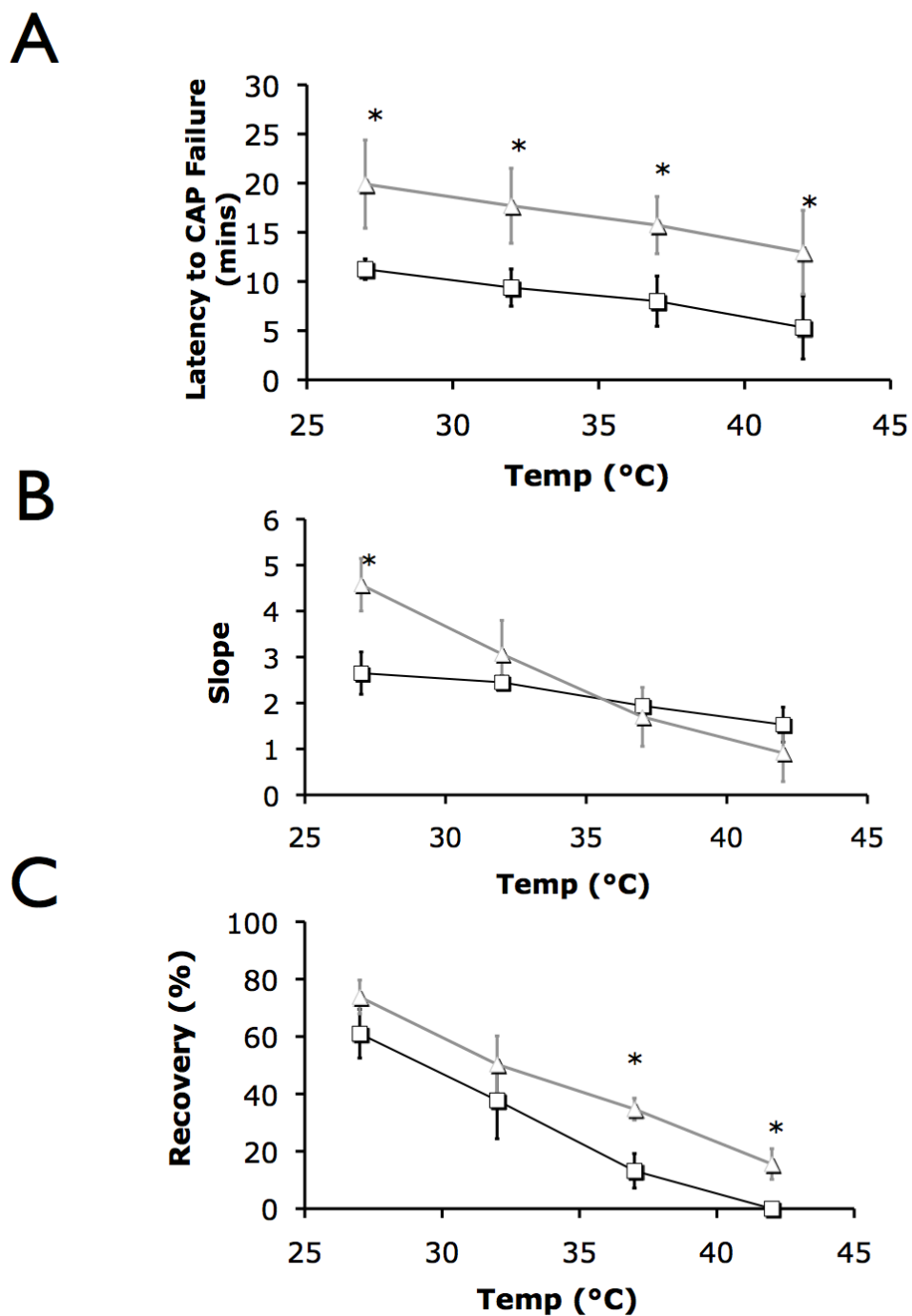


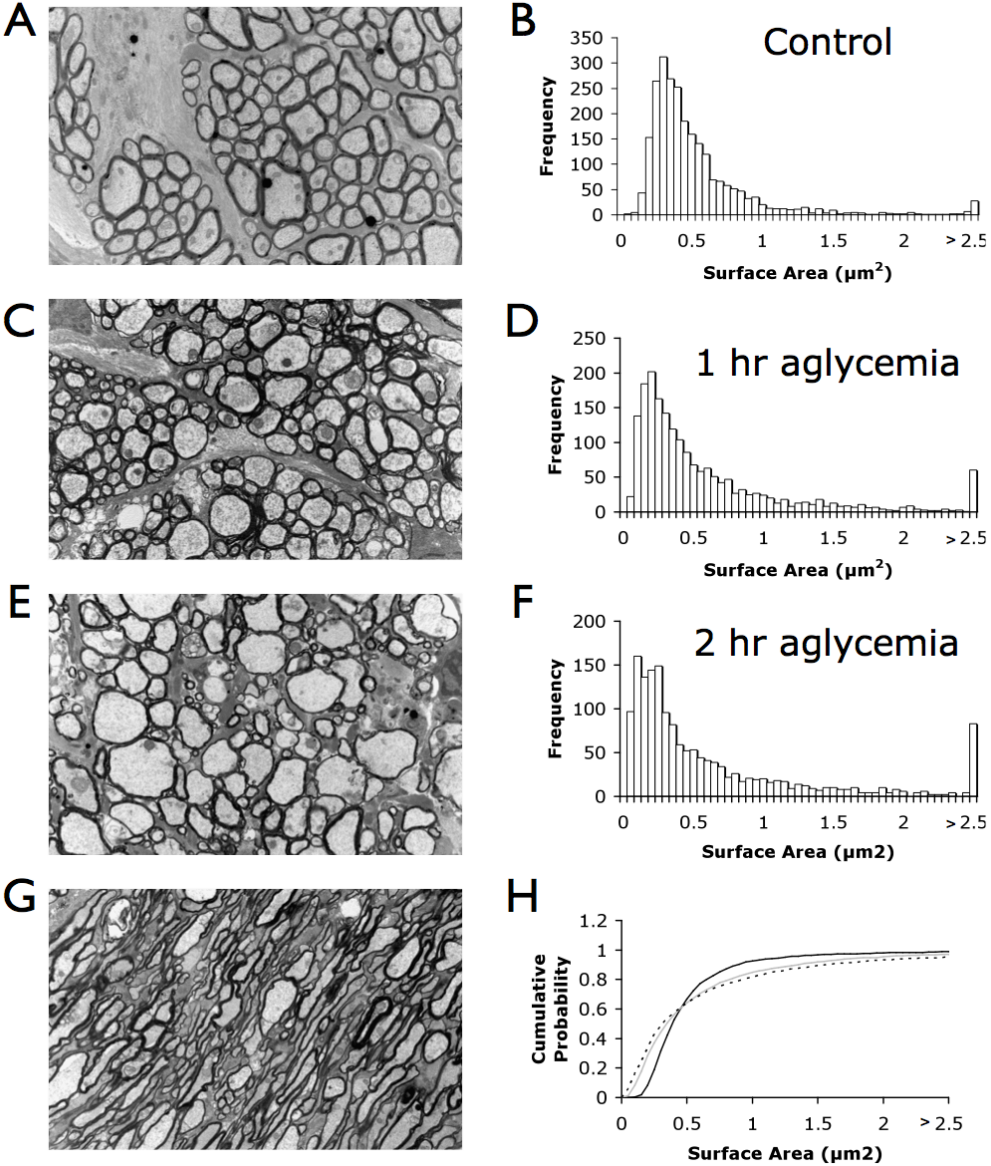
Figure 3.10 The effect of temperature on CAP area parameters for a 1 hour period of aglycemia; comparison of control and glycogen-depleted nerves. **A.** Latency to CAP failure. **B.** Slope of CAP fall. **C.** Recovery of CAP after 1 hour 10 mM glucose post-aglycemia. Open squares show glycogen-depleted MONs and control values from Fig. 3.6 are shown by open triangles for comparison. * denotes $p < 0.05$ for comparisons between control and glycogen-depleted MONs at the same temperature ($n = 4$).

3.3.7 Morphology of aglycemic injury at 37 °C

MONs showed good preservation upon fixing as previously described (Allen et al., 2006). Figure 3.11.A shows a transverse section of a control MON, which was incubated in 10 mM glucose. All axons are myelinated in the adult MON, with myelin visible as a dark ring surrounding the axoplasm, in which mitochondria are sometimes visible. A frequency histogram of axon surface area showed that surface area distribution was skewed towards larger areas (Fig. 3.11.B), with a modal surface area of 0.35 - 0.40 μm^2 . Data from 3 nerves with a total of 44 ROIs; total number of axons was 2465 with an average of 56.0 ± 15.3 axons per ROI. The mean surface area of all the axons was $28.6 \pm 7.3 \mu\text{m}^2$ per ROI, thus the average surface area of each axon was $0.525 \pm 0.131 \mu\text{m}^2$.

In MONs exposed to 1 hour of aglycemia followed by a 1 hour recovery period in 10 mM glucose aCSF, axons were visibly different to control axons. Axons were more rounded in profile, and there appeared to be more axons with a large surface area (Fig. 3.11.C). However the frequency histogram revealed that the peak frequency moved in the direction of smaller sized axons, in contrast to initial impressions based on the obvious presence of more large axons. The population of large axons is represented by surface areas of 2.5 μm^2 or larger, of which there are a larger proportion (3.1% vs. 1.1%) than the control (Fig. 3.11.D), and modal surface area was 0.25 - 0.30 μm^2 . Data from 4 nerves with a total of 42 ROIs; total number of axons was 1914 with an average of 45.6 ± 13.0 axons per field. The mean surface area of all the axons was $27.5 \pm 6.1 \mu\text{m}^2$ per ROI, thus each axon had on average a surface area of $0.643 \pm 0.209 \mu\text{m}^2$.

Figure 3.11 Morphological effects of aglycemia on MON axons at 37°C. **A.** Control nerves incubated in 10 mM glucose showed good preservation with all axons myelinated and mitochondria present in the axoplasm. **C & E.** MONs exposed to aglycemia for 1 or 2 hours, respectively, showed large, rounded, swollen axons, but also an increase in smaller sized axons. Scale bars 2 μm. **B, D & F.** Frequency histograms showing the size distribution of the axons. **G.** Longitudinal section of MON exposed to aglycemia for 1 hour showing ‘string of pearls’ indicative of localised ballooning of axons. Scale bar 2 μm. **H.** The cumulative probability of axon counts shows a sigmoidal relationship for control axons (black line), but aglycemia exposure for 1 (grey line) or 2 hours (dotted line) resulted in an increase in smaller sized axons (> 0.4 μm²) and an increase in the proportion of larger (> 2.5 μm²) axons.



This pattern was augmented in the MONs exposed to aglycemia for 2 hours. The modal surface area was 0.15 – 0.20 μm^2 from 31 ROIs from 3 nerves with 5.2% of axons 2.5 μm^2 or greater. Total number of axons was 1566 with an average of 50.5 ± 11.5 axons per field. The mean surface area of all the axons was $33.1 \pm 6.1 \mu\text{m}^2$ per ROI, thus each axon had on average a surface area of $0.693 \pm 0.215 \mu\text{m}^2$.

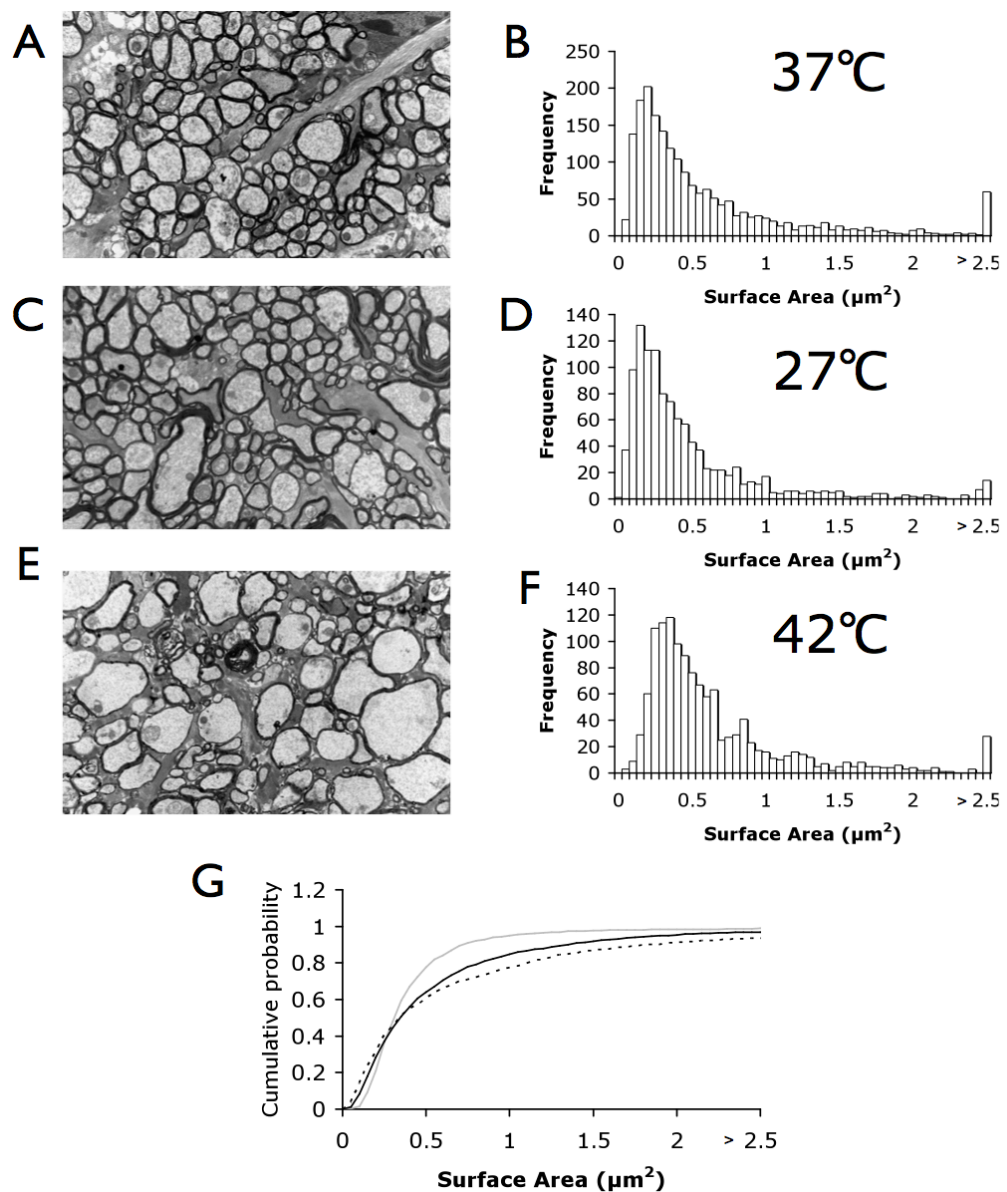
The cumulative probability provides an alternate representation of the data. In control conditions the curve is sigmoidal in shape with the 0.5 probability occurring at about 0.35 μm^2 . Exposure to aglycemia shifts the curve to the left at surface areas less than 0.4 μm^2 , indicative of an increase in the number of smaller axons. For example 8.4% of axons have a surface area of 0.2 μm^2 or less in control conditions, but this increased to 28.5% in nerves exposed to aglycemia for 1 hour. However, at surface areas greater than 0.4 μm^2 the curve is flattened indicative of an increase in the number of larger axons than in control conditions (Fig. 3.11.H).

3.3.8 Morphology of temperature-dependence of aglycemic injury

The effect of temperature on axon morphology in MONs exposed to 1 hour of aglycemia was examined at 27°C, 37°C and 42°C. Experiments at 37°C are the same as those described above (Fig. 3.11.C and D) with an additional illustration of an ROI for comparative purposes (Fig. 3.12.A and B) and data are as previously described. In MONs exposed to aglycemia at 27°C the axon morphology appeared similar to control tissue with smaller sized axons and less ballooning of axons (Fig. 3.12.C). The frequency histogram shows the modal surface area at 0.25 – 0.30 μm^2 from 2 MONs with 32 ROIs and 1098 axons, thus an average of 34.3 axons per field. The mean surface area of all axons was 16.49 μm^2 thus each axon had a surface area of 0.480 μm^2 , with only 0.75% of axons having a surface area of 2.5 μm^2 or greater. In MONs exposed

to aglycemia at 42°C axons appeared grossly swollen. The modal surface area was 0.40 – 0.45 μm^2 from 3 MONs with 1261 axons in 39 ROIs, an average of 32.3 axons per field. The mean surface area of all axons was 20.47 μm^2 thus each axon had a surface area of 0.636 μm^2 , with 2.2% of axons were 2.5 μm^2 or greater. The cumulative probability showed that temperature had the effect expected based on the data in Fig 3.12.H, namely that decreasing temperature led to decreased probability of large surface area, whereas the converse occurred at higher temperatures.

Figure 3.12 Temperature-dependent effects of aglycemia. **A.** MONs exposed to 1 hr aglycemia at 37°C showed moderate axonal swelling. **C.** In MONs exposed to aglycemia for 1 hour at 27°C the pathological effects were less evident with MONs lacking grossly swollen axons. **E.** MONs exposed to aglycemia at 42°C showed grossly swollen axons, swollen intra-axonal mitochondria, as well as numerous small axons. Scale bars 2 μm . **B, D** and **F.** Frequency histograms of axons exposed to aglycemia at 37°C, 27°C or 42°C, respectively. **G.** Cumulative probability of axon counts shows that MONs exposed to aglycemia at 42°C (dotted line) display more small axons, as well as larger axons compared to MONs exposed to aglycemia at 37°C (black line). Conversely the neuroprotective effects of hypothermia (27°C) are demonstrated by the decreased proportion of larger axons (grey line).



3.4 Discussion

I set out to test the hypothesis that hypothermia and glycogen content are neuroprotective in the isolated mouse optic nerve (MON) during periods of aglycemia. The MON contains glycogen, which acts as an endogenous energy reserve, thus the aims were several-fold. Firstly, to demonstrate that hypothermia and glycogen are neuroprotective, secondly to demonstrate the effect of hypothermia on oxygen consumption and glycogen metabolism, and finally to compare the relative scale of any beneficial effects of glycogen content or hypothermia

3.4.1 Prevention of Injury During Aglycemia

During aglycemia or hypoglycemia glucose delivery to tissue is below that required for normal tissue function, resulting in tissue glucose levels falling below the concentration required to saturate hexokinase, which in turn causes the rate of glucose metabolism to fall (Dienel, 2009). This sequence of events then leaves a shortfall in the energy supply required for normal tissue function. Without a sufficient energy supply, function is lost and a series of pathological events are set in motion, which cause tissue injury and cell death. Neurological deficits due to loss of myelin and axonal damage can result from this kind of injury to CNS white matter (Mori et al., 2006). There is an effort ongoing to understand these injury processes and prevent or minimise any impact.

Aglycemia can be induced experimentally in the MON and its effects are seen as a fall in CAP area over time as axonal conduction fails. Axonal conduction can be restored by restoring the glucose supply to the nerve but often recovery is incomplete, an indication of irreversible axon injury. The degree of the recovery is inversely related to the duration of the aglycemic episode. Clinically the central symptoms of hypoglycemia, predominantly caused by

iatrogenic insulin injection, can progress from confusion and memory impairment ultimately to seizure, coma and death in the absence of intervention (Frier and Fisher, 2007). There is currently no therapeutic strategy to combat systemic hypoglycemia, aside from rapid restoration of euglycemia by introduction of exogenous glucose. The MON can be used to evaluate and explore possible interventions which may either delay conduction failure, prevent permanent injury or both in CNS white matter.

3.4.2 The Protective Role of Hypothermia

The results presented in this chapter demonstrate that whereas mild hypothermia protects MON axons exposed to aglycemia, hyperthermia aggravates aglycemic injury. Mild hypothermia has been reported as neuroprotective during such brain trauma as ischemia (Busto et al., 1987) and seizures (Liu et al., 1993). Both of these conditions can result in energy imbalance where the energetic demands of the tissue are not met by blood borne supply of glucose and oxygen. *In vitro* studies have shown that in both grey and white matter mild hypothermia is neuroprotective during ischemia (Busto et al., 1987), and anoxia (Stys et al., 1992) or hypoglycemia (Shin et al., 2010) in isolation. The most obvious reason for this neuroprotection induced by hypothermia is by decreasing the metabolic requirement of the tissue.

In grey matter the mechanism of hypoglycemic injury is excitotoxicity, where decreasing ATP levels lead to elevations of extracellular glutamate, which activates post-synaptic glutamate receptors. This leads to a multiple step process involving Ca^{2+} influx, mitochondrial Ca^{2+} deregulation, reactive oxygen species production, DNA damage, polyADP-ribose polymerase-1 activation, mitochondrial permeability transition and mitochondria-to-nucleus translocation of apoptosis-inducing factors (Shin et al., 2010). There is also accumulating evidence that influx of zinc, which can lead to ROS and PARP-1 production, plays a key role in neuronal death (Suh et al., 2008). In contrast,

the mechanism of axon death in white matter appears to be via a non-excitotoxic mechanisms involving toxic Ca^{2+} influx via L-type Ca^{2+} channels that are activated by the membrane depolarization following ATP exhaustion (Brown et al., 2001a; Brown et al., 2001b; Fern et al., 1995), and reversal of the Na^+ - Ca^{2+} exchanger activated by increasing intracellular Na^+ levels (Brown et al., 2001a; Stys et al., 1992). The sequence of events leading to cell death following Ca^{2+} influx in white matter is unknown but are likely to resemble those of grey matter.

3.4.3 Morphometric Analysis of Nerve Injury

Morphometric analysis of aglycemic injury consisted of axon counts in combination with measures of cross sectional surface area from transverse sections of MON. Our goal in these studies was not to investigate the sub-cellular effects of aglycemia, but rather to correlate aglycemia-induced changes in axon morphology with measurements of axon conduction. We have chosen to express axon size in terms of surface area rather than diameter for the following reasons. Measuring axon diameter at the shortest distance bisecting the axon will tend to underestimate the surface area calculated from this diameter as not all axons will be cut perpendicular to the axon cylinder, and thus not all axons will appear spherical, rather they will appear as oblongs, and such diameter measurement would underestimate the surface area (James et al., 2010). The distribution of axon size was skewed in the direction of larger axons as previously reported in mouse (Allen et al., 2006), rat (Garthwaite et al., 1999) and hamster (James et al., 2010). All axons are included in counts and those considered pathological were not excluded due to the subjective nature of such judgements. Initial impressions of MONs exposed to aglycemia at 37°C were of an overall increase in axon surface area. However although some axons did indeed swell there were a large number of smaller axons. Indeed our cumulative probability data shows an increase in the number of smaller axons in MONs exposed to aglycemia compared to

control MONs. This may be explained with reference to the longitudinal section of the aglycemic MON, where a 'string of pearls' appearance of axons is seen. This phenomenon has been previously demonstrated in ischemic MON axons, where the swelling of axons was focal with the intervening sections of axons appearing shrunken (Garthwaite et al., 1999). This almost certainly explains the shift in the frequency distribution of axon sizes towards smaller axons rather than towards larger axons. A similar less than expected shift in frequency distribution has been reported in ischemic MON axons (Garthwaite et al., 1999). This effect was augmented in MONs exposed to 2 hours of aglycemia. The cumulative probability of MON surface area demonstrates a less steep relationship in MONs exposed to aglycemia with a crossover at $0.4 \mu\text{m}^2$ resulting in greater frequency of axons below $0.4 \mu\text{m}^2$ and less above $0.4 \mu\text{m}^2$ compared to control. However reference to the frequency histograms shows more axons $> 2.5 \mu\text{m}^2$ in aglycemia treated axons, indicating the development of larger swollen oedematous axons. Similarly the effects of temperature reveal morphological differences. In MONs exposed to 1 hour of aglycemia at 37°C there is the appearance of large swollen axons, whose numbers decrease if the temperature was decreased to 27°C during the aglycemic episode. Conversely increasing the temperature to 42°C during the aglycemic insult resulted in an increase in the number of axon $> 2.5 \mu\text{m}^2$. Reference to the cumulative probability highlighted this trend, namely that decreased temperature led to smaller number of swollen axons, but that hyperthermia led to an increased number of swollen axons. Calculations of axons size showed that the average axon surface area increased upon exposure to aglycemia, and that the duration of aglycemia led to greater surface area. Similarly hypothermia led to decreased surface area of MONs exposed to aglycemia, whereas hyperthermia had the opposite effect. These results complement the electrophysiology results indicating the neuroprotective effects of hypothermia.

A possible limitation of this study was that the effect of temperature alone on axon morphology was not examined. This decision was made due to the fact

that changes in temperature which lasted for the length of time used within these experiments had no irreversible effect on CAP area. The assumption was made that if axons were undergoing morphological changes as an effect of the change in temperature, these would be represented by a change in the profile of the CAP.

3.4.4 The Role of Brain Glycogen

MONs contain endogenous glycogen, located in astrocytes (Cataldo and Broadwell, 1986), which acts as an energy buffer to provide the tissue with energy substrate in the face of aglycemia (Brown et al., 2003). However, glycogen content is limited and once reserves are exhausted axon conduction fails (Wender et al., 2000; Brown et al., 2003). Toxic Ca^{2+} influx is subsequently triggered, followed by irreversible injury, the extent of injury related to the duration of glucose withdrawal (Fig. 3.3 and Brown et al., 2001). Here it has been shown that the protective effects of hypothermia are in part mediated by a decreased rate of glycogen metabolism. Glycogen content of the MON remained elevated after 20 mins of aglycemia at 27 °C, revealing a slower mobilisation of this energy store than at 37°C. This observation is no doubt due to the reduced demand for glycosyl units by tissue at lower temperatures. Oxygen consumption also reflected this as it was decreased at 27°C compared to 37°C. It is interesting to note that the oxygen consumption was the same for nerves in the presence and absence of glucose over a 30 minute period, indicating that glycogen can supply glycosyl units at an equivalent rate to that of normal glucose consumption.

Glycogen was neuroprotective at all temperatures tested with regards to delaying CAP failure, with depletion of glycogen prior to aglycemia accelerating loss of axonal conductivity. This is an important observation with clinical relevance as disruption in action potential conduction is likely to lead to some of the symptoms of hypo/aglycemia described above. The ability of

glycogen to delay CAP failure was greater at 42°C than even a reduction in temperature to 27°C in glycogen-depleted nerves. The results of this study suggest that the possibility that brain glycogen content may help protect against symptoms of hypoglycemia should be further explored.

Post-injury recovery was also influenced by the availability of glycogen, but this was only significant at 37°C and 42°C. The extent of the neuroprotection offered by glycogen stores can be seen by comparing CAP recovery between different conditions. MONs which were glycogen-depleted prior to aglycemia showed less recovery at 37°C than those with glycogen present which were exposed to aglycemia at 42°C. The harmful effects of hyperthermia are well documented but this result shows that the presence of glycogen is equally important for post-aglycemia recovery of axonal function in white matter. This raises clinical considerations for patients prone to insulin-induced hypoglycaemia. If brain glycogen in these patients is below normal then they may be more vulnerable to the CNS effects of hypoglycemia. It is a well known aspect of hypoglycemia that because of hypoglycemia unawareness, one episode of hypoglycemia increases the probability of other subsequent hypoglycemic events (Frier and Fisher, 2007). The significance of this clinical observation in relation to these results is that the glycogen depletion that occurs during hypoglycemia may not be replenished to baseline levels before the next hypoglycemic episode. It may be possible to develop methods to restore or up-regulate brain glycogen to protect against hypoglycemic symptoms. Controlling glycogen content of the brain is a much more realistic and practical method of reducing the likelihood and severity of aglycemic injury since dietary or pharmacological methods affecting glycogen content would be easier to implement than therapeutic cooling.

3.4.5 Summary

In conclusion these results demonstrate that ambient temperature influences the degree of injury incurred by adult MON during aglycemia, with hyperthermia aggravating axonal injury, whereas, hypothermia reduces injury. A major contributory factor in the neuroprotection afforded by hypothermia is the presence of glycogen, which provides energy substrate to axons during periods of aglycemia, and whose decreased utilisation due to decreased tissue energy demand during hypothermia prolongs the neuroprotective effect. The importance of glycogen in protecting white matter from aglycemic injury is clear as glycogen-depletion is as harmful to tissue recovery as hyperthermia. This study suggests that there is good reason to focus more attention on the role of brain glycogen as an energy substrate and neuroprotective agent.

Chapter Four

Real-time measurement of lactate using biosensors reveals that glycogenolysis contributes to extracellular lactate in the mouse optic nerve.

4.1 Introduction

4.1.1 *Lactate in the CNS*

The role of lactate in the CNS is an intensely debated topic that polarises researchers. Some see lactate as a minor contributor to brain energy metabolism, whereas others support the view that it is an important oxidative fuel for neurons. The dogmatic view of glucose metabolism was established when the biochemical pathways of energy metabolism were being characterised (Pellerin and Magistretti, 2003). Tradition states that the brain requires a constant supply of glucose, and that other metabolic substrates for energy metabolism play an insignificant role in brain energetics (Greutter et al., 1992). Specifically lactate was regarded as a waste product of anaerobic metabolism that served no further useful function (Huckabee, 1958). This view was challenged by Pellerin and Magistretti (1994) who claimed that lactate was a major energy substrate in the brain, when they put forward their astrocyte-neuron lactate shuttle hypothesis (ANLSH). This model introduced lactate as an important metabolic substrate and reignited interest in some older studies which showed that lactate could support brain function (See Chapter 1). The newfound interest in lactate even led to the proposition that lactate is always the end product of glycolysis and therefore the substrate for mitochondria (Schurr, 2006). This hypothesis is considered a more extreme stance but strong arguments dictate that lactate cannot simply be dismissed as a metabolic dead-end.

Lactate is present in the brain at appreciable concentrations, typically around 0.5 - 1 mM under resting conditions, with some studies reporting up to 3 mM (Erlichman and Leiter, 2010). The concentration of lactate rises as a result of increased neural activity (Kuhr et al., 1988; During et al., 1994). The relative contributions of oxidative and anaerobic metabolism may play a pivotal role in lactate dynamics. Increased metabolic demand can occur very rapidly in nervous tissue during high frequency action potential firing. Studies have

shown that during neuronal activation an increase in the rate of glycolysis is triggered which is greater than the concurrent increase in oxidative metabolism (Fox et al., 1988). The up-regulation of glycolysis causes an increase in lactate production although oxygen is present in adequate quantities. The energy yield from glycolysis is much smaller than that from full oxidative metabolism of glucose. This energy, however, is available rapidly. In sub-cellular locations such as astrocyte processes that are too small to contain mitochondria, glycolysis may represent the more suitable method to generate the energy needed for homeostatic processes such as K^+ clearance from the extracellular space. In this case lactate may be released from the cell. Since, if allowed to accumulate intracellularly the lactate would inhibit key metabolic reactions and reduce the rate of glycolysis (Dietl et al., 2010). Convention would suggest that lactate produced in this manner is removed from the local area or removed from the brain entirely via venous drainage (Zimmer and Lang, 1975; Leegsma-Vogt et al., 2003). There are other possibilities as to the fate of this lactate, which include oxidation of lactate (Madsen et al., 1999), possibly within neurons (Pellerin, 2004). The precise contributions of oxidative and non-oxidative metabolism during neuronal activation are still under question, a key variable being the nature of the stimulus. In white matter it has been reported that some axons can survive without oxidative metabolism. In both the mouse and rat optic nerve some axonal activity is maintained under anoxic conditions (Tekkok et al., 2003). The magnitude of anoxic resistance in the optic nerve declines with age (Hamner et al., 2011). Anoxic resistance may be a property of CNS white matter as the corpus callosum shows similar anoxic resistance to that observed in the optic nerve, whereas, hippocampal grey matter does not (Tekkok and Ransom, 2004). The mechanism that underlies white matter resistance to anoxia is not fully understood (Hamner et al., 2011). It is also not clear as to whether some axons remain able to function normally whilst some lose the ability to conduct, or whether all axons have a partial sensitivity to anoxia and generate action potentials of reduced amplitude under anoxic conditions (Tekkok and Ransom, 2004)..

4.1.2 Lactate in White Matter

In common with a/hypoglycemic injury (Chapter 3) much of the focus on lactate metabolism in the brain has been centred around grey matter. However, lactate may be as equally important in white matter. In white matter lactate is released from astrocytes and is able to support axonal conduction (Tekkok et al., 2005). This raises the consideration that a model similar to the ANLSH may apply to white matter. The ANLSH's focus on glutamatergic synapses may, on initial inspection, appear to rule out any relevance to white matter. However, glutamate release and re-uptake, as well as the presence of glutamate receptors, have been shown in the optic nerve (a white matter tract) (Tekkok et al., 2007). There also exists the possibility that lactate shuttling within white matter may exist, but be dependent on a process such as K^+ clearance rather than glutamate recycling.

4.1.3 Glycogen is a Source of Lactate

A source of lactate in the CNS is glycogen metabolism. It has been shown that during energy deprivation in white matter glycogen stores in astrocytes can be mobilised and released as lactate to be taken up by axons to sustain their energy demands (Brown et al., 2005; 2007). The same mechanism can provide energy for axonal activity during high frequency stimulation (Brown et al., 2005). A dynamic role for glycogen in brain energetics has also been proposed. The glycogen shunt model argues that glycogen is more than a quiescent energy store and that prior to entering the glycolytic pathway a significant fraction of glucose passes through glycogen molecules (Walls et al., 2009). Recently, glycogenolysis and the associated lactate shuttling have been shown to be necessary for memory formation in the rat hippocampus (Suzuki et al., 2011). The accumulating evidence gives a strong indication that glycogen and lactate metabolism in the CNS are important pathways in normal brain

functioning, but the precise role and contribution of glycogen has yet to be determined.

4.1.4 Biosensors

It has proven difficult to experimentally confirm many of the theories and models of brain energy metabolism, with much of the evidence being circumstantial or based on modelling studies. This has been in the most part due to the complexity of the tissue and the inter-dependence of different cell types. Many of the experiments used to investigate the assorted hypotheses have involved measurement of lactate in nervous tissue. A range of methodologies, including magnetic resonance (Mangia et al., 2003), autoradiography (Lear and Kasliwal, 1991), microdialysis (Fray et al., 1996) and biosensors (Hu and Wilson, 1997) have been employed to track changes in brain lactate under various conditions with each of these having their own particular advantages and disadvantages.

Enzyme-based biosensors have a number of advantages when compared to other methods used to measure lactate; they are relatively simple and low cost to use, they are small and minimally disrupt tissue, can be applied both *in vivo* and *in vitro* and have an excellent temporal resolution enabling real-time measurement of a specific metabolite. The use of biosensors to determine real-time concentrations and fluxes of metabolites and signalling molecules in brain tissue has provided important insights in a number of areas (Hu and Wilson, 1997; Dale et al., 2005). Biosensors have not yet been used to investigate lactate in white matter, and the putative contribution of glycogen metabolism, which, as discussed above, is a topic with important unresolved questions.

4.1.5 Aims

The aim of the experiments in this chapter was to study lactate dynamics in white matter by establishing the use of an enzyme-based lactate biosensor to monitor lactate release from the mouse optic nerve (MON). The isolated MON preparation is a widely used model for white matter, which has been used to study both normal physiological and pathological processes (Bolton and Butt, 2005). The first objective was to evaluate the biosensors, and then to determine whether lactate is produced by the MON. Secondly, the relationship between glucose availability and lactate production was sought. As lactate is implicated in glycogen metabolism, the relationship between glycogen and lactate in the MON was also examined.

4.2 Methods

All methods are described in detail in Chapter 2. Briefly; axon conduction in the isolated mouse optic nerve was monitored by recording the stimulus-evoked CAP and expressed as the normalised area under the CAP. Simultaneous recording of the extracellular lactate signal was achieved by use of an enzyme-based lactate biosensor (see Fig. 2.4). Latency to CAP failure, and time to fall of the lactate signal during aglycemia, were measured as the time to 50 % normalised CAP area and lactate signal, respectively.

4.3 Results

4.3.1 Biosensor Calibration and Specificity

The enzyme-based biosensor for lactate used in these experiments is designed with a selectivity layer to ensure that the signal is specific for lactate, in common with other sensors that share this construction (Dale et al., 2005). Before using these sensors to record lactate in the optic nerve they were calibrated in the experimental chamber used to record optic nerve CAPs. Firstly, the specificity of the signal for lactate was compared against a number of compounds which would be used in later experiments. The sensor was positioned in the tissue bath constantly perfused with aCSF in the absence of any tissue. The compounds tested were: zero glucose aCSF, 10 mM glucose, 10 mM fructose, 20 mM pyruvate, 5 mM L-lactate and 5 mM D-lactate. D-lactate is an optical isomer of L-lactate that is metabolically inert but that will compete with L-lactate on binding sites (Tekkok et al., 2005). Fig. 4.1.A shows that pipetting compounds onto the sensor caused a small negative deflection as an addition artefact and only L-lactate gave a strong signal, with D-lactate evoking a small signal. Fig. 4.1.B shows the sensor response when aCSF containing 1 mM lactate was perfused into the chamber. A smooth increase in lactate signal was observed which then plateaued. Returning to a lactate-free aCSF solution caused the lactate signal to return to zero within 3 minutes. Performing this experiment provided an indication of the time required for a solution to fully perfuse the tissue chamber and therefore the dead space of the perfusion system.

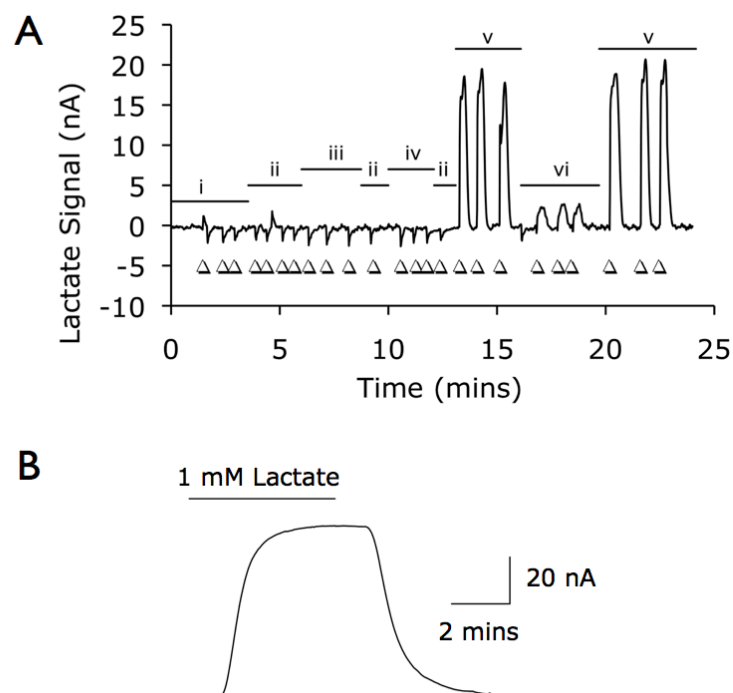


Figure 4.1 Response of lactate biosensor in the laminar flow perfusion chamber. **A)** Specificity of signal; aCSF containing the following compounds were pipetted into the chamber (arrow heads) to determine any potential interference. i) zero glucose aCSF ii) 10 mM glucose iii) 10 mM fructose iv) 20 mM pyruvate v) 5 mM L-lactate vi) 5 mM D-lactate. **B)** Wash in and wash out times of the perfusion system.

Secondly, the standard curve for the sensor's response to known lactate concentrations was determined (Fig. 4.2). The sensor showed a linear current response to lactate concentrations in the range of 10 - 800 μM , which was in agreement with their advertised sensitivity (<http://www.sarissa-biomedical.com>) Above this concentration range the sensor's response was not linear but did not plateau at concentrations tested (up to 10 mM). The sensor's response was found to be linear across the entire concentration range when plotted on a logarithmic scale, verifying its exponential nature (Fig. 4.2.C).

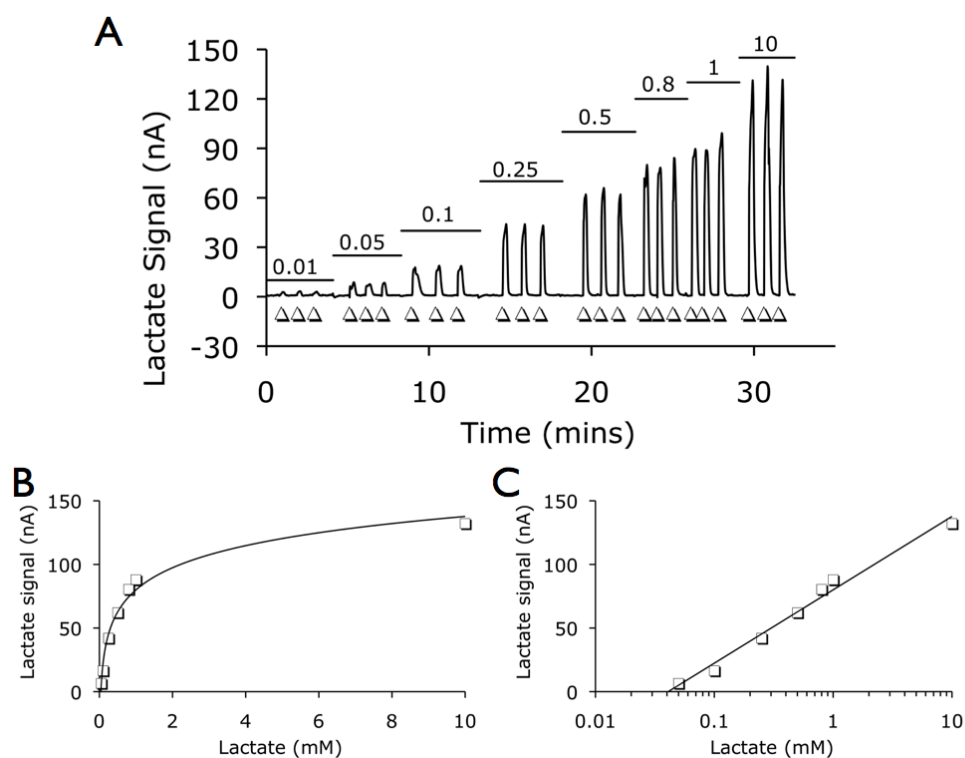


Figure 4.2 Calibration curve for lactate biosensor. Pipetting lactate onto the biosensor in the perfusion chamber gave a dose-dependent increase in lactate signal from the sensor. **A)** Raw trace from calibration experiment; additions are indicated by arrows under trace and the lactate concentration (mM) is given by the number above the trace. **B)** Lactate concentration plotted against peak lactate signal from the biosensor. **C)** Data from B plotted on a logarithmic scale for lactate concentration. For B and C, data are mean values ($n = 3$) from one sensor. SDs are too small to be visualised on the figure (maximum = 4.46 nA).

4.3.2 Lactate is Produced by the Mouse Optic Nerve

The mouse optic nerve (MON) produces lactate when minimally stimulated and supplied with glucose as an external energy substrate. Positioning an enzyme-based lactate biosensor in close proximity to the MON revealed that lactate was released from the nerve at a stable rate. The lactate sensor reading was interpreted as a proxy for extracellular lactate in the nerve (see Discussion). The extracellular lactate concentration in the optic nerve was 440

$\pm 86.0 \mu\text{M}$ ($n=3$) in aCSF containing 10 mM glucose when the supra-maximal CAP was evoked every 30 seconds. This value was obtained by calibrating the biosensor against a known range of lactate concentrations in the bath at the end of the experiment. It was found that the position of the sensor relative to the nerve, i.e. how much of the sensor was in contact with the nerve, could alter the strength of the signal observed. For this reason the lactate signal in further experiments was expressed as a normalised value. This was calculated by dividing by the stabilised lactate signal for each nerve in 10 mM glucose. A null electrode was not used after it was determined that the background noise measured by the null was not great enough to warrant subtraction from the signal of the lactate sensor.

4.3.3 The Relationship Between Glucose Supply and Extracellular Lactate

The effect of ambient glucose upon the lactate concentration was investigated by altering the concentration of glucose supplied to the nerve between 0.5 - 30 mM (Fig 4.3). Fig. 4.3.A shows that the concentration of lactate measured was unaffected by glucose concentrations between 5 and 30 mM. The lactate signal was not significantly different to that at 10 mM glucose for 5 and 30 mM ($p > 0.05$). At a glucose concentration of 2 mM and below the concentration of lactate fell, which prompted measurement of the lactate signal at lower glucose concentrations. The lactate signal for nerves incubated in 2 mM glucose was $82.6 \pm 6.2\%$ of that for 10 mM glucose, this dropped to $63.4 \pm 5.6\%$ and $32.6 \pm 4.2\%$ for 1 and 0.5 mM glucose, respectively ($n = 3$ for each glucose concentration). Each of these readings were significantly different from control conditions at 10 mM glucose ($p < 0.05$). Nerve activity, as indicated by CAP area, was maintained despite falling lactate levels at glucose concentrations of 1 and 2 mM, but partially fell when the MON was bathed in aCSF containing 0.5 mM glucose (Fig 4.3.B). The concentration-response of lactate release from the MON in different external glucose concentrations is summarised in Fig. 4.3.C.

Figure 4.3 The relationship between external glucose concentration and lactate production in the MON. Extracellular lactate was recorded with a biosensor positioned against the MON whilst the glucose concentration in the bathing aCSF was altered. The lactate signal increased with higher glucose concentrations but plateaued at 5 mM glucose. The lactate signal is shown as normalised against the stable signal seen with a bathing glucose concentration of 10 mM. **A.** Lactate signal (solid line) and CAP area (open squares) for glucose concentrations between 5 and 30 mM. Lactate remained stable at all glucose concentrations above 2 mM. **B.** Lactate signal and CAP area for glucose concentrations of 5 mM and below. The lactate signal fell in a manner that was glucose-dependent. CAP area was maintained until a glucose concentration of 0.5 mM upon which it partially fell. Figure continues on the next page.

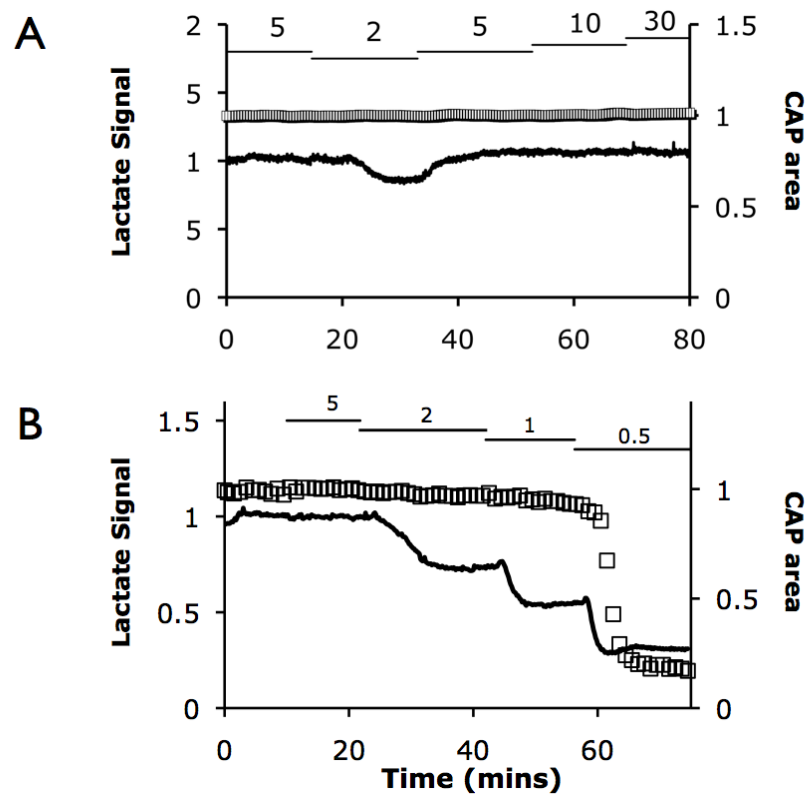
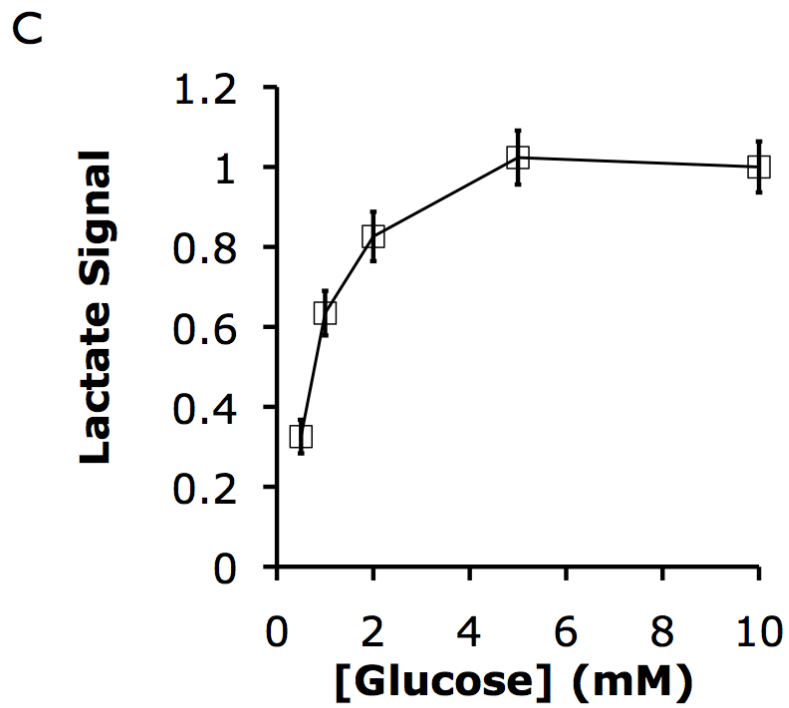


Fig 4.3 (cont.) C. Plot of glucose concentration versus normalised lactate signal ($n = 3$, error bars show S.D.).



4.3.4 Extracellular Lactate with Fructose as the Sole Energy Substrate

MON function has previously been shown to be partially supported by fructose (Allen et al., 2006; Meakin et al., 2007), therefore, the effect of substituting glucose with fructose upon the lactate signal was tested. Supplying the MON with 10 mM fructose caused a drop in the normalised lactate signal to 0.18 ± 0.01 . Increasing the fructose concentration to 25 mM led to an increase in normalised lactate signal to 0.62 ± 0.02 , this still being less than the lactate signal in the presence of 10 mM glucose.

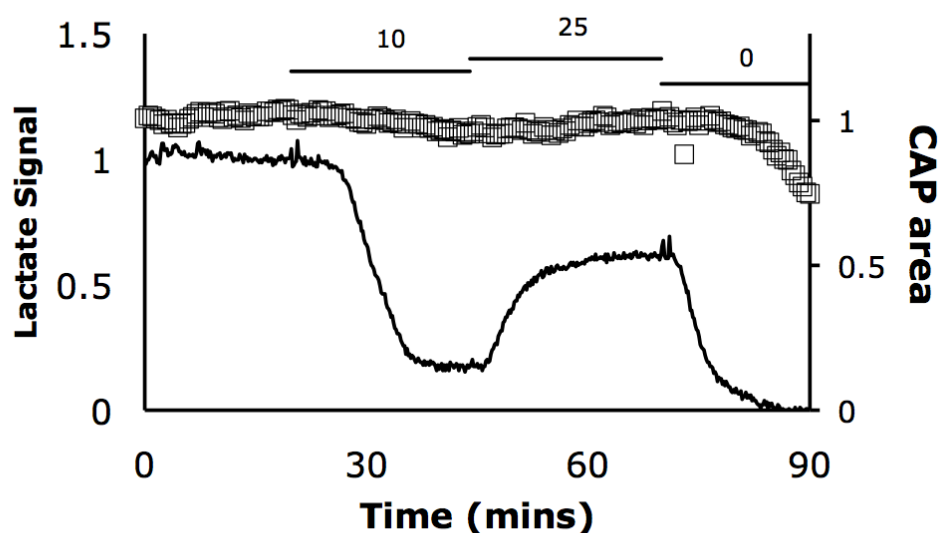


Figure 4.4 The effect of fructose on the lactate signal and CAP area of the MON. The experiment commenced in control aCSF (10 mM glucose) which was switched to 10 mM, 25 mM or 0 mM fructose (indicated by black bars) in the absence of glucose. The lactate signal (solid line, left axis) fell in 10 mM fructose, partially recovered in 25 mM fructose and was lost in 0 mM. CAP area (open squares, right axis) was maintained in 10 mM and 25 mM fructose but began to fall in 0 mM (aglycemia).

4.3.5 Lactate Production Requires Glycolytic Metabolism of Glucose

Figure 4.5.A shows the effect of a period of aglycemia upon CAP area and lactate signal in the MON. Aglycemia was induced by replacing the standard aCSF bathing the nerve with an aCSF solution made up lacking glucose. The extracellular lactate concentration fell to zero in a sigmoidal manner reaching 50% after 10.2 ± 0.2 mins with a latency to CAP failure of 28.4 ± 0.8 mins ($n = 4$).

The effect of inhibiting glycolysis upon lactate production and nerve activity was investigated by the addition of 1 mM iodoacetate (IA), an irreversible inhibitor of the glycolytic enzyme glyceraldehyde-3-phosphate dehydrogenase (GAPDH) (see Chapter 1, Fig. 1.2). Figure 4.5.C shows that addition of IA to the aCSF resulted in a rapid decrease of lactate concentration in the nerve reaching 50% after 5.5 ± 0.2 mins. This was followed by a complete failure of the CAP with a latency to failure of 16.7 ± 1.1 mins ($n = 4$). Both of these falls were significantly accelerated in comparison to those seen after induction of aglycemia by removal of glucose from the aCSF ($p < 0.05$) (see also Fig. 4.8.C-D).

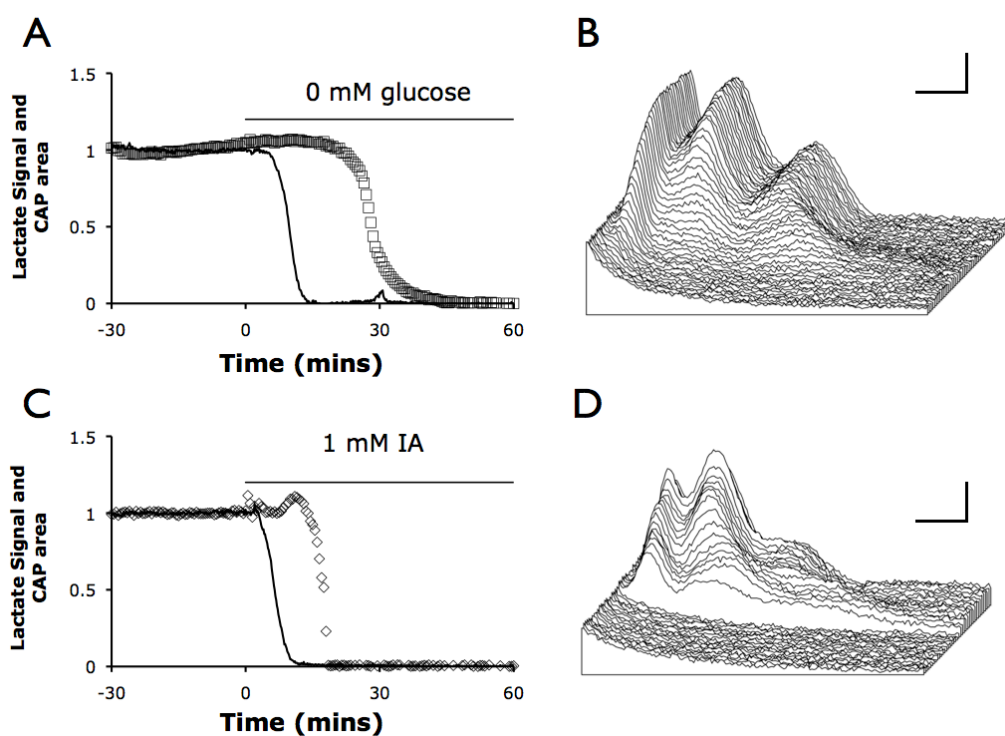


Figure 4.5 The effect of aglycemia and glycolytic inhibition on the MON CAP and lactate release. **A.** Induction of aglycemia caused a fall in extracellular lactate as monitored by a lactate-sensitive biosensor (solid line), which was followed by a delayed fall in CAP area (open squares) ($n = 4$). **B.** CAP traces during aglycemia, rearmost traces are first chronologically with traces commencing at $t = -10$ min from A. The fall in CAP area over time is clearly seen. **C.** Inhibiting glycolysis using 1 mM sodium iodoacetate (IA) caused a qualitatively similar effect, but this was accelerated for both lactate and CAP area in comparison to aglycemia ($n = 4$). **D.** CAP traces during exposure to IA. Scale bars for B and D are 1 ms (x-axis) and 1 mV (y-axis).

4.3.6 Inhibition of Oxidative Metabolism in the MON

Oxidative energy metabolism was blocked by using 1 mM NaCN to inhibit the electron transport chain (See Chapter 1 Fig. 1.3). The blockade of the electron transport chain causes a rapid energy deficit and depolarisation of axons in rodent optic nerve (Leppanen and Stys, 1997). The disruption of axonal function in this manner is seen as a fall in CAP area to 0 after less than 10 mins. Lactate concentration in the MON initially increased after cyanide administration, but gradually fell to below the control concentration.

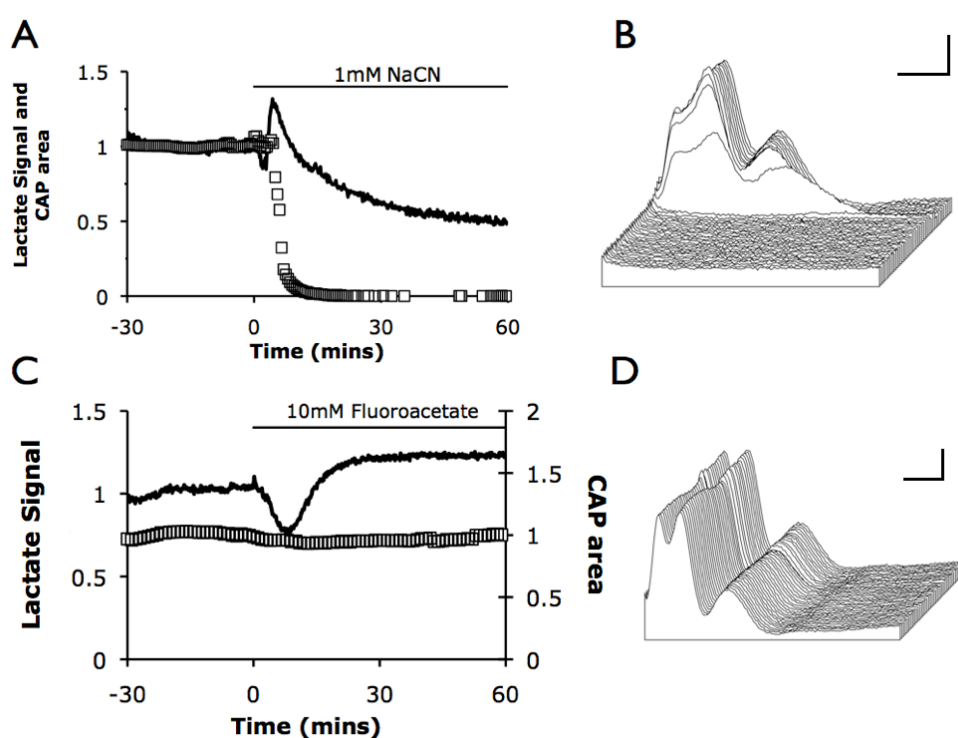


Figure 4.6 Inhibiting oxidative metabolism in the MON affects lactate production. **A.** Non-specific inhibition of the electron transport chain by 1 mM NaCN. Cyanide caused a very rapid fall in CAP area (open squares, right axis) and an initial rise in lactate followed by a slow but incomplete fall (solid line, left axis) ($n = 3$). **B.** CAP traces during cyanide exposure, rearmost traces are first chronologically with traces commencing at time = -10 min from A. **C.** Disruption of TCA cycle flux in astrocytes by 10 mM sodium fluoroacetate (FA). Normalised CAP signal is shown on the right y-axis for clarity ($n = 3$). **D.** CAP traces during exposure to FA. Scale bars for B and D are 1 ms (x-axis) and 1 mV (y-axis).

Selective disruption of astrocyte energy metabolism was investigated by applying 10 mM sodium fluoroacetate (FA) to the nerve. FA is rapidly taken up by astrocytes where it exerts toxic effects by inhibiting the TCA cycle (Fonnum et al., 1997). FA is first converted to fluorocitrate which then acts as a suicide inhibitor of the enzyme aconitase (Swanson and Graham, 1994). Fig. 4.6 shows that 10 mM FA had no effect on CAP area but affected the lactate concentration. Lactate initially decreased before increasing to a concentration above the control value prior to FA exposure, 20 mins after FA exposure the normalised lactate signal was 1.23 ± 0.01 relative to baseline.

4.3.7 Glycogen Metabolism Contributes to Extracellular Lactate

The observation that inhibition of glycolysis caused a more rapid loss of lactate and CAP area than bathing the nerve in glucose-free aCSF raised the possibility that glycogen metabolism may be contributing to the lactate signal. Astrocytic glycogen is used to form lactate which fuels axons during aglycemia in the mouse optic nerve (Brown et al., 2003; 2005). The glycogen phosphorylase inhibitor 1,4-dideoxy-1,4-imino-D-arabinitol (DAB) has been successfully used to prevent glycogen metabolism in the optic nerve (Walls et al., 2008). DAB was used at a concentration of 1 mM as would achieve the greatest inhibition of GP within the concentration range of DAB that Walls et al. recommended for experimental use. The effect of DAB on MON lactate release was examined and it was found that incubating MONs in aCSF containing 1 mM DAB and 10 mM glucose caused the lactate release to fall upon addition of DAB. Twenty minutes after introduction of aCSF containing DAB the normalised lactate signal was 0.78 ± 0.02 , there was, however, no effect on CAP area (Fig. 4.7.A). Under control conditions in the MON preparation this result shows that $22 \pm 2.4\%$ ($n = 3$) of extracellular lactate is the result of glycogenolysis.

The glycogen shunt model of brain energy metabolism (Shulman et al., 2001) predicts that under increased energy demands, the contribution of glycogen to ATP generation will increase. This theory was examined by stimulating MONs at a higher frequency than the control frequency of one CAP every 30 seconds. A stimulus frequency of 10 Hz increased the lactate signal by 50 % and led to a small increase in CAP area, due to broadening of the CAP area. Applying DAB to MONs stimulated at 10 Hz resulted in a decrease in the lactate signal (Fig. 4.7.B). The relative decline in lactate in the combined presence of DAB and 10 Hz stimulation was greater than that observed with DAB under control conditions. The proportion of lactate derived from glycogen metabolism was taken as the relative fall in lactate signal between pre-incubation and 20 mins after incubation with 1 mM DAB, which at 10 Hz was $33.9 \pm 2.0 \%$, whereas at 0.03 Hz glycogen accounted for $22.2 \pm 2.4 \%$, a significantly lower contribution ($p < 0.001$) (Fig. 4.7.C).

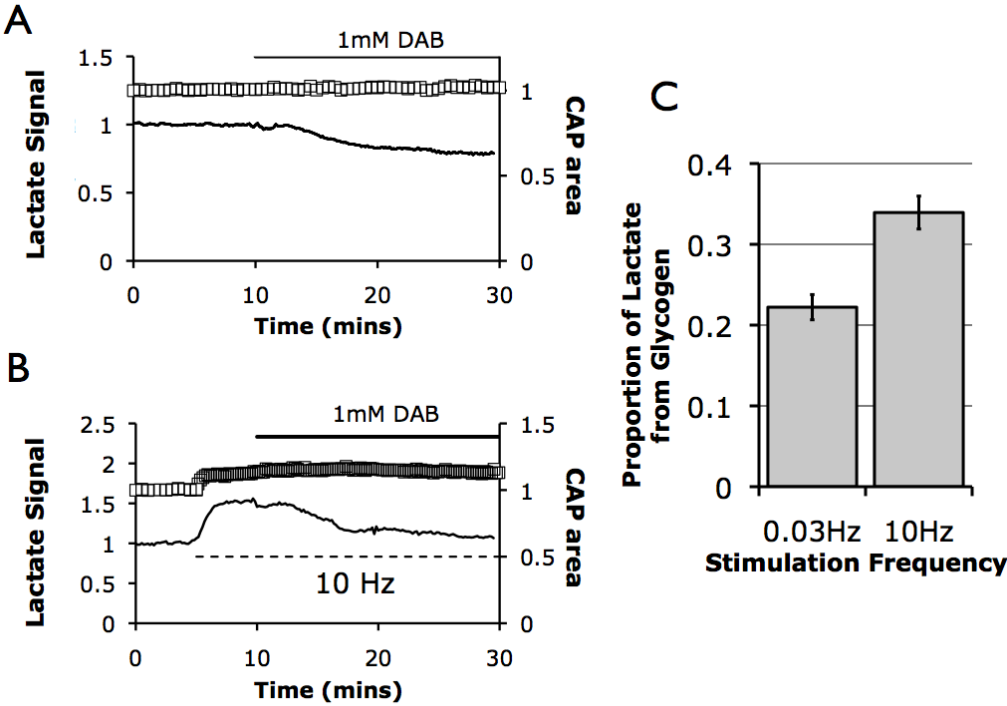


Figure 4.7 The contribution of glycogen metabolism to lactate production and release. **A.** 1 mM DAB caused a decrease in lactate signal in the MON (solid line, left axis) without affecting CAP area (open squares, right axis). **B.** Stimulating the nerve at a higher frequency (10 Hz) increased lactate production in the MON, and addition of 1 mM DAB during the 10 Hz stimulation resulted in a decrease in lactate signal. **C.** The ratio of lactate signal prior to, and after application of 1 mM DAB was calculated from A and B. A greater proportion of lactate was derived from glycogen when the nerve was under increased metabolic demand during the high frequency stimulus (n = 3).

The effect of both increasing or decreasing glycogen availability on lactate release and CAP area during aglycemia was determined. Glycogen availability was increased by pre-incubating nerves for 2 hours in 30 mM glucose (Brown et al., 2003), to negate any effects of increased glucose in the extracellular space prior to aglycemia the nerve was exposed to 10 mM glucose for 10 minutes before glucose withdrawal. Based on Fig. 4.1.B, this should be sufficient time for the complete exchange of solutions. Using pre-incubation in 30 mM glucose to increase glycogen content resulted in an increase in the latency to both the fall of lactate released by the nerve and CAP failure. Lactate concentration reached 50 % after 12.2 ± 1.7 mins and the latency to CAP failure was 33.2 ± 1.1 mins (Fig 4.8.A). To achieve the opposite effect of limiting glycogen availability during aglycemia nerves were exposed to 1 mM DAB (a glycogen phosphorylase inhibitor) throughout the experiment. Although DAB causes an increase in the glycogen content it is rendered inaccessible by the inhibitory effect of DAB on glycogen phosphorylase (Walls et al., 2008). DAB caused the lactate concentration to reach 50 % after 7.8 ± 1.0 mins and CAP failure to occur after 23.3 ± 1.5 mins (Fig 4.8.B).

Figure 4.9 shows the effect on CAP area and lactate release in the MON of: aglycemia, aglycemia with up-regulated glycogen, aglycemia in the presence of DAB, and for comparison the effect of inhibition of glycolysis by IA. All conditions led to loss of the lactate signal prior to CAP failure which was complete in all cases. For comparison the data are presented in figure 4.9.C-D, and all data points for CAP failure and loss of lactate signal were statistically significant from the control condition, which was aglycemia after 2 hours pre-incubation in 10 mM glucose ($p < 0.05$).

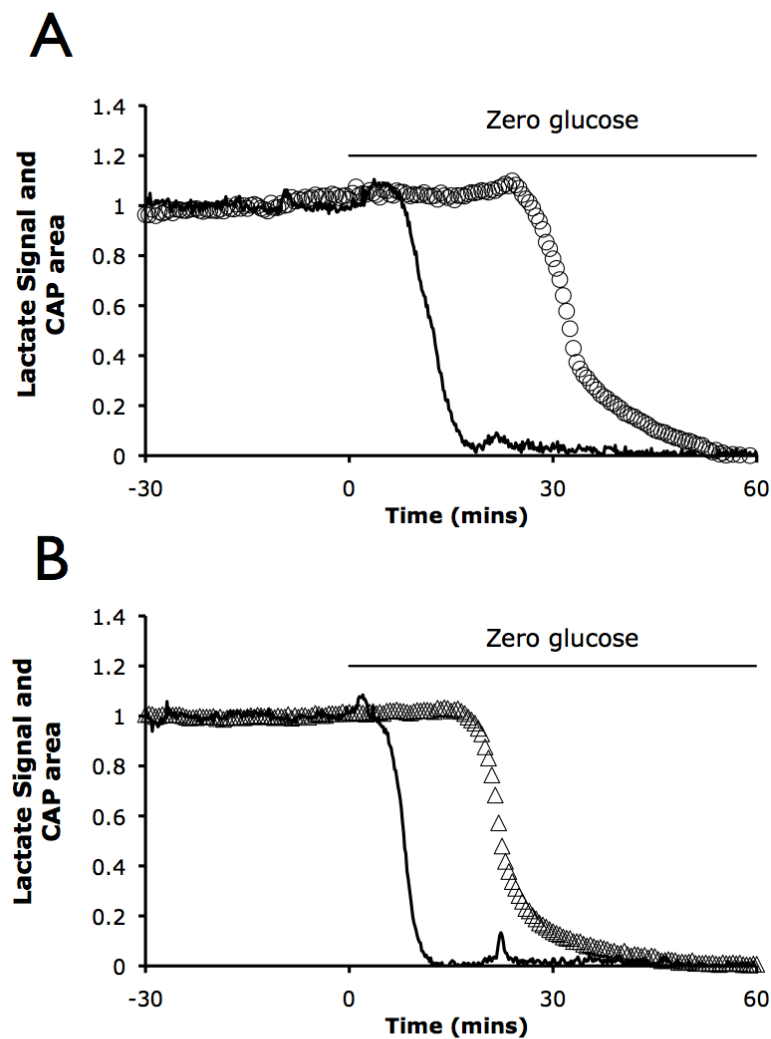
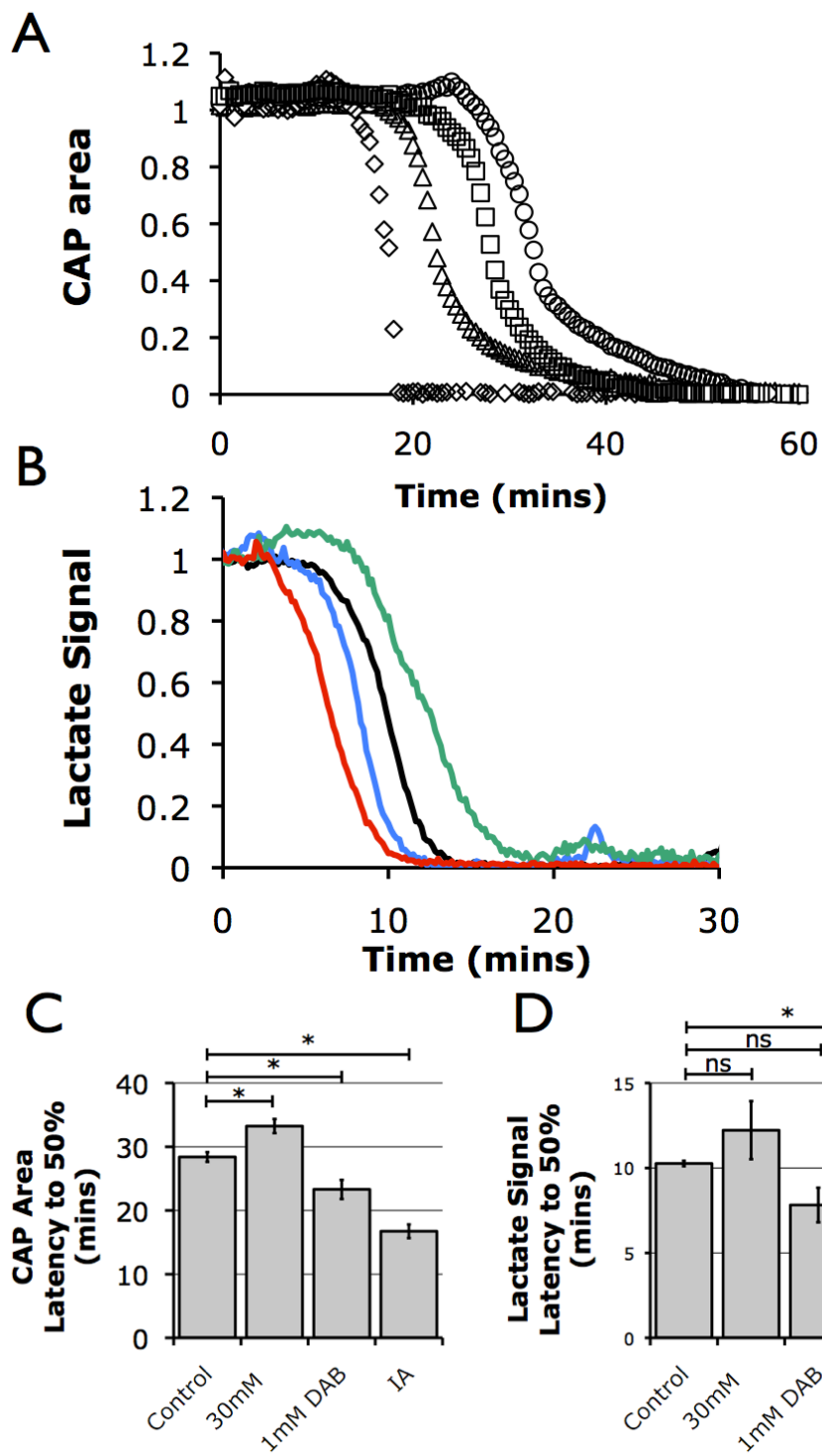


Figure 4.8 Increasing glycogen content and decreasing glycogen availability in the MON affects the latency to failure of the CAP and the fall in lactate signal during aglycemia. **A.** Glycogen stores were up-regulated by a pre-incubation of MONs in 30 mM glucose aCSF for 2 hours prior to aglycemia. In the 10 mins before aglycemia 10 mM glucose aCSF was introduced to allow glucose concentration in the nerve to equilibrate to control levels. Increasing glycogen availability delayed CAP failure (open circles) and loss of lactate signal (solid line). **B.** Glycogenolysis was inhibited by 1 mM DAB throughout the experiment which had no effect on the CAP when glucose was available but accelerated the decline in CAP area (open triangles) and loss of lactate signal (solid line) during aglycemia ($n = 4$). See figure 4.9 for comparison.

Figure 4.9 (following page) Comparison of the effects of aglycemia on CAP area under a range of metabolic conditions. **A.** Normalised CAP area in the presence of glycolytic inhibition with 1 mM IA (\diamond), 1 mM DAB (Δ), aglycemia after pre-incubation in 10 mM glucose (\square), and aglycemia after pre-incubation in 30 mM glucose (\circ). **B.** Normalised lactate signal with glycolytic inhibition with 1 mM IA (red), aglycemia in the presence of 1 mM DAB (blue), aglycemia after pre-incubation in 10 mM glucose (black) and aglycemia after pre-incubation in 30 mM glucose (green). **C.** Comparison of delay to CAP failure. **D.** Comparison of lactate falls; n = 4 for all, * denotes $p < 0.05$, n.s.: not significant.



4.4 Discussion

There is an ongoing controversy regarding lactate and the role that it plays in CNS energy metabolism. One body of evidence that challenges the primacy of glucose as the main energy substrate used by neurons and instead suggests that lactate is a key source of energy (Pellerin and Magistretti, 1994; Mangia et al., 2003; Pellerin, 2004). A counter argument maintains the traditional and dogmatic view that the major source of energy for axons is glucose and that lactate is not a significant energy substrate for neurons (Chih and Roberts, 2003; Leegsma-Vogt et al., 2003). Either way, the findings in this field have important implications for normal brain physiology, clinical conditions, and the principles underlying brain imaging (Bonvento et al., 2005). Research into CNS energy metabolism has often focused on grey matter as it has a higher metabolic rate than white matter (Dienel, 2009), and is widely accepted as the tissue responsible for cognition. However, white matter (which comprises 50 % of brain volume (Zhang and Sejnowski, 2000) should not be ignored, since it connects brain areas, is vulnerable to pathology and associated deficits in function (Goldberg and Ransom, 2002). Injury to white matter is a major source of disability following stroke and it is vulnerable to even short periods of ischemia (Pantoni et al., 1996). The experiments described in this chapter were carried out to determine whether lactate plays a role in white matter energy metabolism, and to shed further light on what is perhaps one of the more lively debates in neuroscience.

4.4.1 Biosensors for Real-Time Measurement of Lactate

The first objective of the experiments described in this chapter was to evaluate the use of a commercially-available enzyme-based lactate biosensor in order to measure lactate release from the optic nerve in real time. Prior to experimental use with tissue the sensor was checked for its specificity and calibrated in the perfusion chamber which was used to record electrical activity in the MON.

The specificity of the sensor's response to lactate was good, and the current response of the sensor was linear in a physiological range of lactate concentrations. A wide signal to noise ratio allowed for clear recordings to be made of changes in extracellular lactate even in the absence of a null sensor, which is not the case for many biosensor applications (Dale et al., 2005).

When biosensors are used to measure the concentrations of substances in the extracellular space (ECS) it is important to be aware of what constitutes the signal. A stable concentration of lactate in the ECS as measured by the sensor is achieved by a balance between cellular lactate release, cellular lactate uptake and lactate wash out into the tissue bath. This is shown schematically in Figure 4.10. Changes in the lactate concentration or lactate signal in these experiments are a summation of the relative contribution of these lactate fluxes.

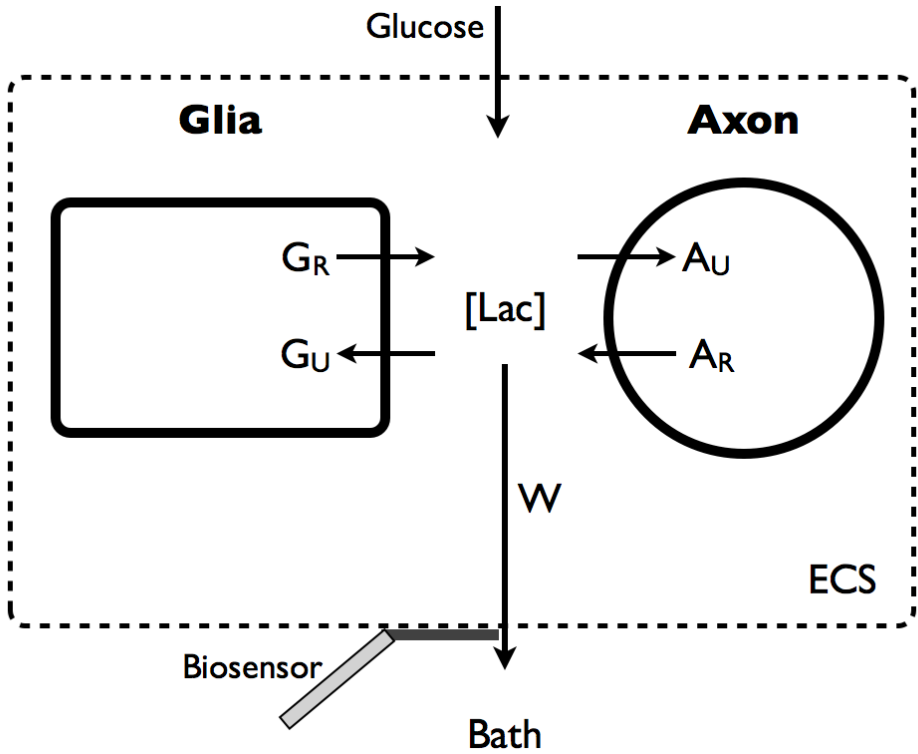


Figure 4.10 Schematic of the factors affecting extracellular lactate in the isolated mouse optic nerve preparation. A proxy for extracellular lactate [Lac], the signal recorded amperometrically by the biosensor, is a combination of lactate release by glia (G_R), release from axons (A_R), uptake by glia (G_U), uptake by axons (A_U), and (W) the washout from the ECS into the tissue bath across the porous membranes of the pia mater and arachnoid (broken line). The exact rates of these lactate fluxes, with the exception of W , cannot be directly determined by biosensors alone.

4.4.2 Extracellular Lactate in White Matter

Lactate is present in the extracellular space of the brain. In humans and rats the concentration of lactate in the brain ECS is greater than in plasma, suggesting significant lactate production within the limits of the blood brain barrier (BBB) (Abi-Saab et al., 2002). Blood lactate concentration is independent of lactate levels in the brain (Kuhr et al., 1988) meaning that lactate in the brain is produced locally i.e. within the BBB. The results presented in this chapter indicate that lactate is produced and released into the ECS of the mouse optic nerve (MON). The MON provides a useful model system for studying the role of lactate in white matter as it is devoid of synapses and neuronal cell bodies and thus is a simple model comprising of two cellular compartments (Butt et al., 2004). The MON can also be maintained *in vitro* for many hours while the ability of axons to conduct is monitored by recording the stimulus-evoked compound action potential (CAP). Using a lactate oxidase-based biosensor it has been shown here that the *in vitro* MON preparation has an extracellular lactate concentration of 0.44 mM under resting conditions. This lactate signal and the CAP are stable over a period of many hours indicating that lactate production is not associated with injured or otherwise compromised tissue.

The concentration of lactate in the brain ECS has been previously documented in a number of experimental systems. Typically under resting conditions a lactate concentration between 0.5 - 2 mM has been reported (Kogure et al., 1974; Medina et al., 1975). Quantification of lactate in the rat striatum using microdialysis revealed a baseline concentration of 0.56 mM (Taylor et al., 1994). The value obtained here in the optic nerve (0.44 mM) is possibly an underestimation due to low metabolic demand of the tissue at rest and the positioning of the lactate biosensor. Biosensors were positioned on the surface of the optic nerve in order to avoid the traumatic injury to the tissue that would occur with insertion of sensor into the nerve. The location of the sensing tip in contact with the nerve rather than inside it means that the

sensor is reading lactate release, which is a proxy of extracellular lactate (see Fig. 4.10). The signal from the sensor is proportional to the surface area that is in contact with the lactate containing solution. In comparison to the calibration readings there is a concentration gradient that will exist across the sensor leading to an under-estimation of lactate within the nerve ECS. It should also be noted that in the perfusion chamber system fresh aCSF is constantly flowing across the tissue (2 ml / min) which may enhance lactate clearance from the tissue (Fig. 4.10). These factors mean that the values obtained *in vitro* and the precise kinetics of the lactate response may vary considerably.

4.4.3 Glucose Availability and Extracellular Lactate

Blood glucose (unlike lactate) correlates with the concentration of lactate in the brain extracellular space: higher blood glucose levels result in increased glucose and lactate concentrations in the brain (Harada et al., 1993). The concentration of lactate in the MON is also related to the externally supplied glucose concentration, below about 5 mM. The value of 0.44 mM lactate was obtained at the control glucose concentration of 10 mM. Increasing the glucose concentration to 30 mM did not have a significant effect upon lactate, neither did lowering the glucose concentration to 5 mM. However, glucose concentrations of 2 mM and below caused a decrease in the lactate concentration measured. This relationship suggests that the lactate production from the nerve saturates at glucose concentrations of about 5 mM and above. This observation along with the stability of CAP conduction at these glucose concentrations points towards the nerve receiving an adequate supply of energy substrate. At 2 mM glucose the lactate concentration decreased but the CAP area remained stable. A reduction in CAP area was only seen at a glucose concentration of 0.5 mM indicating that the minimum glucose concentration that can support axonal activity is between 0.5 - 1 mM. Previous data from the MON shows that at 2 mM glucose and below glycogen-derived lactate supplements the glucose supply (Brown et al., 2003). Systemic glucose

concentration of 2 - 3 mM are considered to be hypoglycemic (Frier and Fisher 2007). However, in the isolated MON preparation the blood-borne delivery of substrates is circumvented. An aCSF glucose concentration of 2 mM is probably accompanied by a ECS glucose concentration of close to 2 mM which is close to the value observed in normoglycemic rat brain (Silver and Erecinska, 1994). The observation that extracellular lactate falls at glucose concentrations of 2 mM and below, whilst the CAP is only affected at a glucose concentration of 0.5 mM possibly indicates that increased oxidation of lactate is occurring and therefore less lactate is released into the extracellular space. Lactate is capable of supporting the MON as the sole energy substrate (Brown et al., 2001) so it is plausible that under these conditions oxidative metabolism of lactate contributes towards ATP production, and compensates for the reduced availability of glucose.

4.4.4 Fructose Metabolism in the Optic Nerve

When fructose was the sole substrate in the aCSF the lactate release was considerably lower than that seen with equimolar glucose (Fig. 4.4). Even at 25 mM fructose the lactate signal was below that seen with 10 mM glucose. This matches observations in cultured astrocytes where the lactate release in the presence of fructose was also less than that when the cells were supplied with glucose (Bergbauer et al., 1996). Metabolism of fructose in astrocytes is most likely limited by the reduced affinity of fructose as a substrate for hexokinase in comparison to glucose (Sols and Crane, 1954). Since some lactate is produced in the presence of fructose, and fructose is converted ultimately to fructose-6-phosphate (see Fig. 1.2), this reinforces that glycolysis is the source of lactate in the MON. Astrocytes in culture have to rely on hexokinase activity to metabolise fructose as they lack fructokinase activity (Bergbauer et al., 1996).

In contrast to these findings in cell culture, fructokinase immuno-reactivity is visible in optic nerve astrocytes and selected axons (Meakin et al., 2007). The role of fructokinase (ketoheokinase) in the brain is not currently known, but its presence suggests at least some fructose metabolism does occur in the brain.

4.4.5 Metabolic Inhibition

Lactate is produced as a possible end product of glycolysis; glucose is metabolised by the chain of glycolytic enzymes resulting in the formation of pyruvate and the generation of energy in the form of ATP. Pyruvate can then be further metabolised oxidatively in mitochondria, or converted to lactate by the enzyme lactate dehydrogenase which forms NAD^+ from NADH in the same reaction. The necessity of glycolysis for lactate formation in the MON was demonstrated by applying iodoacetate (IA), an inhibitor of the glycolytic enzyme glyceraldehyde 3-phosphate dehydrogenase. IA rapidly halted lactate production and resulted in CAP failure, as axonal activity is lost due to the dependence of membrane potential upon a steady supply of glucose. IA has previously been shown to cause a depolarisation of axonal membranes in the optic nerve (Leppanen and Stys, 1997) with the combined effect on all axons seen as the failure of the CAP (Fig. 4.5.C, D).

Aerobic glycolysis is a term given to the glycolytic production of lactate in the presence of physiologically adequate oxygen. Aerobic glycolysis may play an important role generating the energy required for normal neural activity in white matter, but it is not sufficient on its own to support CAP conduction. Figure 4.6 shows that after application of cyanide the CAP fails rapidly. Cyanide inhibits cytochrome c oxidase which disrupts the electron transport chain halting the aerobic production of ATP. The rapid loss of action potential conduction shows that white matter requires aerobic generation of energy to function normally. This has previously been reported in the rodent optic nerve

(Stys et al., 1992). The initial increase in lactate after application of cyanide could be due to either increased glycolytic production of lactate, a reduction in oxidation of lactate or a combination of both.

A subset of MON axons maintain function during anoxia, or in the presence of cyanide (Tekkok et al., 2003). This observation was not seen here since cyanide caused complete failure of the CAP. This discrepancy may be explained due to strain differences between mice used. The CD-1 strain shows the same response as the rat optic nerve which is not resistant to anoxia (Waxman et al., 1994). The age of animals is also a factor as anaerobic function in the mouse optic nerve declines with age (Hamner et al., 2011). Animals used for experiments in this chapter were chosen from within a weight range rather than a specific age, although all animals used were considered adult. The mechanism underlying age-dependent resistance to anoxia is not known, thus it is difficult to explain why no function persisted during chemical anoxia in these mice. Optic nerve diameter is not thought to be important, but there may be differences in glucose metabolism although this is purely speculative at this stage (Hamner et al., 2011).

An observation that has not been previously described is the effect of blocking oxidative metabolism on the lactate concentration in white matter. Cyanide caused a transient increase in lactate before it reached a steady concentration at a value less than that seen before the onset of chemical anoxia. The need for oxidative metabolism to support CAP function may be attributed to the axons which have a high oxidative demand. The stable conduction of CAPs in the MON may not require astrocytic oxidative metabolism as selectively blocking TCA cycle flux in astrocytes with fluoroacetate (FA) does not result in CAP failure. Fig. 4.6 shows the effect of FA, which is a selective toxin for astrocytes, as it is preferentially taken up by these cells where it inhibits the enzyme aconitase (Fonnum et al., 1997). However, experiments with astrocytes in culture show that FA may not impair ATP production as FA did not cause a drop in intracellular ATP (Swanson and Graham, 1994).

4.4.6 Glycogen as a Source of Lactate

Glycogen, the only storage carbohydrate available in the mammalian brain, is located exclusively in astrocytes and can act as an energy reserve providing fuel for axons in the absence of glucose (Ransom and Fern, 1997). Lactate is a product of glycogen metabolism in white matter. Experiments in the optic nerve show that it is lactate that is produced from glycogen that fuels axons during periods of glucose withdrawal (Brown et al., 2007). The availability of glycogen can be influenced prior to aglycemia by either up- or down-regulating glycogen content or pharmacologically blocking glycogen metabolism. The effect of these interventions on axonal conduction during aglycemia has previously been documented in the MON (Brown et al., 2005). The experiments performed by Brown et al. were repeated, but with the addition of monitoring extracellular lactate (Fig. 4.8 and 4.9). It was observed that extracellular lactate persisted longer during aglycemia when glycogen stores were elevated, and that the lactate signal was lost sooner when glycogen metabolism was blocked. The timing of the fall in extracellular lactate is consistent with the fall in glycogen content during aglycemia, as both reach their nadir before CAP conduction begins to fail.

Whether the function of astrocytic glycogen *in vivo* is as a dormant energy reserve may be questionable; consciousness is rapidly lost when the brain is deprived of glucose although these circumstances are rare. Perhaps a more physiologically realistic function of glycogen is as an energy buffer, which may act as a source of energy substrate during times of heightened energy demand. An example of this is that glycogenolysis supports high frequency firing of axons in the optic nerve (Brown et al., 2005). The degree of the increase in demand required to cause mobilisation of glycogen stores need not be great. Glycogenolysis occurs in response to normal sensory stimuli (Swanson et al., 1992), an observation that links glycogen metabolism to normal physiological function. It has been proposed that glycogen may be

used to fuel specific cellular functions in astrocytes which are then up-regulated during neural activity.

4.4.7 Evidence for a Glycogen Shunt

The glycogen shunt model proposes that a proportion of glucose metabolism in the brain is processed via glycogen and that glycosyl residues are constantly being added and removed from the glycogen skeleton as part of normal energy metabolism (Shulman et al., 2001). A glycogen shunt is believed to operate in muscle tissue and evidence shows that the glycogen shunt plays a large role in astrocyte energy metabolism (Walls et al., 2009).

In muscle the glycogen shunt pathway is responsible for the formation of lactate during aerobic exercise (Shulman, 2005). If the glycogen shunt is present and active in neural tissue it could be the source, or a contributing source, of lactate production in the brain. Blocking glycogenolysis caused a fall in extracellular lactate, which reveals that glycogen metabolism contributes to lactate release in the MON under minimally stimulated conditions (Fig. 4.7.A). This supports the notion of constant glycogen metabolism; if glycogen metabolism was only required during periods of high activity or hypoglycemia, then it would not be expected that resting lactate would be affected by the availability of glycogen. The contribution of glycogen to lactate production increases under conditions of higher metabolic demand (Fig 4.7.B,C), an observation that is predicted by the glycogen shunt model (Shulman et al., 2001). High-frequency stimulation of the MON was used to place a high metabolic demand on the tissue. Stimulation frequencies were within the physiological range of the MON (Brown et al., 2005), but the stimulus is unlikely to reflect the firing pattern of the nerve *in vivo*. In astrocytes stimulated by noradrenaline, glycogen shunt activity accounts for 40 % of glucose metabolism (Walls et al., 2009); it appears that glycogen shunt

activity may account for a similar fraction of lactate production in the MON during high-frequency stimulation.

Metabolism of glycogen that results in the formation of lactate may seem an inefficient pathway of energy production when compared to full oxidation of glucose, but under certain conditions it makes metabolic sense. Obtaining glycosyl residues from glycogen is advantageous due to the speed with which glycogen phosphorylase can be activated (Shulman and Rothman, 2001). Computer modelling suggests that fuelling the requirements of astrocytes by glycogenolysis ensures that glucose supplies are preserved for use by neurons (DiNuzzo et al., 2010). The cellular architecture of astrocytes may also be responsible for the use of the glycolytic pathway under fully oxygenated conditions. Astrocytes have many cytoplasmic processes that are too narrow to contain mitochondria, and this could make them at least partly reliant upon glycolytic metabolism of glycogen resulting in lactate production. The increase in lactate production and the greater proportion of lactate which is derived from glycogen during a 10 Hz stimulus can be explained by the rapid rise in energy demand that occurs in astrocytes in response to increased neural activity being fuelled by this pathway. Astrocytes express the transporters necessary for this rapid and high level of lactate trafficking across the membrane (Hertz and Dienel, 2005). One of the major functions of astrocytes that is linked to neural activity is K^+ homeostasis via K^+ uptake and spatial buffering. Ion pumping which is necessary for control of K^+ concentrations inside and outside the cell is associated with glycolysis, and may be the source of lactate production during activation in the optic nerve; this will be explored further in Chapter 5.

Chapter Five

**Activity-dependent
increases in white matter
lactate production are
mediated by
extracellular potassium**

5.1 Introduction

Neural tissue is subject to fluctuating levels of activity, reflected in variations in the energy demands of the tissue. The principle that local increases in energy demand is coupled to increases in glucose and oxygen consumption underpins the rationale behind neuroimaging techniques such as positron-emission tomography (PET) and functional magnetic resonance imaging (fMRI) (Magistretti and Pellerin, 1999). Traditionally it has been assumed that the glucose is metabolised oxidatively in both the resting and active brain (Sokoloff et al., 1977). As brain imaging became widely adopted as a method for studying brain function observations emerged that questioned the traditional view. It was found that the increase in glucose uptake was not matched by an equivalent level of oxygen consumption (Fox et al., 1988; Vaishnavi et al., 2010). The un-coupling between glucose and oxygen consumption raised the possibility that a major contributor to energy metabolism during neural activity is glycolysis and lactate production.

5.1.1 Lactate and Increased Neural Activity

The brain is a highly oxidative organ but increased neural activity is accompanied by an increase in glycolysis. Indirect evidence for lactate production during neuronal activity comes from the increase in glucose metabolism that is not matched by an increase in oxygen consumption necessary for full oxidative metabolism of this glucose (Fox et al., 1988). This effect shows regional variability and is greatest in the pre-frontal cortex and medial and lateral parietal cortex (Vaishnavi et al., 2010).

The increase in glycolysis and lactate production have been linked to recycling of synaptic glutamate. In the previous chapter the results showed that lactate is released from white matter, and that an increase in the rate of action potential conduction led to greater lactate release. These results suggest that

an increase in glycolysis that out-weighs oxidative phosphorylation may also be a response to rising energy demand in white matter.

5.1.2 Lactate and Pathological Conditions

An increase in lactate production in the CNS has also been associated with pathological conditions. Determination of lactate concentration in the blood is used as a clinical test, with increases in lactate interpreted as a negative sign for a patient's outlook (Schurr, 2002). Increases in brain lactate concentration occur as part of the ageing process (Ross et al., 2010) and this elevated lactate in the brain may be a risk factor for Alzheimer's disease (Xiang et al., 2010). Lactate is also raised after stroke and traumatic insults and has long been considered a marker of "brain death" (Paulson et al., 1971). This association of raised lactate with poor prognosis has proven difficult to overcome despite evidence that lactate is an important energy substrate for the brain during recovery from hypoxia (Schurr et al., 1997a; 1997b). The energy demands of the injured tissue are likely to be greater than normal and lactate accumulation at the injury site possibly reflects the tissues enhanced need for energy substrate (Chen et al., 2000).

5.1.3 Aims

There is a lively debate ongoing as to the nature of lactate increases that accompany neural activity. The association between raised lactate and pathological conditions has resulted in a negative dogma surrounding brain lactate even though lactate is produced during normal neural activity. Conflicting evidence and opinions mean that the origin, movement and disposal of lactate are all as yet unresolved important questions. The aim of this series of experiments was to investigate the dynamics of extracellular lactate produced during times of high neuronal activity in white matter. The

mouse optic nerve (MON) was selected as a model tissue in which to perform these experiments.

5.2 Methods

The methods used in this chapter are as detailed in Chapter 2 and Chapter 4.

5.3 Results

5.3.1 Extracellular Lactate Increases During Axonal Activity

5.3.1.1 Effect of Stimulus Frequency

To observe how extracellular lactate concentration related to tissue metabolic demand in the MON, the demand on the tissue was increased by evoking CAPs at higher frequencies than the 0.33 Hz used under standard conditions. The MON was stimulated for 2 minutes at a range of frequencies up to a maximum of 50 Hz while the lactate concentration and CAP were recorded. Figure 5.1.A shows an example trace from one experiment where a MON was stimulated at a range of frequencies between 2 and 50 Hz, being allowed to recover between each stimulus train, with the traces from each stimulus set overlaid. The figure shows that as the stimulus frequency increases the evoked lactate concentration rises and then recovers towards baseline when the increased demand is over. The relationship between lactate concentration and stimulus frequency can be seen in figure 5.1.B, where a stimulation frequency of 60 Hz for 2 mins results in a peak normalised lactate signal of 2.12 ± 0.02 (Fig. 5.1.B).

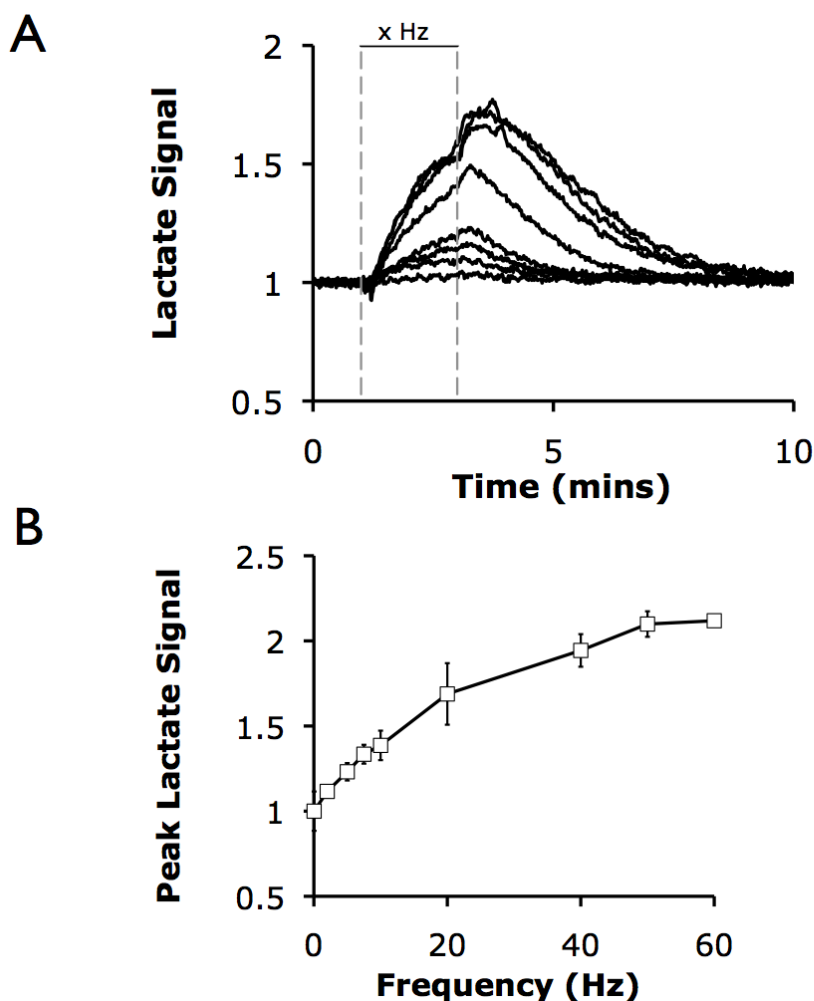


Figure 5.1 The effect of high frequency stimulus on lactate in the MON. **A.** The normalised lactate signal is shown for a single nerve stimulated for 2 mins at frequencies of 2, 5, 7.5, 10, 20, 40, 50 or 60 Hz. The period of increased stimulus frequency is shown by the bar and bordered by broken lines, at other times a CAP was evoked once every 30 s (0.033 Hz). **B.** The peak normalised lactate signal for each frequency is shown, data are mean from 3 nerves.

5.3.1.2 Effect of Stimulus Duration

The effect of the duration of increased stimulation frequency upon lactate concentration was also examined (Fig 5.2). A 50 Hz stimulus was applied to generate a defined number of CAPs between 100 and 6000 (i.e. a stimulus of between 2 and 120 seconds). The peak lactate above baseline rose rapidly for stimuli consisting of between 100 and 2000 action potentials but above this

number the increase appeared to saturate. The maximum increase in lactate signal was seen after a 50 Hz stimulus lasting 120 s (6000 action potentials) which was 2.37 ± 0.02 that of baseline lactate (Fig. 5.2.B).

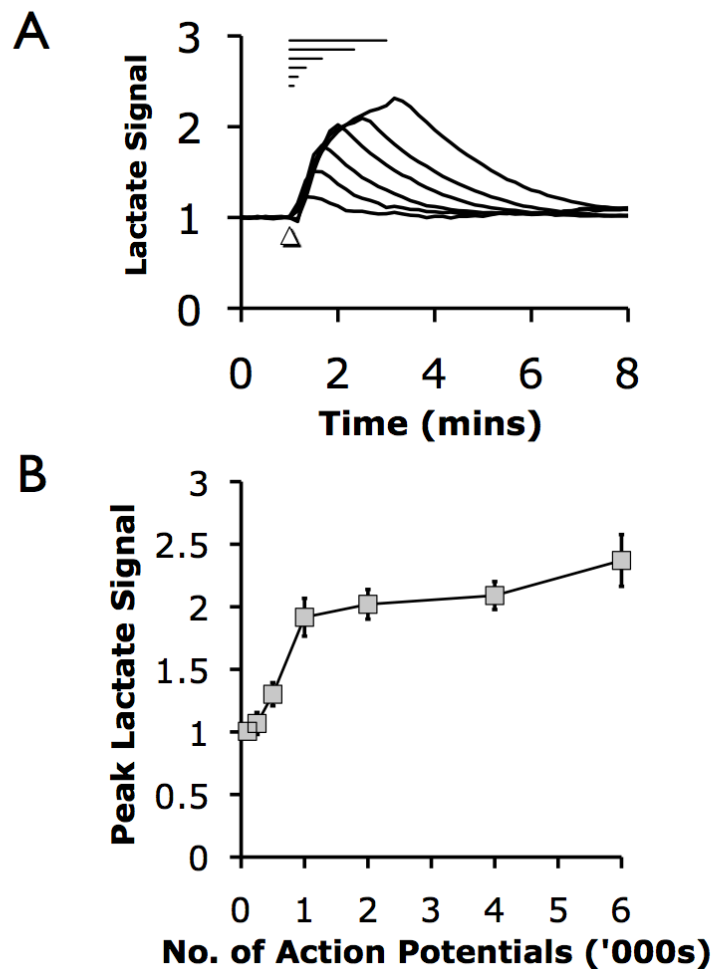


Figure 5.2 The effect of the duration of high frequency stimulus on the lactate signal in the optic nerve. A 50 Hz stimulus was applied to the optic nerve for a defined number of action potentials between 250 (5 s duration) and 6000 (120 s duration). **A.** Lactate response to these stimuli each applied 3 times and averaged for a single nerve. Arrow indicates onset of stimuli and horizontal lines show the durations. Each increase in duration of the stimulus caused a further increase in the lactate signal. **B.** Peak lactate signal for each stimulus ($n = 3$).

5.3.1.3 Analysis of the Lactate Response

Figure 5.3 shows the mean lactate trace ($n = 3$ from a single nerve) of a 2 mins 50 Hz stimulus, with the period of the stimulus indicated as the shaded area. This chart shows that in the first few seconds after stimulus onset there was an initial slight decrease in lactate followed by a rapid increase. Upon returning to stimulating once every 30 s there was a further increase in lactate followed by a gradual return to baseline lactate over a period of 8 -10 mins. The initial dip in lactate was quite small in comparison to the increases seen, and was not always clearly observed at lower stimulation frequencies. The increase in lactate seen at the end of a stimulus was also more pronounced at higher frequencies.

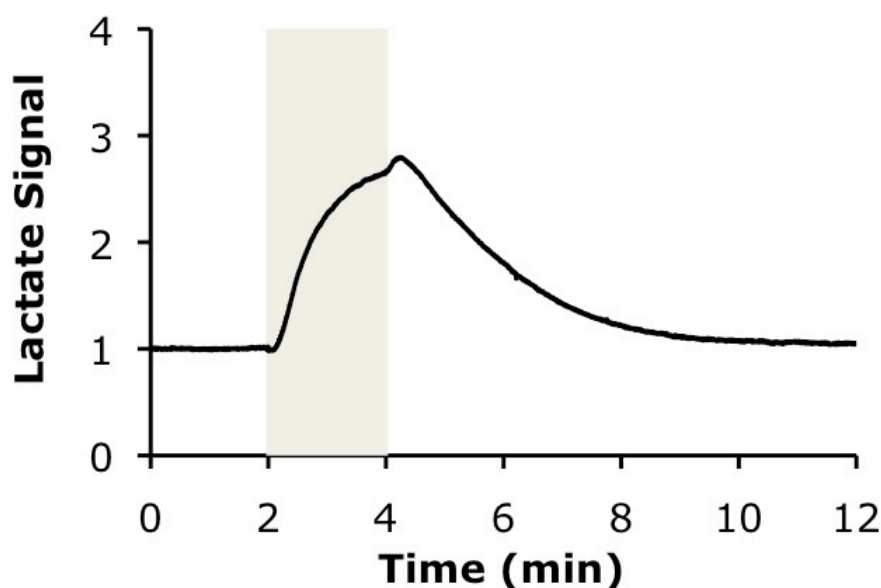


Figure 5.3 Detail of the lactate response to a high-frequency stimulus. An averaged trace of the lactate response of the MON to a 2 min 50 Hz stimulus ($n = 3$). Lactate dips at start of a period of high frequency stimulation and peaks after the stimulus is stopped.

5.3.1.4 Effect of Na⁺ channel block

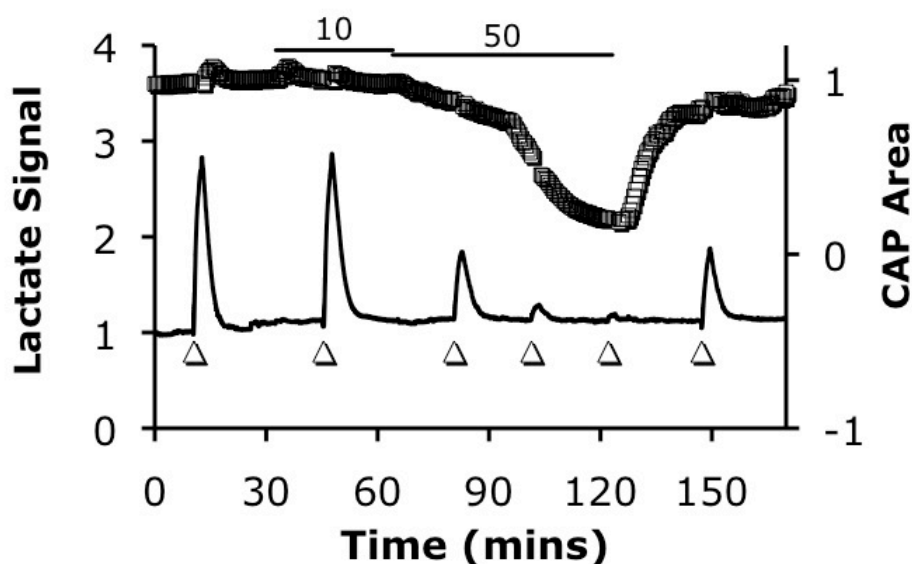


Figure 5.4 The effect of Na⁺ channel block on CAP area and lactate signal in the MON. A representative experiment is shown where the Na⁺ channel blocker TTX was applied to the MON whilst periodic stimuli at 50 Hz for 2 mins were performed (arrows). The concentration of TTX is indicated in nM above the trace, CAP area is represented by open squares (right axis) and lactate via the solid line (left axis). 10 nM TTX had no apparent initial effect so the concentration was increased to 50 nM, which caused a decrease in CAP area. At 50 nM TTX also lowered the lactate response to a high-frequency stimulus with the peak amplitude of lactate for a stimulus decreasing over time. Washout of TTX restored CAP area and partially restored the lactate response to a high-frequency stimulus. The figure shows a single experiment.

The association between lactate production and axonal activity in the form of action potential propagation was further examined by applying the sodium channel blocker TTX (tetrodotoxin). Initially a 10 nM concentration of TTX was applied to the nerve along with a 2 min 50 Hz stimulus. This stimulus produced an increase in lactate that was the same as that seen prior to TTX application, however, there was also no effect observed upon the CAP area

suggesting that ion movement was not significantly affected at this concentration. The TTX concentration was then increased to 50 nM which caused a decline in CAP area and a decrease in the peak lactate response to a 2 min, 50 Hz stimulus. The lactate response to this stimulus then further decreased after subsequent stimuli while there was no change in baseline lactate between stimuli. Washing off the TTX saw a partial recovery in CAP area and peak lactate response to a high frequency stimulus. This experiment with TTX was only carried out once. This must be taken into account when making conclusions from it. The clarity of the effect and its reversibility suggest that future repeats will confirm these results.

5.3.2 Extracellular Potassium Stimulates Lactate Production

5.3.2.1 Effect of Extracellular K^+

High amounts of neuronal activity lead to an increase in extracellular potassium ($[K^+]_o$) in the rodent optic nerve (Ransom et al., 2000; Brown et al., 2001), therefore, the effect of experimentally-induced changes to $[K^+]_o$ upon the extracellular lactate concentration in the MON was examined by exposing nerves to concentrations of K^+ above the control of 3 mM from 4.5 - 15 mM. Increasing the $[K^+]_o$ for 10 mins resulted in a dose-dependent increase in the lactate concentration (Fig. 5.5). The lactate began to fall after $[K^+]_o$ was returned to 3 mM, but after 20 mins had not returned to baseline levels (Fig. 5.5.A). The peak lactate signal at varying $[K^+]_o$ is shown in Fig. 5.5.B. The maximum peak relative to the normalised lactate signal was 2.06 ± 0.14 with a $[K^+]_o$ of 15 mM. The relationship was linear between 3 and 15 mM $[K^+]_o$ unlike that seen for high frequency stimulation, where the lactate signal appeared to saturate when it reached a normalised value of over 2.0. Higher $[K^+]_o$ than 15 mM were not used as these are not seen under physiological conditions (Heinemann and Lux, 1977; Ransom et al., 1986).

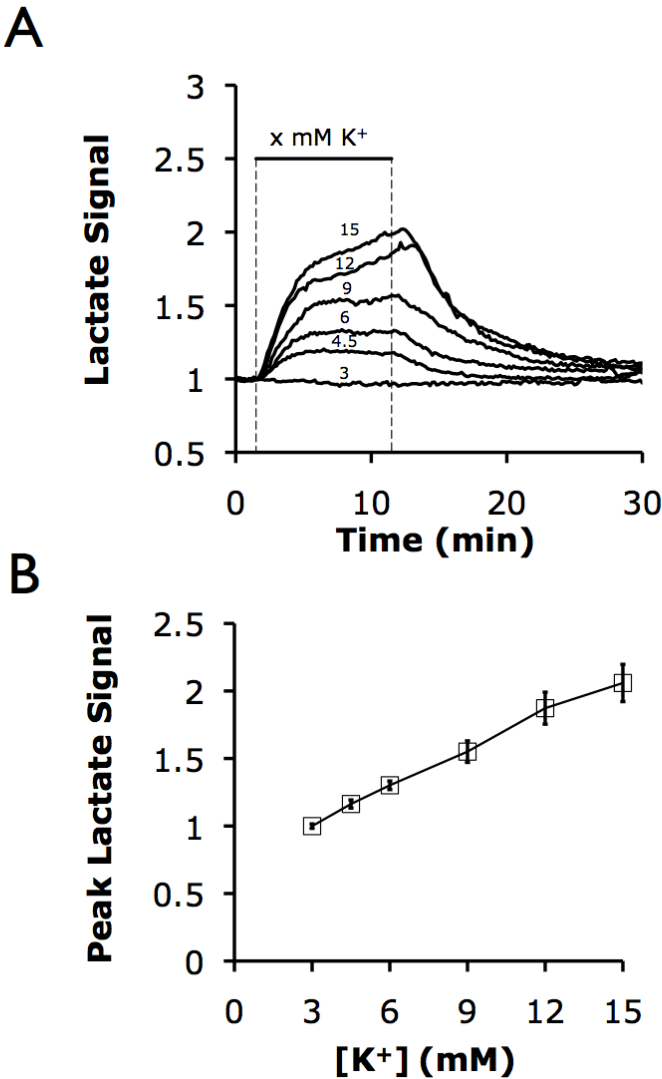


Figure 5.5 The effect of $[K^+]_o$ on lactate release from the optic nerve. Increasing $[K^+]_o$ above the control concentration of 3 mM resulted in an increase in lactate production in the MON. **A.** Normalised lactate signal for a 10 mins exposure to x mM K^+ (given by number above trace). Traces show the mean signal from different experiments overlaid (n = 3). **B.** Peak normalised lactate signal for each concentration of K^+ applied to the MON, lactate signal increased with K^+ (n = 3).

5.3.2.2 Effect of K⁺ Channel Blockers

The influence of K⁺ was further evaluated by observing whether K⁺ channel blockers had any effect upon lactate concentration in the MON. Barium ions (Ba²⁺) are known to interfere with a number of K⁺ channel subtypes (Newman, 1989). In astrocytes Ba²⁺ has been shown to cause depolarisation by blocking the inward rectifier K⁺ channel (Walz et al., 1984). Tetraethylammonium (TEA) is another commonly used K⁺ channel blocker which has been used to study K⁺ conductance in astrocytes (Perillan and Simard, 1999). 2 mM BaCl₂ caused a very large increase in lactate, 3.5 fold compared to a normalised signal. Similarly, TEA produced an increase in lactate, but not as great as that observed for Ba²⁺ (Fig. 5.6).

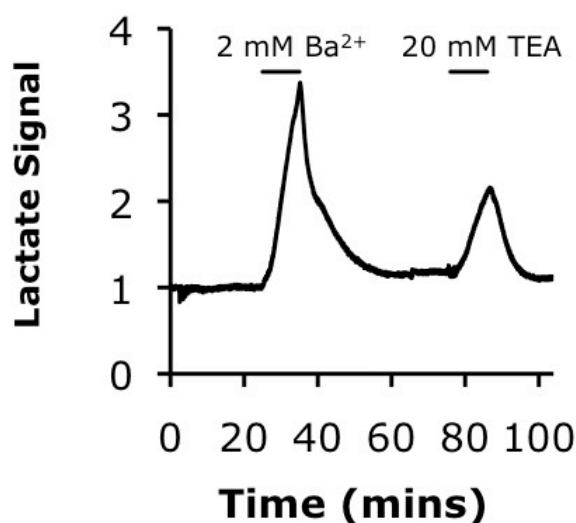


Figure 5.6 The effect of K⁺ channel blockade on lactate in the MON. A 10 minute exposure to 2 mM BaCl₂ caused an increase in lactate signal in the MON which returned to baseline in control aCSF. A similar effect but with a lower increase in signal was seen for 20 mM tetraethylammonium (TEA). The labeled black bars show the period of exposure. This figure shows the trace from a single experiment.

5.3.3 *Post-aglycemia Recovery*

Aglycemia is also known to cause an increase in $[K^+]_o$ which persists when glucose is re-perfused (Brown et al., 2001). The lactate response to aglycemia is shown in Chapter 4. The lactate signal from the MON falls during glucose withdrawal and CAP failure is seen shortly after the lactate reaches zero. To expand upon these findings the lactate signal was recorded during MON recovery post-aglycemia. The effect of re-perfusion of the MON with 10 mM glucose after a 25 minute period of aglycemia is shown in Fig. 5.7. Lactate rose rapidly when glucose was reintroduced to the tissue, as the CAP area recovered the lactate concentration increased above its pre-aglycemia baseline until the CAP area stabilised when the lactate concentration returned to the value it was prior to the insult.

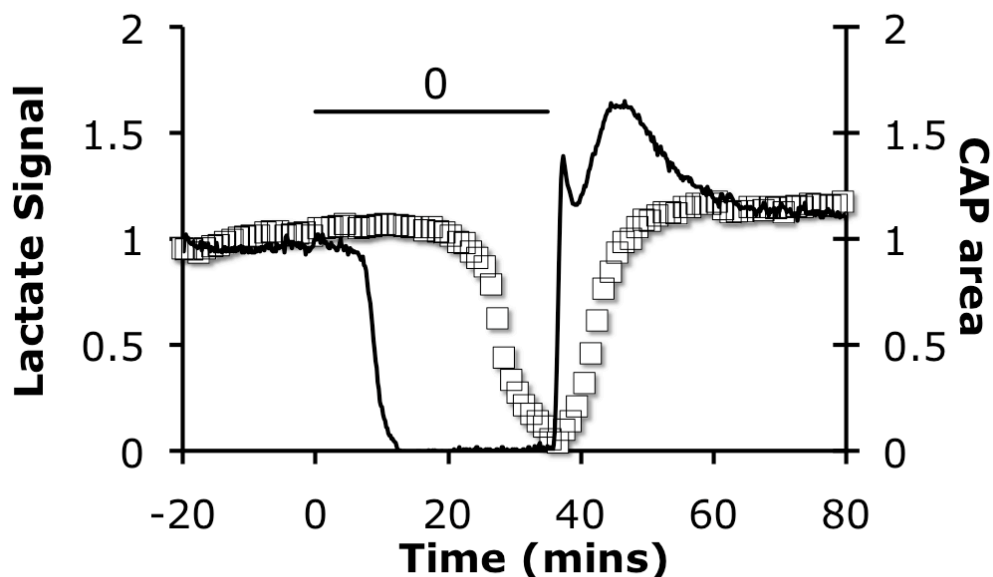


Figure 5.7 The effect of a 25 minute period of aglycemia on MON lactate and CAP area. Aglycemia was induced by replacing control aCSF with zero glucose aCSF (indicated by the bar). The lactate signal (solid line, left axis) decreased and this was followed by a delayed fall in CAP area (open squares, right axis). The CAP area reached 0 at 25 mins when 10 mM glucose was restored to the nerve. Reintroducing glucose cause a rapid spike in lactate signal followed by a sustained period during which the lactate signal deviated above baseline. During this period the CAP recovered completely and equilibrated as the lactate level returned to the pre-aglycemia value (Data are presented as means, $n = 3$).

The effect of a longer period of energy deprivation on the CAP and lactate was examined by reintroducing glucose after 30 mins to allow for complete CAP failure (Fig 5.8). Recovery after this insult was incomplete in the representative trace shown in Fig 5.8. CAP area only recovered to 59 % of its pre-aglycemia value. In experiments such as this with incomplete CAP recovery the lactate signal also did not return to baseline. Lactate remained above the pre-aglycemia concentration but was gradually falling. A subsequent period of

aglycemia was applied to determine what would happen to extracellular lactate when axonal injury was too severe to allow CAP recovery. The latter portion of Fig. 5.8 shows that after a further 90 mins of aglycemia, there is no recovery in CAP area. Reintroducing 10 mM glucose in the second recovery phase led to a rapid increase in lactate signal from the nerve to baseline levels prior to both aglycemic episodes.

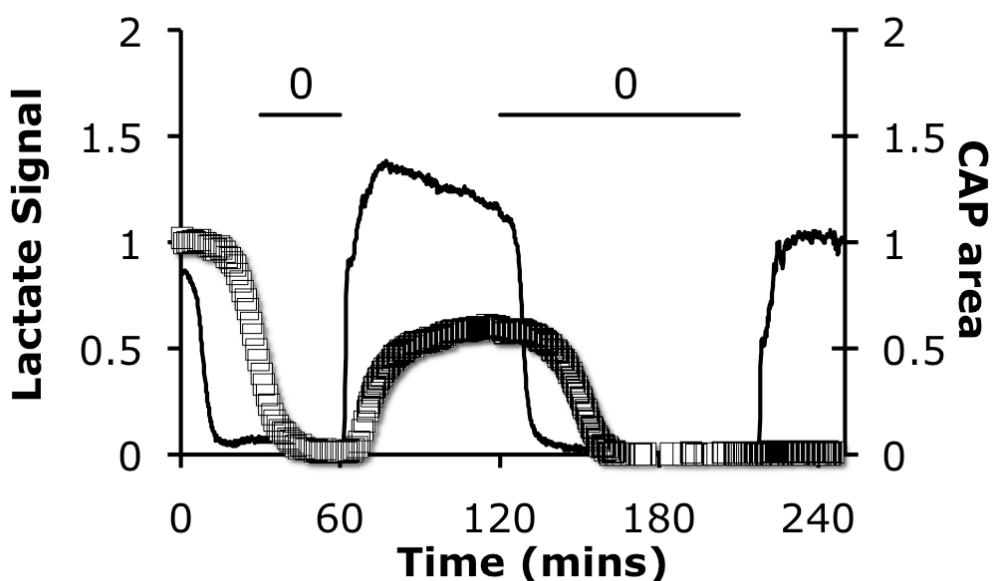


Figure 5.8 The effect of two periods of aglycemia on MON CAP area and lactate. A representative trace is shown for an exposure to 30 mins aglycemia, followed by 60 mins recovery, a second period of aglycemia lasting 90 mins and a final recovery period in 10 mM glucose. During the first period of aglycemia lactate signal and CAP area fall to zero. In the first recovery phase a partial recovery of CAP area is seen along with an elevated lactate level. The second period of aglycemia again caused complete loss of CAP area and lactate signal. A second recovery phase did not reveal any restoration of CAP area, but lactate returned towards baseline.

5.4 Discussion

5.4.1 The Effect of Axonal Activity on Extracellular Lactate

The concentration of extracellular lactate increases when extra metabolic demand is placed upon CNS tissue. In the results presented here this increased metabolic demand is triggered by an increase in the frequency of action potentials conducted by the axons. Seizures are a pathological increase in neural activity which results in increased metabolic demand. Seizure activity has been shown to increase lactate concentrations in CSF and blood (Brooks and Adams, 1975) and locally within the brain (During et al., 1994; Cornford et al., 2002). Increases in lactate can also be generated by experimental stimulation of CNS tissue. The effect of increased axonal activity in the MON is in agreement with these other results in that substantial increases in extracellular lactate are observed upon stimulation of the nerve (Fig. 5.1).

The increase in lactate concentration at higher frequencies appeared to reach a plateau at 50-60 Hz when the peak lactate was not significantly different. The plateau of the lactate concentration is likely to be caused by a rate-limiting step in its production. Whether this is due to glucose supply or enzyme saturation cannot be directly determined from these results, but repeating the stimuli at higher glucose concentrations could reveal whether this was the limiting factor. Other possibilities are saturation of glycolytic enzymes or lactate transport from the cell. High concentrations of lactate can inhibit lactate dehydrogenase thus constraining lactate synthesis (Moorhouse et al., 2010). The maximum increase in lactate brought about by electrical stimulation of the tissue was 2 - 3 times baseline, which is approximately equivalent to that seen in experiments that have used microdialysis to measure brain lactate.

5.4.2 Time Course of Lactate Production

The temporal characteristics of the transient increase in extracellular lactate that accompanies increased neural activity have received much attention in a number of studies. Understanding the mechanisms behind the lactate response will allow a clearer picture of brain energy metabolism to be formed. Microdialysis experiments are capable of revealing the increase in lactate but are not best suited to examine the time course of lactate changes. Since microdialysis is limited in its temporal resolution, due to constraints on the frequency with which quantification can occur. The use of enzyme-based biosensors allows a much greater time resolution of the lactate response to stimulus.

The *in vivo* use of biosensors have shown that a 5 s stimulation of the perforant pathway in the rat hippocampus caused an increase of up to 200% in lactate, which took 10 - 14 mins to return to baseline levels (Hu and Wilson, 1997). In the optic nerve a 120 s stimulus at 60 Hz resulted in a similar lactate increase which then took 4 - 6 mins to return to baseline post-stimulus (Fig. 5.3). The lactate response after stimulation is qualitatively similar in both grey and white matter. A combination of experimental protocol and tissue differences most likely account for the quantitative differences in the lactate response. The isolated MON is constantly bathed in fresh aCSF and is therefore likely to have a faster clearance of lactate from the tissue than exists *in vivo*.

The changes in extracellular lactate in response to a stimulus have been interpreted as supporting the hypothesis that lactate is taken up and oxidised. In the MON upon onset of a period of high-frequency stimulation an initial decrease in lactate is observed. When the stimulus is stopped there is a further increase in the rate of lactate release (Fig. 5.3). These observations may be due to a fraction of the lactate produced by the nerve being taken out of the extracellular space during the stimulus, which is consistent with axonal

uptake and presumably oxidation of lactate. Hu and Wilson (1997) similarly observed a decrease in lactate after initiating a stimulus in the hippocampus (their Figure 1a closely resembles Figure 5.3 in this chapter). As the effect is seen at the onset and termination of an electrical stimulus use of a null sensor would add further confidence to this observation. It is possible that electrical stimulation caused an artefact on the sensor. This would be detected by a null sensor. However, similar decreases in brain lactate content have been observed in the human brain upon the onset of neural activity triggered by a visual stimulus (Mangia et al., 2003). A coinciding dip in NADH fluorescence in neurons at stimulus onset is also seen which is interpreted as an initial response of neuronal oxidation followed by astrocytic glycolysis and extracellular lactate acting as an energy buffer (Kasischke et al., 2004). The results of *in vivo* and *in vitro* experiments are further supported by studies carried out which have utilised computer modelling to recreate the lactate response (Cloutier et al., 2009).

Further evidence to support the notion that lactate is being taken up and oxidised in the MON could be obtained from the use of MCT blockers. MCTs are responsible for lactate transport across cell membranes (Halestrap and Price, 1999). Neurons express MCT2, a different isoform to the MCT1 and 4 expressed by astrocytes (Debernardi et al., 2003; Rafiki et al., 2003). Neuronal MCT2 can be selectively blocked by using the MCT inhibitor 4-CIN at a concentration of 100 μ M (Erllichman et al., 2008). A potential pitfall of the use of 4-CIN is that it has been reported to block pyruvate entry into the mitochondrion (McKenna et al., 2001). However, this effect was observed at higher concentrations (0.25 - 1 mM) than those used to inhibit MCT2. Preliminary experiments were attempted with this compound but they did not generate presentable results. It is predicted that if the theory of lactate uptake by neurons is correct then the extracellular lactate signal in the MON would increase after the application of 4-CIN. Quercetin is another MCT inhibitor but it acts to preferentially block lactate release from astrocytes (McKenna et al., 1998). Comparing the effects of these two MCT inhibitors on

lactate concentration in the MON would enhance our understanding of lactate fluxes in this tissue. These are important experiments which will take precedence in any future work.

The transient lactate response observed after neural activity has been linked to glutamate uptake by astrocytes. However, it has been argued that the energy cost of glutamate uptake by astrocytes is not sufficient to stimulate astrocyte lactate production (Fillenz, 2005). The similarity between the lactate transient in grey matter (Hu and Wilson, 1997; Simpson et al., 2007) and that observed here in white matter also argues against glutamate uptake being the trigger for this metabolic switch. A mechanism which is common to both grey and white matter is more likely.

5.4.3 Potassium Homeostasis and Lactate Production

The resting level of $[K^+]_O$ in the brain is maintained at about 3 mM by a number of tightly controlled regulatory processes (Katzman, 1976). However, local changes in $[K^+]_O$ do occur. The need for tight regulation of $[K^+]_O$ is required as $[K^+]_O$ can influence many of the processes vital to normal brain function. Release of neurotransmitters is influenced by $[K^+]_O$ as is neuronal activity and resting membrane potential. Cerebral blood flow responds to $[K^+]_O$ and importantly for these experiments concerning energy metabolism, both glucose uptake and its subsequent metabolism respond to $[K^+]_O$ (Salem et al., 1975).

Increased neuronal activity causes an elevation in extracellular potassium ($[K^+]_O$) in both grey and white matter (Connors et al., 1982; Ransom et al., 2000). Each individual action potential can lead to a local increase in $[K^+]_O$ of approximately 0.75 mM (Adelman and Fitzhugh, 1975) and the total increase is proportional to the intensity of the neuronal activity. Normal physiological activity can lead to increases in $[K^+]_O$ of up to 12 mM measured in the optic

nerve (Connors et al., 1982). It is possible for $[K^+]_O$ to exceed this concentration under pathological conditions, such as during spreading depression and epileptic activity (Somjen, 2002).

As intense neural activity results in an increase in lactate and $[K^+]_O$, I investigated whether a causal link connected increases in $[K^+]_O$ and lactate release in white matter. A concentration-dependent increase in lactate was observed at $[K^+]_O$ above the normal physiological concentration of 3 mM. The ability of increases in $[K^+]_O$ to evoke lactate release suggests that this lactate release may be astrocytic in origin. This effect could also be replicated by blocking the inward rectifier K^+ channel with Ba^{2+} and TEA (Fig. 5.6), an intervention which depolarises astrocytes (Walz et al., 1984), providing indirect evidence that lactate production and release occurs in astrocytes. A full characterisation of MON lactate release in response to Ba^{2+} and TEA was not carried out since the objective of this experiment was merely to show that disrupting K^+ homeostasis would have an effect on lactate release. In future a full concentration-response relationship may provide further mechanistic detail.

An explanation for lactate release is that increases in $[K^+]_O$ or disruptions to potassium currents (I_K) lead to an increase in energy demand upon the cell as energy is required to maintain the resting balance of ion concentrations and ion gradients across the membrane. Whether this lactate is then used as a metabolic substrate or not further utilised locally remains an open question.

5.4.4 Ion Pumps and Aerobic Glycolysis

Production and release of lactate at times of high neuronal activity or increased $[K^+]_O$ are likely to be brought about by increased tissue energy demand. One of the main requirements for high frequency propagation of action potentials is the rapid return to resting membrane potential in axons.

Maintaining the resting membrane potential is in part due to the activity of the Na^+/K^+ ATPase (the sodium pump) which restores the ionic gradients required for action potentials. This process requires energy which may be derived from aerobic glycolysis, i.e. metabolism of glucose via glycolysis that produces lactate as its end product in the presence of adequate oxygen. Previous measurements of lactate in the brain have shown similar concentrations to that observed *in vitro* in the MON. Therefore, it is unlikely that lactate produced in the MON is due to the tissue being in a state of hypoxia. The potential of hypoxia affecting *in vitro* tissue is important to consider as the blood is an extremely efficient carrier of oxygen.

A link between aerobic glycolysis and Na^+/K^+ transport has been demonstrated in muscle tissue. In vascular smooth muscle oxidative metabolism is generally used to support contractile mechanisms, whereas, glycolysis provides the ATP necessary for membrane ion pumps (Paul et al., 1979). The spatial localisation of the glycolytic enzyme chain in the cell has been put forward as the reason behind this. For white matter, a co-localisation of ion pumps and the enzymatic machinery responsible for glycolysis may be similarly responsible for the production of lactate in response to increased $[\text{K}^+]_o$.

It is possible that attributing lactate production to the action of the sodium pump could provide a common link between lactate release in white matter and the lactate production in grey matter that is incorporated into the ANLSH model.

5.4.5 Lactate and Aglycemia

The response of white matter tissue to glucose withdrawal or aglycemia has been used as a method to understand energy metabolism in this tissue. Understanding the injury mechanisms that underlie aglycemic injury in white

matter also has important clinical implications. Glucose deprivation commonly occurs in conjunction with hypoxia in conditions such as stroke (Siesjö, 1988), but can occur independently in diabetic patients (Frier and Fisher, 2007).

As discussed above maintenance of an energy supply is vital for the brain in both grey and white matter, otherwise the membrane potentials that are required for both glia and neurons to function are dissipated. The question that remains is what happens to the tissue during the period of time where energy is not available. Considering the role of lactate is important from two perspectives: firstly, lactate, produced from astrocytic glycogen is thought to be shuttled to axons providing them with an energy supply during times of energy deprivation; secondly, it has been shown that lactate is an important substrate for CNS tissue following a period of hypoxia (Schurr et al., 1997). Thus, whether lactate plays a similar role post-aglycemia is a clinically relevant question.

Fig. 5.7 shows that when glucose was withdrawn entirely the lactate concentration fell to zero prior to axon conduction failure. The delay between extracellular lactate reaching its nadir and failure of the CAP could be due to the time taken for axons to exhaust the intracellular energy substrates built up prior to aglycemia. Alternatively, astrocytes may still be releasing lactate as a breakdown production of glycogen, but as the uptake rate of lactate by axons is rapid the lactate is not recorded in the extracellular space.

5.5 An Integrated Overview of Lactate in White Matter

The results contained in this chapter and Chapter 4 add to our knowledge of energy metabolism in white matter, and can be discussed in a broader context and integrated into current models of white matter energy metabolism.

5.5.1 Are astrocytes the Source of White Matter Lactate?

Large increases in extracellular lactate accompany periods of intense axonal activity or exposure to high $[K^+]_o$ in white matter. Models of brain energy metabolism propose that astrocytes and neurons have different metabolic responses to increased workload and that the increase in lactate may be associated with a specific cell type. A theory that shows strong popularity is that astrocytes are the main producers of lactate and that this lactate may then be oxidised by neurons. However, these models are generally discussed in the context of grey matter. Determining the origin and fate (see next section) of brain lactate is an important step in producing an accurate model of brain energetics.

Extracellular lactate remains elevated for some time after a period of increased neural activity. The prolonged nature of the increase in lactate seen after stimulation in the hippocampus has been used as evidence to argue that this lactate is not involved in the uptake of synaptic glutamate (Hu and Wilson, 1997). The energy requirement for glutamate uptake by astrocytes has been estimated as 3 % of brain ATP, which is insufficient to stimulate astrocyte glycolysis and lactate production (Fillenz, 2005). The qualitative similarity between the changes in lactate shown here in the optic nerve argues against the involvement of synaptic mechanisms as synapses are absent from the optic nerve. Instead it is likely that the production of lactate is linked to a process

that is common to white and grey matter, namely an increase in extracellular potassium ($[K^+]_O$) that follows increased neural activity. This is supported by the K^+ -induced, concentration-dependent increase in lactate production shown here in white matter (Fig. 5.5).

The observation that lactate production is closely related to $[K^+]_O$ in the optic nerve may be interpreted as hinting towards lactate having an astrocytic origin. Astrocytes are exquisitely sensitive to rises in $[K^+]_O$ and their Na^+ pump can be activated by a rise in $[K^+]_O$ of 1 mM. Conversely, the Na^+ pump on the neuronal membrane is not activated by small changes in $[K^+]_O$, or activated by increases in intracellular $[Na^+]$. The sensitivity of astrocytes to elevated $[K^+]_O$ is related to their role in K^+ regulation.

It has been shown here that in the MON a proportion of the extracellular lactate is derived from glycogen metabolism (Fig. 4.7). This is true even under minimally stimulated conditions, and as glycogen is exclusively located in astrocytes, the source of this lactate will be astrocytic in origin.

Further evidence that the source of lactate is from astrocytes can be taken from Fig. 5.8 which shows that after two 60 minute periods of aglycemia there is no recovery of the CAP but the lactate concentration remains similar to that seen prior to the insult. Absence of the CAP indicates that axons are non-functioning and as astrocytes are less vulnerable to aglycemic insults they are still viable and able to produce lactate.

Astrocytes and axons exhibit a relationship that is highly interdependent which makes determining the source of lactate in the optic nerve difficult and sometimes reliant on circumstantial evidence. Any manipulation which affects one cell type quite often directly affects the other, e.g. both axons and astrocytes have TTX-sensitive channels (Nowak et al., 1987), so administration of TTX will not simply block action potentials, it will alter the physiology of astrocytes too. Even in cases where an intervention is meant to target one cell

type there is likely to be a knock-on effect as axons rely on astrocytes to maintain the extracellular environment. FA, which is selectively taken up by astrocytes, was found to initially reduce lactate production but this was then followed by an increase. This pattern could be due to a direct effect on the astrocytes reducing their ability to produce lactate, and then a secondary effect on the axons as the extracellular environment changes. Confounding factors such as this are perhaps why much of the data which has been used to produce models of CNS energy metabolism has come from cell culture studies on single cell types. Mathematical modelling combined with computer simulations may be a fruitful avenue for examining this cellular relationships. These *in silico* experiments allow manipulations, such as specific alterations in properties of a single cell type, to be performed which would not be possible *in vivo* or *in vitro*. The lactate response during neural activity has already been modelled and its predictive value demonstrated (Cloutier et al., 2009).

5.5.2 The Fate of Extracellular Lactate

The quantities of lactate produced by the MON are high even under minimal activity which would suggest that lactate metabolism is an important component of white matter energetics. The question remains as to the end fate of this lactate. If a mechanism like that proposed by the ANLSH exists in white matter then the lactate released by astrocytes would be taken up by axons to be metabolised oxidatively. The results presented here are equivocal with respect to metabolic shuttling of lactate from astrocytes to axons in white matter. The lactate increase in response to activity occurs after a delay and persists beyond the stimulus which has previously been used to argue against the ANLSH. However, Fig. 5.3 shows that when a 2 min period of 50 Hz stimulation is applied there is an initial drop in lactate concentration before a substantial rise is seen and there is an increase in the gradient of the rising lactate concentration upon cessation of the stimulus. This observation may imply that there is some degree of lactate uptake occurring during this

activity, although it is small in relation to the increase in extracellular lactate that is not taken up by axons.

The ability of astrocytes and neurons to take up and release lactate has often been used as evidence for and against shuttling of lactate between cell types. Monocarboxylate transporters (MCTs) are responsible for lactate transport across the cell membrane and are expressed in white matter. There are eight subtypes of MCT which have different affinities for lactate and show specific expression patterns in the brain. The main subtypes of MCT which are of relevance to white matter are MCT1 and 2, both are expressed in the MON (Tekkok et al., 2005). MCT1 expression has been localised to astrocytes, whereas MCT2 is present of the neuronal cell membrane (Koehler-Stec et al., 1998). It has been suggested that MCT1, which has a lower affinity for lactate, is more suited to lactate export and MCT2 for lactate uptake. The expression pattern in white matter supports the hypothesis of astrocyte lactate release and axonal uptake (Tekkok et al., 2005). Pharmacological inhibition of MCTs has also been used to explore their possible role in brain energetics, 4-CIN accelerates CAP failure during aglycemia and this has been attributed to its application blocking entry of lactate into axons by its specific action on MCT2 (Wender et al., 2000). The use of 4-CIN in intact animals has shown that neurons in the rat retrotrapezoid nucleus take up lactate and this has been cited in support of the ANLSH model (Erllichman et al., 2008). A criticism of the use of MCT blockers such as 4-CIN is that they may also inhibit entry of pyruvate into the mitochondrion and have metabolic effects beyond blocking lactate uptake. More recently, MCT1 expression has been demonstrated in myelin (Rinholm et al., 2011) which implies that the significance of lactate metabolism may not be restricted to the relationship between astrocytes and axons.

The debate surrounding lactate metabolism in the brain has largely focused on two main cell types: neurons and astrocytes. There is evidence to suggest that a two compartment model is insufficient in describing the true picture of

lactate as a metabolic substrate in the brain. Oligodendrocytes are responsible for covering the axons of neurons in the CNS with myelin and they require metabolic substrates in order to synthesise this specialised lipid membrane. Experiments with oligodendrocytes in cell culture reveal that these cells oxidise lactate at a higher rate than astrocytes or neurons and synthesise lipids from lactate to a much greater extent (Sanchez-Abarca et al., 2001). Oligodendrocytes are injured during periods of energy deprivation (Salter and Fern, 2005) and lactate can be used by oligodendrocytes to support myelination under low glucose conditions (Rinholm et al., 2011). These data give rise to the possibility that a fraction of the lactate released by astrocytes in white matter is taken up by oligodendrocytes rather than axons, although the postulated role for MCT1 as a lactate exporter is not in agreement with this. The role of oligodendrocytes and myelin in lactate metabolism warrants further examination in order to integrate it into white matter energy metabolism models.

The fate of increased extracellular lactate in response to neural activity may not be solely restricted to its use as a substrate for oxidative metabolism. The release of lactate possibly contributes to neuro-vascular coupling which in turn may underpin the principles of neuroimaging (Attwell et al., 2010). Imaging the brain has become a widely used technique to study a vast range of normal brain processes and pathologies; because of this it is important to understand the cellular activity that generates the signal underlying this technology.

Chapter Six

A Functional Role for Peripheral Nerve Glycogen

6.1 Introduction

Recent studies have shown that glycogen, located in astrocytes in the CNS, can act as an energy buffer, which may fuel axons during times of increased activity or under aglycemic conditions (Wender et al., 2000; Brown et al., 2003). Much of what is known about glycogen in the CNS is discussed in previous chapters. However, the role of glycogen in the peripheral nervous system has not been addressed in great detail.

There are a number of reasons why the regulation of glycogen may differ in the PNS to that of the CNS. Firstly, the cell type which contains glycogen in the CNS, the astrocytes, are not present in peripheral nerves. Secondly, energy metabolism in peripheral nerves is not restricted to substrates which can cross the blood brain barrier which leaves the potential for the nerves to derive their energy from different sources and pathways than CNS neurons and glia. Thirdly, peripheral nerves have a less reliable supply of energy substrates than CNS tissue as they can be susceptible to postural ischemia as a result of normal body movements. The capillaries supplying peripheral nerves are also of greater diameter than erythrocytes resulting in less efficient oxygen delivery and a greater tendency for anaerobic metabolism (Low et al., 1997). This combination of factors means that the physiology of glycogen metabolism in the CNS cannot be simply applied to the PNS, and thus warrants investigation.

6.1.1 Peripheral Nerve Morphology

Peripheral nerve is a noticeably different tissue compared to the CNS. The PNS is not constrained spatially in the same way as the CNS, where evolutionary pressure dictates that neurons and glia fit inside the limited volume of the skull. The reduced pressure for compaction of the peripheral

nervous system can be seen by the much larger extracellular space in peripheral nerves, and this greater distance between axons and glia is likely to impact upon intercellular communication. Perhaps another hallmark of the increased volume in the periphery is the evolution of axons of much greater diameter than in the CNS, which allows increased conduction velocity necessary for transmitting impulses over the much greater distances that axons traverse. These large axons tend to be present in peripheral nerves which reach to distal body regions and can either be afferent or efferent. Smaller axons are found in autonomic nerves and also grouped in sensory or motor nerves, where they are un-myelinated and conduct slow signals involved in functions such as nociception.

6.1.2 Glial Cells in Peripheral Nerves

In the PNS the glial population is composed of Schwann cells and satellite glial cells, which do not share the same morphology and physiology as CNS glia such as astrocytes and oligodendrocytes. Satellite glial cells are found mainly in peripheral ganglia where they envelop neurons, possibly performing a role analogous to CNS astrocytes (Hanani, 2010). Schwann cells are responsible for myelination in peripheral nerves. Each myelinating Schwann cell myelinates only one axon, in contrast to CNS oligodendrocytes, which can form myelin sheaths around many axons. There are also Schwann cells which support smaller un-myelinated axons forming structures called Remak bundles, where one Schwann cell can surround over 20 axons. The exact number of axons in a single Remak bundle varies with location. In more distal areas the number of axons per bundle tends to be lower (Murrinson and Griffin, 2004).

6.1.3 Energy Metabolism in Peripheral Nerves

Further differences between the CNS and PNS emerge when considering energy metabolism in each of these tissues. These differences start with the fuels available to the cells. In the CNS, axons and their surrounding glial cells are restricted to metabolic substrates that can pass through the blood brain barrier (BBB) or are produced within the brain parenchyma. Peripheral nerves have access to a wider range of possible substrates, as they are not contained within the BBB. Peripheral nerves also differ in their energy demands in comparison to CNS tissue. The brain is well known as a large consumer of energy but peripheral nerves consume relatively little energy (Low et al., 1997).

6.1.4 Glycogen in Peripheral Nerves

Whilst the glycogen content of peripheral nerves has not been functionally characterised in the same way as CNS glycogen, it is not a completely unexplored subject. The presence of glycogen in peripheral nerves has been described in cases of disease and trauma. Glycogen granules have been observed in PNS axons at specific stages of Wallerian degeneration (Zelena et al., 1980). Glycogen is also known to accumulate in nerves of patients with glycogen storage diseases (Komure et al., 1985). A number of studies examining nerves of diabetic patients and animal models of the disease have revealed the presence of glycogen-like deposits (Mancardi et al., 1985; Weiss and Schroder, 1988). These findings would suggest that peripheral nerves have the enzymatic machinery involved in glycogen metabolism, which raises the question as to whether glycogen has a role in non-pathological peripheral nerves. The situation may be the same as in the CNS where neurons have the ability to synthesise glycogen but when glycogen is synthesised in neurons it

causes apoptosis (Magistretti and Allaman, 2007) and hence is associated with pathological states.

The evidence for a physiological role for glycogen in the PNS is less well documented, but it has been reported that sympathetic nerves do contain and synthesise glycogen *in vitro* (De Ribaupierre, 1968). The majority of other references to glycogen in healthy nerves are restricted to the field of embryology, where glycogen is present in the embryonic nerves of a number of species (Gage, 1917). The paucity of recent exploration of this subject may provoke the assumption that there is little to gain from studying glycogen in peripheral nerves. However, demonstrating a role for glycogen in peripheral nerve energy metabolism may have clinical implications for conditions such as diabetes, where peripheral nerve energy metabolism is thought to play a role in the development of peripheral neuropathy (Murakawa et al., 2002; Vincent et al., 2010).

6.1.5 The Sciatic Nerve as a Model

The sciatic nerve is a large nerve in the mammalian body, which has its origin in the spinal cord and innervates the lower limbs. The mouse the sciatic nerve primarily originates from the third and fourth lumbar nerves (L3 and L4), with a small contribution from L5 (Rigaud et al., 2008) It contains myelinated motor axons and a mixture of myelinated and un-myelinated sensory and sympathetic axons (Schmalbruch, 1986). The mouse sciatic nerve (MSN) was chosen as a model peripheral nerve in which to study glycogen metabolism due to its size, ease of access, prevalence in the literature and known susceptibility to peripheral neuropathy. The MSN can be dissected out of the animal and maintained *in vitro*, which allows experimental protocols based on those used to evaluate glycogen and energy metabolism in the CNS (Brown et al., 2003; 2005) to achieve similar objectives for the PNS.

6.1.6 Aims

The primary aim of this work was to determine whether glycogen was present in the mouse sciatic nerve, and whether it could be used to support axon conduction during reduced glucose availability. The cellular localisation of glycogen in peripheral nerve was also examined. The methods used for this study were based on those which determined the location and functional role of glycogen in CNS white matter (Brown et al., 2003).

6.2 Methods

6.2.1 *Electrophysiology*

Compound action potentials (CAPs) were recorded from the isolated mouse sciatic nerve (MSN) as described in Chapter 2. The MSN CAP has two main components: an A fibre and C fibre component (See Results). These components required different stimulus amplitudes to evoke the supra-maximal CAP. The stimulus artefact generated when stimulus amplitude was large enough to evoke the supra-maximal C fibre response obscured the fast A fibre response, therefore, they were not monitored simultaneously.

6.2.2 *Identification of Glycogen Granules*

Glycogen can be visualised in cells by examining electronmicrographs of osmium-stained tissue (Foster, 1960). Glycogen appears in the form of roughly circular granules of densely stained material. The granules are usually between 15 and 40 Å in diameter (Revel, 1960). In order to locate glycogen in the sciatic nerve, electronmicrographs were prepared as described in Chapter 2. To aid the identification of glycogen granules, control nerves were compared with nerves exposed to aglycemia (i.e. glycogen-depleted). For each sample (normal: n = 2 and aglycemia n = 2) 12 fields encompassing juxt-nuclear cell bodies of myelinating Schwann cells were acquired.

6.2.3 *Immunohistochemistry*

Sciatic nerves were processed as described previously (Black et al., 2004). 10 µm cross-sectional cryosections of the sciatic nerves were cut and mounted on Fisher Superfrost Plus glass slides, and the sections were processed for

immunofluorescent detection of glycogen phosphorylase, S-100 and neurofilament. Sections were incubated sequentially in: (1) blocking solution (3 % cold fish skin gelatin (Sigma, St. Louis, MO), 3 % normal donkey serum (Sigma), and 0.1 % Triton X-100 (Sigma) in PBS) for 15 min at room temperature; (2) primary antibodies (goat anti-glycogen phosphorylase (1:100, Santa Cruz Biotechnology, Santa Cruz, CA), mouse anti-S-100 (1:200, Abcam, Cambridge, MA), and chicken polyclonal NF-H (1:5000, Encor, Alachua, FL)) in blocking solution overnight at 4°C; (3) PBS, 6 x 5 min each, (4) secondary antibodies (donkey anti-goat-488 (1:500, Jackson ImmunoResearch, West Grove, PA), donkey anti-mouse-549 (1:500, Jackson ImmunoResearch), and donkey anti-chicken-649 (Jackson ImmunoResearch)) in blocking solution for 6-8 hours at room temperature, (5) PBS 6 x 5 min each. Sections were mounted with Aqua Poly/mount (Polysciences, Warrington, PA) and images were acquired with a Nikon C1 confocal microscope

All other methods were carried out as detailed in Chapter 2.

6.3 Results

6.3.1 Morphology of the Sciatic Nerve

An electron micrograph of a transverse section of sciatic nerve illustrates the heterogeneous morphology of the constituent axons in the sciatic nerve (Fig. 6.1). The axons fall into two main classes, large myelinated fibres (A), and smaller groups of un-myelinated fibres (C) which are ensheathed in Schwann cell cytoplasm, respectively (Fig. 6.1.B - D).

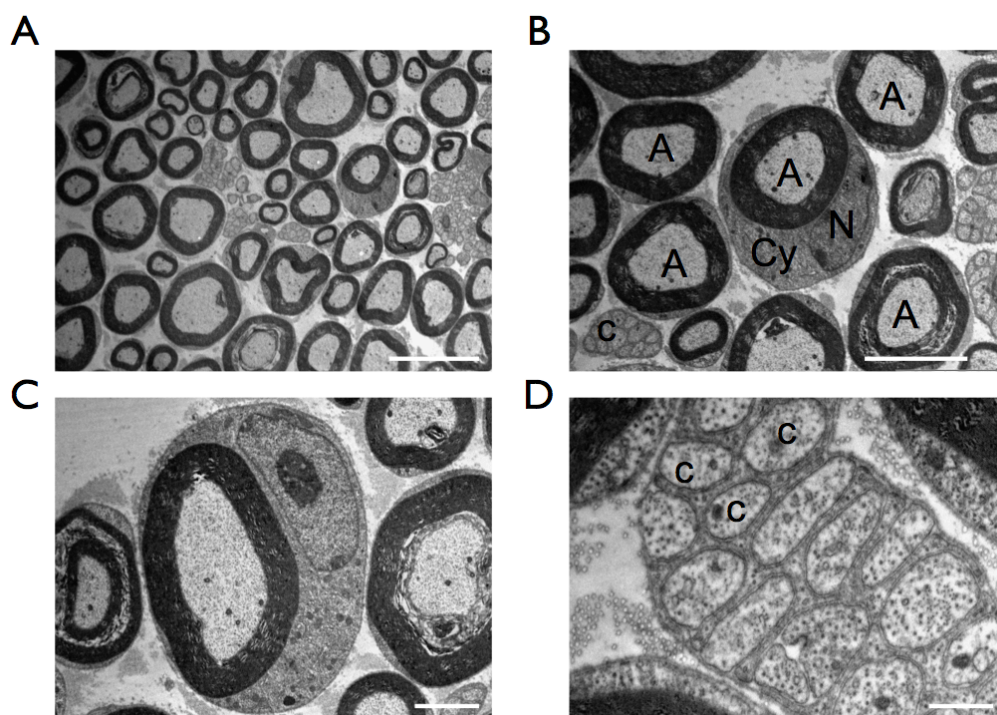


Figure 6.1 Morphology of the mouse sciatic nerve. **A.** Transverse EM of sciatic nerve illustrating the large myelinated fibres that contribute to the A-fibre response, and the smaller un-myelinated C-fibres contributing to the delayed response. **B.** A-fibre (A) showing myelinated axon surrounded by Schwann cell cytoplasm (Cy) and nucleus (N). The C-fibres encapsulated in Schwann cell cytoplasm are also visible (c). **C.** Higher power image illustrating a myelinated A-fibre axon associated with a single Schwann cell. **D.** Groups of un-myelinated C-fibres (c) encapsulated by a single Schwann cell. Scale bars: A 10 μm , B 5 μm , C 2 μm , D 0.5 μm .

6.3.2 The stimulus- evoked compound action potential (CAP) in sciatic nerve

The compound action potential (CAP) evoked by a supra-maximal stimulus is illustrated in Fig. 6.2.A. A small stimulus artefact precedes a large unipolar peak within 1 ms of the stimulus, followed by a smaller bipolar response between 5 to 15 ms after the stimulus artefact (inset, Figure 6.2.A). The large unipolar peak is contributed to by the large myelinated A-fibres and is named the A-peak, whereas the smaller bipolar peak is contributed to by the unmyelinated C-fibres, and is named the C-peak (Ogawa et al., 1984).

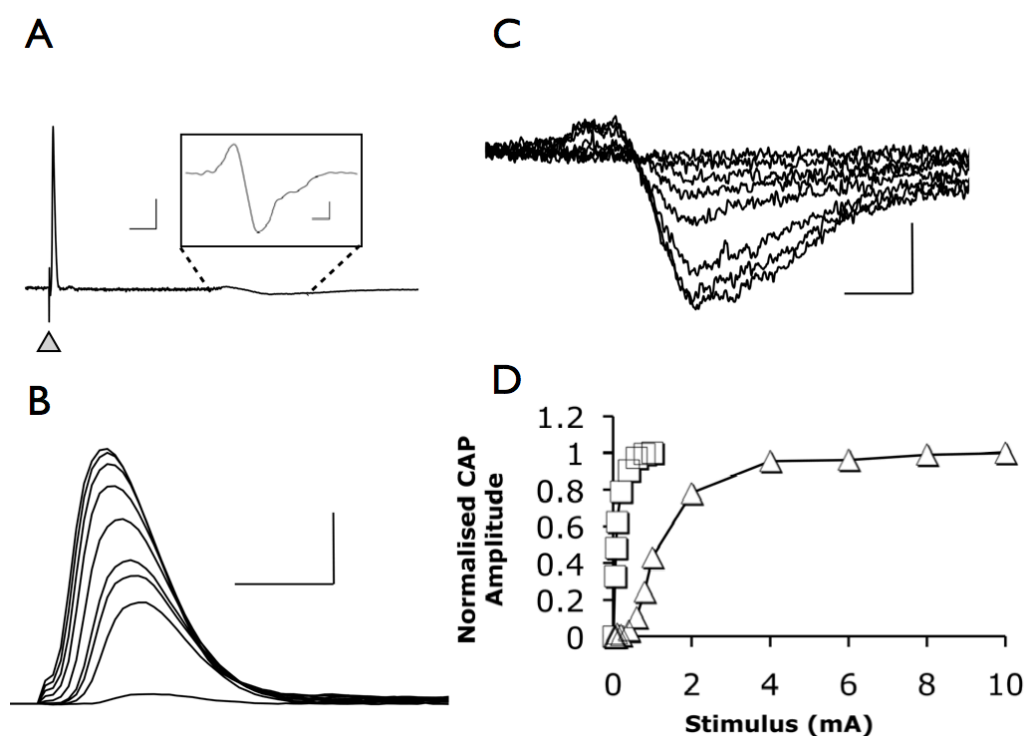


Figure 6.2 Stimulus-evoked CAP. **A.** Individual recording illustrates the large, rapid A-fibre response immediately after the stimulus artefact (shaded arrowhead), followed by the slower and smaller C-fibre bipolar response approximately 10 ms after the stimulus artefact (inset). Scale bars 1 mV and 1 ms; inset scale bars 0.05 mV and 1 ms. **B** and **C.** Increasing the stimulus current results in increased amplitude of the A- and C-fibre response, respectively. Scale bars are 5 mV and 0.25 ms for B and 0.25 mV and 1 ms for C. **D.** Plotting the stimulus intensity versus the normalised amplitude of the A- (\square) and C- (\triangle) fibre CAPs, demonstrates the lower threshold for activation of the A fibres relative to the C-fibres response ($n = 3$).

Stepwise increases in the stimulus current result in increases in the amplitudes of both the unipolar A-peak (Fig. 6.2.B) and the C-peak (Fig. 6.2.C; the amplitude of the C-peak is measured as the difference between the maximum positive peak and the maximum negative peak). The relationship between the normalised peak amplitude and the stimulus current is shown in Figure 6.2.D, illustrating that the A-peak has a much lower threshold than the C-peak, reaching its maximal amplitude at a current stimulus of about 1 mA, a stimulus intensity that only evokes about a quarter of the maximal C-peak response.

6.3.3 Glycogen content of the sciatic nerve

Glycogen content of acutely isolated sciatic nerve was 8.61 ± 0.90 pmol glycogen ($\mu\text{g protein}^{-1}$) ($n = 3$; blood glucose concentration at sacrifice was 9.50 ± 1.80 mM, $n = 18$). Sciatic nerve glycogen content was significantly higher than in acutely isolated optic nerve (6.82 ± 0.40 pmol glycogen ($\mu\text{g protein}^{-1}$); $p = 0.037$) measured using similar methods (Brown et al., 2003).

Glycogen content was stable for many hours in sciatic nerves incubated in 10 mM glucose aCSF. In CNS white matter the glycogen content varies with ambient glucose concentration (Brown et al., 2003). To test whether the same relationship held true for the PNS the effect of bath glucose concentration on sciatic nerve glycogen content was determined. Sciatic nerves were incubated in aCSF with variable glucose concentrations ranging from 2 mM to 30 mM. A pre-incubation period of 60 minutes in 10 mM glucose aCSF preceded each experiment to allow nerves to equilibrate under identical conditions. Nerves were subsequently incubated in the desired glucose concentration by switching the glucose content of the aCSF to the appropriate value for two hours. Nerves were preserved in ice cold 85% ethanol / 15% 30 mM HCl prior to assay to prevent glycogen breakdown. In nerves bathed in 2 mM, 4 mM, 7 mM, 10 mM or 30 mM glucose for two hours, respectively, the glycogen

content was 2.35 ± 0.07 pmol glycogen ($\mu\text{g protein}^{-1}$) ($n = 3$), 7.16 ± 0.53 pmol glycogen ($\mu\text{g protein}^{-1}$) ($n = 3$), 9.68 ± 1.08 pmol glycogen ($\mu\text{g protein}^{-1}$) ($n = 3$), 10.98 ± 1.00 pmol glycogen ($\mu\text{g protein}^{-1}$) ($n = 3$) or 15.21 ± 0.98 ($n = 3$) pmol glycogen ($\mu\text{g protein}^{-1}$) ($n = 3$), respectively (Fig. 6.3). In addition, the glycogen content of sciatic nerves immediately upon removal from the mouse was 8.61 ± 0.90 pmol glycogen ($\mu\text{g protein}^{-1}$) ($n = 3$). These data illustrate an asymptotic relationship between ambient glucose concentration and glycogen content (Fig. 6.3), similar to that seen in mouse optic nerve (Brown et al., 2003).

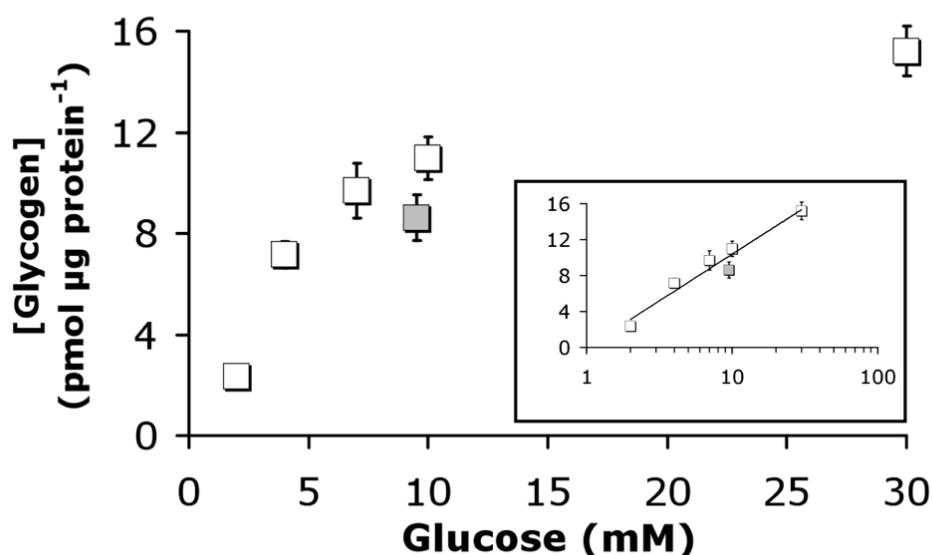


Figure 6.3 Glycogen content of the mouse sciatic nerve. Nerves bathed for 2 hours in 2, 4, 7, 10 or 30 mM glucose showed increasing concentrations of glycogen (open squares: left axis scale pmol glycogen ($\mu\text{g protein}^{-1}$)). Sciatic nerves removed from mice, with a mean blood glucose concentration of 9.5 ± 1.8 mM at the time of death, and immediately frozen for glycogen assay, had a glycogen content of 8.61 ± 0.90 pmol glycogen ($\mu\text{g protein}^{-1}$) (grey square). Inset shows [glucose] (mM) plotted on a logarithmic scale demonstrating the exponential relation between glycogen content and ambient [glucose]. Left axis as main figure.

The presence of labile glycogen in peripheral nerve prompted two questions: (1) can the glycogen provide a utilisable energy substrate to sustain axonal excitability in the absence of glucose, and (2) where is the glycogen located? To investigate the first question the temporal correlation between glycogen content and the ability of the nerve to conduct action potentials during glucose deprivation was studied. The cellular location of glycogen was investigated using electron microscopic techniques as this technique has previously proved successful in identifying glycogen in the optic nerve.

6.3.4 Effects of glycogen content on the CAP during aglycemia

Glycogen stored in astrocytes is used to support axon conduction in white matter during aglycemia (Wender et al., 2000; Brown et al., 2003). In order to test whether the glycogen content of the MSN had a similar functional role the effects of aglycemia on the A-fibre and C-fibre CAP peaks were investigated. Sciatic nerves were removed from the mouse and immediately placed in the interface chamber and perfused with glucose-free aCSF. The A peak was maintained for 1.55 ± 0.52 hours before it failed ($n = 6$), whereas the C-fibre peak lasted only 0.81 ± 0.45 hours ($n = 5$) before failure (Fig. 6.4.A). In separate experiments the glycogen content was systematically manipulated by incubating sciatic nerves in aCSF containing glucose concentrations ranging from 2 to 30 mM before exposing nerves to aglycemia. The C peak had a latency to failure of 0.35 ± 0.29 hours ($n = 6$), 0.57 ± 0.10 hours ($n = 4$) and 0.75 ± 0.09 hours ($n = 4$), respectively, when pre-incubated in 2 mM, 10 mM or 30 mM glucose aCSF, respectively (Figure 6.4.C), whereas the A-fibre peak had a latency to failure of 0.28 ± 0.30 hours ($n = 4$), 2.10 ± 0.34 hours ($n = 4$) and 2.92 ± 0.42 hours ($n = 5$), respectively, following incubation in 2 mM, 10 mM or 30 mM glucose aCSF, respectively (Figure 6.4.B). Plotting latency to CAP failure for the A- and C-fibre peaks relative to the glycogen content in the nerve pre-incubated in 2 mM ($n = 3$), 10 mM ($n = 3$) or 30 mM glucose ($n = 3$) revealed a

saturation response, where increasing glucose concentration led to increases in latency to failure (Figure 6.5.A). The relationship between the glycogen content of the tissue prior to aglycemia and the latency to CAP failure after onset of aglycemia was linear for both the A and C-fibre CAPs, although the slope for the A-fibres was steeper than for the C-fibres (Figure 6.5.C). The values obtained for nerves subjected to aglycemia directly after sacrifice (Fig. 6.5.B) were also plotted on these graphs for comparison.

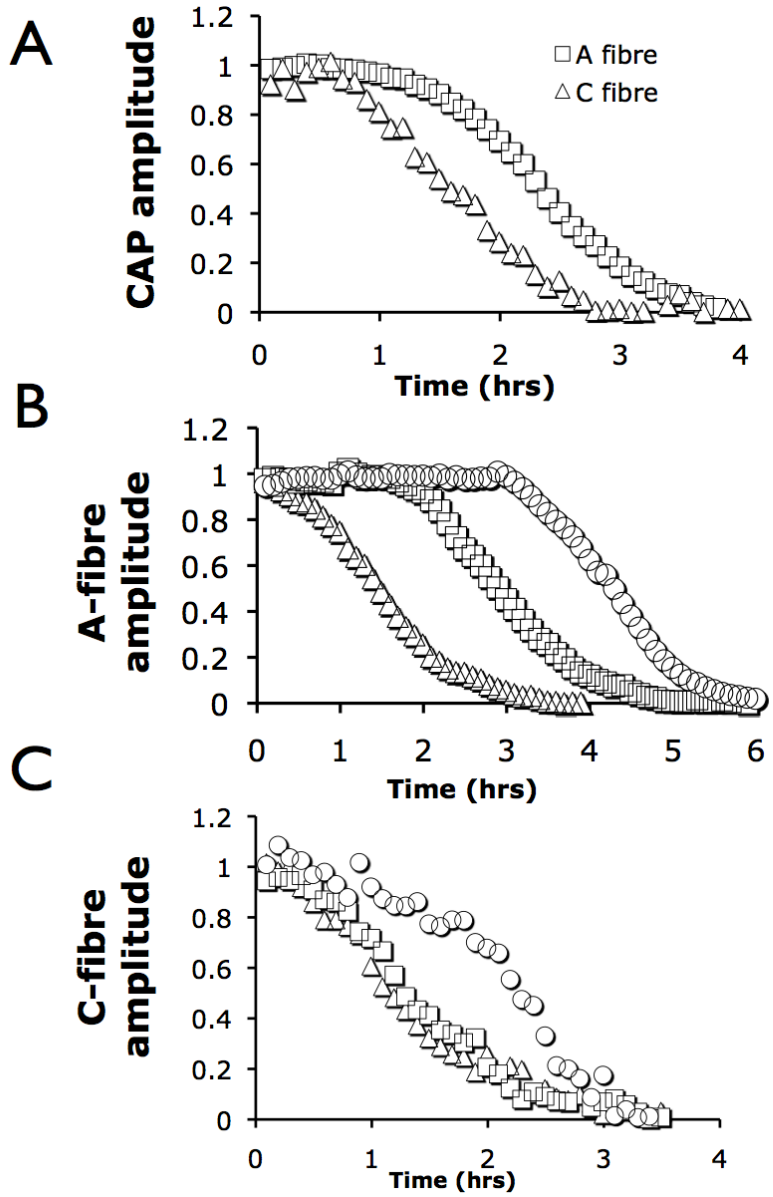


Figure 6.4 Normalised CAP area during aglycemia. **A.** CAPs recorded from sciatic nerves immediately after removal from mouse. Normalised CAP amplitude of the A- (□) and C- (△) fibre peak plotted against time relative to introduction of zero glucose aCSF at 0 hrs. **B.** A-fibre peak in nerves pre-incubated in 2 mM, 10 mM or 30 mM glucose for 2 hours prior to onset of aglycemia at 0 hrs. The peak amplitude was normalised to the value at aglycemia onset. The response was maintained longest in nerves pre-incubated in 30 mM glucose (○), followed by pre-incubation in 10 mM (□) then 2 mM (△) glucose. **C.** The C-fibre peak showed qualitatively the same pattern of failure as the A-fibre response, although the latencies were shorter. Symbols for B also apply. n = 5 in all cases.

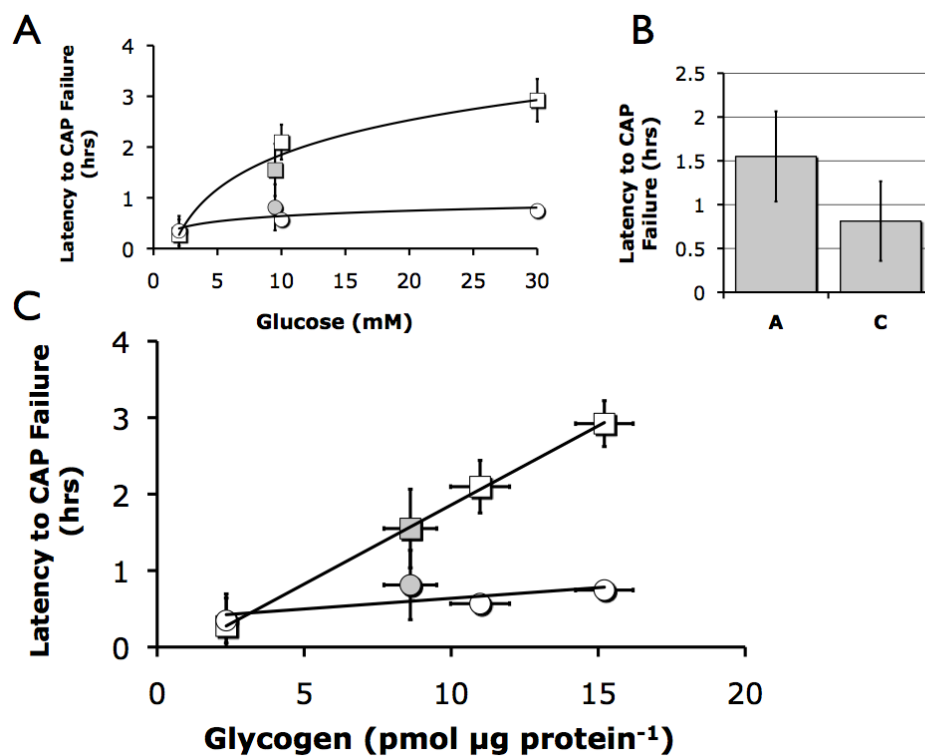


Figure 6.5 Latency to CAP failure during aglycemia for the sciatic nerve. **A.** Relationship between latency to reduction to 95% of baseline value of the A-fibre (\square) and C-fibre (\circ) peak amplitude versus pre-aglycemia bathing glucose concentration. **B.** Latency to CAP failure for nerves in which recordings were carried out immediately on removal from the animal. Directly after sacrifice the blood glucose average was 9.5 mM ($n = 18$) and glycogen content was 8.6 pmol glycogen ($\mu\text{g protein}^{-1}$); these data points are represented on A and C by filled grey symbols. **C.** Relationship between latency to 95% CAP failure and glycogen content at the onset of aglycemia of the A (\square) and C (\circ) peaks, demonstrating a linear relationship for both responses. $n = 3$ unless stated.

6.3.5 Effects of aglycemia on glycogen content and relationship to CAP failure

The effect of removing glucose from the perfusing aCSF (aglycemia) on the A- and C-fibre CAP responses was investigated. At the onset of aglycemia the CAPs were stable. The A-peak initially remained stable and only began to fail 2.10 ± 0.34 hours after the onset of aglycemia. The CAP had almost entirely disappeared by 4.5-hour post onset of aglycemia ($n = 4$). The C-peak failed more rapidly, it began to fall after 0.42 ± 0.11 hours and was completely absent by about 2.5 hours ($n = 4$). The glycogen content at the onset of aglycemia was 10.98 ± 1.00 pmol glycogen ($\mu\text{g protein}^{-1}$) ($n = 3$). Glycogen fell to 7.28 ± 0.71 pmol glycogen ($\mu\text{g protein}^{-1}$) ($n = 3$) after 1 hour of aglycemia, 2.99 ± 0.56 pmol glycogen ($\mu\text{g protein}^{-1}$) ($n = 3$) after 2 hours of aglycemia and 2.31 ± 0.13 pmol glycogen ($\mu\text{g protein}^{-1}$) ($n = 3$) after 4 hours of aglycemia (Fig. 6.6). The continuing presence of glycogen was tightly correlated with the ability of A-fibres to conduct CAPs, although, some glycogen remains even in the absence of glucose (Wender et al., 2000). The excitability of C-fibres, however, was not well correlated with glycogen loss; these fibres failed well in advance of glycogen loss suggesting that their excitability was not supported, or only partially supported, by glycogen breakdown.

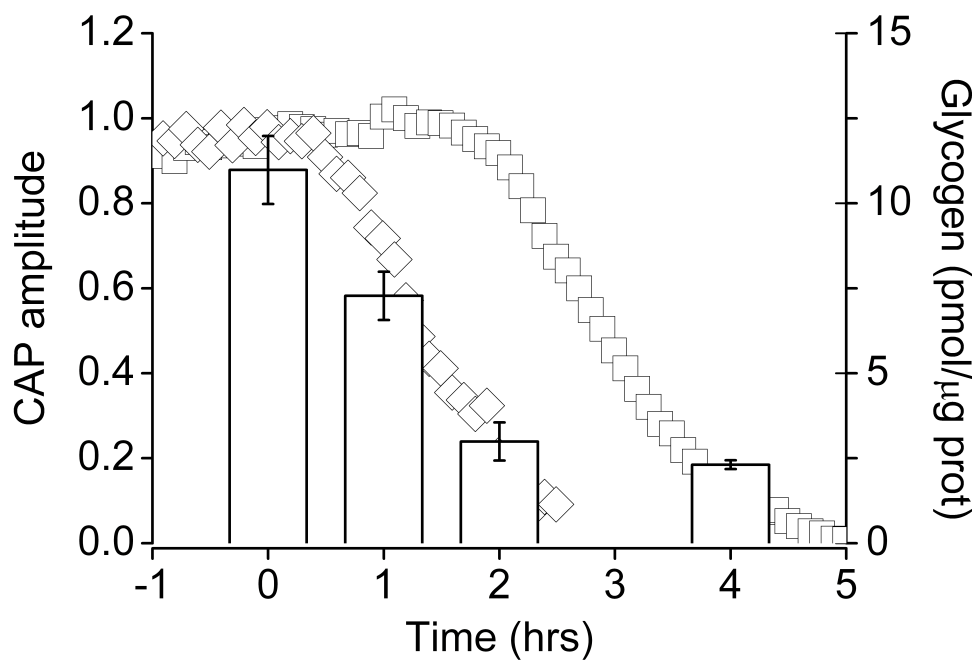


Figure 6.6 Aglycemia and glycogen content of sciatic nerve. Aglycemia resulted in onset of delayed failure of the A-peak after about 2 hours, and total failure after about 4.5 hours (open squares), whereas the C-peak response failed after about 0.5 hours and disappeared by 3 hours. Glycogen content (open columns; right y-axis) decreased during aglycemia, reaching a nadir after about 2 hours which was coincident with the onset of A-peak failure.

6.3.6 Effect of inhibiting glycogen phosphorylase on the CAP

The compound DAB inhibits glycogen phosphorylase (Walls et al., 2008) which prevents glycogen metabolism and accelerates the failure of axonal conduction during aglycemia. The ability of DAB to reduce the latency to CAP failure in the MSN was tested by pre-incubating nerves for 2 hours in aCSF containing either 10 mM glucose, or 10 mM glucose plus 1 mM DAB. Aglycemia was then induced by removing glucose from the aCSF. In the control nerves the A-fibre CAP latency to failure was 2.10 ± 0.34 hours, whereas in the nerves incubated with 1 mM DAB the latency to failure was significantly shorter at 0.64 ± 0.12 hours ($p < 0.0009$ $n = 4$; Fig. 6.7.A and 6.8). The C-fibre latency to failure was 0.58 ± 0.06 hours ($n = 4$) in control conditions and 0.50 ± 0.04 hours ($n = 4$) in the presence of DAB ($p = 0.13$, Fig. 6.7.B and 6.8). As DAB did not have a significant effect on the latency to failure of the C-fibre peak the experiment was repeated but with a pre-incubation in 30 mM glucose to increase glycogen stores. In nerves pre-incubated in 30 mM glucose, or 30 mM glucose plus DAB, the C-fibre latency to failure was 0.75 ± 0.10 hours and 0.71 ± 0.09 hours, respectively; this was again not significantly different between control and DAB-treated ($p = 0.17$, $n = 3$, Fig 6.7.C and 6.8).

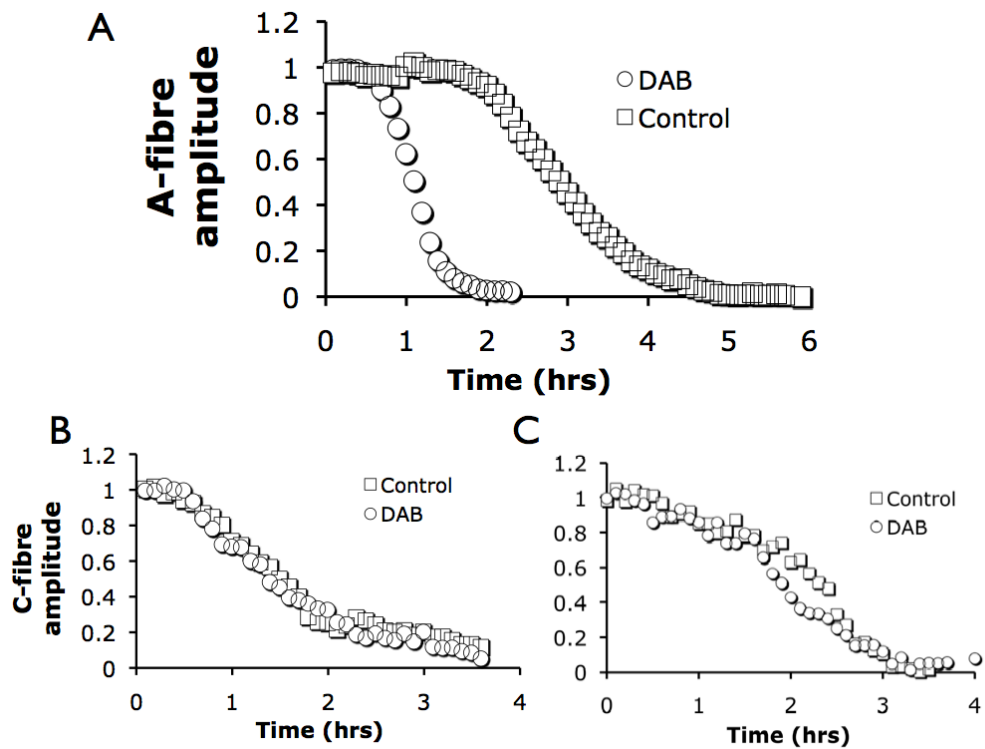


Figure 6.7 Effect of inhibiting glycogen phosphorylase on latency to CAP failure and glycogen content. **A.** Introduction of the glycogen phosphorylase inhibitor DAB resulted in accelerated failure of the A-fibre peak (\circ) relative to control, untreated nerves (\square). **B.** DAB had no effect on latency to CAP failure of C-fibres incubated in 10 mM glucose. **C.** In nerves pre-incubated in 30 mM glucose DAB did not accelerate CAP failure.

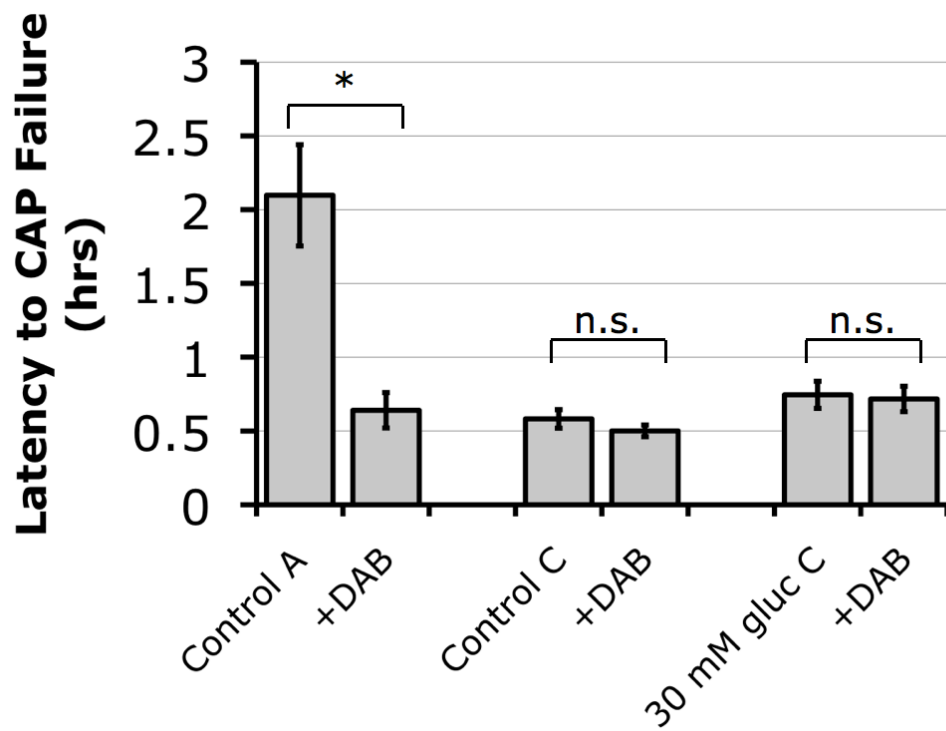


Figure 6.8 Inhibition of glycogen phosphorylase affects A-fibre but not C-fibre survival during aglycemia. DAB significantly accelerated CAP failure after onset of aglycemia in A-, but not C-fibres incubated in 10 mM glucose or 30 mM glucose, although, C-fibre failure was slightly delayed by pre-incubation in 30 mM glucose possibly due to increased extracellular glucose at the start of aglycemia.

To show that DAB was indeed preventing glycogen breakdown during aglycemia the glycogen content was measured. Sciatic nerves were incubated for 2 hours in aCSF containing 10 mM glucose in the presence or absence of 1 mM DAB, then exposed to aglycemia for 2 hours. In control nerves the glycogen content fell from 10.98 ± 1.00 pmol glycogen ($\mu\text{g protein}^{-1}$) to 2.99 ± 0.56 pmol glycogen ($\mu\text{g protein}^{-1}$) ($p = 0.001$, Fig. 6.9) after 2 hour aglycemia, whereas in the DAB-treated nerves the fall in glycogen was attenuated from 14.17 ± 2.37 pmol glycogen ($\mu\text{g protein}^{-1}$) to 12.25 ± 1.50 pmol glycogen ($\mu\text{g protein}^{-1}$) and not significantly lower after 2 hours of aglycemia ($p = 0.3$, Fig. 6.9).

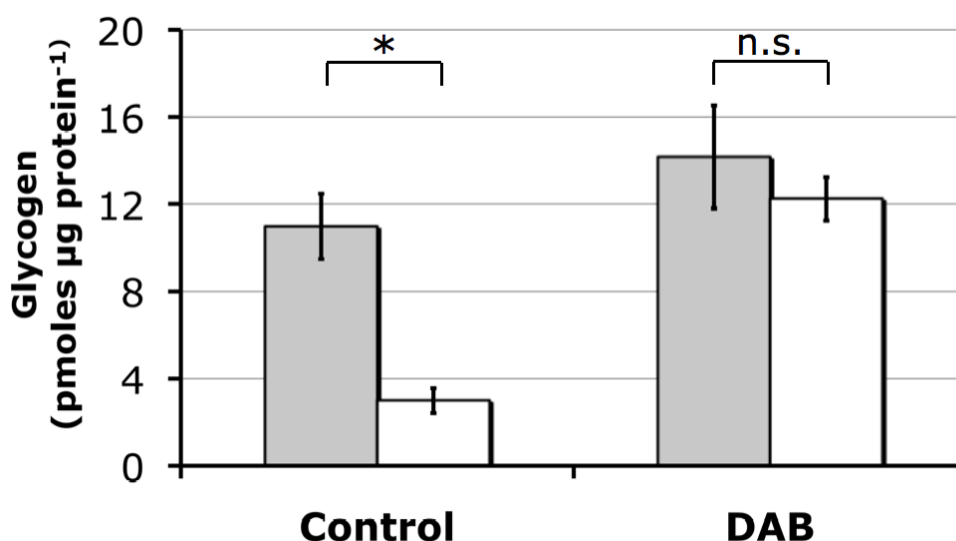
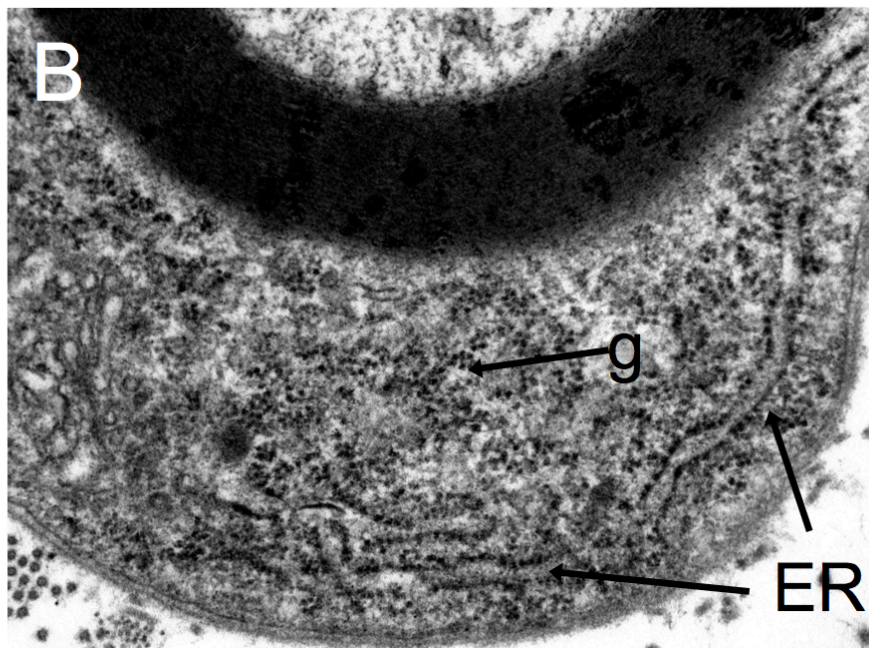
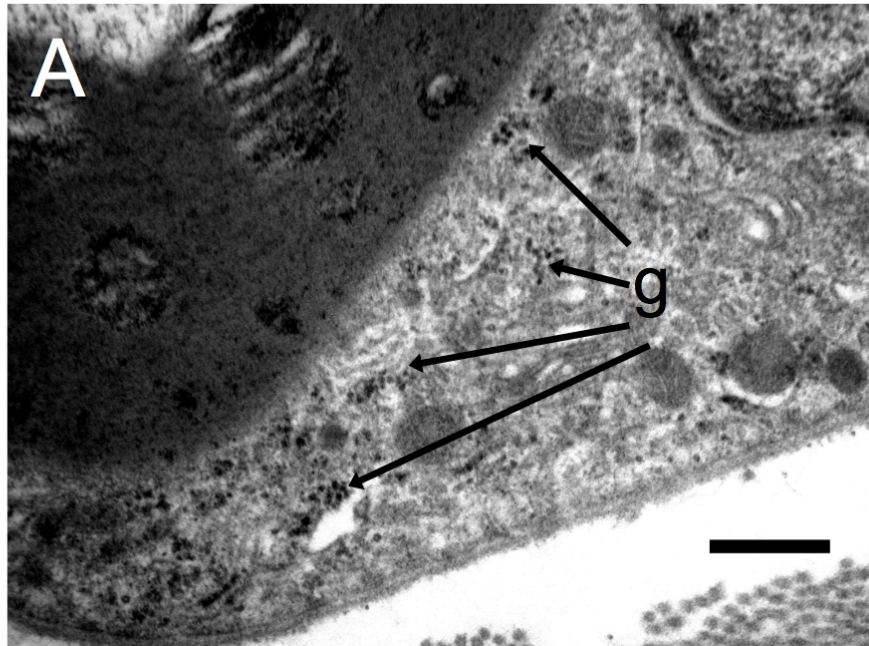


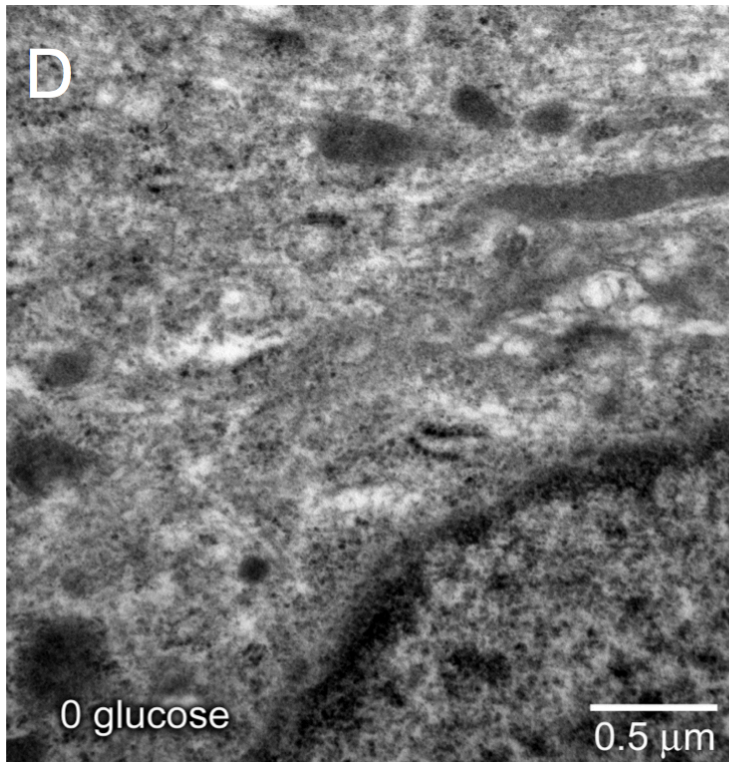
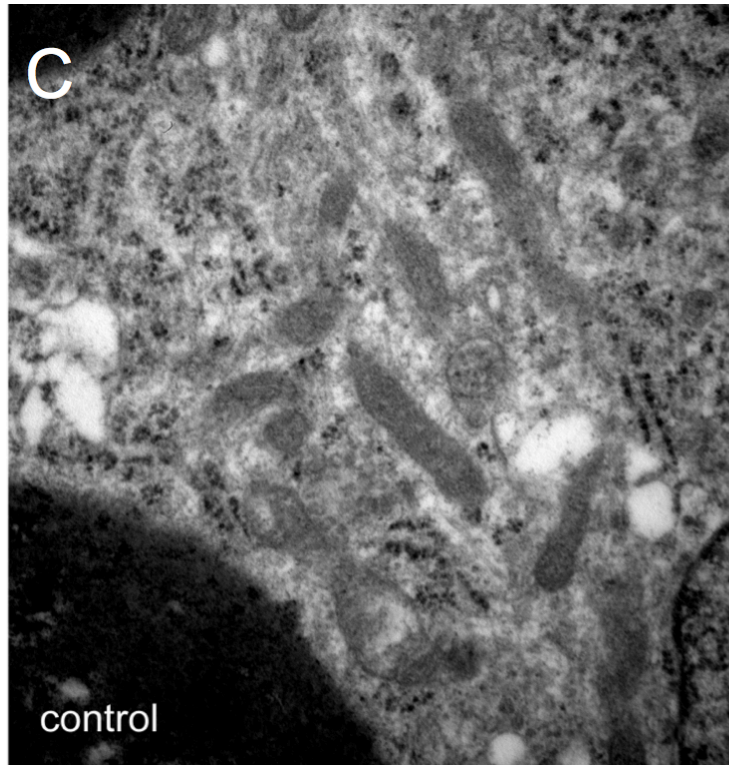
Figure 6.9 Effect of inhibiting glycogen phosphorylase on sciatic nerve glycogen content pre- and post- aglycemia. Glycogen content is shown for nerves incubated in 10 mM glucose for two hours (shaded columns) and after a 2 hour period of aglycemia (open columns). This is shown for control nerves and those maintained in the presence of 1 mM DAB. After 2 hours of aglycemia the glycogen content had significantly fallen in control nerves (* $p < 0.05$, $n = 3$) whereas in nerves incubated in 1 mM DAB throughout the glycogen content had not fallen significantly during aglycemia (n.s. $p > 0.05$, $n = 3$).

6.3.7 Ultrastructural identification of glycogen in sciatic nerve

Electron microscopic studies were carried out on immersion fixed sciatic nerves to identify glycogen. Glycogen was visualised as small densely stained spheres of up to 40 nm diameter and was prominently located in Schwann cell cytoplasm (Fig. 6.10). In nerves exposed to zero glucose aCSF for 2 hours, conditions known to deplete glycogen (see above), the density of glycogen granules decreased (Fig 6.10.D) compared to control nerves (Fig 6.10.C). We made no attempt to quantify glycogen based on the EM images but our strong impression was that the majority of glycogen granules were located in Schwann cell cytoplasm. (A small number of glycogen granules may have been present in some axons.)

Figure 6.10 (next two pages). Location of glycogen in the sciatic nerve determined by electron microscopy. **A.** Glycogen granules (g) are present in Schwann cell cytoplasm of A-fibres, glycogen is visualised as dark spherical granules located throughout the cytoplasm. **B.** Ribosomes attached to endoplasmic reticulum are also present (ER). **D.** Nerves incubated in aglycemic conditions showed a decreased density of glycogen granules compared to control (**C**). Scale bar 500 nm.





6.3.8 Expression of glycogen phosphorylase

At present, robust antibodies to immunocytochemically detect glycogen within fixed tissues are unavailable, and, therefore, as a surrogate, immunohistochemical labelling was performed to determine the presence of the brain isoform (BB) of glycogen phosphorylase, a key enzyme in glycogen metabolism. In the CNS, this enzyme appears to be selectively localised to astrocytes (Pfeiffer et al., 1990), the only cell in the adult brain that contains glycogen (Cataldo and Broadwell, 1986). Staining longitudinal sections of sciatic nerve using the H and E method revealed Schwann cell bodies (purple) interposed between axons (Fig. 6.11.A, pink). Higher power images allowed clear resolution of individual axons with the occasional Schwann cell body (Fig. 6.11.B). Triple labelling studies were carried out using S-100 or neurofilament to localise the glycogen phosphorylase to either Schwann cells or axons, respectively. Glycogen phosphorylase immunolabeling was detected in both axons and Schwann cells, as evidenced by the co-localisation of the glycogen phosphorylase antibodies with markers for axons (neurofilament) or Schwann cells (S-100) (Fig. 6.11.C – F).

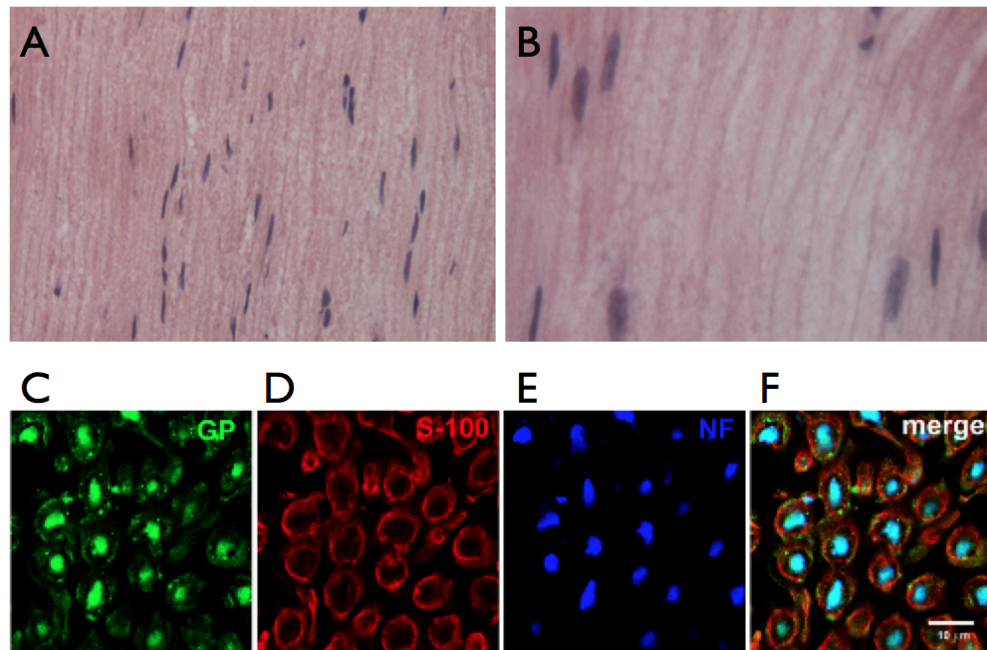


Figure 6.11 Expression of glycogen phosphorylase in sciatic nerve. **A.** H & E staining of longitudinal sections of sciatic nerve revealed Schwann cell bodies as purple oblongs diffusely arranged between axons. **B.** Higher power images revealed individual axons in longitudinal section. **C-F.** Immunohistochemical studies revealed the presence of glycogen phosphorylase (green), whose cellular location was identified using specific cellular markers for Schwann cells (S-100; red) and axons (neurofilament; blue). **F.** Merged images demonstrate that glycogen phosphorylase is detected in both Schwann cell cytoplasm (yellow) and axons (cyan). Scale bar 10 μm .

6.3.9 Role of lactate

Given the cellular location of glycogen and the ability of glycogen to support axon conduction during aglycemia, a transportable conduit must be produced for intercellular transport between the Schwann cell and the axon. The most likely candidate is lactate for the following reasons. Perfusing the sciatic nerve for 4 hours in the presence of 10 mM glucose results in a stable A-fibre CAP. Introduction of aglycemia resulted in a slow, delayed loss of conduction (Fig. 6.12.A) as previously described ($n = 4$). However if aCSF containing 10 mM glucose was reintroduced at 2.5 hrs, when the A-fibre CAP had fallen to approximately 50% of its baseline value, the CAP was fully restored to baseline values ($n = 4$). In a similar manner the A-fibre CAP was fully supported with 20 mM lactate as sole exogenously applied energy substrate ($n = 4$). The A-fibre peak was also fully rescued by introduction of 20 mM lactate aCSF at 2.5 hrs, after partial loss induced by a period of aglycemia from 0 to 2.5 hrs ($n = 4$, Fig. 6.12.B). The C-fibre peak was supported by 10 mM glucose for 4 hours and was rescued by 10 mM glucose (Fig. 6.12.C, $n = 4$) after aglycemia reduced the peak to about half baseline value. In the presence of 20 mM lactate the C fibre CAP was supported although it decreased to below baseline after 4 hours. The C-fibre peak was only partially restored by 20 mM lactate after a period of aglycemia (Fig. 6.12.D, $n = 4$).

Lactate release from the sciatic nerve was measured using an enzyme-based lactate biosensor in the same manner as recordings were made from the optic nerve in Chapters 4 and 5. Fig. 6.13.A shows that the lactate signal remained stable in 10 mM glucose and when aglycemia was induced fell to 50 % of its initial value after 18.2 ± 1.6 mins ($n = 3$). The concentration of lactate released from the sciatic nerve was calculated as 0.18 ± 0.01 mM during exposure to 10 mM glucose (Fig. 6.13.B). This value is lower than that obtained for the optic nerve in Chapter 4.

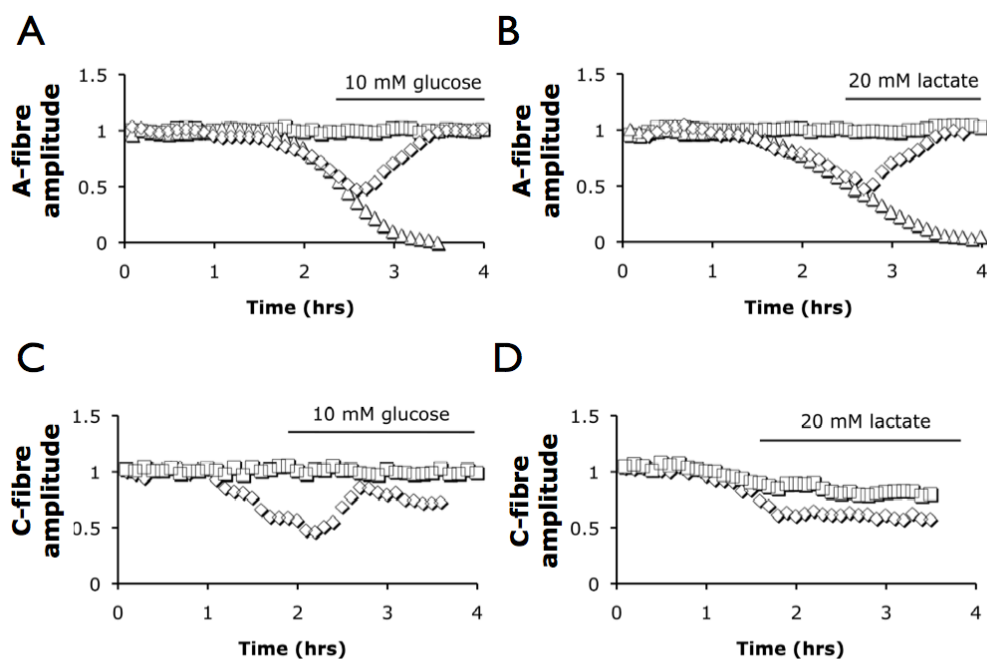


Figure 6.12 Ability of glucose and lactate to sustain and rescue the CAP. **A.** The A-fibre peak was supported for many hours with aCSF containing 10 mM glucose (\square), but introduction of aglycemia at 0 hrs led to delayed failure of the CAP (\triangle). Reintroduction of aCSF containing 10 mM glucose after 2.5 hrs of aglycemia, during which the CAP had fallen to about 50% of baseline value, fully rescued the peak (\diamond). **B.** A similar experiment showed that lactate could support function when present in the aCSF (\square), and also that lactate could rescue function (\diamond) after a 2.5 hr period of aglycemia. **C.** Pre-incubating nerves in 10 mM glucose supported the C-peak conduction, but the CAP was only partially rescued by reintroduction of 10 mM glucose after a period of aglycemia. **D.** In nerves pre-incubated in 20 mM lactate the C-fibre CAP was maintained for several hours but rescuing the CAP after a brief period of aglycemia resulted in incomplete CAP recovery.

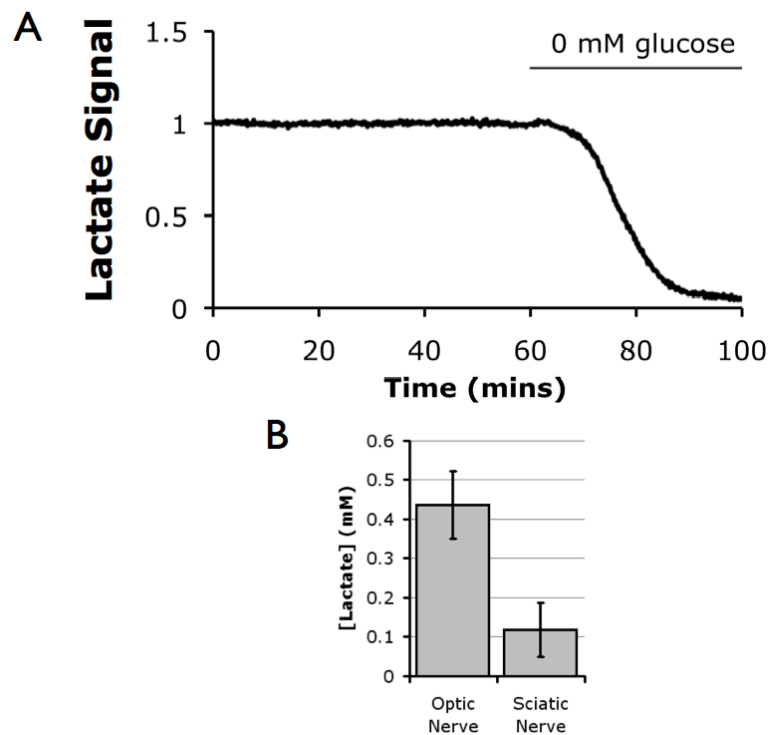


Figure 6.13 Lactate is present in the mouse sciatic nerve and its concentration falls during aglycemia. **A.** A lactate biosensor was positioned in contact with the nerve prior to, and during aglycemia. A lactate signal was present when the nerve was bathed in 10 mM glucose aCSF, but this signal was reduced and was lost during a period of aglycemia ($n = 3$). **B.** The lactate concentration in optic and sciatic nerves was determined by measuring the lactate signal in individual nerves and comparing this to a standard curve of known lactate concentrations. Extracellular lactate was lower in the sciatic nerve than the optic nerve ($n = 4$).

6.4 Discussion

In the experiments described here the mouse sciatic nerve (MSN) was used as a model peripheral nerve to examine the content, cellular location and function of glycogen within the PNS. This study drew influence from those which characterised the glycogen in the CNS using the mouse optic nerve (MON) as a model (Brown et al., 2003; 2005). Many of the findings are, therefore, discussed in direct comparison and contrast with the CNS where a model of glycogen metabolism is well established.

6.4.1 Sciatic Nerve Morphology

The sciatic nerve is one of the largest and longest peripheral nerves in the body and contains a diverse array of axons. An initial step was to examine the morphology of the sciatic nerve and how it related to the observed CAP. Like many peripheral nerves, the sciatic nerve contains both motor and sensory fibres, which conduct action potentials both from and to the CNS, respectively. The directionality of axonal conduction *in vivo* is somewhat irrelevant when the nerves are isolated from the animal with the cell bodies excised, as there is no visible difference between afferent and efferent axons in the TEM images presented here. When recording the CAP all axons are stimulated at the same end of isolated nerve, which will mean that some axons are conducting antidromically. However, this should not matter as isolated axons are equally capable of conducting action potentials in either direction. The possibility that afferent or efferent axons could have different metabolic properties should not be dismissed, but it is beyond the scope of the methods used here to explore this question.

The experiments in this chapter replicate some of those previously conducted in the optic nerve (e.g. Brown et al., 2003; 2005). It is, therefore, useful to make

an initial comparison between the structure of the optic nerve and the MSN. Axons in the sciatic nerve exhibit a much greater range of diameters than the optic nerve. In the adult MON all axons are myelinated, but this is not the case in the adult MSN which contains groups of small un-myelinated fibres.

6.4.2 The Sciatic Nerve Compound Action Potential

The morphological differences between sciatic nerve and optic nerve axons manifest in a markedly different CAP profile. The three-peaked CAP of the adult MON is not seen in the MSN. Instead there is an initial peak, which generally occurs in isolation and displays a faster conduction velocity than the first peak of the MON CAP. This is followed by a slow biphasic peak that is of much smaller amplitude than the first peak. The CAP evoked from the MSN was qualitatively and quantitatively similar to that previously recorded by other groups using suction electrode and sucrose gap methods (Kriz et al., 2000; Matsuka and Spigelman, 2004; Thakor et al., 2009). The large myelinated axons contribute to the fast large amplitude peak and small, un-myelinated axons contribute to the slow, low-amplitude biphasic peak. In myelinated axons the potassium efflux is shielded from the extracellular fluid by the myelin surrounding the axon, but in un-myelinated fibres the extracellular fluid is in contact with the recording electrode (Kocsis and Waxman, 1980), hence the monopolar profile of myelinated axons and the bipolar profile of un-myelinated axons. The biphasic profile of the CAP evoked from un-myelinated axons has also been observed in other peripheral nerves (Vega et al., 2003), in the immature rodent optic nerve (Foster et al., 1982; Fern et al., 1998) and in myelin-deficient rats (Waxman et al., 1990).

6.4.3 The Presence and Location of Glycogen in the Sciatic Nerve

Quantification of sciatic nerve glycogen by biochemical assay showed that the MSN does contain glycogen and that this glycogen content can be up or down-regulated by exposing nerves to glucose concentrations above and below the animals' normal blood glucose concentration (approximately 10 mM). The glycogen content of the nerve was found to be greater than that measured in the MON using the same technique. A 2 hour incubation in 30 mM glucose for the optic nerve resulted in a measured glycogen content of just under 10 pmol glycogen ($\mu\text{g protein}^{-1}$) (Brown et al., 2003), considerably less than the value of 15.2 pmol glycogen ($\mu\text{g protein}^{-1}$) measured in the MSN under identical conditions. The glycogen content of the sciatic nerve incubated in 10 mM glucose was also greater than that in the optic nerve incubated in 30 mM glucose. As these values are corrected for tissue protein content it is clear that the sciatic nerve contains proportionally more glycogen when incubated the same concentration of glucose for 2 hours *in vitro*.

Whilst an assay can detect the presence of glycogen and indeed quantify it, information about its cellular location cannot be determined. It is possible to measure the glycogen content of cultures of individual cell types such as astrocytes and neurons, but this information is not necessarily reflective of the situation *in vivo*. An attempt to locate glycogen granules and determine which cell type(s) they were contained in was made using TEM. Previous experiments using TEM have shown that in the CNS glycogen is almost exclusively located in astrocytes (Brown and Ransom, 2007). The MSN as a peripheral nerve does not contain astrocytes, therefore, clearly glycogen cannot share the same cellular location. Examination of transverse sections of MSN revealed glycogen-like granules located within the cytoplasm of myelinating Schwann cells. Exposing nerves to aglycemia and hence depleting their glycogen content reduced the apparent density of these granules suggesting they are indeed glycogen (Fig. 6.10). No structures similar to

glycogen granules were identified in the axoplasm of myelinated or unmyelinated axons. It should be noted that identification and localisation of glycogen granules within a peripheral nerve warrants a study of its own. It cannot be ruled out that glycogen granules may be found in areas not examined e.g. the axon at the nodes of Ranvier.

The results of immunolabelling of glycogen phosphorylase (GP) in the sciatic nerve provide more incentive for a future in-depth examination of glycogen granules in peripheral nerve as they show that GP is strongly expressed in large axons (Fig. 6.11). A profile of GP expression in rat nervous tissue showed that GP was expressed in neurons of the afferent somatosensory system (Pfeiffer-Guglielmi et al., 2003) and in peripheral axons (Pfeiffer-Guglielmi et al., 2007) as seen in Fig. 6.11. In the MSN GP was also expressed in Schwann cells, which is consistent with the localisation of glycogen just described but in disagreement with previous studies in rat peripheral nerve (Pfeiffer-Guglielmi et al., 2007). A possible explanation for these contrasting observations may be the relative intensity of GP staining between axons and Schwann cells. Fig. 6.11 shows that the GP staining in axons is much more intense and close inspection of the figures presented by Pfeiffer-Guglielmi et al. (2007) hint at possible GP expression outside of the axons. Clearly, the expression of GP in Schwann cells demands further investigation. Irrespective of GP expression in Schwann cells the presence of GP in axons without any detectable glycogen is perplexing. One reason why GP is expressed in peripheral axons may be to prevent glycogen accumulation, as glycogen deposits are pathological for neurons (Magistretti and Allaman, 2007). However, in the CNS, GP is not expressed in axons (Pfeiffer et al., 1990) which would mean that this function of GP would be restricted to peripheral nerves.

6.4.4 Nerve Conduction During Aglycemia

The two main components of the MSN CAP fall in amplitude during aglycemia, indicating that axons become incapable of conducting action potentials. The reason for conduction failure during aglycemia is the same as in the optic nerve (see Chapters 3, 4 and 5). Briefly, withdrawal of energy substrates means that the ion gradients required for propagation of action potentials cannot be maintained. In the MSN the loss of function of myelinated and un-myelinated fibres does not occur at the same time. It was observed that the A-fibre component of the CAP was maintained for a longer duration than the C-fibre component during aglycemia. The only exception to this being after 2 hours incubation in 2 mM glucose prior to aglycemia, it appears that under these conditions both CAP components begin to fail prior to aglycemia, indicating that 2 mM glucose is insufficient to support nerve function as previously described (Brown et al., 2003). The reason why the C-fibre component of the CAP falls before the A-fibre is most likely due to the increased energy demands of C-fibres. Un-myelinated axons require more energy to generate action potentials as the energy required is proportional to membrane capacitance per unit length (Crotty et al., 2006) which is greater in un-myelinated axons (Wang et al., 2008). The difference between A- and C-fibre survival during aglycemia could also be attributed to differences in these axon's access to glycogen if this glycogen has a functional role as an energy store.

6.4.5 A Functional Role for Peripheral Nerve Glycogen

The ability of the MSN CAP to persist during an extended period of aglycemia would seem to suggest that there exists an internal store of energy substrate which can be metabolised to support nerve function. Without an energy supply axons cannot maintain their membrane potentials and therefore cannot propagate action potentials, as these are both energy-dependent processes. It

is proposed here that the glycogen content of the sciatic nerve can be used as an energy store to maintain axonal function in the absence of exogenously supplied glucose. This role for glycogen is analogous to that demonstrated in the rodent optic nerve during glucose deprivation (Ransom and Fern, 1997; Brown et al., 2003). This conclusion is in part drawn from the observation of the correlation between MSN glycogen content prior to aglycemia, and the latency to failure of CAP conduction after glucose is withdrawn. Measurement of nerve glycogen content shows that at the point where function begins to fail, indicated by a steady fall in CAP amplitude, the glycogen content of the nerve has been almost entirely exhausted. The link between CAP failure and glycogen content reaching its nadir has been previously observed in the optic nerve (Brown et al., 2003). Further confirmation of glycogen as the energy store that allows axon function to persist in the absence of glucose comes from inhibiting glycogenolysis. Glycogen phosphorylase is inhibited by DAB, which has been shown to accelerate CAP failure during aglycemia in the optic nerve (Walls et al., 2008). The same observation has now been repeated in the sciatic nerve, where the use of DAB indicates that without glycogen CAP function cannot be maintained during aglycemia.

6.4.6 Glycogen Metabolism Supports only Myelinated Fibres during Aglycemia

Examining the relationship between the glycogen content prior to aglycemia and the latency to CAP failure shows that up or down-regulating the nerve's glycogen content by altering the external glucose concentration determines the length of time conduction persists during aglycemia. This observation is more robust for the A-fibre peak compared to the C-fibre peak. A-fibre latency to failure during aglycemia was well correlated with nerve glycogen content. The A-fibre CAP fell when glycogen stores were depleted, and up-regulating glycogen content had a beneficial effect on the maintenance of conduction during aglycemia. On the other hand, C-fibre amplitude fell before glycogen

was exhausted and there was little effect on CAP failure in the presence of DAB. A small increase in C-fibre latency to failure during aglycemia was seen when nerves were pre-incubated in 30 mM glucose, but it is possible this is due to an increase in extracellular glucose rather than glycogen stores as DAB did not decrease this latency (Fig. 6.7.C and 6.8).

There are a few possible explanations as to why the beneficial effects of glycogen during aglycemia are restricted to myelinated fibres. It is possible that C-fibres have no access to glycogen. Glycogen granules were not identified in Remak Schwann cells surrounding C-fibre axons. However, this could also be explained if the amount of glycogen available to un-myelinated fibres is small and therefore diffusely located in the cytoplasm. Un-myelinated C-fibres have a higher metabolic demand than myelinated axons (Nave, 2010), and if they do have access to small quantities of glycogen their high metabolic demand would likely see these stores exhausted rapidly during aglycemia. Unfortunately, the glycogen assay cannot identify where the glycogen is located in the nerve, it can only determine gross content. If un-myelinated axons do have access to glycogen then it is likely to be a separate pool to that available to myelinated axons. When C-fibre conduction fails there is still over 50 % of the glycogen content of the nerve remaining (Fig. 6.6) suggesting that this is glycogen that C-fibres do not have access to.

The behaviour of myelinated A-fibres appears similar to that observed in the axons of rodent optic nerves (also myelinated) exposed to similar conditions (Brown et al., 2003). The conclusion reached in the case of the optic nerve is that glycogen content is under dynamic control, and can act to provide energy substrate to support axons. The data presented in this chapter point towards a similar situation in myelinated axons in the PNS. Glycogen content is labile and can be catabolised to provide an energy substrate for A-fibre axons in the sciatic nerve.

6.4.7 Glycogen in the PNS vs CNS

The majority of the data described here has also been gathered in equivalent experiments in the optic nerve and comparisons have been discussed. The sciatic nerve shares similarities with the optic nerve in terms of the functional role of glycogen. However, a striking difference is the observation that glycogen in the sciatic nerve can support CAP conduction for a much longer duration than under comparable conditions in the optic nerve. A 2 hour pre-incubation prior to aglycemia with 30 mM glucose will support optic nerve CAPs for around 30 minutes (Brown et al., 2003) whereas, in the sciatic nerve the same incubation will result in CAP failure after 230 minutes, over 7 times longer. This large difference in survival time during aglycemia is most likely due to the greater glycogen content of the nerve combined with the low energy requirements of peripheral nerve (Low et al., 1997). The direct comparison should be approached with caution as the optic nerve CAP is typically measured by its area rather than amplitude due to its more complex profile. Despite this there is a clear difference between the two nerves' abilities to continue to conduct action potentials when external energy substrates are removed.

6.4.8 A Model of Peripheral Nerve Glycogen Metabolism

This study demonstrates that glycogen can act as a source of energy substrate during aglycemia in the sciatic nerve. What remains to be shown is the exact pathway through which this energy substrate is supplied. In the CNS lactate is the product of glycogen breakdown which is then shuttled from glia to the axons – this may also be the case in the PNS. It appears as though lactate has a role in the PNS as lactate is produced by the MSN (Fig. 6.13) as it is by other peripheral nerves (Vega et al., 1998). Under resting conditions lactate is released into the tissue bath where it can be detected with a lactate biosensor which is similar to the CNS (Chapter 4 and 5). Lactate is also capable of

maintaining and restoring axonal conduction in the absence of glucose (Fig. 6.12), a further property shared with the CNS.

The model of PNS glycogen metabolism will depend upon the exact location of the glycogen discussed above but evidence suggests that Schwann cells take up around 75% of the glucose available to peripheral nerves, and that they transfer a metabolic substrate to axons which is thought to be lactate (Vega et al., 2003). Other studies have shown that the MCT1 transporter is expressed on the perineurium (Takebe et al., 2008) which is in fact consistent with either a flux of lactate out of the nerve into the blood, or transfer of plasma lactate to nerve fibres and Schwann cells. MCT transporters are bi-directional and therefore their expression pattern alone is not sufficient to determine direction of lactate transport. Based upon experiments which show staining for GP in the axons of rat vagus nerve by Pfeiffer-Guglielmi et al. (2007) suggest that the lactate transferred from glia to axons may be entered into the gluconeogenesis pathway and in turn used to produce glycogen. This would be in contrast to the situation in the optic nerve where lactate passed from glia to axons is a product of stored glycogen which is then used as an energy substrate (Brown et al., 2004). Future experiments are required to address this issue in further detail. However, preliminary localisation of glycogen to the Schwann cells would suggest that a model closer to that in the optic nerve rather than the one proposed by Pfeiffer-Guglielmi et al. (2007) would hold true for the mouse sciatic nerve. Another factor to consider is that experiments by Pfeiffer-Guglielmi et al. (2003; 2007) were performed in rat rather than mouse where the nerves are larger and diffusion distances increased, which may create a requirement for an energy source to be stored in axons rather than Schwann cells.

6.4.9 Summary

In conclusion, sciatic nerve glycogen content correlates with ability of sciatic nerve to maintain CAP conduction in myelinated axons during substrate withdrawal and once this glycogen is exhausted CAP function begins to fail. The glycogen appears to be located in the Schwann cells, which would suggest a similar model to that of CNS tissue where a substrate is shuttled to the axons from glial cells when required. The candidate molecule for this intercellular exchange is likely to be lactate which is present in the sciatic nerve. However, further investigation is needed in order to confirm the exclusive localisation of glycogen and the role of lactate in peripheral nerves.

Chapter Seven

Summary

This thesis demonstrates novel contributions to our knowledge of energy metabolism in central white matter and peripheral nerves. The summary that follows gives a brief overview of these contributions and also suggests some future directions for further experimentation.

7.1 Central white matter

In this thesis I have demonstrated that the neuroprotective role of glycogen in the MON augments that achieved by clinically utilised degrees of hypothermia. Depletion of nerve glycogen prior to aglycemia results in as severe irreversible damage as that induced by moderate hyperthermia. These findings demonstrate a possible future role for glycogen up-regulation as a therapeutic intervention. However, this comes with the caveat that clinical means of manipulating brain glycogen must be developed. This is unlikely to be simple.

Glycogen metabolism in the MON was also demonstrated under non-pathological conditions. I found that glycogen turnover contributes to the concentration of extracellular lactate observed in the MON. The contribution of glycogen to the lactate signal increases with metabolic demand. This is a feature compatible with the glycogen shunt model (Shulman et al., 2001). Clearly glycogen is not a quiescent energy store in CNS white matter. It is a contributor to the energy metabolism of the MON even under conditions of low metabolic demand.

I went on to further explore the relationship between axonal firing frequency and extracellular lactate. Stimulating the MON at higher frequencies caused the concentration of extracellular lactate to rise. Lactate production is triggered by extracellular K^+ as MON lactate concentration was found to rise with increases in $[K^+]_o$. It was concluded that increases in lactate production

in the MON may be related to the operation of the Na^+ / K^+ ATPase. This ion pump has been shown to use energy derived from glycolysis in muscle tissue (James et al., 1999). A similar association has been put forward for brain tissue and is consistent with the observations presented here. This relationship could be further explored in future by pharmacological inhibition of the Na^+ / K^+ ATPase by the drug ouabain. It would also be interesting to determine whether the proportion of lactate release attributed to glycogen is associated with increased demand on the Na^+ / K^+ ATPase. These experiments could be extended by the use of MCT blockers as discussed in chapter 5. When carried out they may be able to determine whether an ANLSH-like model can be applied to the optic nerve.

7.2 Peripheral Nerves

The role of glycogen in the brain has received an increasing amount of attention in the past decade (Brown, 2004). The same cannot be said of glycogen within peripheral nerves. Although, a role in the supply of energy to axons has been suggested (Pfeiffer-Guglielmi et al., 2007). This conclusion was based upon the presence of the enzyme glycogen phosphorylase within peripheral nerves. An energy store in the form of glycogen might be expected in peripheral nerves due to their structural properties. Large internode distances in myelinated peripheral axons restrict the axoplasm from free access to substrates contained in the extracellular fluid. This has led to the idea that glial cells surrounding the axon could supply nutrients to the internodal areas of the axon (Nave, 2010). Calculations in central axons with shorter internodes suggest that adequate glucose can be taken up by the axon at the node (Harris and Attwell, 2012). However, the authors note that for peripheral axons the node length is such that this might not be the case and the theory put forward by Nave (2010) may hold true.

The results presented in this thesis support the hypothesis that peripheral glia are able to supply energy substrates to axons. Glycogen contained in the Schwann cells surrounding peripheral myelinated axons fulfils this role. It is able to support the activity of myelinated axons in the absence of glucose. In the CNS lactate is released by glycogen-containing astrocytes and taken up by axons. It is presumed that the mechanism with which Schwann cells provide PNS axons with an energy substrate is the same. In this thesis I have shown that lactate is present in the extracellular space of the MSN. In order to confirm that glycogen-derived lactate is the substrate sustaining the activity of myelinated axons during aglycemia it will be necessary to attempt to block lactate uptake with inhibitors of MCTs such as 4-CIN. This experimental method was used to confirm likewise in the MON (Wender et al., 2000). An interesting observation is that un-myelinated PNS axons appear to receive no benefit from glycogen reserves. Whether this property plays a role in conditions such as small fibre neuropathy is an intriguing question.

Experiments presented in this thesis were all conducted *in vitro*. Certain aspects do not reflect the conditions as they are *in vivo*. An example of this is the stimulation of the nerve and the CAPs recorded. The stimulus used to evoke the supra-maximal CAP is not reflective of nerve firing *in vivo*. A frequent criticism of experiments that have looked at nervous system energy metabolism is that results have often not been replicated *in vivo* (Chih and Roberts, 2003). A future direction worth exploring would be transitioning these experiments to an *in vivo* model. This would enable the use of physiological stimuli such as a tail pinch, or a visual stimulus. Confirming the results presented here in such a way would validate the use of *in vitro* models and strengthen the conclusions being made.

References

ABI-SAAB, W. M., MAGGS, D. G., JONES, T., JACOB, R., SRIHARI, V., THOMPSON, J., KERR, D., LEONE, P., KRystal, J. H., SPENCER, D. D., DURING, M. J. and SHERWIN, R. S. (2002). Striking differences in glucose and lactate levels between brain extracellular fluid and plasma in conscious human subjects: effects of hyperglycemia and hypoglycemia. *J Cereb Blood Flow Metab* **22**(3): 271-279.

ADELMAN, W. J., JR. and FITZHUGH, R. (1975). Solutions of the Hodgkin-Huxley equations modified for potassium accumulation in a periaxonal space. *Fed Proc* **34**(5): 1322-1329.

AGARTZ, I., ANDERSSON, J. L. and SKARE, S. (2001). Abnormal brain white matter in schizophrenia: a diffusion tensor imaging study. *Neuroreport* **12**(10): 2251-2254.

ALLAMAN, I., BELANGER, M. and MAGISTRETTI, P. J. (2011). Astrocyte-neuron metabolic relationships: for better and for worse. *Trends Neurosci* **34**(2): 76-87.

ALLEN, L., ANDERSON, S., WENDER, R., MEAKIN, P., RANSOM, B. R., RAY, D. E. and BROWN, A. M. (2006). Fructose supports energy metabolism of some, but not all, axons in adult mouse optic nerve. *J Neurophysiol* **95**(3): 1917-1925.

AMES, A., 3RD (2000). CNS energy metabolism as related to function. *Brain Res Brain Res Rev* **34**(1-2): 42-68.

ANGULO, M. C., KOZLOV, A. S., CHARPAK, S. and AUDINAT, E. (2004). Glutamate released from glial cells synchronizes neuronal activity in the hippocampus. *J Neurosci* **24**(31): 6920-6927.

ARAQUE, A., PARPURA, V., SANZGIRI, R. P. and HAYDON, P. G. (1999). Tripartite synapses: glia, the unacknowledged partner. *Trends Neurosci* **22**(5): 208-215.

ASTRUP, J., SORENSEN, P. M. and SORENSEN, H. R. (1981). Oxygen and glucose consumption related to Na⁺-K⁺ transport in canine brain. *Stroke* **12**(6): 726-730.

ATTWELL, D., BUCHAN, A. M., CHARPAK, S., LAURITZEN, M., MACVICAR, B. A. and NEWMAN, E. A. (2010). Glial and neuronal control of brain blood flow. *Nature* **468**(7321): 232-243.

- ATTWELL, D. and LAUGHLIN, S. B.** (2001). An energy budget for signaling in the grey matter of the brain. *J Cereb Blood Flow Metab* **21**(10): 1133-1145.
- AZEVEDO, F. A., CARVALHO, L. R., GRINBERG, L. T., FARFEL, J. M., FERRETTI, R. E., LEITE, R. E., JACOB FILHO, W., LENT, R. and HERCULANO-HOUZEL, S.** (2009). Equal numbers of neuronal and nonneuronal cells make the human brain an isometrically scaled-up primate brain. *J Comp Neurol* **513**(5): 532-541.
- BAENA, R. C., BUSTO, R., DIETRICH, W. D., GLOBUS, M. Y. and GINSBERG, M. D.** (1997). Hyperthermia delayed by 24 hours aggravates neuronal damage in rat hippocampus following global ischemia. *Neurology* **48**(3): 768-773.
- BAIG, M. R., NAVAIRA, E., ESCAMILLA, M. A., RAVENTOS, H. and WALSS-BASS, C.** (2010). Clozapine treatment causes oxidation of proteins involved in energy metabolism in lymphoblastoid cells: a possible mechanism for antipsychotic-induced metabolic alterations. *J Psychiatr Pract* **16**(5): 325-333.
- BARRON, K. D., MARCIANO, F. F., AMUNDSON, R. and MANKES, R.** (1990). Perineuronal glial responses after axotomy of central and peripheral axons. A comparison. *Brain Res* **523**(2): 219-229.
- BARROS, L. F., BITTNER, C. X., LOAIZA, A. and PORRAS, O. H.** (2007). A quantitative overview of glucose dynamics in the gliovascular unit. *Glia* **55**(12): 1222-1237.
- BERGBAUER, K., DRINGEN, R., VERLEYSDONK, S., GEBHARDT, R., HAMPRECHT, B. and WIESINGER, H.** (1996). Studies on fructose metabolism in cultured astroglial cells and control hepatocytes: lack of fructokinase activity and immunoreactivity in astrocytes. *Dev Neurosci* **18**(5-6): 371-379.
- BINGHAM, E. M., DUNN, J. T., SMITH, D., SUTCLIFFE-GOULDEN, J., REED, L. J., MARSDEN, P. K. and AMIEL, S. A.** (2005). Differential changes in brain glucose metabolism during hypoglycaemia accompany loss of hypoglycaemia awareness in men with type 1 diabetes mellitus. An [11C]-3-O-methyl-D-glucose PET study. *Diabetologia* **48**(10): 2080-2089.
- BITTAR, P. G., CHARNAY, Y., PELLERIN, L., BOURAS, C. and MAGISTRETTI, P. J.** (1996). Selective distribution of lactate dehydrogenase isoenzymes in neurons and astrocytes of human brain. *J Cereb Blood Flow Metab* **16**(6): 1079-1089.

- BLACK, J. A., LIU, S., TANAKA, M., CUMMINS, T. R. and WAXMAN, S. G.** (2004). Changes in the expression of tetrodotoxin-sensitive sodium channels within dorsal root ganglia neurons in inflammatory pain. *Pain* **108**(3): 237-247.
- BLASS, J. P., SHEU, R. K. and CEDARBAUM, J. M.** (1988). Energy metabolism in disorders of the nervous system. *Rev Neurol (Paris)* **144**(10): 543-563.
- BOLTON, S. and BUTT, A. M.** (2005). The optic nerve: a model for axon-glia interactions. *J Pharmacol Toxicol Methods* **51**(3): 221-233.
- BONVENTO, G., HERARD, A. S. and VOUTSINOS-PORCHE, B.** (2005). The astrocyte--neuron lactate shuttle: a debated but still valuable hypothesis for brain imaging. *J Cereb Blood Flow Metab* **25**(10): 1394-1399.
- BOUZIER-SORE, A. K., MERLE, M., MAGISTRETTI, P. J. and PELLERIN, L.** (2002). Feeding active neurons: (re)emergence of a nursing role for astrocytes. *J Physiol Paris* **96**(3-4): 273-282.
- BOYLE, P. J., KEMPERS, S. F., O'CONNOR, A. M. and NAGY, R. J.** (1995). Brain glucose uptake and unawareness of hypoglycemia in patients with insulin-dependent diabetes mellitus. *N Engl J Med* **333**(26): 1726-1731.
- BROER, S., RAHMAN, B., PELLEGGRI, G., PELLERIN, L., MARTIN, J. L., VERLEYSDONK, S., HAMPRECHT, B. and MAGISTRETTI, P. J.** (1997). Comparison of lactate transport in astroglial cells and monocarboxylate transporter 1 (MCT 1) expressing *Xenopus laevis* oocytes. Expression of two different monocarboxylate transporters in astroglial cells and neurons. *J Biol Chem* **272**(48): 30096-30102.
- BROOKS, B. R. and ADAMS, R. D.** (1975). Cerebrospinal fluid acid-base and lactate changes after seizures in unanesthetized man. I. Idiopathic seizures. *Neurology* **25**(10): 935-942.
- BROWN, A. M.** (2001). A step-by-step guide to non-linear regression analysis of experimental data using a Microsoft Excel spreadsheet. *Comput Methods Programs Biomed* **65**(3): 191-200.
- BROWN, A. M.** (2004). Brain glycogen re-awakened. *J Neurochem* **89**(3): 537-552.
- BROWN, A. M.** (2006). A non-linear regression analysis program for describing electrophysiological data with multiple functions using Microsoft Excel. *Comput Methods Programs Biomed* **82**(1): 51-57.

- BROWN, A. M. and RANSOM, B. R.** (2007). Astrocyte glycogen and brain energy metabolism. *Glia* **55**(12): 1263-1271.
- BROWN, A. M., TEKOK, S. B. and RANSOM, B. R.** (2003). Glycogen regulation and functional role in mouse white matter. *J Physiol* **549**(Pt 2): 501-512.
- BROWN, A. M., WENDER, R. and RANSOM, B. R.** (2001). Metabolic substrates other than glucose support axon function in central white matter. *J Neurosci Res* **66**(5): 839-843.
- BROWN, A. M., WENDER, R. and RANSOM, B. R.** (2001). Ionic mechanisms of aglycemic axon injury in mammalian central white matter. *J Cereb Blood Flow Metab* **21**(4): 385-395.
- BROWN, A. M., WESTENBROEK, R. E., CATTERALL, W. A. and RANSOM, B. R.** (2001). Axonal L-type Ca²⁺ channels and anoxic injury in rat CNS white matter. *J Neurophysiol* **85**(2): 900-911.
- BUBBER, P., HARTOUNIAN, V., GIBSON, G. E. and BLASS, J. P.** (2011). Abnormalities in the tricarboxylic acid (TCA) cycle in the brains of schizophrenia patients. *Eur Neuropsychopharmacol* **21**(3): 254-260.
- BUSCHIAZZO, P. M., TERRELL, E. B. and REGEN, D. M.** (1970). Sugar transport across the blood-brain barrier. *Am J Physiol* **219**(5): 1505-1513.
- BUSTO, R., DIETRICH, W. D., GLOBUS, M. Y., VALDES, I., SCHEINBERG, P. and GINSBERG, M. D.** (1987). Small differences in intraschemic brain temperature critically determine the extent of ischemic neuronal injury. *J Cereb Blood Flow Metab* **7**(6): 729-738.
- BUTT, A. M., PUGH, M., HUBBARD, P. and JAMES, G.** (2004). Functions of optic nerve glia: axoglial signalling in physiology and pathology. *Eye (Lond)* **18**(11): 1110-1121.
- CAHN, R. D., ZWILLING, E., KAPLAN, N. O. and LEVINE, L.** (1962). Nature and Development of Lactic Dehydrogenases: The two major types of this enzyme form molecular hybrids which change in makeup during development. *Science* **136**(3520): 962-969.
- CATALDO, A. M. and BROADWELL, R. D.** (1986). Cytochemical identification of cerebral glycogen and glucose-6-phosphatase activity under normal and experimental conditions. II. Choroid plexus and ependymal epithelia, endothelia and pericytes. *J Neurocytol* **15**(4): 511-524.

- CATER, H. L., BENHAM, C. D. and SUNDSTROM, L. E.** (2001). Neuroprotective role of monocarboxylate transport during glucose deprivation in slice cultures of rat hippocampus. *J Physiol* **531**(Pt 2): 459-466.
- CHEN, T., QIAN, Y. Z., DI, X., ZHU, J. P. and BULLOCK, R.** (2000). Evidence for lactate uptake after rat fluid percussion brain injury. *Acta Neurochir Suppl* **76**: 359-364.
- CHIH, C. P. and ROBERTS JR, E. L.** (2003). Energy substrates for neurons during neural activity: a critical review of the astrocyte-neuron lactate shuttle hypothesis. *J Cereb Blood Flow Metab* **23**(11): 1263-1281.
- CLAY, H. B., SILLIVAN, S. and KONRADI, C.** (2011). Mitochondrial dysfunction and pathology in bipolar disorder and schizophrenia. *Int J Dev Neurosci* **29**(3): 311-324.
- CLOUTIER, M., BOLGER, F. B., LOWRY, J. P. and WELLSTEAD, P.** (2009). An integrative dynamic model of brain energy metabolism using in vivo neurochemical measurements. *J Comput Neurosci* **27**(3): 391-414.
- CONNORS, B. W., RANSOM, B. R., KUNIS, D. M. and GUTNICK, M. J.** (1982). Activity-dependent K⁺ accumulation in the developing rat optic nerve. *Science* **216**(4552): 1341-1343.
- CORNFORD, E. M., SHAMSA, K., ZEITZER, J. M., ENRIQUEZ, C. M., WILSON, C. L., BEHNKE, E. J., FRIED, I. and ENGEL, J.** (2002). Regional analyses of CNS microdialysate glucose and lactate in seizure patients. *Epilepsia* **43**(11): 1360-1371.
- CREMER, J. E., BRAUN, L. D. and OLDENDORF, W. H.** (1976). Changes during development in transport processes of the blood-brain barrier. *Biochim Biophys Acta* **448**(4): 633-637.
- CROTTY, P., SANGREY, T. and LEVY, W. B.** (2006). Metabolic energy cost of action potential velocity. *J Neurophysiol* **96**(3): 1237-1246.
- CUMMINS, K. L., PERKEL, D. H. and DORFMAN, L. J.** (1979). Nerve fiber conduction-velocity distributions. I. Estimation based on the single-fiber and compound action potentials. *Electroencephalogr Clin Neurophysiol* **46**(6): 634-646.
- DALE, N., HATZ, S., TIAN, F. and LLAUDET, E.** (2005). Listening to the brain: microelectrode biosensors for neurochemicals. *Trends Biotechnol* **23**(8): 420-428.

DE RIBAUPIERRE, F. (1966). [Synthesis and in-vitro utilization of glycogen in the rat cervical sympathetic ganglion]. *Helv Physiol Pharmacol Acta* **24**(2): C48-49.

DE VIVO, D. C., TRIFILETTI, R. R., JACOBSON, R. I., RONEN, G. M., BEHMAND, R. A. and HARIK, S. I. (1991). Defective glucose transport across the blood-brain barrier as a cause of persistent hypoglycorrhachia, seizures, and developmental delay. *N Engl J Med* **325**(10): 703-709.

DEBERNARDI, R., PIERRE, K., LENGACHER, S., MAGISTRETTI, P. J. and PELLERIN, L. (2003). Cell-specific expression pattern of monocarboxylate transporters in astrocytes and neurons observed in different mouse brain cortical cell cultures. *J Neurosci Res* **73**(2): 141-155.

DIENEL, G. A. and CRUZ, N. F. (2009). Exchange-mediated dilution of brain lactate specific activity: implications for the origin of glutamate dilution and the contributions of glutamine dilution and other pathways. *J Neurochem* **109 Suppl 1**: 30-37.

DIETL, K., RENNER, K., DETTMER, K., TIMISCHL, B., EBERHART, K., DORN, C., HELLERBRAND, C., KASTENBERGER, M., KUNZ-SCHUGHART, L. A., OEFNER, P. J., ANDREESSEN, R., GOTTFRIED, E. and KREUTZ, M. P. (2010). Lactic acid and acidification inhibit TNF secretion and glycolysis of human monocytes. *J Immunol* **184**(3): 1200-1209.

DiNUZZO, M., MANGIA, S., MARAVIGLIA, B. and GIOVE, F. (2010). Glycogenolysis in astrocytes supports blood-borne glucose channeling not glycogen-derived lactate shuttling to neurons: evidence from mathematical modeling. *J Cereb Blood Flow Metab* **30**(12): 1895-1904.

DOMBRO, R. S., HUTSON, D. G. and NORENBURG, M. D. (1993). The action of ammonia on astrocyte glycogen and glycogenolysis. *Mol Chem Neuropathol* **19**(3): 259-268.

DRINGEN, R., GEBHARDT, R. and HAMPRECHT, B. (1993). Glycogen in astrocytes: possible function as lactate supply for neighboring cells. *Brain Res* **623**(2): 208-214.

DURING, M. J., FRIED, I., LEONE, P., KATZ, A. and SPENCER, D. D. (1994). Direct measurement of extracellular lactate in the human hippocampus during spontaneous seizures. *J Neurochem* **62**(6): 2356-2361.

EDWARDS, A. D., WYATT, J. S. and THORESEN, M. (1998). Treatment of hypoxic-ischaemic brain damage by moderate hypothermia. *Arch Dis Child Fetal Neonatal Ed* **78**(2): F85-88.

- ERLICHMAN, J. S., HEWITT, A., DAMON, T. L., HART, M., KURASCZ, J., LI, A. and LEITER, J. C.** (2008). Inhibition of monocarboxylate transporter 2 in the retrotrapezoid nucleus in rats: a test of the astrocyte-neuron lactate-shuttle hypothesis. *J Neurosci* **28**(19): 4888-4896.
- ERLICHMAN, J. S. and LEITER, J. C.** (2010). Glia modulation of the extracellular milieu as a factor in central CO₂ chemosensitivity and respiratory control. *J Appl Physiol* **108**(6): 1803-1811.
- EUGENIN, E. A., SAEZ, C. G., GARCES, G. and SAEZ, J. C.** (1997). Regulation of glycogen content in rat pineal gland by norepinephrine. *Brain Res* **760**(1-2): 34-41.
- EVANS, R. D., WESTON, D. A., McLAUGHLIN, M. and BROWN, A. M.** (2010). A non-linear regression analysis method for quantitative resolution of the stimulus-evoked compound action potential from rodent optic nerve. *J Neurosci Methods* **188**(1): 174-178.
- FERN, R., RANSOM, B. R. and WAXMAN, S. G.** (1995). Voltage-gated calcium channels in CNS white matter: role in anoxic injury. *J Neurophysiol* **74**(1): 369-377.
- FERNANDEZ, P. A., TANG, D. G., CHENG, L., PROCHIANTZ, A., MUDGE, A. W. and RAFF, M. C.** (2000). Evidence that axon-derived neuregulin promotes oligodendrocyte survival in the developing rat optic nerve. *Neuron* **28**(1): 81-90.
- FERNIE, A. R., CARRARI, F. and SWEETLOVE, L. J.** (2004). Respiratory metabolism: glycolysis, the TCA cycle and mitochondrial electron transport. *Curr Opin Plant Biol* **7**(3): 254-261.
- FILLENZ, M.** (2005). The role of lactate in brain metabolism. *Neurochem Int* **47**(6): 413-417.
- FOLEY, J. C., McIVER, S. R. and HAYDON, P. G.** (2011). Gliotransmission modulates baseline mechanical nociception. *Mol Pain* **7**: 93.
- FONNUM, F., JOHNSEN, A. and HASSEL, B.** (1997). Use of fluorocitrate and fluoroacetate in the study of brain metabolism. *Glia* **21**(1): 106-113.
- FOSTER, C. L.** (1960). The demonstration of glycogen in liver cells fixed in osmium tetroxide. *Quarterly Journal of Microscopical Science* **s3-101**(55): 273 - 277.
- FOSTER, R. E., CONNORS, B. W. and WAXMAN, S. G.** (1982). Rat optic nerve: electrophysiological, pharmacological and anatomical studies during development. *Brain Res* **255**(3): 371-386.

- FOX, P. T., RAICHLER, M. E., MINTUN, M. A. and DENCE, C.** (1988). Nonoxidative glucose consumption during focal physiologic neural activity. *Science* **241**(4864): 462-464.
- FRAHM, J., KRUGER, G., MERBOLDT, K. D. and KLEINSCHMIDT, A.** (1996). Dynamic uncoupling and recoupling of perfusion and oxidative metabolism during focal brain activation in man. *Magn Reson Med* **35**(2): 143-148.
- FRAY, A. E., FORSYTH, R. J., BOUTELLE, M. G. and FILLENZ, M.** (1996). The mechanisms controlling physiologically stimulated changes in rat brain glucose and lactate: a microdialysis study. *J Physiol* **496** (Pt 1): 49-57.
- FRIER, B. M. and FISHER, M.** (2007). *Hypoglycemia in Clinical Diabetes 2nd Edition*, John Wiley & Sons.
- FULTON, J. F.** (1928). Observations on the vascularity of the human occipital lobe during visual activity. *Brain* **51**(3): 310-320.
- GAGE, S. H.** (1917). Glycogen in the nervous system of vertebrates. *J Comp Neurol* **27**(3): 451-465.
- GARCIA-MARIN, V., GARCIA-LOPEZ, P. and FREIRE, M.** (2007). Cajal's contributions to glia research. *Trends Neurosci* **30**(9): 479-487.
- GARTHWAITE, G., BROWN, G., BATCHELOR, A. M., GOODWIN, D. A. and GARTHWAITE, J.** (1999). Mechanisms of ischaemic damage to central white matter axons: a quantitative histological analysis using rat optic nerve. *Neuroscience* **94**(4): 1219-1230.
- GIBBS, M. E., ANDERSON, D. G. and HERTZ, L.** (2006). Inhibition of glycogenolysis in astrocytes interrupts memory consolidation in young chickens. *Glia* **54**(3): 214-222.
- GIBBS, M. E., HUTCHINSON, D. S. and SUMMERS, R. J.** (2008). Role of beta-adrenoceptors in memory consolidation: beta3-adrenoceptors act on glucose uptake and beta2-adrenoceptors on glycogenolysis. *Neuropsychopharmacology* **33**(10): 2384-2397.
- GOLDBERG, M. P. and RANSOM, B. R.** (2003). New light on white matter. *Stroke* **34**(2): 330-332.
- GRAEBER, M. B. and STREIT, W. J.** (2010). Microglia: biology and pathology. *Acta Neuropathol* **119**(1): 89-105.
- GREEN, A. R. and SHUAIB, A.** (2006). Therapeutic strategies for the treatment of stroke. *Drug Discov Today* **11**(15-16): 681-693.

- GRUETTER, R.** (2003). Glycogen: the forgotten cerebral energy store. *J Neurosci Res* **74**(2): 179-183.
- GRUETTER, R., NOVOTNY, E. J., BOULWARE, S. D., ROTHMAN, D. L., MASON, G. F., SHULMAN, G. I., SHULMAN, R. G. and TAMBORLANE, W. V.** (1992). Direct measurement of brain glucose concentrations in humans by ¹³C NMR spectroscopy. *Proc Natl Acad Sci U S A* **89**(3): 1109-1112.
- HALESTRAP, A. P. and MEREDITH, D.** (2004). The SLC16 gene family-from monocarboxylate transporters (MCTs) to aromatic amino acid transporters and beyond. *Pflugers Arch* **447**(5): 619-628.
- HALESTRAP, A. P. and PRICE, N. T.** (1999). The proton-linked monocarboxylate transporter (MCT) family: structure, function and regulation. *Biochem J* **343 Pt 2**: 281-299.
- HAMNER, M. A., MOLLER, T. and RANSOM, B. R.** (2011). Anaerobic function of CNS white matter declines with age. *J Cereb Blood Flow Metab* **31**(4): 996-1002.
- HANANI, M.** (2010). Satellite glial cells in sympathetic and parasympathetic ganglia: in search of function. *Brain Res Rev* **64**(2): 304-327.
- HANSEN, T. W.** (2001). Bilirubin brain toxicity. *J Perinatol* **21 Suppl 1**: S48-51; discussion S59-62.
- HARADA, M., SAWA, T., OKUDA, C., MATSUDA, T. and TANAKA, Y.** (1993). Effects of glucose load on brain extracellular lactate concentration in conscious rats using a microdialysis technique. *Horm Metab Res* **25**(11): 560-563.
- HARGREAVES, M.** (2004). Muscle glycogen and metabolic regulation. *Proc Nutr Soc* **63**(2): 217-220.
- HARRIS, J. J. and ATTWELL, D.** (2012). The energetics of CNS white matter. *J Neurosci* **32**(1): 356-371.
- HARTLINE, D. K.** (2011). The evolutionary origins of glia. *Glia* **59**(9): 1215-1236.
- HAWKINS, B. T. and DAVIS, T. P.** (2005). The blood-brain barrier/neurovascular unit in health and disease. *Pharmacol Rev* **57**(2): 173-185.
- HEINEMANN, U. and Lux, H. D.** (1977). Ceiling of stimulus induced rises in extracellular potassium concentration in the cerebral cortex of cat. *Brain Res* **120**(2): 231-249.

- HELLMANN, J., VANNUCCI, R. C. and NARDIS, E. E.** (1982). Blood-brain barrier permeability to lactic acid in the newborn dog: lactate as a cerebral metabolic fuel. *Pediatr Res* **16**(1): 40-44.
- HENNEBERGER, C., PAPOUIN, T., OLIET, S. H. and RUSAKOV, D. A.** (2010). Long-term potentiation depends on release of D-serine from astrocytes. *Nature* **463**(7278): 232-236.
- HEPBURN, D. A., PATRICK, A. W., EADINGTON, D. W., EWING, D. J. and FRIER, B. M.** (1990). Unawareness of hypoglycaemia in insulin-treated diabetic patients: prevalence and relationship to autonomic neuropathy. *Diabet Med* **7**(8): 711-717.
- HERTZ, L. and DIENEL, G. A.** (2005). Lactate transport and transporters: general principles and functional roles in brain cells. *J Neurosci Res* **79**(1-2): 11-18.
- HOUSLEY, G. D.** (2011). Recent insights into the regulation of breathing. *Auton Neurosci* **164**(1-2): 3-5.
- HU, Y. and WILSON, G. S.** (1997). A temporary local energy pool coupled to neuronal activity: fluctuations of extracellular lactate levels in rat brain monitored with rapid-response enzyme-based sensor. *J Neurochem* **69**(4): 1484-1490.
- HUTCHINSON, D. S., SUMMERS, R. J. and GIBBS, M. E.** (2008). Energy metabolism and memory processing: role of glucose transport and glycogen in responses to adrenoceptor activation in the chicken. *Brain Res Bull* **76**(3): 224-234.
- JAMES, E. L., PEACOCK, V. A., EBLING, F. J. and BROWN, A. M.** (2010). Morphological and electrophysiological characterization of the adult Siberian hamster optic nerve. *Anat Sci Int* **85**(4): 214-223.
- JAMES, J. H., WAGNER, K. R., KING, J. K., LEFFLER, R. E., UPPUTURI, R. K., BALASUBRAMANIAM, A., FRIEND, L. A., SHELLY, D. A., PAUL, R. J. and FISCHER, J. E.** (1999). Stimulation of both aerobic glycolysis and Na(+)-K(+)-ATPase activity in skeletal muscle by epinephrine or amylin. *Am J Physiol* **277**(1 Pt 1): E176-186.
- JOHNSON, L. N.** (1992). Glycogen phosphorylase: control by phosphorylation and allosteric effectors. *FASEB J* **6**(6): 2274-2282.
- JUEL, C. and HALESTRAP, A. P.** (1999). Lactate transport in skeletal muscle - role and regulation of the monocarboxylate transporter. *J Physiol* **517** (Pt 3): 633-642.

- KASISCHKE, K. A., VISHWASRAO, H. D., FISHER, P. J., ZIPFEL, W. R. and WEBB, W. W.** (2004). Neural activity triggers neuronal oxidative metabolism followed by astrocytic glycolysis. *Science* **305**(5680): 99-103.
- KATZMAN, R.** (1976). Maintenance of a constant brain extracellular potassium. *Fed Proc* **35**(6): 1244-1247.
- KETY, S. S. and SCHMIDT, C. F.** (1948). The nitrous oxide method for the quantitative determination of cerebral blood flow in man; theory, procedure and normal values. *J Clin Invest* **27**(4): 476-483.
- KIERNAN, M. C., CIKUREL, K. and BOSTOCK, H.** (2001). Effects of temperature on the excitability properties of human motor axons. *Brain* **124**(Pt 4): 816-825.
- KOCHS, E.** (1995). Electrophysiological monitoring and mild hypothermia. *J Neurosurg Anesthesiol* **7**(3): 222-228.
- KOCSIS, J. D. and WAXMAN, S. G.** (1980). Absence of potassium conductance in central myelinated axons. *Nature* **287**(5780): 348-349.
- KOEHLER-STEC, E. M., SIMPSON, I. A., VANNUCCI, S. J., LANDSCHULZ, K. T. and LANDSCHULZ, W. H.** (1998). Monocarboxylate transporter expression in mouse brain. *Am J Physiol* **275**(3 Pt 1): E516-524.
- KOGURE, K., BUSTO, R., SCHEINBERG, P. and REINMUTH, O. M.** (1974). Energy metabolites and water content in rat brain during the early stage of development of cerebral infarction. *Brain* **97**(1): 103-114.
- KOMURE, O., ICHIKAWA, K., TSUTSUMI, A., HIYAMA, K. and FUJIOKA, A.** (1985). Intra-axonal polysaccharide deposits in the peripheral nerve seen in adult polysaccharide storage myopathy. *Acta Neuropathol* **65**(3-4): 300-304.
- KORN, A., GOLAN, H., MELAMED, I., PASCUAL-MARQUI, R. and FRIEDMAN, A.** (2005). Focal cortical dysfunction and blood-brain barrier disruption in patients with Postconcussion syndrome. *J Clin Neurophysiol* **22**(1): 1-9.
- KRIZ, J., ZHU, Q., JULIEN, J. P. and PADJEN, A. L.** (2000). Electrophysiological properties of axons in mice lacking neurofilament subunit genes: disparity between conduction velocity and axon diameter in absence of NF-H. *Brain Res* **885**(1): 32-44.
- KRUGER, G., KLEINSCHMIDT, A. and FRAHM, J.** (1996). Dynamic MRI sensitized to cerebral blood oxygenation and flow during sustained activation of human visual cortex. *Magn Reson Med* **35**(6): 797-800.

KUHR, W. G. and KORF, J. (1988). Extracellular lactic acid as an indicator of brain metabolism: continuous on-line measurement in conscious, freely moving rats with intrastriatal dialysis. *J Cereb Blood Flow Metab* **8**(1): 130-137.

KUM, W., ZHU, S. Q., HO, S. K., YOUNG, J. D. and COCKRAM, C. S. (1992). Effect of insulin on glucose and glycogen metabolism and leucine incorporation into protein in cultured mouse astrocytes. *Glia* **6**(4): 264-268.

LAM, K., SEFTON, A. J. and BENNETT, M. R. (1982). Loss of axons from the optic nerve of the rat during early postnatal development. *Brain Res* **255**(3): 487-491.

LAVOIE, S., ALLAMAN, I., PETIT, J. M., DO, K. Q. and MAGISTRETTI, P. J. (2011). Altered glycogen metabolism in cultured astrocytes from mice with chronic glutathione deficit; relevance for neuroenergetics in schizophrenia. *PLoS One* **6**(7): e22875.

LEAR, J. L. and KASLIWAL, R. K. (1991). Autoradiographic measurement of cerebral lactate transport rate constants in normal and activated conditions. *J Cereb Blood Flow Metab* **11**(4): 576-580.

LEEGSMA-VOGT, G., VENEMA, K. and KORF, J. (2003). Evidence for a lactate pool in the rat brain that is not used as an energy supply under normoglycemic conditions. *J Cereb Blood Flow Metab* **23**(8): 933-941.

LEPPANEN, L. and STYS, P. K. (1997). Ion transport and membrane potential in CNS myelinated axons. II. Effects of metabolic inhibition. *J Neurophysiol* **78**(4): 2095-2107.

LEVI, A. D., GREEN, B. A., WANG, M. Y., DIETRICH, W. D., BRINDLE, T., VANNI, S., CASELLA, G., ELHAMMADY, G. and JAGID, J. (2009). Clinical application of modest hypothermia after spinal cord injury. *J Neurotrauma* **26**(3): 407-415.

LIU, Z., GATT, A., MIKATI, M. and HOLMES, G. L. (1993). Effect of temperature on kainic acid-induced seizures. *Brain Res* **631**(1): 51-58.

LOW, P. A., YAO, J. K., KISHI, Y., TRITSCHLER, H. J., SCHMELZER, J. D., ZOLLMAN, P. J. and NICKANDER, K. K. (1997). Peripheral nerve energy metabolism in experimental diabetic neuropathy. *Neuroscience Research Communications* **21**(1): 49-56.

- LUBOW, J. M., PINON, I. G., AVOGARO, A., COBELLI, C., TREESON, D. M., MANDEVILLE, K. A., TOFFOLO, G. and BOYLE, P. J.** (2006). Brain oxygen utilization is unchanged by hypoglycemia in normal humans: lactate, alanine, and leucine uptake are not sufficient to offset energy deficit. *Am J Physiol Endocrinol Metab* **290**(1): E149-E153.
- MA, D., GUEST, P. C. and BAHN, S.** (2009). Metabonomic studies of schizophrenia and psychotropic medications: focus on alterations in CNS energy homeostasis. *Bioanalysis* **1**(9): 1615-1626.
- MADSEN, P. L., CRUZ, N. F., SOKOLOFF, L. and DIENEL, G. A.** (1999). Cerebral oxygen/glucose ratio is low during sensory stimulation and rises above normal during recovery: excess glucose consumption during stimulation is not accounted for by lactate efflux from or accumulation in brain tissue. *J Cereb Blood Flow Metab* **19**(4): 393-400.
- MAGISTRETTI, P. J.** (2000). Cellular bases of functional brain imaging: insights from neuron-glia metabolic coupling. *Brain Res* **886**(1-2): 108-112.
- MAGISTRETTI, P. J. and ALLAMAN, I.** (2007). Glycogen: a Trojan horse for neurons. *Nat Neurosci* **10**(11): 1341-1342.
- MAGISTRETTI, P. J. and PELLERIN, L.** (1999). Cellular mechanisms of brain energy metabolism and their relevance to functional brain imaging. *Philos Trans R Soc Lond B Biol Sci* **354**(1387): 1155-1163.
- MAGISTRETTI, P. J., PELLERIN, L., ROTHMAN, D. L. and SHULMAN, R. G.** (1999). Energy on demand. *Science* **283**(5401): 496-497.
- MAGISTRETTI, P. J., SORG, O., YU, N., MARTIN, J. L. and PELLERIN, L.** (1993). Neurotransmitters regulate energy metabolism in astrocytes: implications for the metabolic trafficking between neural cells. *Dev Neurosci* **15**(3-5): 306-312.
- MALLOY, P., CORREIA, S., STEBBINS, G. and LAIDLAW, D. H.** (2007). Neuroimaging of white matter in aging and dementia. *Clin Neuropsychol* **21**(1): 73-109.
- MANCARDI, G. L., SCHENONE, A., TABATON, M., TASSINARI, T. and MAINARDI, P.** (1985). Polyglucosan bodies in the sural nerve of a diabetic patient with polyneuropathy. *Acta Neuropathol* **66**(1): 83-86.
- MANGIA, S., GARREFFA, G., BIANCIARDI, M., GIOVE, F., DI SALLE, F. and MARAVIGLIA, B.** (2003). The aerobic brain: lactate decrease at the onset of neural activity. *Neuroscience* **118**(1): 7-10.

MANGOLD, R., SOKOLOFF, L., CONNER, E., KLEINERMAN, J., THERMAN, P. O. and KETY, S. S. (1955). The effects of sleep and lack of sleep on the cerebral circulation and metabolism of normal young men. *J Clin Invest* **34**(7, Part 1): 1092-1100.

MARAN, A., CRANSTON, I., LOMAS, J., MACDONALD, I. and AMIEL, S. A. (1994). Protection by lactate of cerebral function during hypoglycaemia. *Lancet* **343**(8888): 16-20.

MARNER, L., NYENGAARD, J. R., TANG, Y. and PAKKENBERG, B. (2003). Marked loss of myelinated nerve fibers in the human brain with age. *J Comp Neurol* **462**(2): 144-152.

MARTINS-DE-SOUZA, D., HARRIS, L. W., GUEST, P. C. and BAHN, S. (2011). The role of energy metabolism dysfunction and oxidative stress in schizophrenia revealed by proteomics. *Antioxid Redox Signal* **15**(7): 2067-2079.

MATSUKA, Y. and SPIGELMAN, I. (2004). Hyperosmolar solutions selectively block action potentials in rat myelinated sensory fibers: implications for diabetic neuropathy. *J Neurophysiol* **91**(1): 48-56.

McILWAIN, H. (1953). Substances which support respiration and metabolic response to electrical impulses in human cerebral tissues. *J Neurol Neurosurg Psychiatry* **16**(4): 257-266.

McKENNA, M. C., HOPKINS, I. B. and CAREY, A. (2001). Alpha-cyano-4-hydroxycinnamate decreases both glucose and lactate metabolism in neurons and astrocytes: implications for lactate as an energy substrate for neurons. *J Neurosci Res* **66**(5): 747-754.

McKENNA, M. C., TILDON, J. T., STEVENSON, J. H., HOPKINS, I. B., HUANG, X. and COUTO, R. (1998). Lactate transport by cortical synaptosomes from adult rat brain: characterization of kinetics and inhibitor specificity. *Dev Neurosci* **20**(4-5): 300-309.

MEAKIN, P. J., FOWLER, M. J., RATHBONE, A. J., ALLEN, L. M., RANSOM, B. R., RAY, D. E. and BROWN, A. M. (2007). Fructose metabolism in the adult mouse optic nerve, a central white matter tract. *J Cereb Blood Flow Metab* **27**(1): 86-99.

MEDINA, M. A., JONES, D. J., STAVINOHA, W. B. and ROSS, D. H. (1975). The levels of labile intermediary metabolites in mouse brain following rapid tissue fixation with microwave irradiation. *J Neurochem* **24**(2): 223-227.

MICHENFELDER, J. D. and MILDE, J. H. (1991). The relationship among canine brain temperature, metabolism, and function during hypothermia. *Anesthesiology* **75**(1): 130-136.

- MOORHOUSE, A. D., SPITERI, C., SHARMA, P., ZLOH, M. and MOSES, J. E.** (2011). Targeting glycolysis: a fragment based approach towards bifunctional inhibitors of hLDH-5. *Chem Commun (Camb)* **47**(1): 230-232.
- MORETTI, A., GORINI, A. and VILLA, R. F.** (2003). Affective disorders, antidepressant drugs and brain metabolism. *Mol Psychiatry* **8**(9): 773-785.
- MORI, F., NISHIE, M., HOUZEN, H., YAMAGUCHI, J. and WAKABAYASHI, K.** (2006). Hypoglycemic encephalopathy with extensive lesions in the cerebral white matter. *Neuropathology* **26**(2): 147-152.
- MURAKAWA, Y., ZHANG, W., PIERSON, C. R., BRISMAR, T., OSTENSON, C. G., EFENDIC, S. and SIMA, A. A.** (2002). Impaired glucose tolerance and insulinopenia in the GK-rat causes peripheral neuropathy. *Diabetes Metab Res Rev* **18**(6): 473-483.
- MURINSON, B. B. and GRIFFIN, J. W.** (2004). C-fiber structure varies with location in peripheral nerve. *J Neuropathol Exp Neurol* **63**(3): 246-254.
- MUSTAFA, A. K., KIM, P. M. and SNYDER, S. H.** (2004). D-Serine as a putative glial neurotransmitter. *Neuron Glia Biol* **1**(3): 275-281.
- NAVE, K. A.** (2010). Myelination and the trophic support of long axons. *Nat Rev Neurosci* **11**(4): 275-283.
- NEWGARD, C. B., HWANG, P. K. and FLETTERICK, R. J.** (1989). The family of glycogen phosphorylases: structure and function. *Crit Rev Biochem Mol Biol* **24**(1): 69-99.
- NEWMAN, E. A.** (2003). Glial cell inhibition of neurons by release of ATP. *J Neurosci* **23**(5): 1659-1666.
- NIKLASSON, F. and AGREN, H.** (1984). Brain energy metabolism and blood-brain barrier permeability in depressive patients: analyses of creatine, creatinine, urate, and albumin in CSF and blood. *Biol Psychiatry* **19**(8): 1183-1206.
- NOWAK, L., ASCHER, P. and BERWALD-NETTER, Y.** (1987). Ionic channels in mouse astrocytes in culture. *J Neurosci* **7**(1): 101-109.
- OBERHEIM, N. A., TAKANO, T., HAN, X., HE, W., LIN, J. H., WANG, F., XU, Q., WYATT, J. D., PILCHER, W., OJEMANN, J. G., RANSOM, B. R., GOLDMAN, S. A. and NEDERGAARD, M.** (2009). Uniquely hominid features of adult human astrocytes. *J Neurosci* **29**(10): 3276-3287.

OGAWA, S., FINK, B. R. and CAIRNS, A. M. (1984). [Differential vulnerability of mammalian A delta and C fibers to glucose-lack]. *Masui* **33**(5): 469-473.

PANTONI, L., GARCIA, J. H. and GUTIERREZ, J. A. (1996). Cerebral white matter is highly vulnerable to ischemia. *Stroke* **27**(9): 1641-1646; discussion 1647.

PAUL, R. J., BAUER, M. and PEASE, W. (1979). Vascular smooth muscle: aerobic glycolysis linked to sodium and potassium transport processes. *Science* **206**(4425): 1414-1416.

PAULSON, G. W., LOCKE, G. E. and YASHON, D. (1971). Cerebral spinal fluid lactic acid following circulatory arrest. *Stroke* **2**(6): 565-568.

PAVLOVSKY, L., SEIFFERT, E., HEINEMANN, U., KORN, A., GOLAN, H. and FRIEDMAN, A. (2005). Persistent BBB disruption may underlie alpha interferon-induced seizures. *J Neurol* **252**(1): 42-46.

PELLERIN, L., BERGERSEN, L. H., HALESTRAP, A. P. and PIERRE, K. (2005). Cellular and subcellular distribution of monocarboxylate transporters in cultured brain cells and in the adult brain. *J Neurosci Res* **79**(1-2): 55-64.

PELLERIN, L. and MAGISTRETTI, P. J. (1994). Glutamate uptake into astrocytes stimulates aerobic glycolysis: a mechanism coupling neuronal activity to glucose utilization. *Proc Natl Acad Sci U S A* **91**(22): 10625-10629.

PELLERIN, L. and MAGISTRETTI, P. J. (2003). Food for thought: challenging the dogmas. *J Cereb Blood Flow Metab* **23**(11): 1282-1286.

PELLERIN, L. and MAGISTRETTI, P. J. (2004). Neuroenergetics: calling upon astrocytes to satisfy hungry neurons. *Neuroscientist* **10**(1): 53-62.

PELLERIN, L., STOLZ, M., SORG, O., MARTIN, J. L., DESCHEPPER, C. F. and MAGISTRETTI, P. J. (1997). Regulation of energy metabolism by neurotransmitters in astrocytes in primary culture and in an immortalized cell line. *Glia* **21**(1): 74-83.

PERILLAN, P. R., LI, X. and SIMARD, J. M. (1999). K(+) inward rectifier currents in reactive astrocytes from adult rat brain. *Glia* **27**(3): 213-225.

PFEIFFER, B., ELMER, K., ROGGENDORF, W., REINHART, P. H. and HAMPRECHT, B. (1990). Immunohistochemical demonstration of glycogen phosphorylase in rat brain slices. *Histochemistry* **94**(1): 73-80.

- PFEIFFER-GUGLIELMI, B., FLECKENSTEIN, B., JUNG, G. and HAMPRECHT, B.** (2003). Immunocytochemical localization of glycogen phosphorylase isozymes in rat nervous tissues by using isozyme-specific antibodies. *J Neurochem* **85**(1): 73-81.
- PFEIFFER-GUGLIELMI, B., FRANCKE, M., REICHENBACH, A. and HAMPRECHT, B.** (2007). Glycogen phosphorylase isozymes and energy metabolism in the rat peripheral nervous system--an immunocytochemical study. *Brain Res* **1136**(1): 20-27.
- PILEGAARD, H., KELLER, C., STEENSBERG, A., HELGE, J. W., PEDERSEN, B. K., SALTIN, B. and NEUFER, P. D.** (2002). Influence of pre-exercise muscle glycogen content on exercise-induced transcriptional regulation of metabolic genes. *J Physiol* **541**(Pt 1): 261-271.
- POTOCNIK, I., TOMSIC, M., SKETELJ, J. and BAJROVIC, F. F.** (2006). Articaine is more effective than lidocaine or mepivacaine in rat sensory nerve conduction block in vitro. *J Dent Res* **85**(2): 162-166.
- QUISTORFF, B., SECHER, N. H. and VAN LIESHOUT, J. J.** (2008). Lactate fuels the human brain during exercise. *FASEB J* **22**(10): 3443-3449.
- RAFIKI, A., BOULLAND, J. L., HALESTRAP, A. P., OTTERSEN, O. P. and BERGERSEN, L.** (2003). Highly differential expression of the monocarboxylate transporters MCT2 and MCT4 in the developing rat brain. *Neuroscience* **122**(3): 677-688.
- RAICHLE, M. E.** (2003). Functional brain imaging and human brain function. *J Neurosci* **23**(10): 3959-3962.
- RAICHLE, M. E. and GUSNARD, D. A.** (2002). Appraising the brain's energy budget. *Proc Natl Acad Sci U S A* **99**(16): 10237-10239.
- RANSOM, B. R., CARLINI, W. G. and CONNORS, B. W.** (1986). Brain extracellular space: developmental studies in rat optic nerve. *Ann N Y Acad Sci* **481**: 87-105.
- RANSOM, B. R. and FERN, R.** (1997). Does astrocytic glycogen benefit axon function and survival in CNS white matter during glucose deprivation? *Glia* **21**(1): 134-141.
- RANSOM, B. R. and SONTHEIMER, H.** (1992). The neurophysiology of glial cells. *J Clin Neurophysiol* **9**(2): 224-251.
- RANSOM, C. B., RANSOM, B. R. and SONTHEIMER, H.** (2000). Activity-dependent extracellular K⁺ accumulation in rat optic nerve: the role of glial and axonal Na⁺ pumps. *J Physiol* **522 Pt 3**: 427-442.

RASMUSSEN, P., WYSS, M. T. and LUNDBY, C. (2011). Cerebral glucose and lactate consumption during cerebral activation by physical activity in humans. *FASEB J* **25**(9): 2865-2873.

READING, S. A., YASSA, M. A., BAKKER, A., DZIorny, A. C., GOURLEY, L. M., YALLAPRAGADA, V., ROSENBLATT, A., MARGOLIS, R. L., AYLWARD, E. H., BRANDT, J., MORI, S., VAN ZIJL, P., BASSETT, S. S. and ROSS, C. A. (2005). Regional white matter change in pre-symptomatic Huntington's disease: a diffusion tensor imaging study. *Psychiatry Res* **140**(1): 55-62.

REVEL, J. P., NAPOLITANO, L. and FAWCETT, D. W. (1960). Identification of glycogen in electron micrographs of thin tissue sections. *J Biophys Biochem Cytol* **8**: 575-589.

RIGAUD, M., GEMES, G., BARABAS, M. E., CHERNOFF, D. I., ABRAM, S. E., STUCKY, C. L. and HOGAN, Q. H. (2008). Species and strain differences in rodent sciatic nerve anatomy: implications for studies of neuropathic pain. *Pain* **136**(1-2): 188-201.

RINHOLM, J. E., HAMILTON, N. B., KESSARIS, N., RICHARDSON, W. D., BERGERSEN, L. H. and ATTWELL, D. (2011). Regulation of oligodendrocyte development and myelination by glucose and lactate. *J Neurosci* **31**(2): 538-548.

RIVERS, E. P., PARADIS, N. A., MARTIN, G. B., GOETTING, M. E., ROSENBERG, J. A., SMITHLINE, H. A., APPLETON, T. J. and NOWAK, R. M. (1991). Cerebral lactate uptake during cardiopulmonary resuscitation in humans. *J Cereb Blood Flow Metab* **11**(3): 479-484.

ROLLINS, B., MARTIN, M. V., SEQUEIRA, P. A., MOON, E. A., MORGAN, L. Z., WATSON, S. J., SCHATZBERG, A., AKIL, H., MYERS, R. M., JONES, E. G., WALLACE, D. C., BUNNEY, W. E. and VAWTER, M. P. (2009). Mitochondrial variants in schizophrenia, bipolar disorder, and major depressive disorder. *PLoS One* **4**(3): e4913.

ROSS, J. M., OBERG, J., BRENE, S., COPPOTELLI, G., TERZIOGLU, M., PERNOLD, K., GOINY, M., SITNIKOV, R., KEHR, J., TRIFUNOVIC, A., LARSSON, N. G., HOFFER, B. J. and OLSON, L. (2010). High brain lactate is a hallmark of aging and caused by a shift in the lactate dehydrogenase A/B ratio. *Proc Natl Acad Sci U S A* **107**(46): 20087-20092.

ROSSEN, R., KABAT, H. and ANDERSON, J. P. (1943). Acute arrest of cerebral circulation in man. *Arch Neurol Psychiat* **50**: 510-528.

RUST, R. S. (1994). Energy metabolism of developing brain. *Curr Opin Neurol* **7**(2): 160-165.

- SALEM, R. D., HAMMERSCHLAG, R., BRANCHO, H. and ORKAND, R. K.** (1975). Influence of potassium ions on accumulation and metabolism of (14C)glucose by glial cells. *Brain Res* **86**(3): 499-503.
- SANCHEZ-ABARCA, L. I., TABERNERO, A. and MEDINA, J. M.** (2001). Oligodendrocytes use lactate as a source of energy and as a precursor of lipids. *Glia* **36**(3): 321-329.
- SANDOVAL, K. E. and WITT, K. A.** (2008). Blood-brain barrier tight junction permeability and ischemic stroke. *Neurobiol Dis* **32**(2): 200-219.
- SAS, K., ROBOTKA, H., TOLDI, J. and VECSEI, L.** (2007). Mitochondria, metabolic disturbances, oxidative stress and the kynurenine system, with focus on neurodegenerative disorders. *J Neurol Sci* **257**(1-2): 221-239.
- SAXENA, S., BRODY, A. L., HO, M. L., ALBORZIAN, S., HO, M. K., MAIDMENT, K. M., HUANG, S. C., WU, H. M., AU, S. C. and BAXTER, L. R., JR.** (2001). Cerebral metabolism in major depression and obsessive-compulsive disorder occurring separately and concurrently. *Biol Psychiatry* **50**(3): 159-170.
- SCHURR, A.** (2002). Lactate, glucose and energy metabolism in the ischemic brain (Review). *Int J Mol Med* **10**(2): 131-136.
- SCHURR, A.** (2006). Lactate: the ultimate cerebral oxidative energy substrate? *J Cereb Blood Flow Metab* **26**(1): 142-152.
- SCHURR, A., PAYNE, R. S., MILLER, J. J. and RIGOR, B. M.** (1997). Brain lactate is an obligatory aerobic energy substrate for functional recovery after hypoxia: further in vitro validation. *J Neurochem* **69**(1): 423-426.
- SCHURR, A., PAYNE, R. S., MILLER, J. J. and RIGOR, B. M.** (1997). Brain lactate, not glucose, fuels the recovery of synaptic function from hypoxia upon reoxygenation: an in vitro study. *Brain Res* **744**(1): 105-111.
- SCHURR, A., WEST, C. A. and RIGOR, B. M.** (1989). Electrophysiology of energy metabolism and neuronal function in the hippocampal slice preparation. *J Neurosci Methods* **28**(1-2): 7-13.
- SEAQUIST, E. R. and GRUETTER, R.** (2002). Brain glycogen: an insulin-sensitive carbohydrate store. *Diabetes Nutr Metab* **15**(5): 285-289; discussion 289-290.
- SHIN, B. S., WON, S. J., YOO, B. H., KAUPPINEN, T. M. and SUH, S. W.** (2010). Prevention of hypoglycemia-induced neuronal death by hypothermia. *J Cereb Blood Flow Metab* **30**(2): 390-402.

- SHULMAN, G. L., CORBETTA, M., BUCKNER, R. L., RAICHLE, M. E., FIEZ, J. A., MIEZIN, F. M. and PETERSEN, S. E.** (1997). Top-down modulation of early sensory cortex. *Cereb Cortex* **7**(3): 193-206.
- SHULMAN, R. G.** (2005). Glycogen turnover forms lactate during exercise. *Exerc Sport Sci Rev* **33**(4): 157-162.
- SHULMAN, R. G., HYDER, F. and ROTHMAN, D. L.** (2001). Cerebral energetics and the glycogen shunt: neurochemical basis of functional imaging. *Proc Natl Acad Sci U S A* **98**(11): 6417-6422.
- SHULMAN, R. G. and ROTHMAN, D. L.** (2001). The "glycogen shunt" in exercising muscle: A role for glycogen in muscle energetics and fatigue. *Proc Natl Acad Sci U S A* **98**(2): 457-461.
- SIESJO, B. K.** (1988). Hypoglycemia, brain metabolism, and brain damage. *Diabetes Metab Rev* **4**(2): 113-144.
- SILK, T. J., VANCE, A., RINEHART, N., BRADSHAW, J. L. and CUNNINGTON, R.** (2009). White-matter abnormalities in attention deficit hyperactivity disorder: a diffusion tensor imaging study. *Hum Brain Mapp* **30**(9): 2757-2765.
- SILVER, I. A. and ERECINSKA, M.** (1994). Extracellular glucose concentration in mammalian brain: continuous monitoring of changes during increased neuronal activity and upon limitation in oxygen supply in normo-, hypo-, and hyperglycemic animals. *J Neurosci* **14**(8): 5068-5076.
- SIMPSON, I. A., CARRUTHERS, A. and VANNUCCI, S. J.** (2007). Supply and demand in cerebral energy metabolism: the role of nutrient transporters. *J Cereb Blood Flow Metab* **27**(11): 1766-1791.
- SOKOLOFF, L., MANGOLD, R., WECHSLER, R. L., KENNEY, C. and KETY, S. S.** (1955). The effect of mental arithmetic on cerebral circulation and metabolism. *J Clin Invest* **34**(7, Part 1): 1101-1108.
- SOKOLOFF, L., REIVICH, M., KENNEDY, C., DES ROSIERS, M. H., PATLAK, C. S., PETTIGREW, K. D., SAKURADA, O. and SHINOHARA, M.** (1977). The [14C]deoxyglucose method for the measurement of local cerebral glucose utilization: theory, procedure, and normal values in the conscious and anesthetized albino rat. *J Neurochem* **28**(5): 897-916.
- SOLS, A. and CRANE, R. K.** (1954). Substrate specificity of brain hexokinase. *J Biol Chem* **210**(2): 581-595.
- SOMJEN, G. G.** (2002). Ion regulation in the brain: implications for pathophysiology. *Neuroscientist* **8**(3): 254-267.

- STEINMAN, L.** (1996). Multiple sclerosis: a coordinated immunological attack against myelin in the central nervous system. *Cell* **85**(3): 299-302.
- STYS, P. K., RANSOM, B. R. and WAXMAN, S. G.** (1991). Compound action potential of nerve recorded by suction electrode: a theoretical and experimental analysis. *Brain Res* **546**(1): 18-32.
- STYS, P. K., WAXMAN, S. G. and RANSOM, B. R.** (1992). Effects of temperature on evoked electrical activity and anoxic injury in CNS white matter. *J Cereb Blood Flow Metab* **12**(6): 977-986.
- SUH, S. W., AOYAMA, K., MATSUMORI, Y., LIU, J. and SWANSON, R. A.** (2005). Pyruvate administered after severe hypoglycemia reduces neuronal death and cognitive impairment. *Diabetes* **54**(5): 1452-1458.
- SUH, S. W., FREDERICKSON, C. J. and DANSCHER, G.** (2006). Neurotoxic zinc translocation into hippocampal neurons is inhibited by hypothermia and is aggravated by hyperthermia after traumatic brain injury in rats. *J Cereb Blood Flow Metab* **26**(2): 161-169.
- SUH, S. W., HAMBY, A. M., GUM, E. T., SHIN, B. S., WON, S. J., SHELINE, C. T., CHAN, P. H. and SWANSON, R. A.** (2008). Sequential release of nitric oxide, zinc, and superoxide in hypoglycemic neuronal death. *J Cereb Blood Flow Metab* **28**(10): 1697-1706.
- SUH, S. W., HAMBY, A. M. and SWANSON, R. A.** (2007). Hypoglycemia, brain energetics, and hypoglycemic neuronal death. *Glia* **55**(12): 1280-1286.
- SUZUKI, A., STERN, S. A., BOZDAGI, O., HUNTLEY, G. W., WALKER, R. H., MAGISTRETTI, P. J. and ALBERINI, C. M.** (2011). Astrocyte-neuron lactate transport is required for long-term memory formation. *Cell* **144**(5): 810-823.
- SWANSON, R. A.** (1992). Physiologic coupling of glial glycogen metabolism to neuronal activity in brain. *Can J Physiol Pharmacol* **70 Suppl**: S138-144.
- SWANSON, R. A. and CHOI, D. W.** (1993). Glial glycogen stores affect neuronal survival during glucose deprivation in vitro. *J Cereb Blood Flow Metab* **13**(1): 162-169.
- SWANSON, R. A. and GRAHAM, S. H.** (1994). Fluorocitrate and fluoroacetate effects on astrocyte metabolism in vitro. *Brain Res* **664**(1-2): 94-100.

- TAKEBE, K., NIO-KOBAYASHI, J., TAKAHASHI-IWANAGA, H. and IWANAGA, T.** (2008). Histochemical demonstration of a monocarboxylate transporter in the mouse perineurium with special reference to GLUT1. *Biomed Res* **29**(6): 297-306.
- TAYLOR, D. L., RICHARDS, D. A., OBRENOVITCH, T. P. and SYMON, L.** (1994). Time course of changes in extracellular lactate evoked by transient K(+)-induced depolarisation in the rat striatum. *J Neurochem* **62**(6): 2368-2374.
- TEKKOK, S. B., BROWN, A. M. and RANSOM, B. R.** (2003). Axon function persists during anoxia in mammalian white matter. *J Cereb Blood Flow Metab* **23**(11): 1340-1347.
- TEKKOK, S. B., BROWN, A. M., WESTENBROEK, R., PELLERIN, L. and RANSOM, B. R.** (2005). Transfer of glycogen-derived lactate from astrocytes to axons via specific monocarboxylate transporters supports mouse optic nerve activity. *J Neurosci Res* **81**(5): 644-652.
- TEKKOK, S. B. and RANSOM, B. R.** (2004). Anoxia effects on CNS function and survival: regional differences. *Neurochem Res* **29**(11): 2163-2169.
- TEKKOK, S. B., YE, Z. and RANSOM, B. R.** (2007). Excitotoxic mechanisms of ischemic injury in myelinated white matter. *J Cereb Blood Flow Metab* **27**(9): 1540-1552.
- THAKOR, D. K., LIN, A., MATSUKA, Y., MEYER, E. M., RUANGSRI, S., NISHIMURA, I. and SPIGELMAN, I.** (2009). Increased peripheral nerve excitability and local NaV1.8 mRNA up-regulation in painful neuropathy. *Mol Pain* **5**: 14.
- VAISHNAVI, S. N., VLASSENKO, A. G., RUNDLE, M. M., SNYDER, A. Z., MINTUN, M. A. and RAICHLE, M. E.** (2010). Regional aerobic glycolysis in the human brain. *Proc Natl Acad Sci U S A* **107**(41): 17757-17762.
- VAN HALL, G., STROMSTAD, M., RASMUSSEN, P., JANS, O., ZAAR, M., GAM, C., QUISTORFF, B., SECHER, N. H. and NIELSEN, H. B.** (2009). Blood lactate is an important energy source for the human brain. *J Cereb Blood Flow Metab* **29**(6): 1121-1129.
- VAN VEEN, B. K., SCHELLENS, R. L., STEGEMAN, D. F., SCHOONHOVEN, R. and GABREELS-FESTEN, A. A.** (1995). Conduction velocity distributions compared to fiber size distributions in normal human sural nerve. *Muscle Nerve* **18**(10): 1121-1127.

VAN VLIET, E. A., DA COSTA ARAUJO, S., REDEKER, S., VAN SCHAIK, R., ARONICA, E. and GORTER, J. A. (2007). Blood-brain barrier leakage may lead to progression of temporal lobe epilepsy. *Brain* **130**(Pt 2): 521-534.

VEGA, C., MARTIEL, J. L., DROUHAULT, D., BURCKHART, M. F. and COLES, J. A. (2003). Uptake of locally applied deoxyglucose, glucose and lactate by axons and Schwann cells of rat vagus nerve. *J Physiol* **546**(Pt 2): 551-564.

VEGA, C., POITRY-YAMATE, C. L., JIROUNEK, P., TSACOPOULOS, M. and COLES, J. A. (1998). Lactate is released and taken up by isolated rabbit vagus nerve during aerobic metabolism. *J Neurochem* **71**(1): 330-337.

VINCENT, A. M., EDWARDS, J. L., MCLEAN, L. L., HONG, Y., CERRI, F., LOPEZ, I., QUATTRINI, A. and FELDMAN, E. L. (2010). Mitochondrial biogenesis and fission in axons in cell culture and animal models of diabetic neuropathy. *Acta Neuropathol* **120**(4): 477-489.

WALLS, A. B., HEIMBURGER, C. M., BOUMAN, S. D., SCHOUSBOE, A. and WAAGEPETERSEN, H. S. (2009). Robust glycogen shunt activity in astrocytes: Effects of glutamatergic and adrenergic agents. *Neuroscience* **158**(1): 284-292.

WALLS, A. B., SICKMANN, H. M., BROWN, A., BOUMAN, S. D., RANSOM, B., SCHOUSBOE, A. and WAAGEPETERSEN, H. S. (2008). Characterization of 1,4-dideoxy-1,4-imino-d-arabinitol (DAB) as an inhibitor of brain glycogen shunt activity. *J Neurochem* **105**(4): 1462-1470.

WALZ, W., SHARGOOL, M. and HERTZ, L. (1984). Barium-induced inhibition of K⁺ transport mechanisms in cortical astrocytes--its possible contribution to the large Ba²⁺-evoked extracellular K⁺ signal in brain. *Neuroscience* **13**(3): 945-949.

WANG, S. S., SHULTZ, J. R., BURISH, M. J., HARRISON, K. H., HOF, P. R., TOWNS, L. C., WAGERS, M. W. and WYATT, K. D. (2008). Functional trade-offs in white matter axonal scaling. *J Neurosci* **28**(15): 4047-4056.

WAXMAN, S. G., BLACK, J. A., RANSOM, B. R. and STYS, P. K. (1994). Anoxic injury of rat optic nerve: ultrastructural evidence for coupling between Na⁺ influx and Ca²⁺-mediated injury in myelinated CNS axons. *Brain Res* **644**(2): 197-204.

WAXMAN, S. G., DAVIS, P. K., BLACK, J. A. and RANSOM, B. R. (1990). Anoxic injury of mammalian central white matter: decreased susceptibility in myelin-deficient optic nerve. *Ann Neurol* **28**(3): 335-340.

- WEIS, J. and SCHRODER, J. M.** (1988). Adult polyglucosan body myopathy with subclinical peripheral neuropathy: case report and review of diseases associated with polyglucosan body accumulation. *Clin Neuropathol* **7**(6): 271-279.
- WENDER, R., BROWN, A. M., FERN, R., SWANSON, R. A., FARRELL, K. and RANSOM, B. R.** (2000). Astrocytic glycogen influences axon function and survival during glucose deprivation in central white matter. *J Neurosci* **20**(18): 6804-6810.
- WENBERG, R. P., JOHANSSON, B. B., FOLBERGROVA, J. and SIESJO, B. K.** (1991). Bilirubin-induced changes in brain energy metabolism after osmotic opening of the blood-brain barrier. *Pediatr Res* **30**(5): 473-478.
- WHITESELL, R. R., WARD, M., MCCALL, A. L., GRANNER, D. K. and MAY, J. M.** (1995). Coupled glucose transport and metabolism in cultured neuronal cells: determination of the rate-limiting step. *J Cereb Blood Flow Metab* **15**(5): 814-826.
- WHITTAM, R.** (1962). The dependence of the respiration of brain cortex on active cation transport. *Biochem J* **82**: 205-212.
- WIENHARD, K., PAWLIK, G., HERHOLZ, K., WAGNER, R. and HEISS, W. D.** (1985). Estimation of local cerebral glucose utilization by positron emission tomography of [¹⁸F]2-fluoro-2-deoxy-D-glucose: a critical appraisal of optimization procedures. *J Cereb Blood Flow Metab* **5**(1): 115-125.
- WYATT, K. D., TANAPAT, P. and WANG, S. S.** (2005). Speed limits in the cerebellum: constraints from myelinated and unmyelinated parallel fibers. *Eur J Neurosci* **21**(8): 2285-2290.
- WYSS, M. T., JOLIVET, R., BUCK, A., MAGISTRETTI, P. J. and WEBER, B.** (2011). In vivo evidence for lactate as a neuronal energy source. *J Neurosci* **31**(20): 7477-7485.
- XIANG, Y., XU, G. and WEIGEL-VAN AKEN, K. A.** (2010). Lactic acid induces aberrant amyloid precursor protein processing by promoting its interaction with endoplasmic reticulum chaperone proteins. *PLoS One* **5**(11): e13820.
- ZAUNER, A., DAUGHERTY, W. P., BULLOCK, M. R. and WARNER, D. S.** (2002). Brain oxygenation and energy metabolism: part I-biological function and pathophysiology. *Neurosurgery* **51**(2): 289-301; discussion 302.
- ZELENA, J.** (1980). Arrays of glycogen granules in the axoplasm of peripheral nerves at pre-ovoid stages of Wallerian degeneration. *Acta Neuropathol* **50**(3): 227-232.

ZHANG, K. and SEJNOWSKI, T. J. (2000). A universal scaling law between gray matter and white matter of cerebral cortex. *Proc Natl Acad Sci U S A* **97**(10): 5621-5626.

ZIMMER, R. and LANG, R. (1975). Rates of lactic acid permeation and utilization in the isolated dog brain. *Am J Physiol* **229**(2): 432-437.

ZISKIN, J. L., NISHIYAMA, A., RUBIO, M., FUKAYA, M. and BERGLES, D. E. (2007). Vesicular release of glutamate from unmyelinated axons in white matter. *Nat Neurosci* **10**(3): 321-330.

Publications

This section contains an index of publications derived from the work contained in this thesis.

Published

EVANS, R. D., WESTON, D. A., McLAUGHLIN, M. and BROWN, A. M. (2010). A non-linear regression analysis method for quantitative resolution of the stimulus-evoked compound action potential from rodent optic nerve. *J Neurosci Methods* **188**(1): 174-178.

EVANS, R. D., MASON, R., and RANSOM, B. R. (2010) The effects of temperature on glucopenic injury in the mouse optic nerve. *Proc Physiol Soc* **19** C22.

In Press

EVANS, R. D., BROWN, A. M., and RANSOM, B. R. (2012) Functions of Glycogen in the CNS. *Advances in Neurobiology*.

Submitted for review

BROWN, A. M., EVANS, R. D., BLACK, J. and RANSOM, B. R. Peripheral nerve Schwann cell glycogen selectively supports myelinated axon function. *Annals of Neurology*.

In preparation

EVANS, R. D., SMITH, P. A., and BROWN, A. M. Temperature sensitivity of glucopenic injury in the mouse optic nerve, a central white matter tract.

EVANS, R. D., RANSOM, B. R. and BROWN, A. M. Application of biosensors for real-time measurement of lactate in CNS white matter.